CHARACTERIZATION OF NESTIN PROTEINS IN THE GOLDFISH: IMPLICATIONS FOR REGENERATION OF ADULT DOPAMINERGIC NEURONS

MADDIE JOLYANE VENABLES

Thesis submitted to the
Faculty of Graduate and Postdoctoral Studies
University of Ottawa
In partial fulfillment of the requirements for the
Ph.D. degree in the

Ottawa-Carleton Institute of Biology

Thèse soumise à la
Faculté des études supérieures et postdoctorales
Université d'Ottawa
dans le cadre des exigences du programme de
doctorat en biologie

Institut de biologie d'Ottawa-Carleton

Acknowledgements

The writing of this thesis would not have been possible without the help, support and guidance of colleagues, friends and family. First and foremost I would like to express my greatest gratitude to my supervisor, Dr. Vance Trudeau. He was not only my supervisor but also a mentor who guided and directed me through my research journey. The overall experience has been very educational, inspiring and fun! I would also like to thank my Ph.D. advisory committee members, Drs. Marc Ekker, Ajoy Basak, and Steffany Bennett for their guidance and stimulating scientific conversations. A special thank you to Dr. Ajoy Basak who helped with the generation of the nestin antibody and assisted with the mass spectrometry experiment.

Another very helpful group of students, postdocs and technicians are past and present teamendo.ca members! I cannot express how grateful I am for all the help in the lab, supportive group during stressful times, and providing great company during social gatherings and events! Thank you for all your help.

I would like to specifically thank Purva Wagh for her help and support with preliminary studies during my first years in the laboratory and Dr. Laia Navarro-Martín for her help with RACE-PCR and sequencing of the nestin goldfish proteins. Not only did Dr. Navarro-Martín helped me with laboratory experiments but she also introduced me to a new community of friends and the sport underwater hockey, one of my favourite hobbies! A special thank you to Lei Xing for quantifying bromodeoxyuridine-labelling cells on numerous goldfish brain sections as well as assisting with confocal imaging. Another thank you to Connor C. Edington whom helped with the video analysis of the MPTP behavioural studies and Marilyn Vera Chang and Antony D. St-Jacques for providing the fish tracking software. I would also like to thank my honour's student, Wei Seah, whom helped with fish husbandry and general laboratory work during his last 2 years of undergraduate studies. Last but not least, I would like to thank Bernard R. Baum for his tremendous help analyzing all the western blot data using PCA.

Thank you to Bill Fletcher and Christine Archer for maintenance and care of the goldfish. I would also like to acknowledge the University of Ottawa for providing me with graduate scholarships during my studies.

Thank you to my parents for supporting me throughout my entire graduate studies and always believing in my research and teaching goals!

Last but not least, I would like to thank my loving husband Christopher for his endless support and friendship throughout this journey. I started my graduate studies with a boyfriend, then a fiancé and ended with a wonderful and loving husband. Now, at the end of the journey, we are expecting to enlarge our family with our first child! Words cannot express how grateful I am for your continuous encouragement, support, laugh and love. Without you, this journey would not have been as enjoyable and successful. Thank you! xx

Abstract

Nestin is a type VI intermediate filament protein that marks proliferative cells in the central and peripheral nervous system of vertebrates during development and adulthood. Nestin is not only expressed in progenitor cells of neuronal tissues but is also present in muscle, heart, lung, pancreas and skin follicle tissues. The goal of this thesis is to investigate and characterize the nestin protein in goldfish and relate nestin expression to neuroregeneration and brain plasticity events in the adult goldfish forebrain. Currently little is known about nestin function and regulation in vertebrates, especially in fish. In this study we used Rapid amplification of cDNA ends PCR (RACE-PCR) to isolate goldfish *nestin* mRNA. We uncovered several different mRNA transcripts. PCR analysis and sequencing further identified three different *nestin* transcripts of 4003, 2446, and 2126 nucleotides with a predicted protein length of 860, 274, and 344 amino acids respectively. We next applied a multiple-antigenic peptide (MAP) strategy to generate a polyclonal goldfish-specific nestin antibody against a 23 amino acid sequence located at the N-terminal end of goldfish nestin. Western blotting revealed the existence of three different nestin protein isoforms (nestin A, B and C); the first report of nestin isoforms in teleost species. Nestin expression and distribution in the goldfish brain is complex and revealed both individual and tissue-dependent variations. The most remarkable finding following principal component analysis of the western blot data was the uniqueness of the pituitary, hypothalamus and telencephalon. These tissues are proliferative in nature containing progenitor and proliferative cellular pools that are involved in important biological axes such as the motor and reproductive axis. Interestingly, all three tissues were able to change their proliferative cellular profile of nestin protein expression to alleviate the detrimental effects of the neurotoxin 1-methyl-4-phenyl-1,2,3,6-

tetrahydropyridine (MPTP) upon administration. The toxin MPTP destroys dopamine neurons in the fish brain leading to motor deficits and reproductive difficulties. The incorporation of 5-bromo-2'-deoxyuriding (BrdU) into newly synthesized DNA revealed an upregulation of BrdU immunolabeling following MPTP administration in the area telencephali pars dorsalis (Vd) and along the ventricular surface area of the telencephalon suggesting the generation of new neurons in the adult central nervous system. This thesis reports novel nestin isoforms and illustrates regenerative events occurring in the goldfish telencephalon following a neurotoxic insult. This work provides a framework for future investigations of the differential roles and regulation of the nestins to better understand seasonal neuronal plasticity, neuronal regeneration and neuronal circuitry in teleost.

Résumé

La nestine est une protéine de filaments intermédiaires de type VI qui marque les cellules prolifératives dans les systèmes nerveux périphérique et central des vertébrés durant le stade de développement et à l'âge adulte. La nestine se trouve non seulement dans les cellules progénitrices des tissus neuronaux, mais aussi dans les tissus musculaires, cardiaques, pulmonaires et pancréatiques, et dans les follicules de la peau. La présente thèse a pour objectif d'analyser et de caractériser la protéine nestine chez le poisson rouge et d'établir un rapport entre la présence de la nestine et la neuroregénération et neuroplasticité du cerveau antérieur de celui-ci. À l'heure actuelle, on en connait peu sur les fonctions de la nestine et son rôle en matière de régularisation chez les vertébrés, particulièrement chez les poissons. Pour les fins de cette étude, nous avons utilisé une technique d'amplification rapide d'extrémités d'ADNc PCR (RACE-PCR) pour isoler l'ARNm de la *nestine*. Nous avons découvert plusieurs produits de la transcription ARNm. L'analyse et le séquençage PCR ont, de plus, permis d'identifier trois différents produits de la transcription *nestine* de 4003, 2446 et 2126 nucléotides, avec une longueur de protéine prévue de 860, 274 et 344 acides aminés respectivement. Nous avons ensuite fait appel à une stratégie d'antigènes peptidiques multiples pour créer un anticorps polyclonal nestine propre au poisson rouge contre une séquence de 23 acides aminés situés dans la région N-terminale de la nestine. Le transfert de type Western a révélé l'existence de trois protéines isoformes distinctes de la nestine (nestine A, B et C); le premier signalement d'isoformes de nestine chez les téléostéens. L'expression et la répartition de la nestine dans le cerveau du poisson rouge sont complexes et ont révélé des variations à la fois individuelles et dépendantes des tissus. L'une des constatations les plus remarquables suivant l'analyse des données principales du transfert de type Western

concernait le caractère unique de l'hypophyse, de l'hypothalamus et du télencéphale. Ces tissus sont prolifératifs de nature et contiennent des bassins cellulaires progéniteurs et prolifératifs qui jouent un rôle importants dans les axes biologiques, notamment les axes moteur et reproductif. Fait intéressant, ces trois tissus ont réussi à modifier leur profil cellulaire prolifératif lié à l'expression de la protéine nestine afin d'atténuer les effets nuisibles de la neurotoxine 1-méthyle-4-phényle-1,2,3,6-tétrahydropyridine (MPTP) au moment de son injection. La toxine MPTP détruit les neurones de dopamine dans le cerveau du poisson, entraînant des problèmes de motricité et de reproduction. L'incorporation de 5-bromo-2'-deoxyuridine (BrdU) dans l'ADN nouvellement synthétisée a révélé une régulation à la hausse de l'immunomarquage BrdU suivant l'administration de la MPTP dans la zone telencephali pars dorsalis (Vd) et le long de la surface ventriculaire du télencéphale, suggérant la création de nouvelle neurones dans le système nerveux central de l'adulte. La présente thèse fait état de nouveaux isoformes de nestine et de la survenance d'événements régénérateurs dans le télencéphale du poisson rouge à la suite d'une atteinte neurotoxique. Elle fournit également un cadre de travail pour d'autres recherches sur les rôles différentiels et la fonction de régularisation des nestines dans le but de mieux comprendre la plasticité neuronale saisonnière, la régénération neuronale et la circuiterie neuronale chez les téléostéens.

Table of Contents

List of Figures

List of Tables

List of Abbreviations

ALDH1	Aldehyde dehydrogenase 1
BDNF	Brain-derived neurotrophic factor
BLBP	Brain lipid-binding protein
BrdU	Bromodeoxyuridine
Brstem	Brainstem
cdk5	Cyclin-dependent kinase 5
Cereb	Cerebellum
CNS	Central nervous system
D2S	Dopamine D2 short isoform
DA	Dopamine
DAT	Dopamine transporter
Dc	Area dorsalis telencephali pars centralis
DJ-1	Oncogene DJ1
dpi	Days post-injection
E	Epinephrine
ECL	Enhanced chemiluminescence
GABA	γ-aminobutyric acid
GDNF	Glial-derived neurotrophic factor
GFAP	Glial fibrillary acidic protein
GnRH	Gonadotropin-releasing hormone
HRP	Horseradish peroxidase
Hyp	Hypothalamus
IF	Intermediate filament
IHC	Immunohistochemistry
IsO	Isthmic organizer
i.p.	Intraperitoneal
ir	Immunoreactivity
LH	Luteinizing hormone
MAP	Multiple-antigenic peptide
Midbr	Midbrain
MPP^+	1-methyl-4-phenylpyridinium
MPTP	1-methyl-4-phenyl-1,2,3,6-tetrahydropyridine
MW	Molecular weight
NE	Norepinephrine
NF	Neurofilament
NPM	Nucleus telencephali pars medialis
NPO	Nucleus preopticus
NPP	Nucleus preopticus periventricularis
NSC	Neural stem cell
nurr1	Nuclear receptor related 1
OB	Olfactory bulb
olig2	Oligodendrocyte lineage transcription factor 2
otx2	Homolog of *Drosophilia* orthodenticle 2

PAR1	Protease activated receptor 1
PCA	Principal component analysis
PINK1	Pten-induced putative kinase 1
PNS	Peripheral nervous system
Pit	Pituitary
pitx3	Paired-like homeodomain transcription factor 3
PD	Parkinson's disease
POA	Preoptic telencephalic area
RACE-PCR	Rapid amplification of cDNA ends polymerase chain reaction
RGC	Radial glial cell
RT	Room temperature
SAS	Statistical analysis system
SDS	Sodium dodecyl sulfate
SDS-PAGE	Sodium dodecyl sulfate polyacrylamide gel electrophoresis
SELDI-Tof	Surface-enhanced laser desorption ionization time of flight
SGZ	Subgranular zone
Shh	Sonic hedgehog
SN	Substantia nigra
SNc	Substantia nigra pars compacta
SSC	Saline-sodium citrate
SVZ	Subventricular zone
Tel	Telencephalon
TH	Tyrosine hydroxylase
TBS	Tris-buffered saline
TBS-T	Tris-buffered saline with tween
TUNEL	Terminal deoxynucleotidyl transferase-mediated dUTP nick-end labelling
uch-L1	Ubiquitin carboxyl-terminal esterase L1
UTR	Untranslated region
Vd	Area telencephali pars dorsalis
VTA	Ventral tegmental area
Vv	Area telencephali pars ventralis

Chapter 1

General Introduction

1.1. Thesis Overview

The findings of this research project provide a platform for future investigations of dopaminergic (DAergic) neuronal regeneration in the goldfish and increases our knowledge about brain plasticity. The characterization of the nestin proteins in goldfish is presented. Nestin is an intermediate filament (IF) protein and neuronal stem cell (NSC) marker involved in regenerative processes in vertebrates. The studies conducted also investigated cellular death, tissue damage and regeneration mechanisms in goldfish following a neurotoxic insult.

1.1.1. Hypotheses

1) Nestin protein is differentially expressed in the goldfish brain based on sex and in response to MPTP treatment.

2) Dopaminergic neurons regenerate in the area telencephali pars dorsalis (Vd) of the goldfish brain as a recovery mechanism following MPTP insult.

This research project focuses on investigating the neuroanatomical effects of 1-methyl-4-phenyl-1,2,3,6-tetrahydropyridine (MPTP) on DAergic neurons in the goldfish brain, identifying regenerating DAergic neurons following MPTP injection and characterizing the nestin protein during neuronal regeneration. In Appendix A, I first confirmed previous reports (Poli *et al.* 1990; Pollard *et al.* 1992; Goping *et al.* 1995; Lucchi *et al.* 1998) and observed MPTP-induced depletion of dopamine (DA) neurons in the telencephalon and optic tectum as determined using tyrosine hydroxylase (TH)

immunohistochemistry (IHC). Other evidence such as the recovery of catecholamine content, specifically DA and norepinephrine (NE), in the goldfish brain following a neurotoxic insult (Poli *et al.* 1992; Pollard *et al.* 1992) and axonal and tissue regeneration following brain injury (Contestabile *et al.* 1979; Levine 1983; Scherer and Easter 1984; Stuermer 1986) indicates that these DA neurons regenerate following injury or a chemical lesion showing the existence of NSCs in the adult teleost brain. Testing this hypothesis required the generation and validation of the first anti-nestin goldfish antibody presented in Chapter 2. Western blotting experiments suggests that the predicted 98 kDa nestin protein is processed to three smaller fragments in vivo. This study reports for the first time the presence of three novel nestin isoforms in a teleost species.

Nestin protein distribution is sex- and tissue-dependent and reveals a complex expression pattern as described in Chapter 2 and 3. Nestin protein expression also changes following a neurotoxic insult in comparison to control animals (Chapter 3). The changes observed in nestin expression patterns, especially in neurogenic brain regions involved in both reproductive and motor control such as the hypothalamus and telencephalon, could suggest the occurrence of neuronal regeneration. In Chapter 4, we explore the possibility of neuronal regeneration in the ventral telencephalon following the administration of the neurotoxic insult MPTP. Chapter 5 elaborates on the accomplishments of this study and reviews the key findings of this thesis. This thesis advances our knowledge in neuronal brain plasticity and expand on neuronal regeneration following injury in teleost .

1.2. Introduction

Dopamine is a key neurotransmitter that plays an important role in movement, reward mechanism, and reproduction in vertebrates. Abnormalities in the functioning and signaling pathways of DAergic neurons can lead to reproductive difficulties in vertebrates and even neurodegenerative diseases such as Parkinson's disease (PD). A parkinsonian syndrome can be induced in fish (Poli et *al.* 1990; Poli et *al.* 1992; Goping et *al.* 1995; Popesku 2009; Sallinen et *al.* 2009), rodents (Horby et *al.* 1987; Date et *al.* 1990a, 1990b; Lucchi et *al.* 1998; Hamill et *al.* 2007), primates (Burns et *al.* 1983; Pollard et *al.* 1992; Lucchi et *al.* 1998) and humans (Pollard et *al.* 1992; Lucchi et *al.* 1998; Oki et *al.* 2008) by injecting the neurotoxin MPTP. The toxin MPTP causes a degradation of DAergic neurons and a loss of DA innervation in the brain leading to disease. Goldfish are amenable models to study signaling pathways and disease mechanisms because they have the ability to regenerate damaged neurons. For example, Poli et *al.* (1992) showed full recovery of DA levels in the goldfish brain after 6 weeks of injecting the neurotoxin MPTP. Another study documented increases in global transcriptional profiles of genes associated with DA neurogenesis such as *nestin*, nuclear receptor related 1 (*nurr1*), paired-like homeodomain transcription factor 3 (*pitx3*) and homolog of *Drosophilia* orthodenticle 2 (*otx2*) in goldfish following MPTP injection suggesting the occurrence of spontaneous regeneration of hypothalamic DAergic neurons (Popesku 2009). Given the central and unequivocal importance of DA in the inhibition of reproduction by suppression of luteinizing hormone (LH) and its role in motor control, it is important to study and understand the DA signaling pathway in vertebrates (Peter *et al.* 1978; Dufour *et al.* 2005, 2009, 2010; Popesku *et al.* 2008).

The aim of this thesis is to explore the ability of teleost to overcome neuronal death and decreased DA content induced by MPTP toxicity. This study investigates the strong propensity for neuronal remodelling and recovery mechanisms in teleost specifically along the DAergic signaling pathway in the goldfish telencephalon by exploring the nestin proteins. This study explores DAergic regeneration along the motor axis specifically at the area telencephali pars dorsalis (Vd). This work will provide a better understanding of normal plasticity events in teleost as well as cellular turnover and proliferative cell maintenance in the brain.

1.3. Nestin: A multi-cell lineage marker

Nestin is a class VI intermediate filament protein expressed in neural progenitor cells and is present in the cytoskeleton of cells undergoing cellular division (Lendahl *et al.* 1990; Yamaguchi et *al.* 2000; Wiese et *al.* 2004; Michalczyk and Ziman 2005; Mahler and Driever 2007). Nestin is a NSC and progenitor cell marker of multi-lineage origin that is abundant in both the central nervous system (CNS) and peripheral nervous system (PNS) and is also found in other cell types and tissues including cardiomyocytes, dental epithelium and pancreatic progenitor cells (Lendahl *et al.* 1990; Kachinsky *et al.* 1995; Terling *et al.* 1995; Yamaguchi et *al.* 2000; Esni *et al.* 2004; Wiese et *al.* 2004; Mahler and Driever 2007). Nestin has also been identified in endothelial cells of developing blood vessels and skeletal muscle in rats and in Müller cells of the retina and radial glial cells (RGC) in humans (Lendahl *et al.* 1990; Tohyama *et al.* 1992; Sejersen and Lendahl 1993; Zimmermann *et al.* 1994; Mokry and Nemecek 1998; Walcott and Provis 2003). Additional immunohistochemical studies performed in mouse, rat and human showed nestin-expressing cell types in neuronal precursor cells, RGCs and Schwann cells (Wiese

et *al.* 2004; Michalczyk and Ziman 2005; Mahler and Driever 2007; März *et al.* 2010; Carmona *et al.* 2011). Nestin was successfully used as a neurogenic marker by Yamaguchi et *al.* (2000) who generated transgenic mice expressing green fluorescent protein under the regulation of the nestin regulatory genes and was able to track and observe neurogenesis. Mahler and Driever (2007) also demonstrated that nestin could be used as a NSC marker in zebrafish. As goldfish and zebrafish are closely related species from the family Cyprinidae, nestin can also be used as a NSC marker in goldfish and other teleost species.

To elaborate, nestin is abundantly present during early neurogenesis and the observation of nestin expression is directly implicated in tissue regeneration (Frederiksen and McKay 1988; Wiese *et al.* 2004; Michalczyk and Ziman 2005). The upregulation of nestin following injury is indicative of extensive remodeling in both the CNS and PNS as well as in other tissues such as pancreas, skeletal muscle and gastrointestinal tract (Lin *et al.* 1995; Duggal *et al.* 1997; Namiki and Tator 1999; Tsujimura *et al.* 2001; Vaittinen *et al.* 2001; Lardon *et al.* 2002; Wiese *et al.* 2004). The timing of the appearance of nestin in cells is also linked with the formation of lineage-specific progenitor or precursor cells suggesting that nestin upregulation could directly increase DAergic progenitor cell pools following MPTP injection (Wiese *et al.* 2004). More specifically, Wiese *et al.* (2004) observed a transient co-expression of nestin with cell lineage markers such as glial fibrillary acidic protein (GFAP) by performing immunohistochemistry (IHC) on embryonic stem cells *in vitro* at specific time-points that define the induction of progenitor cells into a specific cell lineage. Other *in vitro* experiments also illustrate that embryonic stem cells can first differentiate into nestin-expressing cells and later into

neuronal and glial cells (Fraichard *et al.*, 1995; Strübing *et al.* 1995). Unfortunately the mechanism of re-activation of nestin following injury is not well understood. However, there are studies demonstrating a link between nestin and neuroprotective functions and regenerative events. We can observe NSC deficiencies and increased cellular apoptotic events in a knockout mouse model of nestin where the self-renewal ability of nestin is decreased (Park *et al.* 2010). A similar effect is observed in zebrafish with a morpholino knockdown of nestin where brain and eye developmental defects are evident via the induction of neural proliferative cell apoptosis (Chen *et al.* 2010).

The function of nestin is not well known but the protein is thought to participate in cellular structure and cytoskeletal dynamics in actively dividing cells (Michalczyk and Ziman 2005). Nestin may regulate cytoskeletal dynamics through heteropolymerization and homopolymerization of IF proteins such as vimentin and alpha-internexin (Sjoberg *et al.* 1994; Michalczyk and Ziman 2005). Nestin may also play a role in stabilizing cytoskeletal elements by linking IF proteins to microtubules and microfilaments (Herrmann and Aebi 2000; Michalczyk and Ziman 2005). Although nestin has been well characterized in various mammalian models including mouse, rat and human we are only starting to unravel the role of nestin in fish (Lendahl *et al.* 1990; Dahlstrand *et al.* 1992; Yang *et al.* 2001; Chen *et al.* 2010).

1.4. Neuronal regeneration in goldfish (*Carassius auratus*)

1.4.1. Cellular markers of neurogenesis

Tyrosine hydroxylase is an accepted catecholaminergic marker, especially for DA neurons, that has been well characterized as a DA cell marker and previously used by

many studies for this purpose (Hornby et *al.* 1987; Poli et *al.* 1990; Goping et *al.* 1995; Pollard et *al.* 1996; Rink and Wullimann 2001). Catecholamine describes a group of neurotransmitters that act as hormones in the blood and regulates various endocrine systems such as reproduction and the stress axis (Kastenhuber et *al.* 2010). These catecholamines are known as DA, epinephrine (E) and norepinephine (NE) and they are all synthesized from a common precursor, tyrosine, which undergoes a series of enzymatic reactions dependent on cellular demands. Tyrosine hydroxylase is the rate-limiting enzyme in the biosynthesis of catecholamines (Nagatsu *et al.* 1964).

Firstly, tyrosine undergoes hydroxylation by TH and then decarboxylation by DOPA decarboxylase to form DA (Kuhar *et al.* 1999). Subsequently, DA can be further hydroxylized by DA ß-hydroxylase to give rise to NE (Kuhar *et al.* 1999). Then, phenylethanolamine N-methyltransferase can methylate NE to produce E, the third catecholamine (Kuhar *et al.* 1999). Hornby et *al.* (1987) have shown that TH-immunoreactivity (TH-ir) is present in the cell bodies of DA neurons in the goldfish brain. Popesku (2009) reported that the decrease of DA levels observed after MPTP injection in the goldfish brain coincides with an increase in hypothalamic gene expression of TH and nestin. The observed increase in gene expression of DA and nestin suggests the occurrence of spontaneous regeneration of hypothalamic DAergic neurons in the goldfish brain (Popesku 2009).

There are numerous other markers for neurogenesis including glial fibrillary acidic protein (GFAP), protease activated receptor 1 (PAR1), nuclear receptor related 1 (nurr1), paired-like homeodomain transcription factor 3 (pitx3), dopamine transporter (DAT), and aldehyde dehydrogenase 1 (ALDH1). For example, GFAP and nestin are present in NSCs

cultured from brain cortex astrocytes of injured rat brains and these NSCs were capable of differentiating into neurons and glia (Itoh et *al.* 2006). The ability of marking and measuring neurogenic markers will provide insight into regenerative states of various tissues in vertebrates.

1.4.2. Regenerative ability

Goldfish can regenerate damaged cells, tissues, and axons in the CNS as a recovery mechanism following disease or injury but little is known about the regenerative pathway (Levine 1983; Scherer and Easter 1984). Axonal regeneration is defined as "the re-growth of a severed axon from the same axotomised neuron" and neuronal regeneration is defined as "the replacement of lost cells or tissues from NSCs" (Becker and Becker 2008). The rapid increase in genes involved in both neurogenesis and DAergic neuroregeneration including *nestin*, *nurr1*, *pitx3*, *otx2*, *TH*, *DAT*, dopamine D2 short isoform (*D2S)*, glial-derived neurotrophic factor (*GDNF)*, *GFAP*, oligodendrocyte lineage transcription factor 2 (*olig2)*, pten-induced putative kinase 1 (*PINK1)*, cyclin-dependent kinase 5 (cdk5), oncogene DJ1 (DJ-1), ubiquitin carboxyl-terminal esterase L1 (*uch-L1)* and ß-*actin* following 4-7 days post-injection (dpi) of MPTP is coincident with a short recovery period in the goldfish brain providing further evidence towards neuronal regeneration as a recovery mechanism (Popesku 2009; Popesku *et al.* 2012). For example, olig2 is involved in DA neuron development by committing DA precursor cells in zebrafish (Borodovsky *et al*. 2009).

Scherer and Easter (1984) have reported on axonal regeneration in the trochlear nerve of goldfish. In addition, Stuermer (1986) reported the ability of goldfish to regenerate the

retinotectal pathway even though regenerating axons often divert from their normal growing path to reach their target sites. Axonal regeneration in the optic nerve has also been coupled to increased protein synthesis and axonal transportation of proteins such as tubulin, actin, glycoproteins and other proteins along the optic tract 8 days following optic nerve injury (Murray and Grafstein 1969; Springer and Agranoff 1977; Benowitz et *al.* 1981). Contestabile et *al.* (1979) have also reported a regenerative potential in the goldfish brain in regenerating catecholamine innervation following chemical lesion with 6-hydroxydopamine (Contestabile et *al.* 1979). All of the above studies indicate that the goldfish has high regenerative ability in reforming axonal tracts and tissues in the CNS and could therefore have the ability to regenerate DA neurons in the telencephalon as a recovery mechanism following a neurotoxic insult.

1.4.3. Neurogenesis of dopamine neurons

Neurons are generated from progenitor cells that arise from neuronal stem cells during development and in the mature vertebrate brain (Yamaguchi et *al.* 2000). Stem cells are defined as unspecialized and undifferentiated cells capable of self-renewing themselves via cell division as well as developing into numerous tissue-specific and organ-specific cell types during early life and growth (Vankelecom 2007). Stem cells have an asymmetric division giving rise to one equivalent stem cell, thereby sustaining the stem cell pool in a given tissue or organ, and gives rise to one daughter/progenitor cell (Vankelecom and Gremeaux 2009).

Neuroepithelial cells are progenitor cells arising from embryonic stem cells in early development (Fig. 1.1). As the organism develops, these progenitor neuroepithelial cells

multiply and proliferate and form the ventricular zone in the CNS (Barry et *al.* 2014). Later in development, the neuroepithelial cells serve as NSCs and exhibit self-renewal and multipotency capabilities (Barry et *al.* 2014). They then mature into transit-amplifying cells called RGCs that express nestin and can be identified using the marker brain lipid-binding protein (BLBP) (Wiese et *al.* 2004; Barry et *al.* 2014). Radial glial cells have multi-lineage capability and can differentiate to give rise to astrocytes, oligodendrocytes, and neurons. More specifically, DA neurons can arise from the differentiation of RGCs in the brain by the regulation of various transcriptional factors and signals (Fig. 1.1). RGCs major role is to provide guidance during neuronal migration of newborn neurons (Götx and Barde 2005; Barry et *al.* 2014).

Differentiation of DAergic neurons in the teleost midbrain is very similar to mammalian mesencephalic DAergic neuronal development; however, the origin of the DA precursor cells differs in early induction of DA neurons (Riddle and Pollock 2003). To elaborate, the midbrain DA neuron precursors in zebrafish migrate from the ventral diencephalons in comparison to the isthmic organizer (IsO) in the mammalian midbrain, which is located at the mesencephalic/metencephalic boundary (Rink and Wullimann 2001, 2002; Wullimann and Rink 2001, 2002; Holzschuh *et al.* 2003; Ma 2003). The predominant DA neuronal signals and transcriptional factors leading to DA neuron generation include Notch signalling, nurr1, sonic hedgehog (Shh) glycoprotein, Wnt proteins, pitx3 and otx-2 factors (Fig. 1.1) (Kapsimali et *al.* 2001; Riddle and Pollock 2003; Castelo-Branco et *al.* 2005; Dirian et *al.* 2014). For example, nurr1 receptor is involved in neuronal differentiation of DAergic neurons in the substantia nigra (SN) and ventral tegmental area (VTA) of mice (Castillo *et al.* 1998). Nurr 1 is also important for

regulating the expression of the biosynthetic enzyme TH and dopamine transporter DAT (Prakash and Wurst 2006). Pitx3, nurr1, Wnt, otx2 and Shh have been shown to be important players in mammalian DAergic neuron development (Prakash and Wurst 2006; Smidt and Burbach 2007). Similarly, nurr1 and pitx3 are important for DAergic neuron development in teleost (Filippi *et al.* 2007; Blin *et al*. 2008; Luo *et al.* 2008). The upregulation of genes relating to neurogenesis and to the development and maturation of DA neurons could give us insight into the permissive factors involved in goldfish regenerative mechanism following MPTP injection.

Furthermore, the transitions from one IF type to the next marks important differentiation steps undergone by proliferative cells to differentiate into a neuron (Mahler and Driever 2007). Characterizing the nestin IF could be a key concept in understanding the transition time-points from NSC to a neuronal cell in the goldfish brain. There is a sequential order of transition steps between the various IF types to give rise to the mammalian CNS during development. In the developing mammalian CNS, class I and class II IFs are observed and these represent the cytokeratins (Dahlstrand *et al.* 1992). Following neurulation, class VI IFs (eg. nestin) and class III IFs (eg. desmin) appear in the cytoskeleton. During terminal neural differentiation, a downregulation of nestin is followed by the induction of class IV IFs (eg. neurofilaments) (Dahlstrand *et al.* 1992). There is also transient expression of other IFs types such as alpha-internexin (class IV) during CNS development and GFAP (class III) expressed in astrocytes (Dahlstrand *et al.* 1992). In this thesis, nestin expression was extensively studied to investigate the regenerative possibilities in the goldfish telencephalon and observe brain plasticity and regular proliferative cell maintenance in the proliferative cell pools.

The mammalian CNS expresses some level of plasticity and flexibility where new neurons can be generated, however, the mechanism remains unknown (Yamaguchi et *al.,* 2000). In early mammalian development, RGCs are abundant in the brain but, as development progresses, only a few RGCs persist in the mammalian adult brain. In adulthood, the neurogenic areas become segregated into two main neurogenic areas known as the subventricular zone (SVZ) lining the ventricle and the subgranular zone (SGZ) of the dentate gyrus (März *et al.* 2010). Throughout the adult mammalian brain, RGCs can only be found in the olfactory bulb (OB), the telencephalon, the SVZ and SGZ (Liu et *al*. 2006; Brunne et *al.* 2010). On the other hand, RGCs in the adult teleost fish are present early during development and are more abundant throughout adult life in the various neurogenic areas including the telencephalon contributing to teleost increased neurogenic capabilities (Zupanc and Clint 2003; Mahler and Driever 2007; Pelligrini *et al.* 2007; März *et al.* 2010; Zupanc and Sîrbulescu 2011; Barry et *al.* 2014).

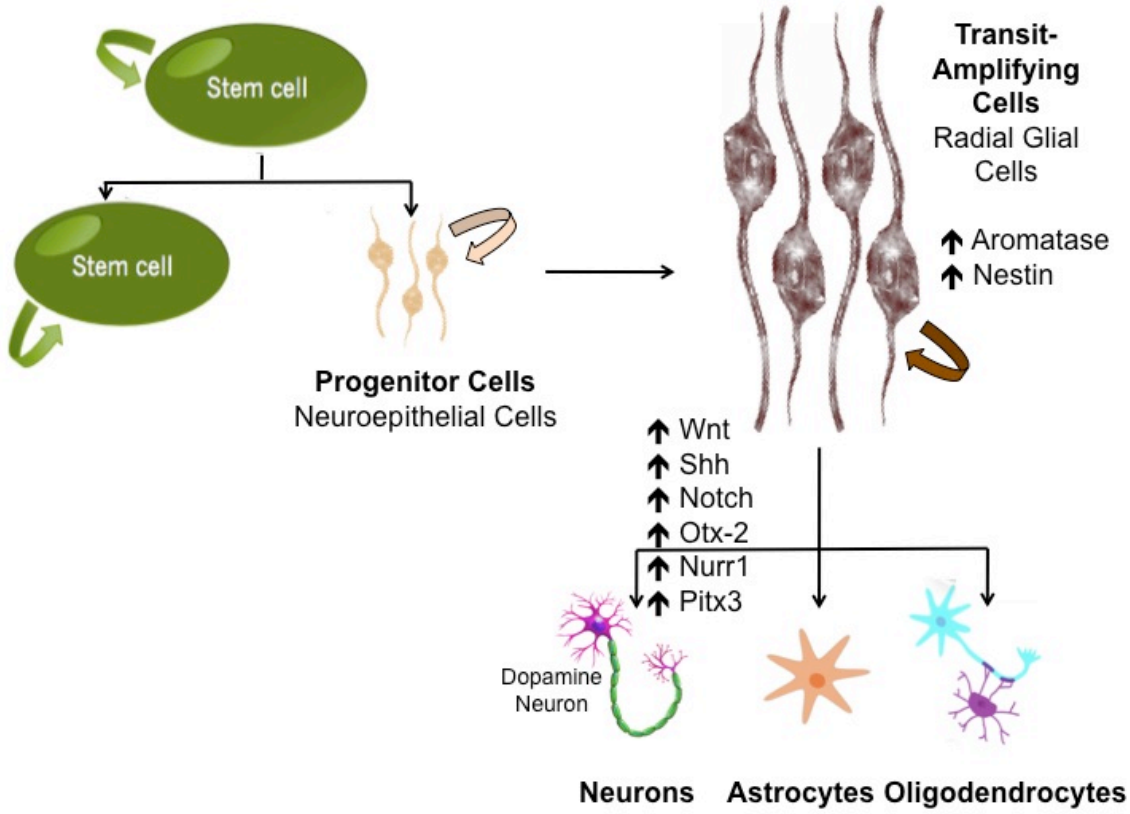

Figure 1.1. Simplified dopamine neuronal differentiation pathway during development and in adulthood of teleost. The figure outlines and highlights key signaling factors and players in teleost neurogenesis and DAergic neuron regeneration. The figure is not to scale, see text for details.

1.5. Neurotoxicity of 1-methyl-4-phenyl-1,2,3,6-tetrahydropyridine (MPTP)

1.5.1. Mechanism of action

MPTP is a neurotoxin that is a useful tool for the study of neurogenesis after neuronal damage. After injection *in vivo*, MPTP is converted to 1-methyl-4-phenylpyridinium (MPP^+) in the brain by the enzyme monoamine oxidase B of glial cells specifically astrocytes and serotonergic neurons in the primate brain and selectively taken up by DA neurons via a dopamine transporter (Chiba *at al.* 1984; Javitch and Snyder

1984; Westlund *et al.* 1985; Snyder *et al.* 1986; Singer et *al.* 1987; Pollard et *al.* 1992, 1996; Gainetdinov *et al.* 1997). In turn, MPP^+ accumulates in the brain and inhibits complex I of the respiratory chain on the inner membrane of the mitochondria inducing anoxia, anaerobic respiration and cell death (Vyas *et al.* 1986; Singer et *al.* 1987; Tipton and Singer 1993; Sriram et *al.* 1997; Sallinen et *al.* 2009). Goping et *al.* (1995) have demonstrated, using light and electron microscopy, that injection of MPTP in the goldfish leads to progressive irregularities of neuronal nuclei and granularization of nucleoplasm. These histochemical abnormalities were observed in the adult goldfish telencephalon especially near the ventricle followed by cellular abnormalities in the preoptic area (POA) and hypothalamus (Goping *et al.* 1995; Sallinen *et al.* 2009). These areas are involved in DAergic brain signaling for both the reproductive and motor axis (Sallinen et *al.* 2009). Pollard et *al.* (1996) were among the first to suggest the goldfish as a model for Parkinson's disease (PD) to study neuronal control of motricity.

1.5.2. Neurotoxicity effects of MPTP on catecholamines

The highest level of catecholamines can be found in the forebrain of the goldfish, which comprises the midbrain's optic tectum and the telencephalon (Goping et *al.* 1995). MPTP injection selectively depletes DA and NE in the telencephalon, hypothalamus, optic tectum and cerebellum of the adult goldfish brain (Poli *et al.* 1990; Pollard *et al.* 1992; Goping *et al.* 1995; Lucchi *et al.* 1998). MPTP injection also reduced TH-ir and DA levels in DAergic neurons of the goldfish retina (Guarnieri *et al*. 1989; Poli *et al.* 1990). Tyrosine hydroxylase-ir was reduced at the mid-telencephalic level near the area ventralis (Vv) and the cytoplasmic processes of TH-ir neurons were reduced (Poli *et al.* 1990). In addition, morphological changes were observed in the affected TH-ir neurons

where the cytoplasmic matrix of TH-ir neurons in the POA was condensed and the endoplasmic reticulum and mitochondria were swollen following MPTP treatment (Poli *et al.* 1990). Interestingly, the selective depletion of DA and NE in the forebrain of the goldfish coincides with the loss of mobility after MPTP injection (Poli et *al.* 1992; Pollard *et al.* 1992; Lu *et al.* 2014). The neurotoxic effects of MPTP appear to be specific to catecholaminergic neurons as no significant changes were observed in the glutamatergic, cholinergic, and GABAergic markers in the goldfish brain (Poli et *al.* 1992). A parallel decrease of DA and NE has also been reported in PD patients in the basal ganglia, the neocortical, and the limbic structures of the brain (Scatton et *al.* 1983).

In goldfish, DA content in the brain (forebrain, midbrain, cerebellum and vagal lobe) reaches its lowest level 3-5 days following injection of MPTP (Poli *et al.* 1990; Pollard *et al.* 1992; Youdim *et al.* 1992). Interestingly, Poli et *al.* (1992) reported full recovery of DA levels in the telencephalon, diencephalon and medulla oblongata in the goldfish brain after 6 weeks of MPTP injection and partial recovery of other catecholamine 4 weeks after injection. Norepinephrine recovery to baseline levels following MPTP injection has been reported to take longer than DA recovery (Poli et *al.* 1992). Pollard *et al.* (1992) reported reversible changes in DA and NE levels in the goldfish brain following MPTP administration where NE and DA levels were lowest at 5 dpi and DA levels returned to baseline levels by 8 days followed by recovery of NE towards normal levels. The catecholamine recovery described in various studies in the goldfish further supports the concept of neuronal regeneration and brain plasticity events following a neurotoxic insult. The findings of these studies led us to formulate the hypothesis that DA neurons are regenerating in the telencephalon following a complex mechanism of neuronal

remodelling. These data indicate that goldfish are susceptible to MPTP toxicity and the areas affected undergo neurochemical changes that are relevant to changes observed in primates. The telencephalon was the focus of this research thesis as this brain tissue has a high neurogenic capacity, is abundant in proliferative cells where RGCs reside and is involved in important biological and behavioural functions such as motricity and reproduction.

1.5.3. Effects of MPTP on neuronal markers

In goldfish, Popesku (2009) reported an upregulation of TH, DAT, nestin, nurr1, pitx3, otx2, GDNF, GFAP, and D2S coincident with the recovery of DA levels following MPTP injection. Similarly, an increase in TH and DAT expression was observed in mouse and monkey following the injection of MPTP (Ohye *et al.* 1995; Goulet *et al.* 1999; Kuhn *et al.* 2003; Miller *et al.* 2004). The upregulation of nestin has also been observed in the mammalian substantia nigra (SN) following MPTP treatment where the DAergic neurons involved in mammalian motricity reside (Zhao *et al.* 2003).

Furthermore, an increase of olig2, PINK1, cdk5, DJ-1, uch-L1, and β-actin was observed following 4-7 days of MPTP injection (Popesku 2009). Some of these markers are signals and transcription factors that specifically trigger DA neuronal differentiation (Saucedo-Cardenas *et al.* 1998; Riddle and Pollock 2003; Smidt *et al.* 2003; Vernay *et al.* 2005; Martinat *et al.* 2006; Smits and Smidt 2006; Filippi *et al.* 2007; Omodei *et al.* 2008; Borodovsky *et al.* 2009; Jacobs *et al.* 2009). For example, otx2, pitx3 and nurr1 are important factors involved in the development and maturation of DAergic neurons in the mammalian mesencephalon and zebrafish ventral diencephalon (Saucedo-Cardenas *et al.* 1998; Riddle and Pollock 2003; Smidt *et al.* 2003; Vernay *et al.* 2005; Martinat *et al.*

2006; Smits and Smidt 2006; Filippi *et al.* 2007; Omodei *et al.* 2008; Jacobs *et al.* 2009). In rat, nurr1 is required for the expression of TH and may serve a protective role for the degeneration of DAergic neurons observed in PD (Sakurada *et al.* 1999; Saijo *et al.* 2009). The changes in gene expression following the injection of MPTP further corroborate the idea of neuronal regeneration to repair damaged tissues in the brain.

1.6. Goldfish as a model organism

1.6.1. Role of dopamine in Parkinson's Disease

Dopamine participates in four different pathways in the vertebrate CNS, which are the mesolimbic, the mesocortical, the tuberoinfundibular, and the nigrostriatal pathways (Riddle and Pollock 2003; Kastenhuber et *al.* 2010). The mesolimbic pathway is involved in motivation and transmits DA from the ventral tegmental area (VTA) of the midbrain to the limbic system via the nucleus accumbens (Mogensen *et al.* 1980; Björklund and Dunnett 2007; Iversen and Iversen 2007; Van den Heuvel and Pasterkamp 2008). The mesocortical pathway is involved in cognitive control, motivation and emotional response and transmits DA from the VTA to the frontal cortex (Björklund and Dunnett 2007; Van den Heuvel and Pasterkamp 2008; Kabanova *et al.* 2015). The tuberoinfundibular pathway is involved in the secretion of certain hormones such as prolactin and transmits DA from the hypothalamus via the arcuate nucleus to the pituitary gland (Porter *et al.* 1990; Benskey *et al.* 2014). Finally, the nigrostriatal pathway is involved in voluntary movement in mammals and originates in the substantia nigra pars compacta (SNc) and innervates the telencephalic dorsal striatum (Marshall *et al.* 1974; Hornby et *al.* 1987; Goping et *al.* 1995; Olanow and Tatton 1999). The destruction of

cells in the nigrostriatal pathway produces observable motor deficits in vertebrates (Goping et *al.* 1995; Horby et *al.* 1987; Poli et *al.* 1992; Sallinen et *al.* 2009). For example, severe motor deficiencies were observed in a cat following MPTP-injection (Schneider and Markham 1986).

Parkinson's disease is a CNS disease characterized by loss of axonal tracts as well as loss of specific cells and tissues relating to motor function (Becker and Becker 2008). The Parkinson-like symptoms such as bradykinesia and tremors can be generated in goldfish (Poli et *al.* 1990; Poli et *al.* 1992; Goping et *al.* 1995; Popesku 2009), zebrafish (Sallinen et *al.* 2009), rodents (Horby et *al.* 1987; Date et *al.* 1990a, 1990b; Lucchi et *al.* 1998; Hamill et *al.* 2007), primates (Burns et *al.* 1983; Pollard et *al.* 1992; Lucchi et *al.* 1998) and humans (Pollard et *al.* 1992; Lucchi et *al.* 1998; Oki et *al.* 2008) following MPTP injection. Unlike mammalian models, the behavioural bradykinesia observed in goldfish treated with MPTP is reversible where the greatest bradykinetic effects are observed at 3-4 dpi and goldfish recover to non-observable motor deficits following 6 dpi of MPTP (Poli et *al* 1992; Pollard *et al.* 1992). The bradykinetic behaviours observed in goldfish are described as decreased swimming activity and increased resting time (Pollard *et al.* 1992). Goldfish (*Carassius* auratus*)* are among many model organisms used for neuroendocrine studies and they are an excellent model organism because they are cost effective and provide neuroanatomical homologues to that of higher vertebrates for studying the DA signaling pathway (Pollard et *al.* 1992; Popesku et *al.* 2008). The goldfish blood-brain barrier is also greatly abbreviated thus some toxins and other compounds can easily enter the brain, making the goldfish an attractive animal model (Weinreb and Youdim 2007).

Parkinson's disease is characterized by the degradation of DA synthesizing neurons in the SNc and loss of DA innervation to the striatum (Sirinathsinghju et *al.* 1988; Goping et *al.* 1995; Oki et *al.* 2008; Sallinen et *al.* 2009). The toxin MPTP causes a depletion of DAergic neurons in the striatum and the SNc of primates as well as a depletion of TH-ir cell bodies and fibers in the SNc (Schneider and Markham 1986; Adams *et al.* 1989; Burns e*t al.* 1983; Chiueh *et al.* 1984; Hallman *et al.* 1985; Heikkila *et al.* 1984a; Irwin *et al.* 199; Langston *et al.* 1984; Schneider *et al.* 1986; Waters *et al.* 1987). A similar degradation of DA neurons has been observed in the goldfish brain following MPTP injection and parallels a parkinsonian syndrome observed in humans affected by PD (Poli et *al.* 1990; Pollard et *al.* 1992; Goping et *al.* 1995).

Although a substantia nigra has not yet been definitively identified in the goldfish, immunocytochemical and evolutionary studies suggest the nucleus telencephali pars medialis (NPM) as a homologous structure to the SNc (Goping *et al.* 1995). The NPM is susceptible to damage following MPTP injection and innervates a striatal area in the telencephalon of the goldfish brain providing further evidence to its homology to the SNc (Goping et *al.* 1995). The damage observed to neurons in the NPM is similar to that observed in SNc neurons in mammals (Pollard et *al.* 1992; Goping et *al.* 1995; Lucchi et *al.* 1998). The SNc is most likely not in the goldfish midbrain as observed in mammalian models as there is no TH-ir bodies observed in this region based on IHC (Hornby *et al.* 1987; Hornby and Piekut 1990). The NPM structure identified in the goldfish corresponds to the previously identified area dorsalis, pars centralis (Dc) of the goldfish telencephalon (Peter *et al.* 1975; Hornby and Piekut 1990; Goping *et al.* 1995).

Furthermore, the Vd in the goldfish brain has been proposed as the homologous structure to the striatum of mammals based on immunocytochemical evidence and depletion of DA following MPTP injection (Franzoni *et al.* 1986; Sas *et al.* 1990; Pollard *et al.* 1992; Goping *et al.* 1995; Wullimann and Mueller 2004). The neuronal irregularities and malformations observed in DAergic cell populations after MPTP treatment are located in the forebrain of the goldfish telencephalon, including the Vd, NPM and POA (Goping *et al.* 1995). Sas *et al.* 1990 reported that the ventral region of the teleost telencephalon, thought to be the equivalent brain structure to the mammalian striatum, receives DAergic innervation from other telencephalic neurons. For these reasons, the telencephalon is most likely the location where DAergic regeneration occurs to reestablish DA signaling and innervation following MPTP injection. All of these studies provide evidence that the basic neural circuits and endocrine signaling pathways of goldfish are comparable to those of primates making the goldfish an excellent model to study PD and neuronal remodelling. The ability of goldfish to reverse the behavioural impairments and neurochemical effects of MPTP as well as recover quickly from MPTP toxicity could be a result of shorter distances traveled by proliferative cells to the affected areas to undergo regeneration and thus contributes to the observed high neurogenetic brain capacity in the goldfish brain.

1.6.2. Role of dopamine in reproduction

Much of our knowledge of DA signaling in teleosts comes from analysis of the inhibitory role of DA in reproduction (Peter *et al.* 1978). Several neuropeptides and receptors are involved in the neuroendocrine regulation of teleost reproduction (Guilgur *et al.* 2006; Klausen *et al.* 2002; Lethimonier *et al.* 2004; Trudeau *et al.* 2000; Trudeau

1997). This thesis provides a platform for future studies focusing on the effects of DA in the neuroendocrine regulation of teleost reproduction. There is a dual neuroendocrine control of reproduction in teleost involving both DA and gonadotropin-releasing hormone (GnRH) (Dufour *et al.* 2010). Both DA and GnRH regulate the release of LH, a hormone produced from the gonadotrophs in the pituitary, which triggers gonadal growth, sex steroids and sex pheromone synthesis as well as sperm production and ovulation in teleost (Trudeau 1997). Dopamine is the single most potent inhibitor of reproduction in teleosts (Dufour *et al.* 2010). Dopamine acts as an inhibitor of LH release whereas GnRH stimulates the release of LH from the pituitary gonadotrophs and thereby both neuropeptides regulate teleost reproduction (Stacey *et al.* 1979; Dufour et *al.* 2005, 2009, 2010). Dopamine acts directly on the gonadotrophs in the pituitary to inhibit LH release and inhibits GnRH-stimulated LH release in the brain thereby inhibiting reproduction in fish (Omeljaniuk *et al.* 1987; De Leeuw *et al.* 1989).

The DA neurons involved in the inhibition of LH release are localized in the nucleus preopticus (NPO) and extend to the pituitary (Peter and Paulencu 1980; Kah *et al.* 1987). More specifically, DA inhibits the release of LH in the teleost brain via the D1 receptor on the GnRH neurons in the teleost brain and via the D2 receptor on the gonadotrophs of the pituitary (Kebabian and Calne 1979; Monsma *et al.* 1989; Yu and Peter 1990). In teleosts, a disinhibition of DA is necessary to obtain a surge of LH release and ovulation (Stacey et *al.* 1979; Chang and Peter 1983). As a result, the goldfish expresses a distinct pattern of DA expression throughout the seasonal reproductive cycle allowing the organism to reproduce only at sexual maturity (Trudeau *et al.* 1993; Dufour et *al.* 2005; Le Page et *al.* 2010). Although DA also has a role in reproduction in other

species such as amphibians, birds and mammals, it only plays a key inhibitory role in fish.

Physical or chemical lesions in the CNS can alter DA brain content and levels providing a venue to study DA signaling pathways involved in reproduction. Injection of MPTP reduces the abundance of DA synthesis and release in the brain thereby decreasing DA's inhibitory effect on LH release and ovulation and potentiates release of LH by GnRH (Peter *et al*. 1986). MPTP leads to a depletion of DA in the telencephalic POA and hypothalamic region of the goldfish brain, two areas involved in teleost reproduction and control (Peter and Paulencu 1980; Ball 1981; Kah *et al.* 1987; Poli et *al.* 1990; Anglade *et al.* 1993; Goping et *al.* 1995). Remarkably, goldfish exhibit brain plasticity and remodeling capability and thus have the ability to counteract the negative effect of MPTP-induced DA depletion in the telencephalic and POA (Poli et *al.* 1990; Goping et *al.* 1995). It appears that the goldfish reproductive cycle returns to basic hormonal control a few days following MPTP injection as DA levels rise and return to basal levels (Poli et *al.* 1992; Pollard et *al.* 1992). MPTP-treatment studies could provide further insight into the molecules involved in brain plasticity and seasonal neuronal remodelling in teleost. Also, increasing our body of knowledge of DA regulation could have a major implication for inducing spawning of teleosts in aquaculture.

Furthermore, several lesional and behavioural studies in goldfish have demonstrated that fibrous telencephalic projections to the hypothalamus and from hypothalamus to the pituitary regulate courtship behaviour and spawning during the reproductive season (Oka and Ueda 1981; Kyle and Peter 1982; Koyama *et al.* 1984; Fryer *et al.* 1985). There are also telencephalic fibers connecting the telencephalic POA

to the hypothalamic nuclei such as the nucleus preoticus (NPO) and nucleus preopticus periventricularis (NPP) (Airhart *et al.* 1988). For example, lesions in the Vv or the PN leads to spawning impairments in male goldfish (Kyle and Peter 1982; Koyama *et al.* 1984).

Seasonal neuronal remodeling and cellular maintenance are two important events to ensure regular motor activity and successful reproduction of fish at the optimal time during life meaning at sexual maturity, during the breeding season, and at the proper annual gonadal growth cycle. For example, Zhang *et al.* (2009) studied seasonal changes on gene expression profile and identified genes in the hypothalamus that were differentially expressed during different stages of the goldfish reproductive cycle such as *aromatase b* and *calmodulin*. All of these events are interlinked and can be affected by injury, disease and exposure to environmental or chemical toxins. Understanding the normal cellular maintenance events of proliferative pools in teleost in normal conditions as well as following a neurotoxic insult will provide the basis to understanding brain plasticity events in adult fish. These studies will provide a foundation to understanding neuronal remodelling and link the participation of nestin into regenerative mechanisms employed by fish to alleviate the toxicity effects of MPTP.

Chapter 2

Characterization of multiple nestin isoforms in the goldfish brain

2.1. Introduction

Nestin is an intermediate filament (IF) protein that is mostly found in cells undergoing mitosis, for example cells undergoing cellular division in both the central nervous system (CNS) and peripheral nervous system (PNS) (Wiese *et al.* 2004; Michalczyk and Ziman 2005; Mahler and Driever 2007). Nestin is often used as a progenitor cell marker in many species and labels cells such as radial glia that exhibit self-renewal and multipotency capabilities (Michalczyk and Ziman 2005; Mahler and Driever 2007; März *et al.* 2010; Carmona *et al.* 2011). Teleost fish have abundant progenitor cells and, compared to humans, have a higher capacity to regenerate neurons following injury. Nestin function and the subsequent upregulation of nestin observed following injury could be the key to understanding cellular regeneration. In this study, we characterized the nestin proteins in the goldfish, a species with exceptional capacities for adult neurogenesis and CNS repair (Levine 1983; Scherer and Eater 1984; Zupanc and Sîrbulescu 2011).

Nestin-positive cells have the ability to give rise to neurons and glial cells upon cellular differentiation (Wiese *et al.* 2004; Mahler and Driever 2007). The subependymal zone of the lateral ventricle and the subgranular zone of the dentate gyrus in the hippocampus are the only two distinct proliferative areas in the adult mammalian brain that give rise to new neurons (Alvarez-Buylla and Garcia-Verdugo 2002; Taupin and Gage 2002; Goldman 2003; Garcia *et al.* 2004; Merkle *et al.* 2004; Doetsh and Hen 2005; Lledo and Saghatelyan 2005). On the other hand, teleost fish have numerous neurogenic

areas especially in the forebrain and these areas are dense with progenitor and stem cells. More specifically, the telencephalon has a remarkable neurogenetic capacity especially near the ventral and dorsal telencephalic areas (Mahler and Driever 2007; März *et al.* 2010). The proliferative areas are identified as the ventricular zones of the telencephalon, the diencephalon, the midbrain-hindbrain boundary, and the ciliary marginal zone of the retina in teleosts (Michalczyk and Ziman 2005).

Several studies have explored the various roles of the nestin protein. One study reported that nestin can affect the efficiency of a cell to move particles (e.g., vesicles) intracellularly, thereby providing structural and functional support during cellular proliferation (Michalczyk and Ziman 2005; Chen *et al.* 2010; Carmona *et al.* 2011). Nestin can also control the localization and partitioning of IFs within the cytoskeleton, thereby affecting the distribution of cellular components during mitosis (Michalczyk and Ziman 2005; Chen *et al.* 2010). This suggests that nestin plays a role in reorganizing cytoskeletal filaments, thus controlling cellular dynamics by regulating the polymerization of various IFs (Mahler and Driever 2007). Although many functional properties of nestin protein have been proposed, its mechanism of action at the molecular level still remains unclear.

Data to date suggest that the nestin protein contains a short amino terminal and a long carboxyl end and is fairly well conserved among species such as chicken, mouse, rat, zebrafish, frog and human (Mahler and Driever 2007; Chen *et al.* 2010). Severe developmental malformations such as morphological abnormalities are visible in zebrafish morphants that are injected with a nestin morpholino (Chen *et al.* 2010). These abnormalities included decreased body and head growth, small eyes, underdeveloped

retinal lens, brain defects, and developmental defects of motor neurons, axons, and glial cells in the brain (Chen *et al.* 2010). These morphants also exhibited decreased proliferative cell niches in the developing nervous system resulting in fewer progenitor cells possibly caused by cellular apoptosis and death (Chen *et al.* 2010). All of these observations suggest that nestin is involved in the mechanism controlling neurokinetic capacity and regenerative cellular processes.

Characterization of the nestin protein in teleosts could provide a better understanding of the mechanisms underlying brain plasticity. Herein we investigate the nestin protein in the goldfish brain and describe the generation of the first fish-specific nestin antibody, a new tool to study teleost neurogenesis. The characterization of 3 novel nestin isoforms in the goldfish could also provide insight into neurogenic capabilities in other vertebrates.

2.2. Materials and methods

2.2.1. Animal maintenance

Adult female goldfish (*Carassius auratus*) were purchased from a commercial supplier (Mt. Parnell Fisheries Inc., Mercersburg, PA, USA) and maintained at 18˚C under a natural-simulated photoperiod on standard flaked goldfish food. Fish were kept in 70L tanks (15-18 fish/tank). All procedures were performed according to the guidelines of the Canadian Council on Animal Care and were approved by the University of Ottawa animal care committee. Goldfish were anesthetized using 3-aminobenzoic acid ethylester (MS-222; 0.05% in water, Sigma Chemicals) for all handling and sampling procedures.

2.2.2. Rapid amplification of cDNA ends-polymerase chain reaction (RACE-PCR)

Five female goldfish brain was dissected and frozen on dry ice immediately and stored at -80°C. Total RNA was isolated using RNeasy mini kit (Qiagen, Toronto, Canada, 74134). The GeneRacer™ Kit (Invitrogen, Burlington, Canada, L150201) was used to obtain the 5'- and 3'-ends of goldfish *nestin (nes)* cDNA following the manufacturer's instructions. To obtain the 5'-mRNA end of goldfish *nes,* the mRNA was initially dephosphorylated and then the mRNA cap structure was removed and replaced with GeneRacer™ RNA Oligo using RNA ligase. Reverse transcription was performed on the mRNA using Thermo Scientific Maxima First Strand cDNA Synthesis Kit (Invitrogen, Burlington, Canada, K1642). The cDNA was used to amplify both 3' and 5' RACE-PCR using the GeneRacer™ Primer specific to the GeneRacer™ RNA Oligo sequence and gene-specific primers (Table 2.1). The gene-specific primers were designed using Primer3 Software (http://bioinfo.ut.ee/primer3-0.4.0/) based on the partial goldfish *nes* cDNA sequence (GenBank FJ855222.1). Goldfish *nes* cDNA was cloned using a nested and external PCR approach with a Platinum Taq DNA Polymerase High Fidelity enzyme (Invitrogen, Burlington, Canada). The PCR cycling parameter consisted of 2 min at 94˚C; 5 cycles of 30 sec at 94˚C and 1 min at 72˚C; 5 cycles of 30 sec at 94˚C and 1 min at 70˚C; 25 cycles of 30 sec at 94˚C, 30 sec at 65˚C and 1min at 68˚C and a final extension of 10 min at 68˚C. PCR products were cloned into either pCR4-TOPO vector (Invitrogen, Burlington, Canada) or pGEM-T Easy Vector (Promega, WI, USA) and at least 3 different clones were sequenced using Applied Biosystems 3730 DNA Analyzer at the Ottawa Health Research Institute. Based on the obtained sequence for goldfish *nestin A (nesa)* transcript (GenBank KT373807), a second round of RACE-PCR was performed

to obtain the complete 3'-end of goldfish *nesa* transcript using new gene-specific primers (Table 2.2). Procedures were performed as explained above.

2.2.3. Production of rabbit anti-goldfish nestin antiserum

A polyclonal antibody against goldfish nestin was generated using a multiple antigenic peptide (MAP) strategy (Basak *et al.* 1995). The peptide used was composed of 23 amino acids VVSIQRQKAKNAQAEAQRKLMES, located at the N-terminal of goldfish nestin (GenBank FJ855222.1). This peptide sequence was selected based on secondary structure, antigenicity and hydrophilicity analyses using the proteomics tools in the Expasy website (www.expasy.ch). The peptide was synthesized on a 4-branched lysine MAP core to form the immunogenic peptide nestin23-MAP (MW 10,456 g/mol). A total of 6 rabbits were used to generate the anti-nestin antibody. Nestin23-MAP (1 mg) was suspended by vortexing in 0.2 ml of pure glacial acetic acid (ACROS) and then 0.8 ml of sterile distilled water was added to the solution. The solution was further mixed with ~2.2 ml Freund's complete adjuvant for the first injection into rabbits. For all subsequent injections ~2.2 ml of Freund's incomplete adjuvant was used. The injections were administered at the interval of every 4 weeks with 2 intramuscular injections of 0.25 ml and 5 subcutaneous injections of 0.2 ml for a total injection volume of 1.5 ml per rabbit. Blood sample (~1.5 ml) was collected every 14 days following injections until the final bleed at 4 months post the initial injection. Preliminary serum analysis by dot and western blotting indicated that rabbit 9 had the highest titer and this anti-serum was used in all subsequent experiments.

2.2.4. Protein extraction and SDS-PAGE

Brain tissues and pituitaries of sexually regressed female goldfish (26 g ± 7g body weight; 1.8±0.5, gonadosomatic index) were obtained in June – August for protein extraction and western blotting. The tissues were dissected and immediately frozen in dry ice and stored at -80°C until analysis. A photograph showing the various goldfish brain regions is presented in Supplementary Figure 2.1. Tissues were homogenized in various volumes of homogenizing buffer (HEPES, pH 7.5; NaCl, 150 mM; EDTA, 1mM; NaF, 1 mM; $NaVO_3$, 0.1 mM; ß-glycerophosphate, 10mM). The soluble proteins in the homogenate were separated from the pellet by centrifugation (12,000 rpm; 12 min; 4˚C). Protein samples each containing 20µg were prepared for SDS-PAGE analysis by adding 3x reducing sample buffer (0.15M Tris-HCl, pH 6.8; 24% v/v glycerol; 4.8% SDS; and 0.06% bromophenol blue) and 2-mercaptoethanol. The protein samples were boiled for 15 min at 65˚C and subsequently chilled on ice for 2 min before loading them into each lane of a 10% SDS-polyacrylamide gel. Following electrophoresis protein band separation, the gel was transferred to an Immobilon-P transfer membrane (Millipore, Toronto, Canada) using the semi-dry transfer cell (Bio-Rad, Mississauga, Canada) at 20V for ~70 min.

2.2.5. Western blot analysis

Western blot analysis was used to determine the specificity of the rabbit anti-nestin goldfish antibody. The nestin antibody (1:500) was pre-absorbed overnight at 4˚C with 1µM nestin23-MAP or nestin23 linear peptide. The antibody was diluted in a blocking buffer (1x TBS; 0.3% Tris-Base, 0.8% NaCl; 0.02% KCl, pH 8; 1% fat-free

milk powder, and 0.05% v/v Tween 20). The membranes with the protein samples were incubated in blocking buffer for 1hr at room temperature, and then exposed to anti-nestin antibody at 1:500 or purified mouse anti-ß-actin monoclonal antibody (Cedarlane, Burlington, Canada, CLT9001; 4µg/ml) or rabbit anti-actin antibody (Sigma, Oakville, Canada, A2066, 1:1200) diluted in blocking buffer overnight at 4˚C. The next day, the membrane was washed in a series of washes of 1xTBS-T (1xTBS with 0.05% v/v Tween 20) and 1xTBS. The protein standard ladder (Precision plus protein western C standards 161-0385, Bio-Rad, Mississauga, Canada) on the membrane was separated from the remaining protein samples. The ladder was incubated with precision protein StrepTactin-HRP conjugate (Bio-Rad, Mississauga, Canada, 161-0376) diluted in blocking buffer at room temperature for 1.5 hrs. The membrane with the protein samples was incubated in the secondary antibody ECL peroxidase labelled anti-rabbit antibody (GE Healthcare, Mississauga, Canada, NA934, 1:50000) diluted in blocking buffer for 1.5 hrs. The protein bands and the ladder on the membrane were detected using an ECL Prime Western Blotting Detection Reagent kit (GE Healthcare, Mississauga, Canada, RPN2232) as recommended by the manufacturer. The chemiluminescent signals on the membranes were detected with the Fusion FX5 detector system (MBI Lab equipment, Montreal, Canada) or with the ChemiDoc^{TM} XRS+ molecular imager system (Bio-Rad, Mississauga, Canada) and quantified using the ImageJ1.43I software (Rasband 1997-2014). Exposure times ranged from 1s to 5 min depending on signal intensity.

2.2.6. Mass Spectrometry

Female goldfish brain protein extract (40 µg) was loaded on a 10% SDS-polyacrylamide gel and separated by electrophoresis. The different protein bands were

revealed in the gel after Coomassie blue staining. The protein bands at molecular weights ~30, 40 and 70 kDa (Fig. 2.1) were excised from the gel. Aqueous NH_4HCO_3 (100 µl; 25 mM) was added to each gel band in order to allow it to swell and then digested with the enzyme trypsin (10 µl, 0.1µg/ml) overnight at 37˚C. The following day, 100 µl of 50% ACN/NH_4HCO_3/5%HOAC was added, then the sample was vortexed (~3-5 min) and centrifuged (Eppendorff, 10 000 r.p.m., 15 min), and the supernatant collected. The residual gel was extracted 3 additional times in a similar manner and all supernatants containing the soluble proteins were combined and completely evaporated overnight in a lyophilizer. The residue thus obtained was re-dissolved in 10 µl of 25 mM NH_4HCO_3/50%ACN and then spotted (2x2 ml) on re-usuable gold plates and mass spectra determined using a Surface-Enhanced Laser Desorption Ionization Time of Flight (SELDI-TOF) instrument (Protein Chips, Ciphergen Biosystems Inc., Fremont, Ca, USA). The material was allowed to dry at room temperature and another 2 µl of energy absorbing matrix solution (CHCA) was added. The CHCA (α-cyano-4-hydroxycinnamic acid, Fluka, 28480) solution was prepared by dissolving 10 mg of the material in a mixture of 500 µl of 0.1% TFA/water and 500 µl of acetonitrile (ACN). The mass spectral results were analyzed using the Ciphergen Protein Chip software v3.2.0.

2.2.7. Statistical analysis of western blot immunoreactivity signals

Canonical discriminant analysis and principal component analysis (PCA) were used as dimension-reduction techniques because western blot analysis determined that nestin expression is complex. The 3 major immunoreactive bands (~30, 40 and 70 kDa; Fig. 2.1) varied in presence and intensity in a tissue-dependent manner and were considered for further analysis. Canonical discriminant analysis for the different nestin

proteins obtained from female goldfish (n=10) was performed using the PROC DISCRIM and PROC CANDISC modules in SAS (Statistical Analysis System, v9.4, Cary, NC, USA) software. A scree plot outlining a principal component factor analysis of protein expression obtained from the western blots was performed to reveal the components providing the most variance observed in the data set. The SAS software was also used for PCA, which provided a series 2D score plots where the two principal components that encompass the most variance within the data set are shown as the x- and y-axes. The 2D plot provides a visual overview of all of the samples and their potential groupings. Following the visualization of grouped samples in the PCA, a 3D plot was created using NTSYS-pc (Rohlf 2009). Thus, three principal components for the nestin protein expression provided a better visual representation of all the samples and their potential groupings. The 3D plot also identifies the discriminating factors between the female goldfish group in terms of nestin protein expression. The PCA was used to compare each isoform across tissues and to identify the patterns of isoform expression in the various brain regions and whole pituitary.

2.2.8. Phylogenetic analysis

Phylogenetic analysis of nestin was conducted using MEGA5 (Tamura *et al.* 2011). Human vimentin was used as the outgroup in the phylogenetic tree and evolutionary history was inferred using the Neighbor-Joining Method with a bootstrap consensus of 1000 replicates to represent the evolutionary history of the taxa analyzed (Felsenstein 1985; Saitou and Nei 1987). The branches that correspond to partitions reproduced in less than 80% bootstrap replicates were collapsed. The evolutionary distances were computed using the Poisson correction method (Zuckerkandl and Payling

1965) and are in the units of the number of amino acid substitutions. A total of 73 amino acid sequences were used in the analysis and all were obtained from Ensembl with the exception of *Carassius auratus* transcript A, B, and C. All ambiguous positions were removed for each sequence pair and a total of 2886 positions were present in the final dataset.

2.3. Results

2.3.1. Isolation and characterization of goldfish nes mRNAs

We utilized RACE-PCR to isolate goldfish *nes* mRNAs in goldfish brain. The results showed the presence of two different 5'-UTR ends where both contained the same initiation codon but one had a deletion of 320 nucleotides (Supplementary Figure 2.2). Two different 3'-UTR ends were also evident. Three different bands were detected suggesting the presence of three different goldfish *nes* transcripts. The bands were fully sequenced resulting in 4003, 2446 and 2126 nucleotides. The goldfish *nes* mRNA sequences a, b, and c were submitted to GenBank and have the following accession numbers KT373807, KT373808 and KT373809, respectively. These three mRNAs are predicted to encode for 860, 274 and 344 amino acids, respectively (Fig. 2.2).

2.3.2. Anti-nestin antiserum specificity

Identification of three different mRNA sequences and subsequent protein predictions suggested the presence of multiple nestin isoforms (Fig. 2.2B). As a result, we used a multi-antigenic peptide (MAP) strategy to generate a goldfish-specific nestin antibody. Western blot analysis was performed to assess the specificity of the antibody by pre-incubating the nestin antiserum with nestin23-MAP peptide (Fig. 2.1). Western blot

analysis of proteins extracted from sexually mature female goldfish telencephalon tissue revealed the presence of three major protein bands of ~30, 40 and 70 kDa (Fig. 2.1). On the other hand, there were no bands detected when the antiserum was pre-absorbed with nestin23-MAP peptide (Fig. 2.1) or with nestin-23 linear peptide (not shown).

2.3.3. Characterization of nestin-positive immunoreactive protein bands by mass spectrum analysis

Nestin-immunopositive bands in western blot were analysed using mass spectrometry of their enzyme (trypsin) digests. The representative mass spectrum of one typical trypsin (unit of activity 0.164 nmol/hr/µl) digest is shown in Fig. 2.3. To determine the identity of each protein band, we compared the observed molecular weights of all fragments with those of calculated values based on the predicted amino acid sequence of the nestins we cloned (GenBank accession no. KT373807, KT373808 and KT373809). The calculated theoretical molecular weights of nestin fragments following trypsin digestion were obtained from the peptide cutter tool in Expasy website (http://web.expasy.org/peptide_cutter/). This western blot and mass spectral data suggest the existence of 3 isoforms of nestin protein in goldfish brain. The amino acid sequences obtained for all 3 bands from the mass spectral data correspond to the predicted amino acid sequences of goldfish nestin isoform A, B and C (Fig. 2.1). Importantly, all protein sequences obtained from the mass spectrum analysis contain the 23-amino acid peptide epitope used to generate the goldfish anti-nestin antibody, further supporting high antibody specificity.

Based on comparison of observed mass spectra of trypsin digests of the 30 kDa protein band with the theoretical values, there is a 67% identity match of this protein as nestin. In a similar manner the 40 kDa band exhibited an identity match of 63% with nestin protein. The 70 kDa protein band showed a much higher identity match of 72% as a nestin protein. Therefore, all bands on the western blot correspond to either one of the three goldfish nestin isoforms (Fig. 2.1). Based on the mass spectral analysis, the observed 30 kDa band corresponds to goldfish nestin isoform B with a calculated molecular weight (MW) of 27.08 kDa and an amino acid length of 229. The 40 kDa band likely corresponds to goldfish nestin isoform C with a calculated MW of 36.21 kDa with a length of 306 amino acids. The 70 kDa band likely corresponds to goldfish nestin isoform A with a calculated MW of 74.29 kDa with a length of 656 amino acids.

2.3.4. Distribution of nestin proteins in female goldfish brain and pituitary

The expression of nestin in pituitary, hypothalamus, telencephalon, optic tectum, midbrain, cerebellum, vagal lobe, and brainstem was qualitatively analyzed by western blotting (Fig. 2.4). Based on 10 different western blots of brain tissues and pituitaries, the major nestin protein bands appear at different frequencies (Table 2.3). The ~40 kDa band is clearly evident in all goldfish brain tissues and pituitary, and has the highest signal intensity in comparison to the other bands. The ~70 kDa band is present in all tissues except for the hypothalamus. However, the 70 kDa band appears at a lower frequency in the telencephalon and the midbrain compared to the other tissues based on 10 female goldfish western blots. There is also another nestin immunoreactive protein band of ~75 kDa evident in the female goldfish brain and pituitary western blot. Although this protein band is absent from the pre-absorption western blot, it is likely that the ~70 kDa and ~75

kDa bands represent the same sequence with one having a post-translational modification. The 75 kDa band was only evident after longer exposures and at a lower frequency. The ~75 kDa band is present in all the tissues except for the hypothalamus and the telencephalon. The ~30 kDa band is present in all the brain tissues and pituitary; this band is very faint and only appears at higher exposure times compared to the other bands. Although it is present in all the brain tissues and pituitary, it appears at a lower frequency in the pituitary, hypothalamus, telencephalon and brain stem in comparison to the other tissues.

The scree plot (Fig. 2.5A) reveals that the first three components provide the greatest variability in the nestin protein expression data set as the line straightens after the third principle component. The 2D plot (Fig. 2.5B) obtained from PCA illustrates that the telencephalon is projected on the positive side of both the x- and y-axes. The eigenvectors of the telencephalon also point in a different principal direction in comparison to the other groupings. The telencephalon corresponds to the greatest positive direction on axis 2 having the most positive variation in comparison to the other data points. The plot illustrates that the data set is best classified based on the expression pattern of nestin in the different tissues in the goldfish brain. The hypothalamus and brainstem also contribute in the positive area, but very close to axis 1, whereas pituitary, cerebellum, optic tectum, midbrain and vagal lobe contribute in the negative area of axis 2, but remain very close in proximity to axis 1.

The 3D plot (Fig. 2.6) considers the first three principal components for the nestin expression pattern in female goldfish. As seen in Fig. 2.5B, the telencephalon has the greatest variance in comparison to the other data points and provides further validity of

the results obtained from the 2D plot. In comparison to the 2D plot, the pituitary is observed on axis 3 followed by optic tectum and hypothalamus contributing to the positive areas; followed by the midbrain, cerebellum, vagal lobe and brainstem on the negative side of axes 2 and 3. In other words, pituitary and telencephalon are pulling in opposite directions mainly on axes 2 and 1 (both Fig. 2.5B and 2.6); and the two against the rest of the eight variables. The midbrain, cerebellum and vagal lobe are also high on axis 3 and 1 whereas the brainstem is highest on axis 1 and lowest on axis 3.

2.3.5. Nestin protein is conserved in vertebrates

Sequence comparison of three goldfish nestin isoforms shows that they share overall highly similar sequences, while they display a small difference at the C-terminal short region. For example, compared to isoform A, isoform B has 3 unique residues at C-terminus and isoform C has 31 unique residues (Supplementary Figure 2.3). The high identity is also observed in the *nestin* mRNA a, b and c sequences. The observation that the beginning of the sequence for both mRNA and protein are identical suggests that these three isoforms are products of the same *nes* gene, but they are generated by a common mechanism of alternative splicing.

Goldfish nestin A is very similar to nestin proteins in zebrafish and other fish. Multiple amino-acid alignments of goldfish nestin isoform A, B and C against 73 other vertebrate nestin protein sequences illustrates evolutionary conservation (Supplementary Figure 2.4). Goldfish nestin A has 70% sequence identity with zebrafish (*Danio rerio*); 46% with medaka (*Oryzias latipes*); and 45% with princess cichlid (*Neolamprologus brichardi*). Goldfish nestin A has a 35% ± 5% average identity with all other vertebrate

species (BLASTP 2.2.29+, NCBI). Goldfish nestin B has 84% sequence identity with zebrafish; 57% with Mexican tetra (*Astyanax mexicanus*); and 53% with Atlantic herring (*Clupea harengus*). Goldfish nestin B has a 41% ± 9% average identity with all other vertebrate species (BLASTP 2.2.29+, NCBI). Goldfish nestin C has 85% sequence identify (*Danio rerio*); 58% (*Astyanax mexicanus*); and 54% (*Clupea harengus*) and has an average of 43% identity ± 9% with all other vertebrate species (BLASTP 2.2.29+, NCBI).

In mammals, nestin protein is predicted to be approximately 174-210 kilodalton (kDa) in molecular weight and can be detected using mammalian nestin antibodies (BLASTP 2.2.29+, NCBI; http://web.expasy.org/translate/). In teleosts, the predicted molecular weights of the nestin protein varies among species from 140 kDa in the Southern platyfish (*Xiphophorus maculatus);* 143 kDa in the zebrafish (*Danio rerio*) to 185 kDa in the Spotted gar (*Lepisosteus oculatus)* measured using the proteomics tools for protein translation in the Expasy website (http://web.expasy.org/translate/) (Cunningham *et al.* 2015). Although other teleost nestin isoforms have not yet been identified, we identified mammalian nestin isoforms in the prairie vole, squirrel, mouse, rat, pig, buffalo, chimpanzee and human (BLASTP 2.2.29+, NCBI). All of the nestin protein sequences and molecular weights in both mammals and teleosts are predictions only, and were obtained based on extensive database searches of nestin mRNA sequences via NCBI and Ensembl websites. More specifically, the predicted nestin protein sequences were obtained using a protein translation tool and protein molecular weights were measured using proteomics tools in the Expasy website (http://web.expasy.org/translate/).

An analysis of conserved domain using the pfam domain database (Finn *et al.* 2014) revealed that the first 322 amino acids of the goldfish nestin isoform A, the first 271 amino acids of the goldfish nestin B and the first 315 amino acids of the goldfish nestin C contain the conserved intermediate filament module (pfam00038) (Marchler-Bauer and Bryant 2015).

2.3.6. Predicted structure of the goldfish nes gene

We further examined the genomic structures of *nes* homologs in other species where the information was available and we found all *nes* genes share a four exon genomic structure (Fig. 2.2A). Using zebrafish and human *nes* genomic structures as the reference, we propose a likely genomic structure for the goldfish *nes* gene. This analysis reveals that the long length of *nes* isoform A (compared to typical intermediate filaments) is likely due to the extended transcription of the 4th exon (Fig. 2.2B). By contrast, the isoform B is probably derived from exon 1whereas the isoform C is derived from the fusion of exon 1 and exon 2.

Specifically, the goldfish *nesa* mRNA is 4003 base pairs (bp) in length and includes 149 bp of 5' untranslated region (UTR), the transcription start site, and a 2580 bp open reading frame giving rise to a predicted protein sequence of 860 amino acids in length. A poly-A signal, AATAAA, was found in the 3'end of the nucleotide sequence. Based on the zebrafish *nestin* mRNA sequence, we predict that goldfish *nesa* mRNA is likely composed of 4 different exons of 813 bp, 125 bp, 74 bp, and 1568 bp in length. The predicted transcription start site is 82 bp downstream of the predicted TATA box motif. The goldfish *nesb* mRNA is 2446 bp in length and includes 149 bp of 5' UTR, the

transcription start site, and 822 bp open reading frame giving rise to a predicted protein sequence of 274 amino acids in length. The poly-A signal AATAAA, was identified in the 3'end of the nucleotide sequence. Similarly, based on the zebrafish *nes* mRNA sequence, we predict that goldfish *nesb* mRNA is composed of exon 1 containing 822 bp in length. The transcription start site is 82 bp downstream of the TATA box predicted motif. The goldfish *nesc* mRNA is 2126 bp in length and includes 149 bp of 5' UTR, the transcription start site, and a 1032 bp open reading frame giving rise to a protein sequence of 344 amino acids in length. The poly-A signal AATAAA, was identified in the 3'end of the nucleotide sequence. Based on the zebrafish *nes* mRNA sequence, we predict that goldfish *nesc* mRNA is composed of two exons of 813 and 219 bp in length. The transcription start site is 82 bp downstream of the predicted TATA box motif.

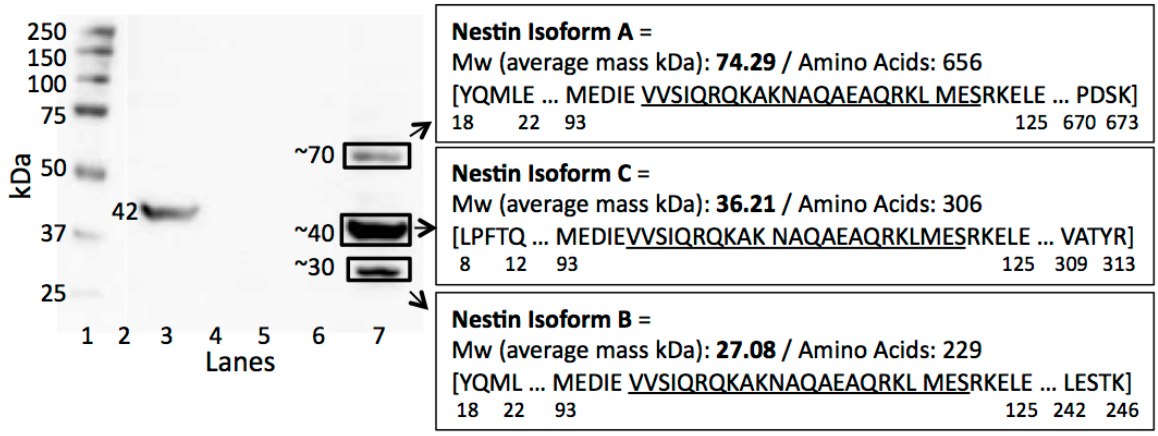

Figure 2.1. Western blot analysis of female goldfish brain extracts using anti-nestin rabbit antibody. Lane 1 represents the standard ladder and lane 3 is a positive control and illustrates the actin protein size at 42 kDa. Lane 5 is a negative control where the anti-nestin antibody was pre-absorbed overnight with the goldfish nestin23-MAP prior to using the solution as the primary antibody in the western blot. The antigen preabsorption experiment confirms the specificity of the rabbit anti-goldfish nestin antibody. Lane 7 represents the nestin precursor protein processed into 3 smaller fragments of ~30, 40 and 70 kDa. Using mass spectrometry and RACE-PCR analysis, the bands have been identified as either nestin isoform A, B, or C. The underlined protein sequence represents the epitope of the anti-nestin antibody generated using the MAP strategy. The numbers under the protein sequence denotes the position of the amino acids within the predicted nestin isoform protein sequence A, B and C.

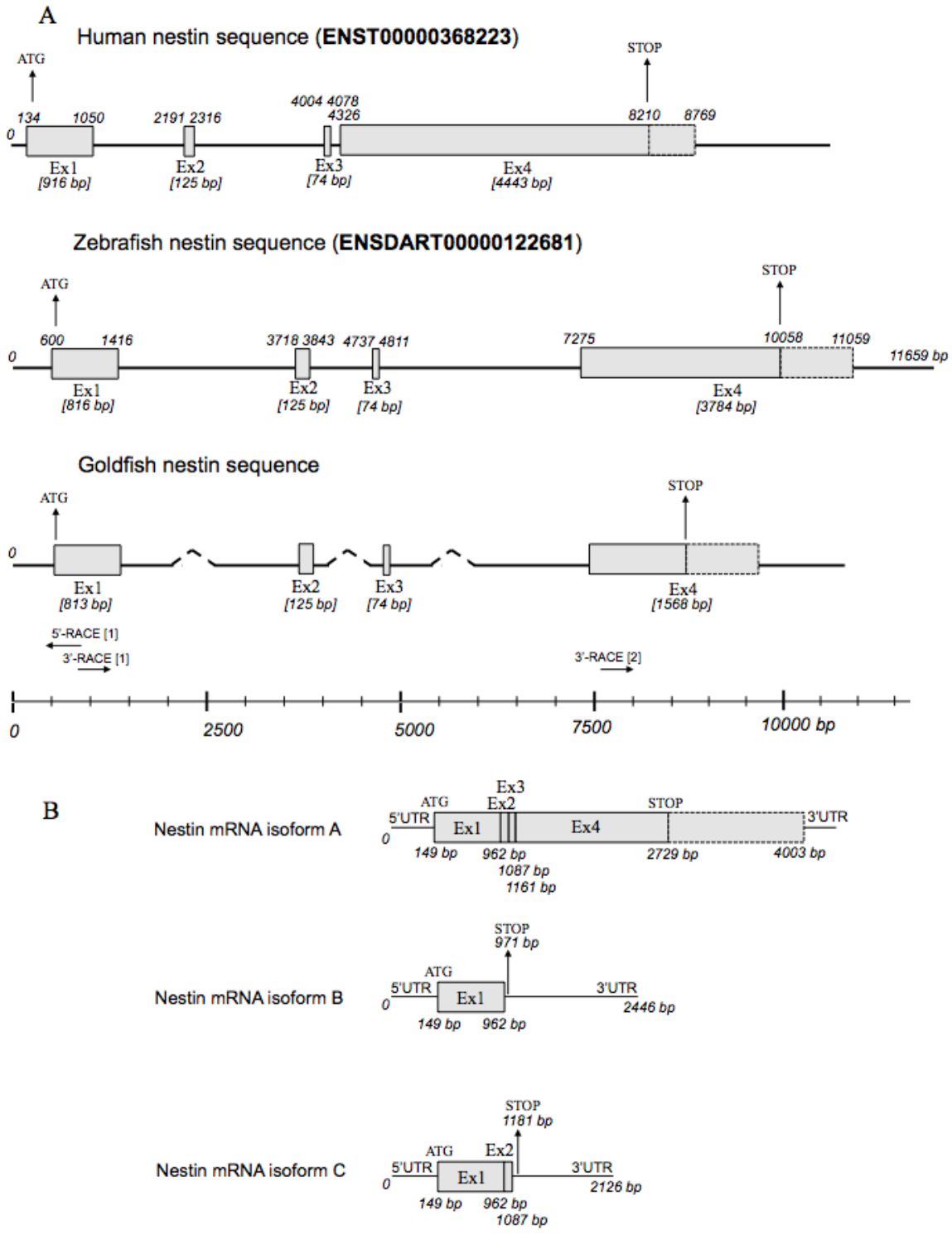

Figure 2.2. A) Schematic diagram representing the human, zebrafish and goldfish *nes* gene organization. Base pair numbers are indicated in italics and exons by grey boxes. B) Schematic diagram representing the 3 different *nes* transcripts identified in the goldfish brain using RACE-PCR.

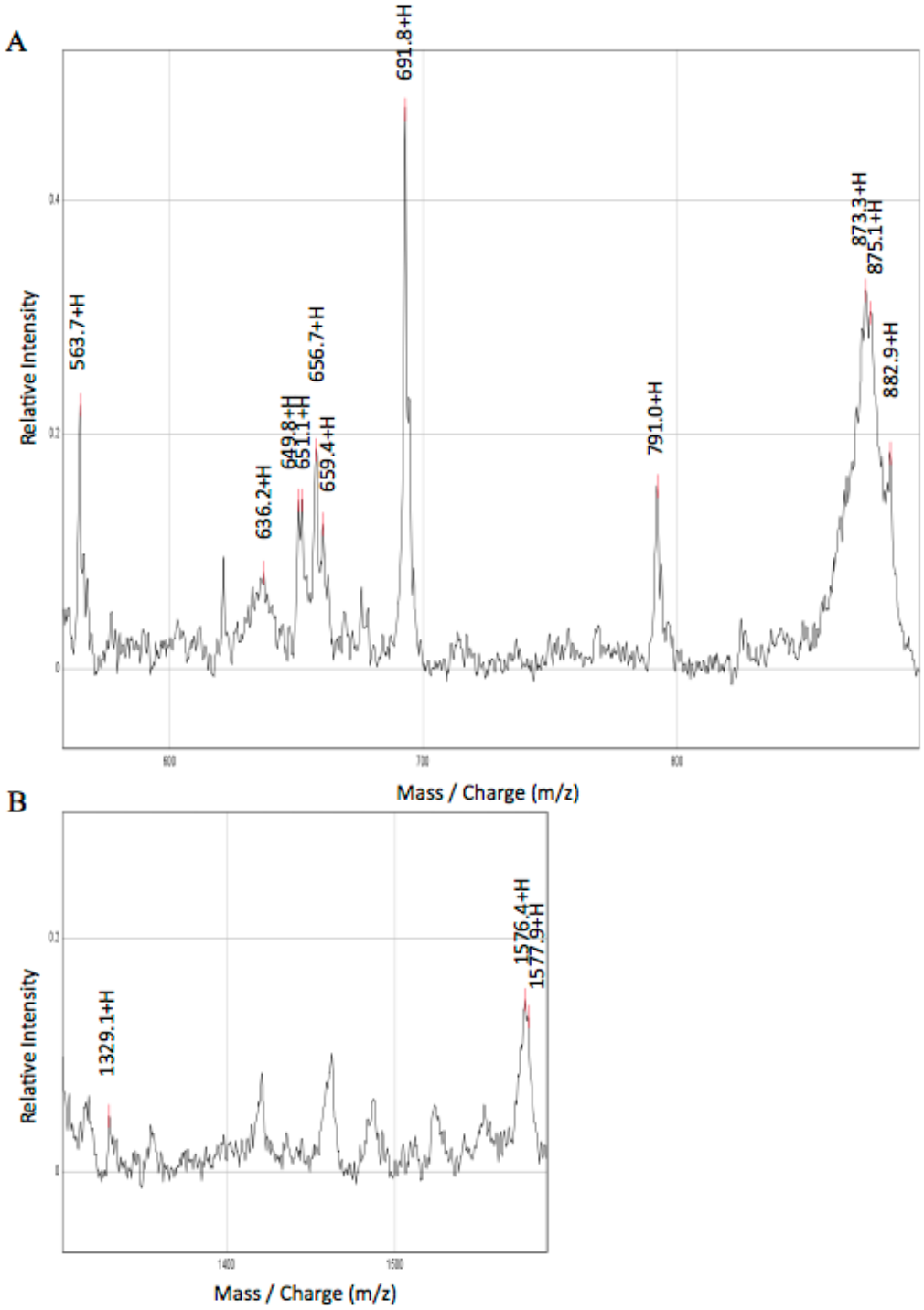

Figure 2.3. The SELDI-tof mass spectrum of one representative sample of trypsin digest of a Coomassie stained protein band at ~70 kDa in 10% SDS-PAGE. The observed m/z values of various peaks as labelled in the figure are in good agreement with the corresponding calculated values derived from the sequence obtained in this study of nestin isoform A (GenBank KT373807) upon trypsin digestion. The multiple groups of peaks in close proximity at m/z 649.8 and 651.1; 656.7 and 659.4; 873.3 and 875.1 (Figure 2.3A) as well as 1576.4 and 1577.9 (Figure 2.3B) represent isotopic forms of the same fragment peak. Please note that Figures 2.3A and 2.3B are the expanded sections of interest from the complete mass spectrum of the crude digest.

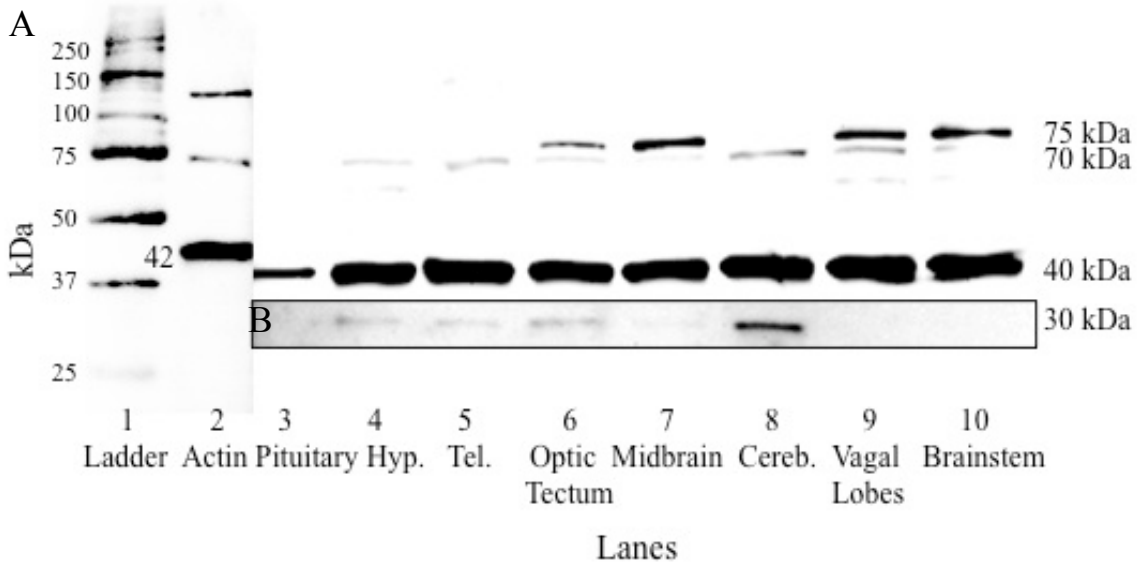

Figure 2.4. Western blot analysis of nestin protein distribution patterns in the goldfish female brain and pituitary. Lane 1 is the standard ladder, lane 2 is the positive control of ß-actin at 42 kDa, lane 3 is goldfish pituitary, lane 4 is hypothalamus, lane 5 is telencephalon, lane 6 is optic tectum, lane 7 is midbrain, lane 8 cerebellum, lane 9 is vagal lobes, and lane 10 is brainstem. The insert B illustrates the 30 kDa band at a longer exposure time (5 min) in comparison to western blot A (1 min).

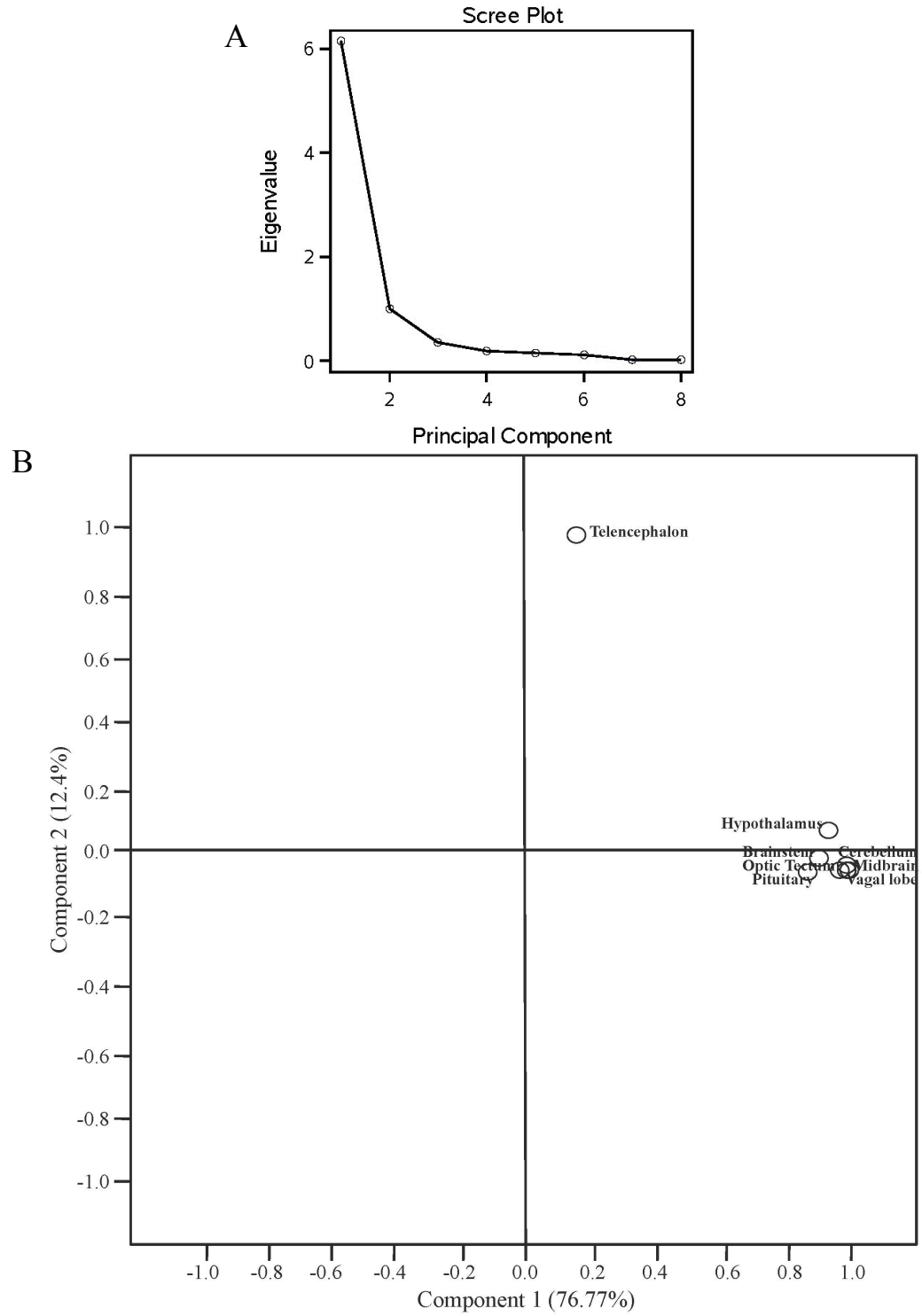

Figure 2.5. A**)** A principal component analysis of nestin protein expression obtained from western blots of female goldfish (n=10) displayed as a scree plot. The scree plot shows that the first three principal components best describe the variation within the data as the line straightens after component 3. The remaining components explain a very small proportion of the variance of nestin protein expression. B**)** Canonical analysis of nestin protein expression data obtained from western blots separating the variables pituitary, hypothalamus, telencephalon, optic tectum, midbrain, cerebellum, vagal lobe and brain stem of female goldfish (n=10) on a 2D plot. Variation explained as percent in brackets.

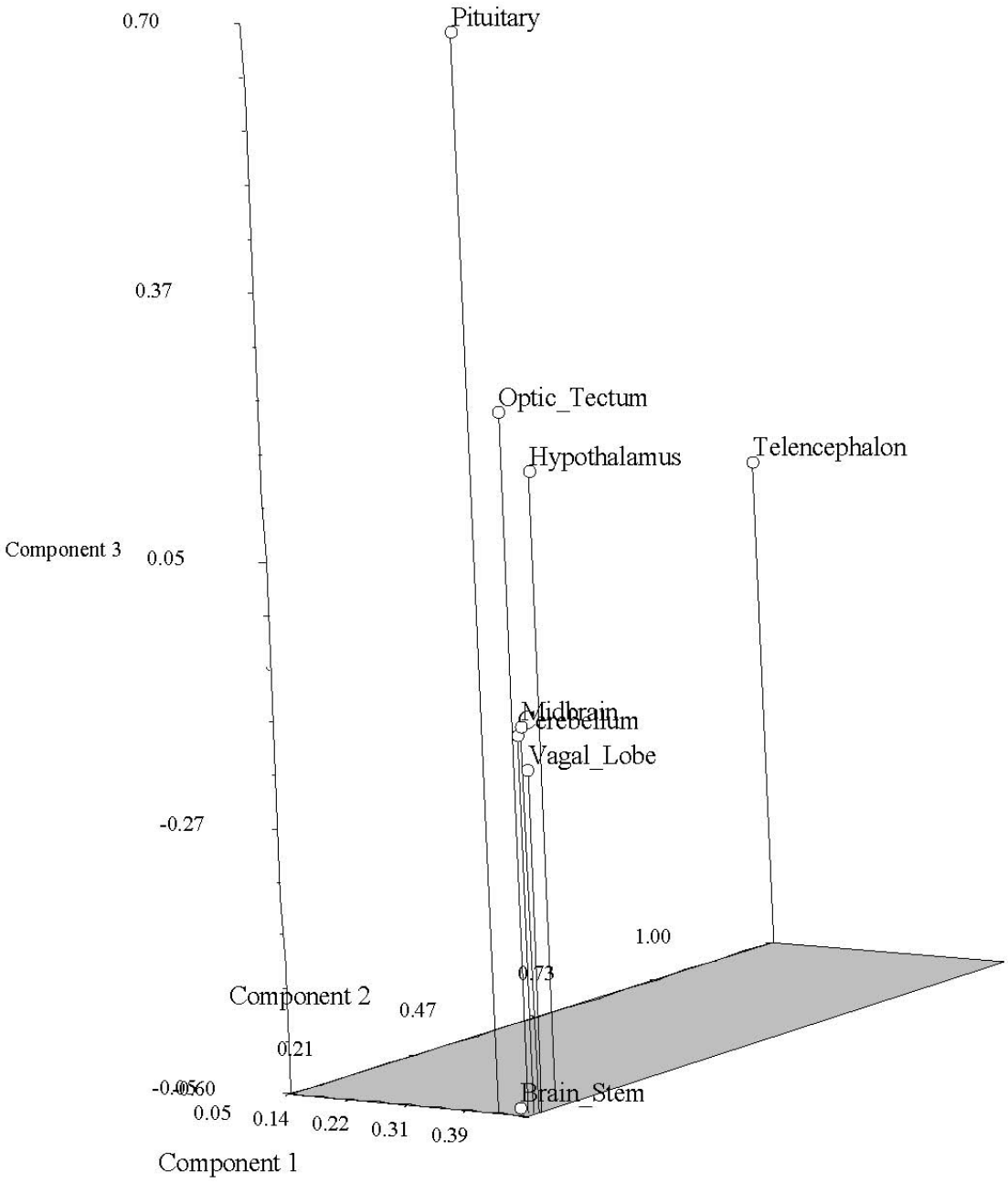

Figure 2.6. Three-dimensional score plot of the first three principal components for the nestin protein expression in the female goldfish group (n=10) separating the factors pituitary, hypothalamus, telencephalon, optic tectum, midbrain, cerebellum, vagal lobe and brain stem. Variance of component 1 explained is 76.77%; component 2 is 12.4% and component 3 is 4.43%.

Table 2.1. Primers used for RACE-PCR (Fw, forward; Rv, reverse; gf, goldfish).

Primer Name	Primer Sequence (5'->3')
GeneRacer™ 5' Primer Fw	GGACTGGAGCACGAGGACACTGA
5'_gfnestin_RACE1 Fw	AAGGACAGCCTGGGGCAGCAGATAGA
GeneRacer™ 5' Primer nested Fw	GGACACTGACATGGACTGAAGGAGTA
5'_gfnestin_RACE1 nested Fw	CAAGATGTCCCTGGGCCTGGAAGTG
GeneRacer™ 3' Primer Rv	GCTGTCAACGATACGCTACGTAACG
3'_gfnestin_RACE1 Rv	CTTCCTCCAGGCCTCCTCCAGCATC
GeneRacer™ 3' Primer nested Rv	CGCTACGTAACGGCATGACAGTG
3'_gfnestin_RACE1 nested Rv	CCTGCTGGTTCCCTGCTGCTCTTG
3'_gfnestin_RACE2 Fw	GGGAAGGATGAGGACACTGA
3'_gfnestin_RACE2 nested Fw	AAATGGCTCGGATTTCACAC

Table 2.2. Gene-specific primers used for second round of RACE-PCR to obtain goldfish *nes* transcript A (Fw, forward; gf, goldfish).

Primer Name	Primer Sequence (5'->3')
3'_gfnestin_GSP_RACE2 Fw	GGGAAGGATGAGGACACTGA
3'_gfnestin_GSP_RACE2 nested Fw	AAATGGCTCGGATTTCACAC

Table 2.3. Nestin protein band frequency in the different brain tissues and pituitaries based on 10 female goldfish western blots (n=10)

Nestin protein band	Pit.	Hyp.	Tel.	Optic tectum	Mid.	Cereb.	Vagal lobe	Brainst.
75 kDa	3	0	0	2	3	3	4	4
70 kDa	6	0	1	4	1	3	5	3
40 kDa	10	10	10	10	10	10	10	10
30 kDa	1	3	2	6	6	8	6	2

Pit: pituitary; Hyp: hypothalamus; Tel: telencephalon; Mid: midbrain; Cereb; cerebellum; Brainst: brainstem

2.4. Discussion

This study reports for the first time the presence of multiple nestin isoforms in a teleost fish. The 3 *nes* mRNAs identified in the goldfish were named *nesa, nesb* and *nesc* transcripts. The sequencing of each transcript resulted in 4003, 2446 and 2126 nucleotides encoding for 860, 274 and 344 amino acid predicted sequence, respectively. The identification of three different novel isoforms for nestin in goldfish could be the key to understanding brain plasticity and maintenance of proliferative cellular pools in teleosts as there could be interplay between the nestin isoforms to give rise to innate neurogenic abilities.

The zebrafish genomic structure was used as a reference to construct a putative genomic structure of goldfish *nes* as they are closely related species from the family Cyprinidae. Both species have undergone a teleost-specific whole-genome duplication event at the base of the teleost lineage (Glasauer and Neuhauss 2014). Although different *nes* transcripts or proteins have not previously been identified in teleosts, the generation of the first fish-specific nestin antibody reported here could reveal the existence of various isoforms in other species. Further evidence for the existence of different nestin isoforms stems from the evolutionary and genomic similarities between teleost species. For example, we determined that the four coding exons of *nesa* are similar to the exons of zebrafish *nes*. To elaborate, the *nesa* is composed of all 4 coding exons, transcript B is composed of coding exon 1, and transcript C is composed of coding exons 1 and 2 based on the comparison with the zebrafish *nes* mRNA sequence. The genomic structure of *nes* is also known in several mammalian species including mouse, rat and humans, and we have also identified putative nestin isoforms in other mammalian species such as in the

prairie vole, squirrel, mouse, rat, pig, buffalo, chimpanzee and human following extensive database searches (BLASTP, NCBI; http://web.expasy.org/translate/). Most mammalian nestins contain four exons, as proposed for the goldfish *nesa* transcript. However, the number of exons varies greatly among fish species; four in the zebrafish (*Danio rerio*), five in spotted gar (*Lepisosteus oculatus*) and six in Southern platyfish (*Xiphophorus maculatus)* based on Ensembl database searches (Cunningham *et al.* 2015).

Sequence analysis and genomic structure predictions suggest that the multiple goldfish nestins are products of alternative splicing. To be noted, the three transcripts are predicted to yield three proteins sharing an identical N-terminal intermediate filament (IF) core domain, whereas they have differing C-terminal regions. The N-terminal IF core domain is located at amino acid 15-322 in nestin isoform A; 15-271 in nestin isoform B; and 15-315 in nestin isoform C of the goldfish. A common feature in IF evolution is the great expansion of IF members to generate cell-specific heteropolymers (Fuchs and Weber 1994). This structural feature suggests that goldfish nestin is indeed involved in controlling, at least partly, cellular dynamics by regulating the polymerization of cytoskeletal elements. This functional role for nestin has been proposed and discussed by several other authors including Michalzyck and Ziman (2005), Mahler and Driever (2007) and Chen *et al.* (2010). Functional studies of different classes of IF proteins have shown that polymerizations occur mostly between the conserved IF regions (Steinert and Roop 1988; Fuchs and Weber 1994; Herrmann and Aebi 2000). The C-terminal region of IFs is likely to interact with other proteins in a cell-specific manner. Hence, the multiple nestin isoforms with a variable C-terminal region may generate another level of complexity for nestin interactions. The application of similar diversity modes by

employing different C-terminal regions is known for human neurofilament (NF) proteins (NF-L, NF-M, NF-H) (Lees *et al.*, 1988). However, different from NFs where gene duplication events are at the foundation of C-terminal diversity, alternative splicing likely leads to nestin diversity in goldfish. We suggest that the extraordinary brain plasticity exhibited by goldfish and other teleosts could be related to the diversity of nestin proteins we report. This would be an additional mechanism complimentary to the abundance of stem-like radial glial cell and regenerative capacity of the adult teleost CNS (Zupanc and Sîrbulescu 2011; Elisabeth *et al.* 2015).

Western blotting revealed that nestin immunoreactivity is present in all adult goldfish brain areas, similar to the situation observed for developing mammalian CNS (Lin *et al.* 1995). In contrast, the distribution of nestin becomes restricted to only the few proliferative areas of the adult mammalian CNS (Wiese *et al.* 2004; Michalczyk and Ziman 2005; Mahler and Driever 2007; Chen *et al.* 2010). Three major, and several minor nestin isoforms, were evident in the goldfish brain and pituitary tissue. The ~40 kDa band (corresponding to Transcript C) is the most common one and is found in all tissues. We speculate that transcript C is a major form of the protein and possibly has a function in maintaining and sustaining proliferative cells throughout adult life. The ~30 kDa protein band (Transcript B) is also present in low amounts in all the brain regions and pituitary which are tissues that undergoes cellular proliferation and cellular turnover. The ~70 kDa band is the second most common form of nestin protein found in the goldfish brain and is most similar to the nestin forms previously identified in other teleost species.

Both individual and tissue-dependent variations in the presence and relative abundance of these different goldfish nestins indicate a dynamic pattern of production and necessitated both discriminant and principal component analyses. It is clear that the telencephalon was distinct amongst the tissues examined. This is significant because the telencephalon undergoes high cellular proliferation during both embryogenesis and adulthood (Mahler and Driever 2007; März *et al.* 2010). The teleost telencephalon contains a large amount of RGCs especially near the ventricular layer and contains numerous proliferative cell pools and thus unparalleled neurogenetic capacity (Zupanc and Clint 2003; Mahler and Driever 2007; Pelligrini *et al.* 2007; März *et al.* 2010; Zupanc and Sîrbulescu 2011). Numerous studies have reported the ability of the goldfish to regenerate damaged tissues and cells following chemical or physical lesions in the CNS (Contestable *et al.* 1979; Levine 1983; Scherer and Easter 1984; Zupanc and Sîrbulescu 2011). The main determinants indentifying the telencephalon as the most variable tissue of nestin expression amongst the other 7 tissues is the frequency and intensity of the nestin isoform bands. More specifically, based on the frequency of detection of the nestin immunoreactive bands, nestin isoform A (~70 kDa) and B (~30 kDa) appear less frequently in the telencephalon of the goldfish compared to the vagal lobe tissue.

In conclusion, we have generated the first antibody against a fish nestin, and have identified and confirmed by gene sequencing and proteomic methods 3 different nestin isoforms in the female goldfish brain. The presence and patterns of distribution of the isoforms were complex, revealing tissue-dependent expression. The ~40 kDA isoform was consistent in presence and expression in all tissues examined, and thus may be

constitutively expressed, as would be expected for a key cytoskeletal element. The most striking finding following both PCA and discriminant analysis of the western blot data was the uniqueness of the telencephalon. Close examination of expression patterns in 10 individual females revealed that the 70 kDa band was absent on 9/10 of these animals at the time they were sacrificed for tissue sampling. Clearly, the functions of these different isoforms must be determined, perhaps using knockdown and overexpression methods in cell culture (e.g., in goldfish radial glial cells; Xing et al. 2015). Nevertheless, these data permit speculation of the roles of nestin isoforms. Morpholino knockdown experiments by Chen *et al.* (2010) suggest that nestin suppression enhances cellular apoptosis of neural progenitor cells in the developing zebrafish brain, a function that appears to be independent of its role in the cytoskeleton. The isoform they knocked down in zebrafish likely corresponds to the 70 kDa protein we identified in goldfish. Therefore, the low expression or absence of the 70 kDa isoform in the telencephalon is associated with the unparalleled capacity for neurogenesis in the teleost telencephalon (Pellegrini *et al.* 2007; 2015; Diotel et al. 2010). Perhaps there is a biochemical or functional relationship between the 70 kDA band and the other major nestin bands contributing to the neurogenic capacity of varying brain tissues. Consequently, it will be important to determine the expression of the multiple nestin proteins following neurotoxin-induced neuronal degeneration and subsequent regeneration in the telencephalon.

Chapter 3

Sex and tissue-dependent effects of MPTP on nestin protein distribution in the goldfish brain and pituitary

3.1. Introduction

Teleosts have unparalleled neurogenic capacity and contain several proliferating areas in the brain that are active not only during early development but during adulthood (Yoon 1975; Raymond and Easter 1983; Stuermer 1988). Adult fish have a much higher capacity and rate of neurogenesis in the central nervous system (CNS) compared to birds, mammals and other terrestrial vertebrates (Alvarez-Buylla 1990; Ekström *et al.* 2001; Zupanc 2001; Chapouton *et al.* 2007; Kaslin *et al.* 2008; Zupanc 2008). Nestin is an intermediate filament (IF) protein that marks neural stem cells (NSC) in the brain of zebrafish, mouse, rat and humans and can be used to observe proliferative cells and thus neurogenesis in the CNS and peripheral nervous system (PNS) (Lendahl *et al.* 1990; Yamaguchi *et al.* 2000; Wiese *et al.* 2004; Michalczyk and Zyman 2005; Mahler and Driever 2007). Nestin expression is linked to neurogenetic activity and its expression pattern can reveal an organism's neurogenetic state (Wiese *et al.* 2004). Interestingly, adult cellular proliferation and neurogenesis are differentially expressed in both female and male zebrafish (Zikipoulos *et al.* 2000, 2001; Ampatzis and Dermon 2007). For example, the male zebrafish cerebellum expresses a higher rate of proliferation than female fish (Ampatzis and Dermon 2007). This present study investigated sex differences in various goldfish brain structures by investigating the distribution of nestin isoforms in male and female adult goldfish. Currently, three novel nestin isoforms have been identified in the goldfish brain (nestin A,B and C) and these are differentially expressed in normal brain tissues (Chapter 2).

To elaborate, sex differences in neurogenesis are not only observed in fish but also exist in various brain areas of birds and mammals (Ampatzis and Dermon 2007). For example, sex differences are evident in the adult rat olfactory bulb where males have more newborn cells than females (Peretto *et al.* 2001). Adult neurogenesis and cellular proliferation also occur at different rates in the male adult songbird compared to females where males have a higher neurogenic rate (Goldman and Nottebohm 1983; Nordeen and Nordeen 1989; Rasika *et al.* 1994; Hidalgo *et al.* 1995). The sex differences observed in neurogenetic activity and expression are thought to link neurogenesis to specific animal behaviours. For example, increased neurogenesis in male songbirds likely contributes to courtship behaviour and song production during adolescence and adulthood (Goldman and Nottebohm 1983; Nordeen *et al.* 1987; Nordeen and Nordeen 1989; Rasika *et al.* 1994; Hidalgo *et al.* 1994). In teleosts, sex differences in neurogenesis have been identified in the dorsal hypothalamus, an area involved in reproductive behaviour, where females had a higher density of newborn neurons than males (Zikipoulos *et al.* 2000, 2001). Sex-specific differences in teleost neurogenesis could explain the greater capacity of certain brain areas to undergo plasticity events in the adult goldfish brain.

During early vertebrate development following the onset of neurulation, nestin is abundantly expressed, then as the organism develops, nestin expression decreases and becomes restricted to proliferative areas of the CNS (Wiese *et al.* 2004; Michalczyk and Ziman 2005; Mahler and Driever 2007; Rutherford *et al.* 2010). When terminal differentiation is established, nestin is specifically replaced by other tissue-specific IF proteins in the cytoskeleton such as glial fibrillary acidic protein (GFAP) and neurofilaments (Lendahl *et al.* 1990; Lin *et al.* 1995; Michalczyk and Ziman 2005). In

adult vertebrates, nestin expression is reestablished and upregulated following cellular and tissue injury in the muscle and nerve tissues especially in the proliferative areas of both the CNS and PNS (Lin *et al.* 1995; Michalczyk and Ziman 2005; Carmona *et al.* 2011). Nestin upregulation following injury could be a potential function of the IF protein to increase cellular proliferation in the injured brain. Nestin could influence cell proliferation in neurogenetic tissues such as the telencephalon and hypothalamus but also in the pituitary, optic tectum, midbrain, cerebellum, vagal lobe and brainstem. Teleosts contain numerous proliferative areas, the forebrain exhibiting the greatest amount of proliferative pools especially along the ventricular surface area (Zupanc and Horschke 1995; Ekström *et al.* 2001; Zupanc *et al.* 2005; Adolf *et al.* 2006; Grandel *et al.* 2006; Zupanc and Zupanc 2006; Kaslin *et al.* 2009; März *et al.* 2010; Schmidt *et al.* 2013; Pelligrini *et al.* 2015).

The upregulation of nestin following injury suggests neuronal regeneration as a means to heal and repair damaged cells and tissues. In this study, the neurotoxin 1-methyl-4-phenyl-1,2,3,6-tetrahydropyridine (MPTP) was used to injure the teleost brain. This neurotoxin induces a Parkinsonian-like syndrome in fish, rodents, primates and humans leading to a depletion of dopamine (DA) neurons in the brain (Burns *et al.* 1983; Hornby *et al.* 1987; Date *et al.* 1990a, 1990b; Poli *et al.* 1990; Poli *et al.* 1992; Pollard *et al.* 1992; Lucchi *et al.* 1998; Hamill *et al.* 2007; Oki *et al.* 2008). Studies in fish and mammals have shown that not only nestin is upregulated following injury but there is also a significant activation of glial cells coincident with the depletion of DA neurons (Lin *et al.* 1995; Michalczyk and Ziman 2005; Carmona *et al.* 2011; Blesa *et al.* 2012; Yokoyama *et al.* 2010). The role of glial activation following MPTP administration in

teleost is not well understood, however, glial cells in teleost are known to produce glial cell line-derived neurotrophic factors (GDNF) and brain-derived neurotrophic factor (BDNF) which are involved in DA neuronal survival, decreasing DA neuronal apoptosis and promoting axonal growth and regeneration (Lin *et al.* 1993; Lykissas *et al.* 2007; Pellegrini *et al.* 2007; Yasuhara *et al.* 2007). Nestin-positive cells and glial cells could act as a cellular reserve that is activated to proliferate, migrate and differentiate to heal damaged tissues in teleost species (Lin *et al.* 1995; Namiki and Tator 1999; Wiese *et al.* 2004).

The investigation of the distribution and sex-specific expression patterns of nestin in injured teleost brain could reveal a role of nestin as a player in regulating the progenitor cell niches in the adult brain and provide insight into neurogenic capabilities in vertebrates. Teleost cellular remodeling capabilities were also investigated by observing actin, another IF protein that is highly conserved among vertebrates, found in the cytoskeleton of all cells and involved in numerous functions including motility, exocytosis and phagocytosis (True 1990).

3.2. Materials and methods

3.2.1. Animal maintenance

Adult female and male goldfish (*Carassius auratus*) were purchased from a commercial supplier (Mt. Parnell Fisheries Inc., Mercersburg, PA, USA) and maintained at 18˚C under a natural-simulated photoperiod on standard flaked goldfish food. Fish were kept in 70L tanks (15-18 fish/tank). All procedures were performed according to the guidelines of the Canadian Council on Animal Care and were approved by the University of Ottawa animal care committee. Goldfish were anesthetized using 3-aminobenzoic acid

ethylester (MS-222; 0.05% in water, Sigma Chemicals) for all handling and sampling procedures.

3.2.2. Experimental and sampling procedures

The dopaminergic neurotoxin, 1-methyl-4-phenyl-1,2,3,6-tetrahydropyridine (MPTP), was purchased from Sigma-Aldrich (M0896, Oakville, Canada) and dissolved in 0.6% saline to give a dose of 50 μg/g body mass of fish at 2 μL/g. Sexually regressed female goldfish (June-August; ~22 g ± 1.5 body weight; 2.2 ± 0.3 gonadosomatic index; n=32) and male goldfish (June-August; ~19 g ± 1.4 body weight; 1.3 ± 0.2 gonadosomatic index; n=31) either received a single injection of MPTP at time t_0 or a control saline 0.6% injection (2 μL/g) similar to the treatment schedule used in Pollard *et al.* (1992) and Goping *et al.* (1995). Female and male goldfish were sacrificed at 4 and 7 days post-injection (dpi). The whole pituitary, pituitary, hypothalamus, telencephalon, optic tectum, midbrain, cerebellum, vagal lobe and brainstem were dissected. All dissections were performed in the morning. The samples were stored at -80 ˚C until RNA and protein extraction. The gonadosomatic index was calculated by dividing the gonad weight by body weight of the goldfish x 100.

3.2.3. RNA extraction, quality control and cDNA synthesis

Only female hypothalamus and telencephalon tissues were used for RNA extraction. The female hypothalamus and telencephalon tissues were homogenized using stainless steel beads in an MM301 Mixer Mill (Retsch, Newton, PA, USA) at 20 Hz for 4 min. The isolation of total RNA from adult female goldfish hypothalamus and telencephalon brain tissue was performed using RNeasy Micro Kit (Qiagen, Toronto,

ON, Canada) as described in the manufacturer's protocol. Upon purification, concentration and quality of all samples was assessed using NanoDrop ND-1000 spectrophotometer (Thermo Fisher Scientific, Waltham, MA, USA) and 2100 Bioanalyzer (Agilent Technoloeis, Mississauga, ON, Canada). RNA integrity values of samples ranged from 8.1 to 9.8, which is above the recommended minimum value of 5 for quantitative real-time RT PCR (qPCR) applications (Fleige and Pfaffl, 2006). Total cDNA was prepared from 1-5 µg total RNA using Maxima cDNA synthesis kit (Thermo Scientific, Waltham, MA, USA) as described by the manufacturer. Each 20 µl reaction was diluted 100-fold in nuclease-free water and used as the template for the real-time qPCR assays. All female goldfish hypothalamus and telecephalon cDNA samples from different time points and treatments were synthesized in parallel.

3.2.4. Quantitative real-time RT-PCR (qPCR)

Real-time RT-PCR assays based on SYBR green were used to validate relative gene expression. Primers used in the present study were designed using Primer3 (http://primer3.sourceforge.net/) and synthesized by Invitrogen (Table 3.1). The Maxima SYBR green qPCR Master Mix (Thermo Scientific, Waltham, MA, USA) and CFX96 Real-Time PCR Detection System (Bio-Rad, Mississauga, Canada) were used to amplify and detect the transcripts of interest. Data were analyzed using the Bio-Rad software package. The relative standard curve method was used to calculate relative mRNA abundance between samples, which were normalized using NORMA-GENE algorithm (Heckmann *et al.* 2011). The data are presented as means + SEM of gene expression from 8 biological replicates (assayed in duplicate) for each group.

3.2.5. Statistical analysis of quantitative real-time RT-PCR (qPCR)

All data were first tested for normality and those data with non-normal distribution were subjected to $\log_{10}$ transformations prior to statistical analyses. All data were presented as a mean + SEM. Comparison of two groups was performed using Student's t-test (two-tailed) in SPSS Statistics (version 21). P-values less than or equal to 0.05 were considered statistically significant.

3.2.6. Protein extraction and SDS-PAGE

Protein extraction of the pituitary and seven different brain tissues were obtained from 20 female (10 control and 10 MPTP-treated goldfish) and 19 (9 control and 10 MPTP-treated goldfish) male goldfish for western blotting. Refer to Chapter 2 Materials and methods section 2.2.6 for methods details.

3.2.7. Western blot analysis

Western blot analysis was used to determine the expression pattern of nestin and ß-actin protein on the seven brain tissues and pituitary. Refer to Chapter 2 Materials and methods section 2.2.7 for methods details.

3.2.8. Statistical analysis of western blot immunoreactivity signals

Canonical and classificatory discriminant analyses, and principal component analysis (PCA) were used as dimension-reduction techniques because western blot analysis determined that nestin protein expression patterns are complex. The major and minor nestin immunoreactive bands varied in presence and intensity in a tissue-dependent manner and were considered for further analysis. The expression pattern of ß-actin was

also analysed. Canonical discriminant analysis for the different nestin protein isoforms and ß-actin obtained from female goldfish (n=10); male goldfish (n=9); MPTP-treated female goldfish (n=10) and MPTP-treated male goldfish (n=10) was performed using the PROC DISCRIM and PROC CANDISC modules in SAS (Statistical Analysis System, v9.4, Cary, NC, USA) software. Scree plots outlining a principal component factor analysis of nestin and ß-actin protein expression obtained from the western blots were performed to reveal the components providing the most variance observed in the data set. An example can be found in Supplementary Fig 3.1. The SAS software was also used for PCA, which provided a series of 2D score plots where the two principal components that encompass the most variance within the data set are shown as the x- and y-axes. The 2D plot provides a visual overview of all of the samples and their potential groupings. Following the visualization of grouped samples in the PCA, 3D plots were created using NTSYS-pc (Rohlf 2009) for nestin protein expression only. Thus, three principal components for the nestin protein expression provided a better visual representation of all the samples and their potential groupings. The 3D plots also identify the discriminating factors between the goldfish groups in terms of nestin protein expression. The PCA was used to compare the nestin isoforms and ß-actin across tissues and to identify sex and treatment pattern differences of protein expression in the various brain regions and whole pituitary.

The canonical plots are presented as bar charts on a frequency axis with different ranges dependent on the number of groups (n) analyzed. The frequency axis ranged from 0 to 10 or 0 to 100% dependent on the number of groups in order to maintain consistency

between data sets. The frequencies were established so that there is only one axis for 2 groups and all other axes were also represented on one axis for comparative purposes.

3.3. Results

3.3.1. Effects of MPTP on ß-actin mRNA levels in the female hypothalamus and telencephalon

At 4 dpi of MPTP, *ß-actin* expression was significantly increased by 2 fold in the hypothalamus and significantly increased by 2.6 fold in the telencephalon relative to control (P=0.001 and P=0.004 respectively) (Fig. 3.1A). However, at 7 dpi of MPTP, *ß-actin* expression was only significantly increased by 1.9 fold in the hypothalamus (P=0.029) and there were no effects of MPTP observed on the expression of *ß-actin* in the telencephalon (P=0.532) (Fig. 3.1B).

3.3.2. Effects of MPTP on nes mRNA levels in the female hypothalamus and telencephalon

Student's t-test analysis was performed to determine the effects of MPTP on the expression of three *nestin* transcripts; *nestin A* transcript (*nesa*) (GenBank KT373807), *nestin B* transcript (*nesb*) (GenBank KT373808) and *nestin C* transcript (*nesc*) (GenBank KT373809) or the overall expression of all three nestin transcripts (*nestin* All; *nesall*) in the female goldfish hypothalamus and telencephalon.

At 4 dpi of MPTP, the *nesall* and *nesc* expression level in the hypothalamus were significantly decreased by 27% and 60% respectively following MPTP (P=0.001), but there were no effects of MPTP on *nesa* (P=0.705) or *nesb* (P=0.199) in the hypothalamus relative to control (Fig. 3.2). In the telencephalon, the expression of *nesa* was

significantly decreased by MPTP by 33% (P=0.037), but there were no effects of MPTP on *nesall* (P=0.0596), *nesb* (P=0.616) or *nesc* (P=0.339) (Fig. 3.2). At 7 dpi of MPTP, there were no effects of MPTP on *nesall* (P=0.137), *nesa* (P=0.143), *nesb* (P=0.605) or *nesc* (P=0.205) in the hypothalamus and no effects of MPTP on *nesall* (P=0.571), *nesa* (P=0.794), *nesb* (P=0.499) or *nesc* (P=0.942) in the telencephalon relative to control (Fig. 3.3).

3.3.3. Distribution of ß-actin protein in female and male goldfish brain and pituitary

The protein levels of ß-actin (Mw 42 kDa) in the pituitary, hypothalamus, telencephalon, optic tectum, midbrain, cerebellum, vagal lobe, and brainstem were qualitatively analyzed by western blotting in female (Fig. 3.4A) and male (Fig. 3.4B) goldfish. Based on the western blots, the 42 kDa ß-actin immunoreactive band was consistently detected in all samples but the intensity of the band varied based on tissue and fish. Canonical and classificatory analyses as well as PCA were used to investigate the differences in intensity levels of ß-actin in the western blots (See section 3.3.8.1 below).

3.3.4. Effects of MPTP on ß-actin protein distribution in female and male goldfish brain and pituitary

The protein expression of ß-actin in the pituitary, hypothalamus, telencephalon, optic tectum, midbrain, cerebellum, vagal lobe, and brainstem was qualitatively analyzed by western blotting in MPTP-treated female (Supplementary Figure 3.2) and MPTP-treated male goldfish (Supplementary Figure 3.3). Canonical and classificatory analyses

as well as PCA were used to investigate the differences in intensity levels of ß-actin in the western blots following MPTP treatment (See sections 3.3.8.2 and 3.3.8.3 below).

3.3.5. Distribution of nestin proteins in female and male goldfish brain and pituitary

The expression of nestin in pituitary, hypothalamus, telencephalon, optic tectum, midbrain, cerebellum, vagal lobe, and brainstem was qualitatively analyzed by western blotting in female (See Chapter 2; Fig. 2.4) and male (Fig. 3.5). Based on the western blots, the major nestin protein bands appear at different frequencies (Table 3.2 and 3.3 respectively). For both female and male goldfish, the ~40 kDa band is evident in all goldfish brain tissues and pituitary, and has the highest signal intensity in comparison to the other bands. The ~70 kDa band is present in all tissues except for the hypothalamus in the female, whereas the ~70 kDa band is present in all tissues in the male goldfish, although it appears at a low frequency (1-2 out of 9). There is also another nestin immunoreactive (-ir) protein band of 75 kDa evident in the female and male goldfish brain and pituitary western blot. Although the ~75 kDa protein band is absent from the pre-absorption western blot (Chapter 2; Fig. 2.1), we believe both the ~70 kDa and ~75 kDa bands represent the same peptide sequence with one having a post-translational modification on the protein. The 75 kDa band is evident due to the longer exposure of the membrane to detect immunoreactive bands (See Chapter 2; Section 2.3.4). The ~75 kDa band is present in all the tissues except for the hypothalamus and the telencephalon in the female fish and the pituitary and cerebellum in the male fish. The ~30 kDa band is present in all the brain tissues and pituitary in the female fish similarly to the male fish except for the pituitary; this band is very faint and only appears at higher exposure times compared to the other bands. In the male goldfish western blot (Fig. 3.5), a ~45 kDa

nestin-ir band is also present in the midbrain and vagal lobe, we believe both the ~40 kDa and ~45 kDa bands represent the same peptide sequence with one having a post-translational modification on the protein.

The scree plot (Supplementary Figure 3.1A) of the nestin-ir protein bands of male goldfish reveals that the first two components provide the greatest variability in the nestin protein expression data set as the line straightens after the second principle component. The male goldfish 2D plot (Fig. 3.6A) obtained from PCA illustrates that the pituitary is projected on the positive side of both x- and y-axes in comparison to the telencephalon in the female goldfish 2D plot (Chapter 2; Fig. 2.5B). The eigenvectors of the pituitary also point in a different principal direction in comparison to the other groupings. The pituitary corresponds to the greatest positive direction on axis 2 having the most positive variation in comparison to the other data points. The plot illustrates that the data set is best classified based on the expression pattern of nestin in the different tissues in the male goldfish brain. In the male goldfish brain, the hypothalamus and optic tectum also contribute in the positive area, but very close to axis 1, whereas the telencephalon, midbrain, cerebellum, brainstem and vagal lobe contribute in the negative area of axis 2, but remain very close in proximity to axis 1.

The 3D plot (Fig. 3.6B) considers the first three principal components for the nestin expression pattern in male goldfish. As seen in Fig. 3.6A, the pituitary has the greatest variance in comparison to the other data points and provides further validity of the results obtained from the 2D plot. In comparison to the 2D plot, the vagal lobe is observed on axis 3 followed by the brainstem and optic tectum contributing to the positive areas; followed by the cerebellum, telencephalon, midbrain and hypothalamus on

the negative side of axes 3. In other words, the pituitary and vagal lobe are clustering in opposite directions mainly on axes 2 and 1 (both Fig. 3.6A and 3.6B); and the two against the rest of the eight variables. The brainstem, optic tectum, cerebellum, telencephalon and midbrain are also high on axis 3 and 1 whereas the hypothalamus is highest on axis 1 and lowest on axis 3.

3.3.6. Effects of MPTP on nestin protein expression in female goldfish brain and pituitary

The expression of nestin in pituitary, hypothalamus, telencephalon, optic tectum, midbrain, cerebellum, vagal lobe, and brainstem was qualitatively analyzed by western blotting in MPTP-treated female goldfish (Fig. 3.7 and 3.8). Based on 10 different western blots of brain tissues and pituitaries for MPTP-treated female goldfish, the major nestin protein bands appear at different frequencies (Table 3.4). The ~40 kDa band is evident in all goldfish brain tissues and pituitary, and has the highest signal intensity in comparison to the other bands. The ~70 kDa band is present in all tissues and appears most frequently in the midbrain (60%). The ~75 kDa band is present in all the tissues except for the hypothalamus although it appears at a low frequency in the pituitary, telencephalon and cerebellum. The ~75 kDa band is present most frequently in the midbrain (70%). The ~30 kDa band is present in all the brain tissues and pituitary but at a lower frequency in the pituitary and the brainstem (20%); this band is very faint and only appears at higher exposure times compared to the other bands.

3.3.7. Effects of MPTP on nestin protein expression in male goldfish brain and pituitary

The expression of nestin in pituitary, hypothalamus, telencephalon, optic tectum, midbrain, cerebellum, vagal lobe, and brainstem was qualitatively analyzed by western blotting in MPTP-treated male goldfish (Fig. 3.9 and 3.10). Based on 10 different western blots of brain tissues and pituitaries for MPTP-treated male goldfish, the major nestin protein bands appear at different frequencies (Table 3.5). The ~40 kDa band is evident in all goldfish brain tissues and pituitary, and has the highest signal intensity in comparison to the other bands. The ~70 kDa band is present in all tissues but at a very low frequency of 10-30%. The ~75 kDa band is present in all the tissues except for the hypothalamus and the telencephalon and it appears at a low frequency in all the other tissues (20-30%). The ~30 kDa band is present in all the brain tissues except for the pituitary. However, the 30 kDa band appears at a low frequency in the telencephalon (20%) and this band is very faint and only appears at higher exposure times compared to the other bands.

3.3.8. Sex-specific differences of ß-actin protein expression in goldfish based on canonical and classificatory discriminant analyses

3.3.8.1. Control female and male goldfish at 4 and 7 dpi

The female and male control goldfish groups at 4 dpi (Fig. 3.11A) and at 7 dpi (Fig. 3.11B) are classified separately in the canonical and classificatory discriminant analyses. In the 4 dpi goldfish group, the female and male fish cluster at opposite ends of the x-axis; where the female are at the negative end and the male at the positive end. This indicates a clear sex difference in the expression pattern of ß-actin. Similarly, at 7 dpi the

female and male fish cluster at opposite ends of the x-axis but they are separated by a smaller distance along the x-axis; the females along the negative end and the males along the positive end. This indicates a clear differential expression of ß-actin protein based solely on sex at both 4 and 7 dpi.

3.3.8.2. Control versus MPTP-treated female and male goldfish at 4 dpi

The control and MPTP-treated female goldfish groups at 4 dpi (Fig. 3.11C) are classified separately in the canonical and classificatory discriminant analysis. The control and MPTP-treated female fish cluster at opposite ends of the x-axis; where the control female are at the negative end and the MPTP-treated female at the positive end. This indicates a clear difference in the expression pattern of ß-actin between the female treatment groups. Similarly, the control and MPTP-treated male goldfish groups at 4 dpi (Fig. 3.11D) are classified separately in the canonical and classificatory discriminant analyses. The control and MPTP-treated male fish cluster at opposite ends of the x-axis; where the control males are at the negative end and the MPTP-treated males at the positive end. This indicates a distinction in the expression pattern of ß-actin between the male goldfish treatment groups at 4 dpi. When combining both sexes of control and MPTP-treated goldfish at 4 dpi and analyzing the entire group for sex differences (Supplementary Figure 3.4A), the goldfish are not clearly separated on opposite ends of the x-axis based on sex. However, there is a clear distinction and separation between the male MPTP-treated goldfish, which are on the negative end of the x-axis at -1.5, and the control and MPTP-treated female goldfish, which are located at the midpoint and the positive end of the x-axis. At the midpoint, there is an overlap of ß-actin expression pattern for control male and female as well as MPTP-treated female goldfish. On the

other hand, the male control goldfish are clustering at the negative end of the x-axis whereas the control and MPTP-treated female are clustering at the positive end of the x-axis. Overall, when observing the differences based soley on sex, the ß-actin immunoreactive protein bands of the male goldfish have a tendency to plot on the negative end of the x-axis whereas the female goldfish are on the positive end. There is no clear difference based on sex due to the overlap of male and female goldfish at the midpoint. With regards to treatment, there is no clear separation of ß-actin-ir between the control and MPTP-treated goldfish. However, there is a separation between the expression pattern of male and female MPTP-treated goldfish at 4 dpi where the males are clustering at the negative end of the x-axis at -1.5 and the females are clustering at the positive end of the x-axis spanning from the midpoint to 3.0. The MPTP-treated female goldfish and the control male goldfish have a bell-shaped ß-actin expression pattern spanning the positive end of the x-axis from 0 to 3 and the negative end of the x-axis from -3 to 0 respectively.

3.3.8.3. Control versus MPTP-treated female and male goldfish at 7 dpi

The control and MPTP-treated female goldfish groups at 7 dpi (Fig. 3.12A) are found separately in the canonical and classificatory discriminant analysis. The control and MPTP-treated female fish cluster at opposite ends of the x-axis; where the control female are at the negative end and the MPTP-treated female at the positive end. This indicates a clear difference in the expression pattern of ß-actin between the female treatment groups. Similarly, the control and MPTP-treated male goldfish groups at 7 dpi (Fig. 3.12B) are classified separately in the canonical and classificatory discriminant analysis. The control and MPTP-treated male fish cluster at opposite ends of the x-axis;

where the control males are at the negative end and the MPTP-treated males are at the positive end. This indicates a distinction in the expression pattern of ß-actin between the male goldfish treatment groups at 7 dpi. When combining both sexes of control and MPTP-treated goldfish at 7 dpi and analyzing the entire group for sex differences (Supplementary Figure 3.4B), the goldfish are not clearly separated on opposite ends of the x-axis based on sex. However, there is a clear distinction and separation between the expression pattern of ß-actin in the female MPTP-treated goldfish, which are on the negative end of the x-axis between -0.75 and -0.25, and the expression pattern in the control female goldfish, which span the positive end of the x-axis between +0.75 to 3.75 as observed in (Fig. 3.12A). There are two points of overlap in the ß-actin expression profile. At -0.75 the control male goldfish and the MPTP-treatment male and female goldfish overlap. The second overlap is observed at +0.75 where the control male and female goldfish and the MPTP-treated male goldfish overlap. Overall, when observing the differences based on sex solely, there is no trend present as overlaps of ß-actin expression are present. However, there are differences observed in the expression pattern in the female treatment groups. The MPTP-treated male goldfish have a bell-shaped ß-actin expression pattern spanning the negative end of the x-axis from -0.75 and +0.75.

3.3.8.4. Control versus MPTP-treated female and male goldfish at 4 and 7 dpi

When combining both 4 dpi and 7 dpi female control and MPTP-treated goldfish groups and analyzing the sex differences (Fig. 3.12C), the goldfish are not separated on opposite ends of the x-axis based on sex. However, the expression pattern of ß-actin in the MPTP-treated 4 dpi and 7 dpi female fish cluster at opposite ends of the x-axis; where the MPTP-treated 4 dpi females are at the positive end between 0 and 2.4 and the MPTP-

treated 7 dpi females are at the negative end between -2.4 and -1.2. This indicates a distinction in the expression pattern of ß-actin between the female MPTP-treatment groups. All the groups except for the MPTP-treated female 7 dpi group have a bell-shaped ß-actin expression pattern spanning the negative and positive end of the x-axis. On the other hand, when visualizing both 4 dpi and 7 dpi male control and MPTP-treated goldfish groups and analyzing the sex differences (Fig. 3.12D), the goldfish are not separated on opposite ends of the x-axis based on sex. However, the control 4 dpi and 7 dpi male fish cluster at opposite ends of the x-axis; where the expression pattern of ß-actin in the control 4 dpi males are at the positive end between 2.25 and 3.75 and the control 7 dpi males are at the negative end between -0.75 and -2.25. This indicates a distinction in the expression pattern of ß-actin between the male control groups. The control 4 dpi and the MPTP-treated 4 dpi male fish also cluster at opposite ends of the x-axis; where the control 4 dpi male fish are at the positive end between 2.25 and 3.75 and the MPTP-treated 4 dpi male fish are at the negative end between -0.75 and -3.75. This indicates a distinction in the expression pattern of ß-actin between the male control and MPTP-treatment groups at 4 dpi. When combining both sexes of control and MPTP-treated goldfish at 4 dpi and 7 dpi and analyzing the entire group for sex differences (Supplementary Figure 3.4C), some goldfish groups express ß-actin differently and thus are separated on opposite ends of the x-axis based on sex and treatment. The protein expression pattern of the control male 4 dpi group and the MPTP-treated female goldfish cluster at opposite ends of the x-axis; where the control male 4 dpi are on the negative end of the x-axis at -2 and -1 whereas the MPTP-treated female goldfish are on the positive axis from 0 to 3. The protein expression pattern of the control male 4 dpi group

and the MPTP-treated male 4 dpi group cluster on opposite ends of the x-axis; the control male 4 dpi group are on the negative side on -2 and -1 whereas the MPTP-treated male 4 dpi group cluster on the positive end of the axis between 0 and 2. The MPTP-treated female 7 dpi goldfish and the MPTP-treated male 4 dpi goldfish cluster on opposite ends of the axis; the MPTP-treated female 7 dpi group are on the negative end between -1 and 0 whereas the MPTP-treated 4 dpi male group cluster on the positive end between 0 and 2. The MPTP-treated female 4 dpi and 7 dpi groups cluster on opposite ends of the x-axis. The MPTP-treated female 4 dpi group clusters on the positive end of the axis between 0 and 3 whereas the MPTP-treated 7 dpi female group clusters on the negative end from -1 and -3. This indicates a distinction in the expression pattern of ß-actin between the female MPTP-treatment groups; the control male 4 dpi and MPTP-treated female and male groups; and a separation between the MPTP-treated female 7 dpi and the MPTP-treated male 4 dpi. As a result, both sex and treatment differences are observed among the various goldfish groups. At the midpoint and at -1, we can observe overlaps of ß-actin protein expression of 6 different groups indicating some similarity in the expression pattern of ß-actin however the frequency of goldfish overlap is smaller at the -1 point versus the midpoint 0. The ß-actin-ir of the control female at 4 dpi is distributed evenly spanning the x-axis from -2 and 2. The MPTP-treated 7 dpi female goldfish group exhibits the greatest negative projection on the x-axis versus the MPTP-treated 4 dpi female group which is clustering on the positive end.

3.3.9. Principal component analysis of ß-actin protein expression patterns

3.3.9.1. Control versus MPTP-treated female goldfish at 4 and 7 dpi

The scree plot of 4 dpi and 7 dpi female control and MPTP-treated goldfish groups reveals that the first three components provide the greatest variability in the data set as the line straightens after the third component. The 2D plot (Fig. 3.13A) obtained from PCA illustrates that both the telencephalon and hypothalamus are projected on the positive side of both x- and y-axes. The eigenvectors of the telencephalon and hypothalamus also point in a different principal direction in comparison to the other groupings. The telencephalon and hypothalamus correspond to the greatest positive direction on axis 2 having the most positive variation in comparison to the other data points. The cerebellum also contributes in the positive area, but very close to axis 1 whereas pituitary, optic tectum, midbrain, vagal lobe and brainstem contribute in the negative area of axis 2 but remain very close in proximity to axis 1 with the exception of the brainstem. The brainstem projects on the negative side of the y-axis. The eigenvector of the brainstem also points in a different principal direction in comparison to the other groupings, clustering in the opposite direction of the telencephalon and hypothalamus. The brainstem corresponds to the greatest negative direction on axis 2 but to a lesser extent than the positive cluster observed from the telencephalon and hypothalamus. Therefore, when comparing control and MPTP-treated female goldfish at 4 and 7 dpi, the plot illustrates that the data set is best classified based on the expression pattern of ß-actin in the telencephalon and hypothalamus. These tissues have the greatest variance and best describe the distribution pattern.

3.2.9.2. Control versus MPTP-treated male goldfish at 4 and 7 dpi

The scree plot of 4 dpi and 7 dpi male control and MPTP-treated goldfish groups reveals that the first three components provide the greatest variability in the data set as the line straightens after the third component. The 2D plot (Fig. 3.13B) obtained from PCA illustrates that the pituitary followed by the hypothalamus and then the telencephalon are projected on the positive side of both x- and y-axis. The eigenvectors of the pituitary, hypothalamus and telencephalon also point in a different principal direction in comparison to the other groupings. The pituitary corresponds to the greatest positive direction on axis 2 having the most positive variation in comparison to the other data points. The optic tectum, midbrain, cerebellum, vagal lobe and brainstem project on the negative side of the y-axis. The optic tectum and midbrain contribute in the negative area but are very close to axis 1 whereas the cerebellum, vagal lobe and brainstem contribute in the negative area of axis 2. The eigenvector of the brainstem points in a different principal direction in comparison to the other groupings, clustering in the opposite direction of the pituitary, hypothalamus and telencephalon. The brainstem corresponds to the greatest negative direction on axis 2 but to a lesser extent than the positive cluster observed from the pituitary and hypothalamus. Therefore, when comparing control and MPTP-treated male goldfish at 4 and 7 dpi, the plot illustrates that the data set is best classified based on the expression pattern of ß-actin in the pituitary and hypothalamus. These tissues have the greatest variance and best describe the distribution pattern.

3.3.9.3. Control versus MPTP-treated female and male goldfish at 4 and 7 dpi

The scree plot of 4 dpi and 7 dpi male and female control and MPTP-treated goldfish groups reveals that the first three components provide the greatest variability in the data set as the line straightens after the third component. The 2D plot (Fig. 3.13C) obtained from PCA illustrates that the hypothalamus and telencephalon are projected on the positive side of both x- and y-axes. The eigenvectors of the hypothalamus and telencephalon also point in a different principal direction in comparison to the other groupings. The hypothalamus and telencephalon correspond to the greatest positive direction on axis 2 having the most positive variation in comparison to the other data points. The pituitary and optic tectum also project on the positive side of both x- and y-axes but are very close to axis 1. In comparison, the cerebellum, midbrain, vagal lobe and brainstem project on the negative side of the y-axis. The cerebellum, midbrain and vagal lobe contribute in the negative area but are very close to axis 1 whereas the brainstem contributes in the negative area of axis 2. The eigenvector of the brainstem points in a different principal direction in comparison to the other groupings, clustering in the opposite direction of the hypothalamus and telencephalon. The brainstem corresponds to the greatest negative direction on axis 2 but to a lesser extent than the positive cluster observed from the hypothalamus and telencephalon. Overall, when comparing control and MPTP-treated male and female goldfish at 4 and 7 dpi, the plot illustrates that the data set is best classified based on the expression pattern of ß-actin in the hypothalamus and telencephalon. These tissues have the greatest variance and best describe the distribution pattern.

3.3.10. Sex-specific differences of nestin protein expression pattern in goldfish based on canonical and classificatory discriminant analyses

3.3.10.1. Control female and male goldfish at 4 and 7 dpi

The canonical and classificatory discriminant analysis of the goldfish groups for nestin protein expression pattern are not as evident as the ß-actin expression pattern. The female and male control goldfish groups at 4 dpi (Supplementary Figure 3.5A) and the female and male control goldfish group at 7 dpi (Supplementary Figure 3.5B) are classified separately in the canonical and classificatory discriminant analyses although there are two and three points of sex overlaps along the x-axis respectively. To elaborate, in the 4 dpi goldfish group, the female and male fish cluster at opposite ends of the x-axis. The female cluster mostly towards the positive end spanning from -1.2 and 3.6 whereas the male cluster mostly towards the negative end spanning from 0 to -3.6. This indicates a distinction in the expression pattern of nestin based on sex. However, there are two points of overlap at -1.2 and at the midpoint 0. At the midpoint, 26% of the female and 23% of the male goldfish overlap. The overlap at -1.2 is much smaller with 1% each of the female and male goldfish. Similarly, in the 7 dpi goldfish group, the female and male fish cluster at opposite ends of the x-axis but over a smaller separation distance along the x-axis. The female fish cluster mostly towards the positive end spanning from -1 and 3 whereas the male fish cluster mostly towards the negative end spanning from 0 to -3. This indicates a distinction in the expression pattern of nestin based on sex. However, there are three points of overlap at -1, the midpoint 0 and 1. At the midpoint, this is where we observed the greatest overlap with 24% of the females and 19% of the male goldfish.

The overlap at -1 is smaller with 8% of the female and 2% of the male goldfish. The overlap at 1 is the smallest with 2% of each of the female and male goldfish.

3.3.10.2. MPTP-treated female and male goldfish at 4 and 7 dpi

The female and male MPTP-treated goldfish groups at 4 dpi (Supplementary Figure 3.5C) and the female and male MPTP-treated goldfish groups at 7 dpi (Supplementary Figure 3.5D) are found separately in the canonical and classificatory discriminant analysis although there are four and two points of sex overlaps along the x-axis respectively. To elaborate, in the 4 dpi MPTP-treated goldfish group, the female and male fish cluster at opposite ends of the x-axis. The female cluster mostly towards the negative end spanning from 1.5 to -3.5 whereas the male cluster mostly towards the positive end spanning from 2.5 to -1.5. This indicates a distinction in the expression pattern of nestin based on sex. However, there are four points of overlap spanning from 1.5 to -1.5. The 0.5 point on the x-axis has the greatest female and male overlap with 15% of the females and 20% of the male goldfish. This is followed by the overlap at point -0.5 with 10% of the females and 6% of the males. The next overlap is at point -1.5 with 6% of the females and 1% of the males. The smallest overlap is observed at point 1.5 with 1% of the females and 4% of the males. Similarly, in the 7 dpi MPTP-treated goldfish group, the female and male fish cluster at opposite ends of the x-axis. The female cluster mostly towards the positive end spanning from -1.2 to 3.6 whereas the male cluster mostly towards the negative end spanning from 1.2 to -3.6. This indicates a distinction in the expression pattern of nestin based on sex. However, there are three points of overlap at -1.2, the midpoint 0 and 1.2. At the midpoint, this is where we observed the greatest overlap with 23% of the females and 24% of the male goldfish.

This is followed by the overlap at point 1.2 with 7% of the females and 2% of the males. The smallest overlap is observed at point -1.2 with 2% of the females and 4% of the males.

3.3.10.3. Control versus MPTP-treated female and male goldfish at 4 dpi

The female control and MPTP-treated 4 dpi groups (Supplementary Figure 3.6A) are found separately in the canonical and classificatory discriminant analysis although there are two points of sex overlap along the x-axis. To elaborate, the female control and MPTP-treated 4 dpi groups cluster at opposite ends of the x-axis. The female control 4 dpi group clusters mostly towards the negative end spanning from 1.2 to -3.6 whereas the 7 dpi female group clusters mostly towards the positive end spanning from -0.75 to 3.75. This indicates a distinction in the expression pattern of nestin based on treatment. However, there are two points of overlap at point -0.75 and point +0.75. The +0.75 point on the x-axis has the greatest overlap with 22% of the 4 dpi control females and 20% of the MPTP-treated 4 dpi female goldfish. The smallest overlap is observed at point -0.75 with 9% of the 4 dpi control females and 11% of the MPTP-treated 4 dpi female goldfish. Similarly, in the male control and MPTP-treated 4 dpi groups (Supplementary Figure 3.6B), the groups cluster at opposite ends of the x-axis. The 4 dpi control males cluster mostly towards the negative end spanning from 0.5 to -2.5 whereas the MPTP-treated 4 dpi males cluster mostly towards the positive end spanning from -0.5 to 3.5. This indicates a distinction in the expression pattern of nestin based on treatment. However, there are two points of overlap at -0.5 and +0.5. The greatest overlap is observed at -0.5 with 20% of the 4 dpi control males and 18% of the MPTP-treated 4 dpi male goldfish. The smallest overlap is observed at point +0.5 with 2% of the 4 dpi control males and 7%

of the MPTP-treated 4 dpi males. When combining both sexes of control and MPTP-treated goldfish at 4 dpi and analyzing the entire group for sex differences (Supplementary Figure 3.6C), there are no clear distinctions or separations between groups based on sex or treatment as there are many points of overlap. The general trends observed are the control female 4 dpi goldfish are clustering at the most positive end of the x-axis spanning from -1.2 to 3.6. The MPTP-treated 4 dpi female goldfish also cluster mostly towards the positive end of the x-axis spanning from 0 to 3.6 except for one outlier at -3.6. The male control 4 dpi goldfish are clustering at the most negative end of the x-axis spanning from 1.2 to -4.8. The MPTP-treated 4 dpi male goldfish are more neutral and have a bell-shaped motif surrounding the midpoint between -1.2 and 1.2. However, there are three points of overlap where all 4 groups are found near the midpoint from -1.2 to 1.2.

3.3.10.4. Control versus MPTP-treated female and male goldfish at 7 dpi

The female control and MPTP-treated 7 dpi groups (Supplementary Figure 3.7A) cluster at opposite ends of the x-axis. The 7 dpi control females cluster mostly towards the negative end spanning from 2.4 to -3.6 whereas the MPTP-treated 7 dpi females cluster mostly towards the positive end spanning from 0 to 3.6. This indicates a distinction in the expression pattern of nestin based on treatment. However, there are three points of overlap at +2.4, +1.2 and the midpoint 0. The greatest overlap is observed at the midpoint with 26% of the 7 dpi control females and 29% of the MPTP-treated 7 dpi female goldfish. This is followed by the overlap at point +1.2 with 2% of the 7 dpi control females and 3% of the 7 dpi females. The smallest overlap is observed at point +2.4 with 2% of the 7 dpi control females and 1% of the MPTP-treated 7 dpi females.

Similarly, in the male control and MPTP-treated 7 dpi groups (Supplementary Figure 3.7B) are found separately in the canonical and classificatory discriminant analysis although there are two points of sex overlap along the x-axis. To elaborate, the control and MPTP-treated 7 dpi male groups cluster at opposite ends of the x-axis. The male control 7 dpi group clusters mostly towards the positive end spanning from -0.75 to 3.75 whereas the 7 dpi MPTP-treated male group clusters mostly towards the negative end spanning from 0.75 to -5.75. This indicates a distinction in the expression pattern of nestin based on treatment. However, there are two points of overlap at point -0.75 and point +0.75. The +0.75 point on the x-axis has the greatest overlap with 22% of the 7 dpi control males and 20% of the MPTP-treated 7 dpi male goldfish. The smallest overlap is observed at point -0.75 with 10% of the 7 dpi control males and 11% of the MPTP-treated 7 dpi male goldfish. When combining both sexes of control and MPTP-treated goldfish at 7 dpi and analyzing the entire group for sex differences (Supplementary Figure 3.7C), there are no clear distinctions or separations between groups based on sex or treatment as there are many points of overlap. The general trends observed are the MPTP-treated female 7 dpi goldfish are clustering at the most positive end of the x-axis spanning from -1.5 to +6.0. The control 7 dpi male goldfish are clustering at the most negative end of the x-axis spanning from +1.5 to -6.0. The MPTP-treated and the control 7 dpi male goldfish are more neutral and have a bell-shaped motif surrounding the midpoint between -1.5 and 1.5. However, there are three points of overlap where all 4 groups are found near the midpoint from -1.5 to +1.5.

3.3.10.5. Control versus MPTP-treated female and male goldfish at 4 and 7 dpi

The female control and MPTP-treated groups at both 4 dpi and 7 dpi (Supplementary Figure 3.8A) are not classified separately in the canonical and classificatory discriminant analysis when analyzing the entire group for sex differences. There are no clear distinctions or separations between groups as there are many points of overlap along the x-axis. The general trends observed are the MPTP-treated female 7 dpi goldfish are clustering at the most positive end of the x-axis spanning from -0.6 to 5.4 and has the highest positive value of 5.4. In comparison, the control female 4 dpi goldfish has the most negative value at -4.2 but has a wide-range distribution from 3 to -4.2. The MPTP-treated female 4 dpi and control female 7 dpi cluster more towards the negative end of the x-axis spanning from 0.6 to -1.8 and 1.8 to -3 respectively. No other distinctions are evident based on the canonical analysis. The greatest overlap is observed at -0.6 where all four groups are located. The male control and MPTP-treated groups at both 4 dpi and 7 dpi (Supplementary Figure 3.8B) are not classified separately in the canonical and classificatory discriminant analysis when analyzing the entire group for sex differences. There are no clear distinctions or separations between groups as there are many points of overlap along the x-axis. The general trends observed are the MPTP-treated male 4 dpi goldfish are clustering at the most positive end of the x-axis spanning from -0.75 to 3.75 and has the highest positive value of 3.75. In comparison, the control female 7 dpi goldfish has the most negative value at -4.2 and spans the x-axis from 0.75 to -6.75. The control and MPTP-treated males at 4 dpi cluster more towards the midpoint spanning the x-axis from -2.25 to -0.75 and -2.25 to 2.25 respectively. No other

distinctions are evident based on the canonical analysis. The greatest overlap is observed at +0.75 where all four groups are located.

When combining both sexes of control and MPTP-treated goldfish at 4 dpi and 7 dpi and analyzing the entire group for sex differences (Supplementary Figure 3.8C), some goldfish groups are separated on opposite ends of the x-axis based on sex and treatment groups. The control female 4 dpi and 7 dpi groups and the control male 4 dpi surround the midpoint of the x-axis from -0.75 to 2.25 and -0.75 to 0.75 respectively. On the other hand, the MPTP-treated groups cluster either on the positive or negative end of the axis in comparison to the controls. More specifically, the MPTP-treated female 4 dpi goldfish cluster towards the negative end spanning the x-axis from 2.25 to -5.75. The MPTP-treated male 4 dpi goldfish cluster toward the positive end of the x-axis spanning from -0.75 to 3.75. The MPTP-treated female 7 dpi group clusters towards the positive end of the x-axis spanning from -0.75 to 6.75 and has the highest positive value at 6.75. The control male 7 dpi groups cluster towards the negative end of the x-axis spanning from 0.75 to -6.75 and has the highest negative value at -6.75. Although there are several overlaps of groups with the largest overlap observed at -0.75, several trends can be observed as described above.

3.3.11. Principal component analysis (PCA) of nestin protein expression patterns

3.3.11.1. Control versus MPTP-treated female and male goldfish at 4 dpi

The scree plot (Supplementary Figure 3.1B) of control versus MPTP-treated 4 dpi female and male goldfish groups reveals that the first two components provide the greatest variability in the data set as the line straightens after the second component. The 3D plot (Fig. 3.14A) considers the first three principal components for the nestin

expression pattern in 4 dpi female and male control and MPTP-treated goldfish groups. The telencephalon has the greatest variance in comparison to the other data points. But, on axis 3 the pituitary followed by the hypothalamus are on the positive areas; followed by the rest of the five tissues on the negative side of axes 3. In other words, the telencephalon and pituitary are clustering in opposite directions mainly on axes 2 and 3; and the two against the rest of the eight variables. The optic tectum is also high on axis 3 whereas the midbrain, vagal lobe, brainstem and cerebellum are among the highest on axis 1 and lowest on axis 3.

3.3.11.2. Control versus MPTP-treated female and male goldfish at 7 dpi

The scree plot (Supplementary Figure 3.1C) of control versus MPTP-treated 7 dpi female and male goldfish groups reveals that the first two components provide the greatest variability in the data set as the line straightens after the second component. The 3D plot (Fig. 3.14B) considers the first three principal components for the nestin expression pattern in 7 dpi female and male control and MPTP-treated goldfish groups. The pituitary has the greatest variance in comparison to the other data points. But, on axis 3 the telencephalon followed by the hypothalamus and vagal lobe are on the positive areas; followed by the rest of the four tissues on the negative side of axes 3. In other words, the pituitary is clustering in the opposite direction to the telencephalon and hypothalamus mainly on axes 2 and 3; and the three against the rest of the eight variables. The midbrain, optic tectum, brainstem and cerebellum are among the highest on axis 1 and lowest on axis 3.

3.3.11.3. Control versus MPTP-treated female and male goldfish at 4 and 7 dpi

The scree plot of 4 and 7 dpi female control and MPTP-treated goldfish groups reveals that the first two components provide the greatest variability in the data set as the line straightens after the second component. The 2D plot (Fig. 3.14C) obtained from PCA illustrates that the telencephalon is projected on the positive side of both x- and y-axes. The eigenvectors of the telencephalon also points in a different principal direction in comparison to the other groupings. The telencephalon corresponds to the greatest positive direction on axis 2 having the most positive variation in comparison to the other data points. The hypothalamus also contributes in the positive area, but very close to axis 1 whereas the cerebellum, vagal lobe, optic tectum, midbrain, pituitary and brainstem contribute in the negative area of axis 2 but remain very close in proximity to axis 1. Therefore, when comparing control and MPTP-treated female goldfish at 4 and 7 dpi, the plot illustrates that the data set is best classified based on the expression pattern of nestin in the telencephalon. The telencephalon tissue has the greatest variance and best describe the protein distribution pattern.

The 3D plot (Fig. 3.14D) considers the first three principal components for the nestin expression pattern in 4 and 7 dpi female control and MPTP-treated goldfish groups. As seen in Fig. 3.14C, the telencephalon has the greatest variance in comparison to the other data points and provides further validity of the results obtained from the 2D plot. But, on axis 3 the pituitary followed by the hypothalamus and vagal lobe are on the positive areas; followed by the rest of the four tissues on the negative side of axes 3. In other words, the telencephalon and pituitary are clustering in opposite directions mainly on axes 2 and 3; and the two against the rest of the eight variables. The hypothalamus and

vagal lobe are also high on axis 3 whereas the optic tectum, cerebellum, brainstem and midbrain are among the highest on axis 1 and lowest on axis 3.

The scree plot of 4 and 7 dpi male control and MPTP-treated goldfish groups reveals that the first two components provide the greatest variability in the data set as the line straightens after the second component. The 2D plot (Supplementary Figure 3.9A) obtained from PCA illustrates that the pituitary is projected on the positive side of both x- and y-axes. The eigenvectors of the pituitary also points in a different principal direction in comparison to the other groupings. The pituitary corresponds to the greatest positive direction on axis 2 having the most positive variation in comparison to the other data points. The hypothalamus also contributes in the positive area, but very close to axis 1 whereas the optic tectum, telencephalon, midbrain, brainstem, vagal lobe and cerebellum contribute in the negative area of axis 2 but remain very close in proximity to axis 1. Therefore, when comparing control and MPTP-treated male goldfish at 4 and 7 dpi, the plot illustrates that the data set is best classified based on the expression pattern of nestin in the pituitary. The pituitary has the greatest variance and best describes the nestin protein distribution pattern.

The 3D plot (Supplementary Figure 3.9C) considers the first three principal components for the nestin expression pattern in 4 and 7 dpi male control and MPTP-treated goldfish groups. As seen in Supplementary Figure 3.9A, the pituitary has the greatest variance in comparison to the other data points and provides further validity of the results obtained from the 2D plot. But, on axis 3 the brainstem followed by the vagal lobe are on the positive areas; followed by the rest of the five tissues on the negative side of axes 3. In other words, the pituitary and brainstem are clustering in opposite directions

on all axes 1,2 and 3; and the two against the rest of the eight variables. The vagal lobe is also high on axis 3 whereas the cerebellum, hypothalamus, optic tectum, cerebellum, and midbrain are among the highest on axis 1 and lowest on axis 3.

The scree plot of 4 and 7 dpi male and female control and MPTP-treated goldfish groups reveals that the first two components provide the greatest variability in the data set as the line straightens after the second component. The 2D plot (Supplementary Figure 3.9B) obtained from PCA illustrates that the telencephalon is projected on the positive side of both x- and y-axes. The eigenvectors of the telencephalon also points in a different principal direction in comparison to the other groupings. The telencephalon corresponds to the greatest positive direction on axis 2 having the most positive variation in comparison to the other data points. On the other hand, the hypothalamus, optic tectum, brainstem, cerebellum, midbrain, vagal lobe and pituitary contribute in the negative area of axis 2 but remain very close in proximity to axis 1. Therefore, when comparing control and MPTP-treated female and male goldfish at 4 and 7 dpi, the plot illustrates that the data set is best classified based on the expression pattern of nestin in the telencephalon. The telencephalon tissue has the greatest variance and best describe the protein distribution pattern. Overall, when comparing control and MPTP-treated male and female goldfish at 4 and 7 dpi, the plot illustrates that the data set is best classified based on the expression pattern of nestin in the telencephalon. This tissue has the greatest variance and best describes the distribution pattern.

The 3D plot (Supplementary Figure 3.9D) considers the first three principal components for the nestin expression pattern in 4 and 7 dpi male and female control and MPTP-treated goldfish groups. As seen in Supplementary Figure 3.9B, the telencephalon

has the greatest variance in comparison to the other data points and provides further validity of the results obtained from the 2D plot. But, on axis 3 the pituitary followed by the hypothalamus are on the positive areas; followed by the rest of the five tissues on the negative side of axes 3. In other words, the telencephalon and pituitary are clustering in opposite directions mainly on axes 2 and 3; and the two against the rest of the eight variables. The hypothalamus is also high on axis 3 whereas the optic tectum, vagal lobe, midbrain, brainstem and cerebellum are among the highest on axis 1 and lowest on axis 2 and 3.

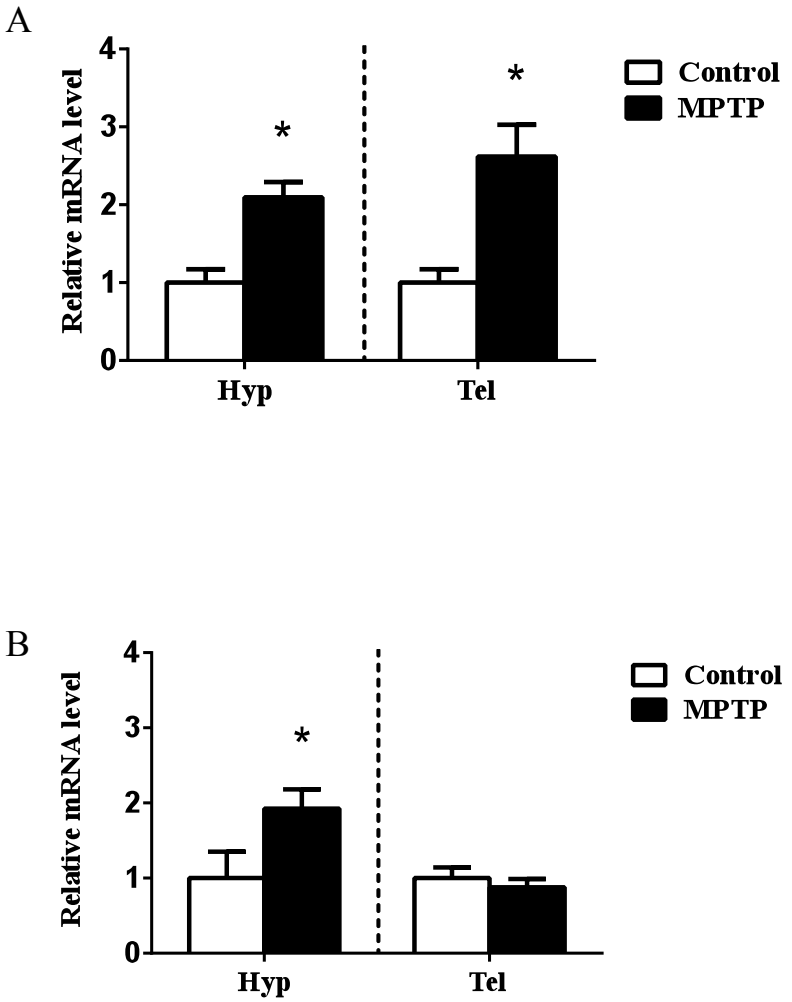

Figure 3.1. Quantitative real-time PCR analysis showing variations in the relative amounts of the mRNA encoding genes of goldfish *ß-actin* in the telencephalon and hypothalamus of female goldfish injected with A) MPTP (4 dpi) and B) MPTP (7 dpi). Bars represent the mean + SEM in 8 different cDNA samples; values for each sample were determined in duplicate. Student T-test was performed to test the effects of MPTP.

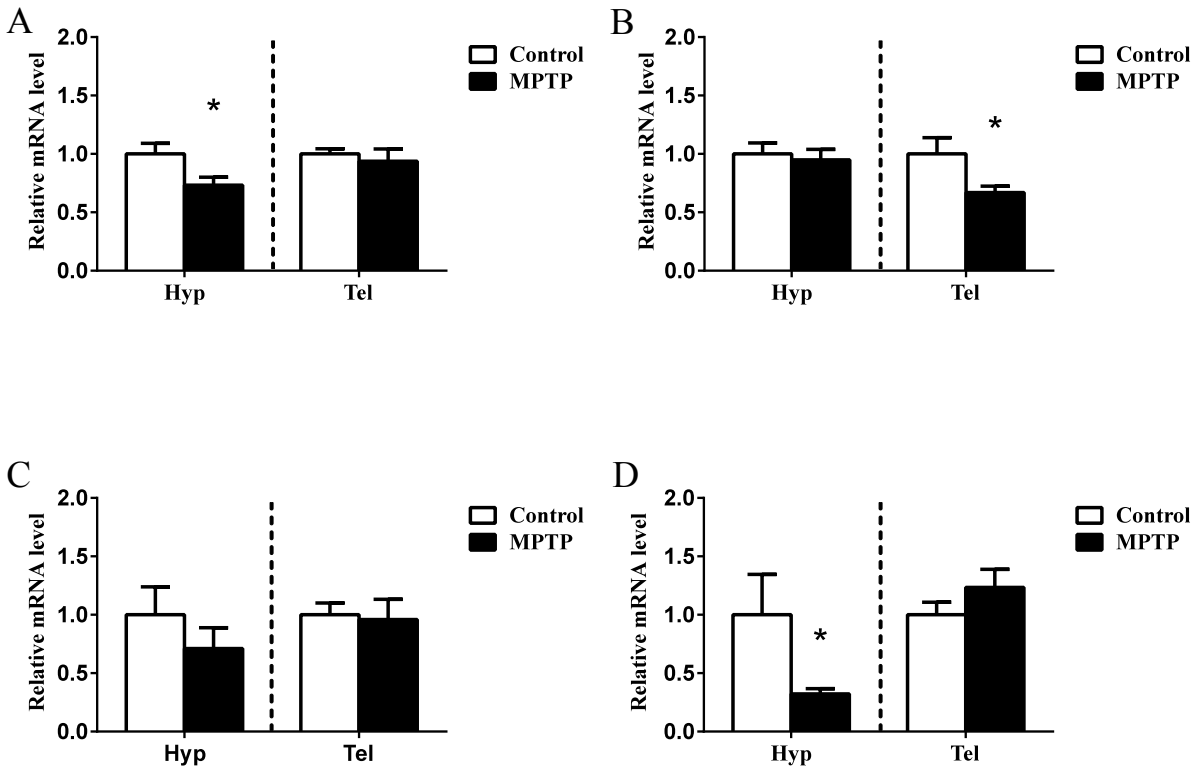

Figure 3.2. Quantitative real-time PCR analysis showing variations in the relative amounts of the mRNA encoding genes of goldfish A) *nesall*, B) *nesa*, C) *nesb* and D) *nesc* in the telencephalon and hypothalamus of female goldfish injected with MPTP (4 dpi). Bars represent the mean + SEM in 8 different cDNA samples; values for each sample were determined in duplicate. Student T-test was performed to test the effects of MPTP.

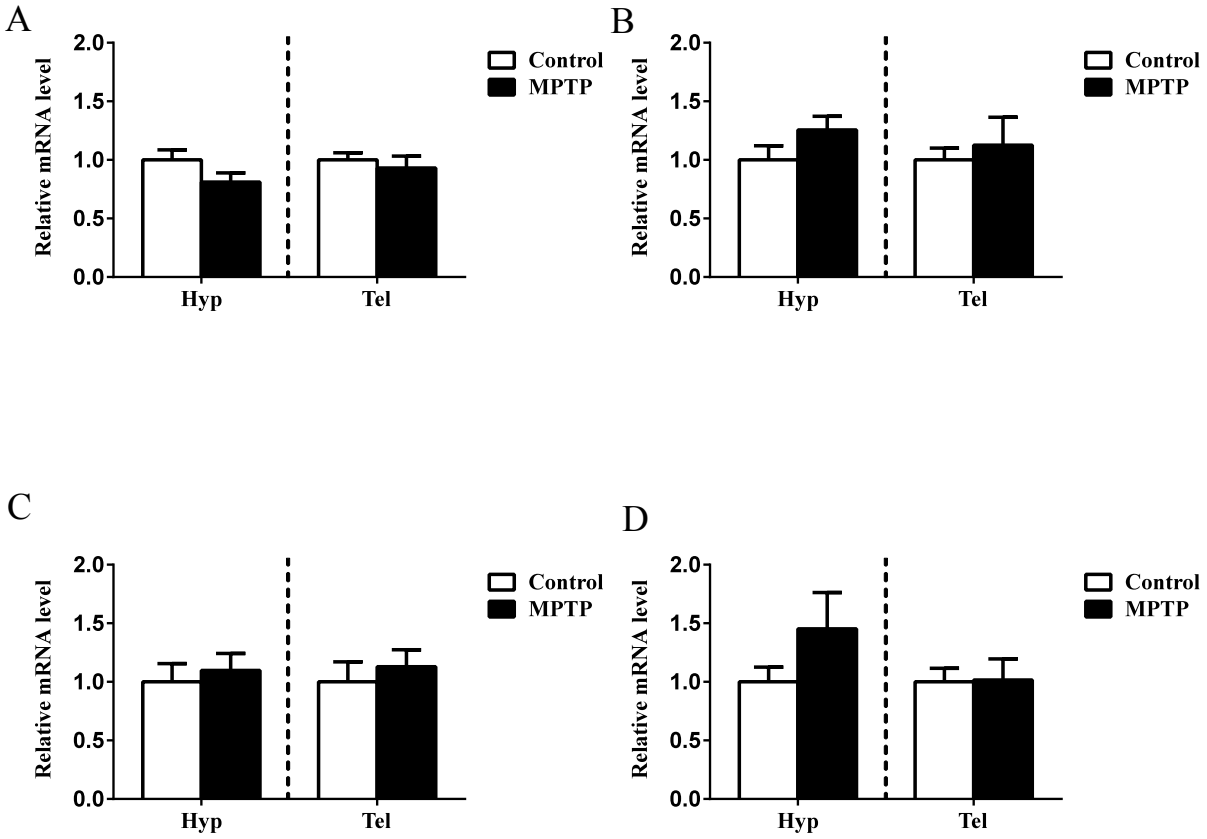

Figure 3.3. Quantitative real-time PCR analysis showing variations in the relative amounts of the mRNA encoding genes of goldfish A) *nesall*, B) *nesa*, C) *nesb* and D) *nesc* in the telencephalon and hypothalamus of female goldfish injected with MPTP (7 dpi). Bars represent the mean + SEM in 8 different cDNA samples; values for each sample were determined in duplicate. Student T-test was performed to test the effects of MPTP.

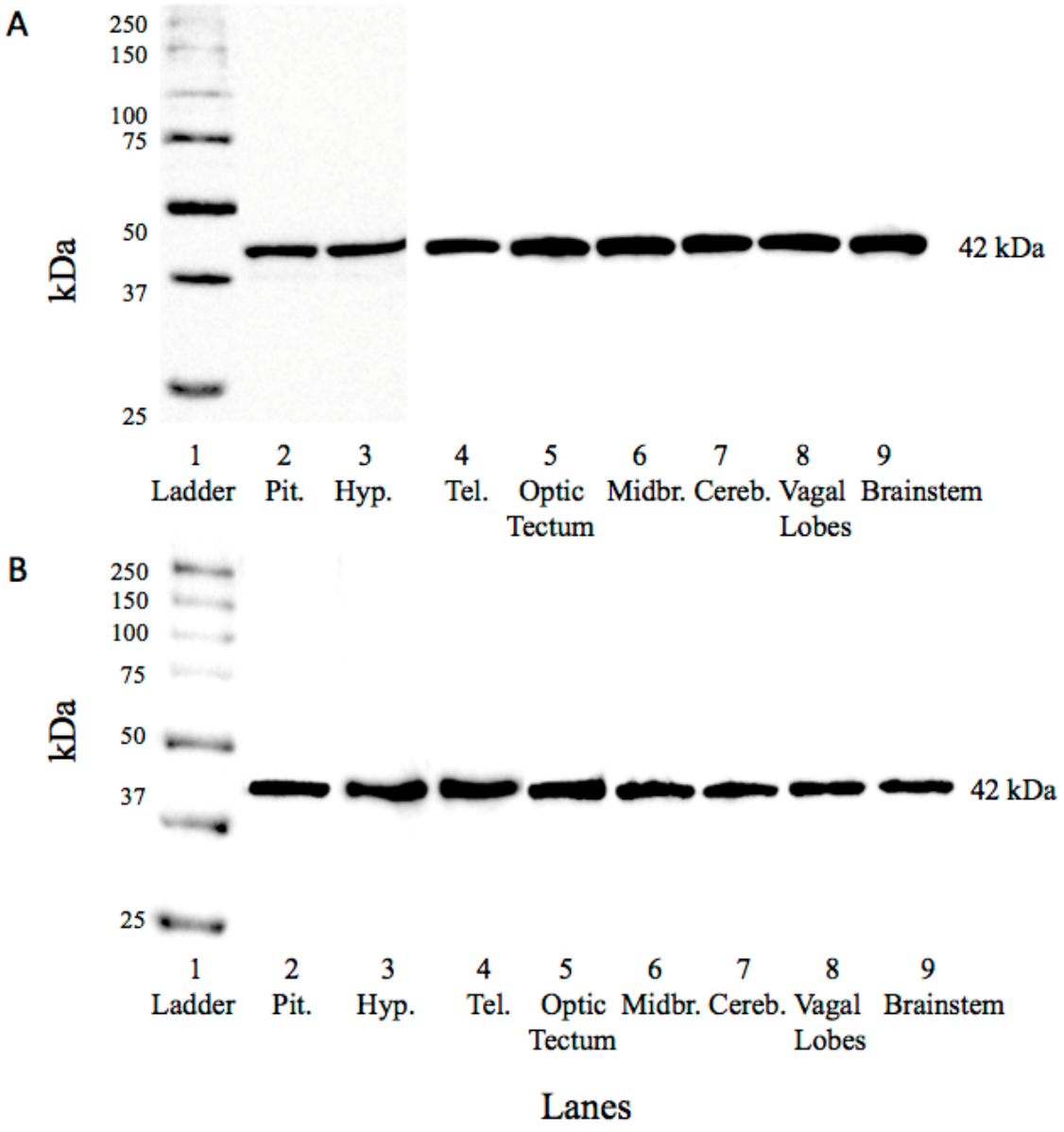

Figure 3.4. Western blot analysis of ß-actin protein distribution patterns (42 kDa) in the brain and whole pituitary of A) female and B) male goldfish. Lane 1 is the standard ladder, lane 2 is goldfish pituitary (Pit), lane 3 is hypothalamus (Hyp), lane 4 is telencephalon (Tel), lane 5 is optic tectum, lane 6 is midbrain (Midbr), lane 7 cerebellum (Cereb), lane 8 is vagal lobes and lane 9 is brainstem.

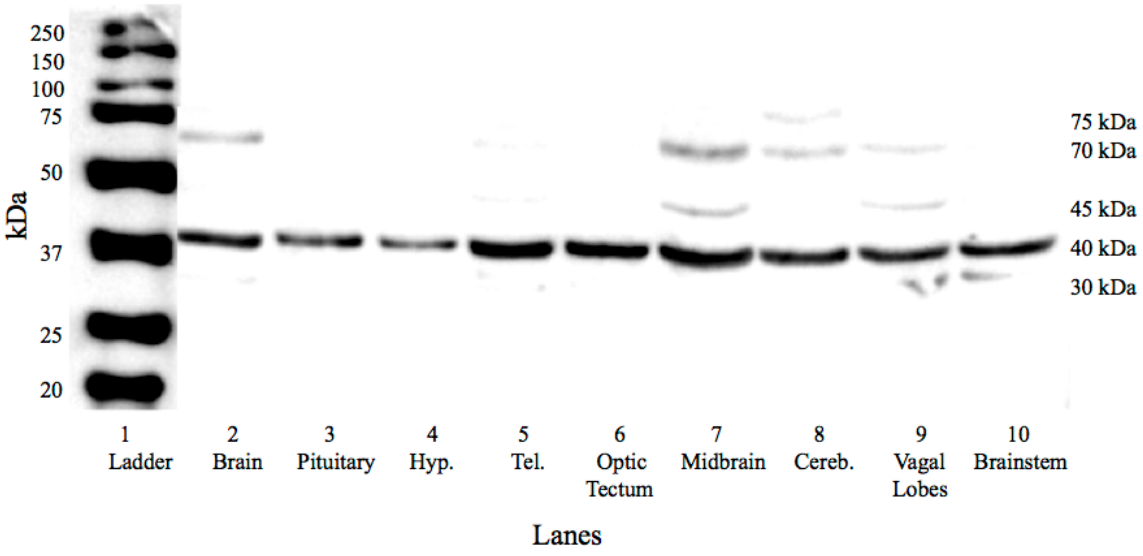

Figure 3.5. Western blot analysis of nestin protein distribution patterns in the goldfish male brain and whole pituitary. Lane 1 is the standard ladder, lane 2 is a whole-brain protein extract, lane 3 is goldfish pituitary, lane 4 is hypothalamus (Hyp), lane 5 is telencephalon (Tel), lane 6 is optic tectum, lane 7 is midbrain, lane 8 cerebellum (Cereb), lane 9 is vagal lobes and lane 10 is brainstem.

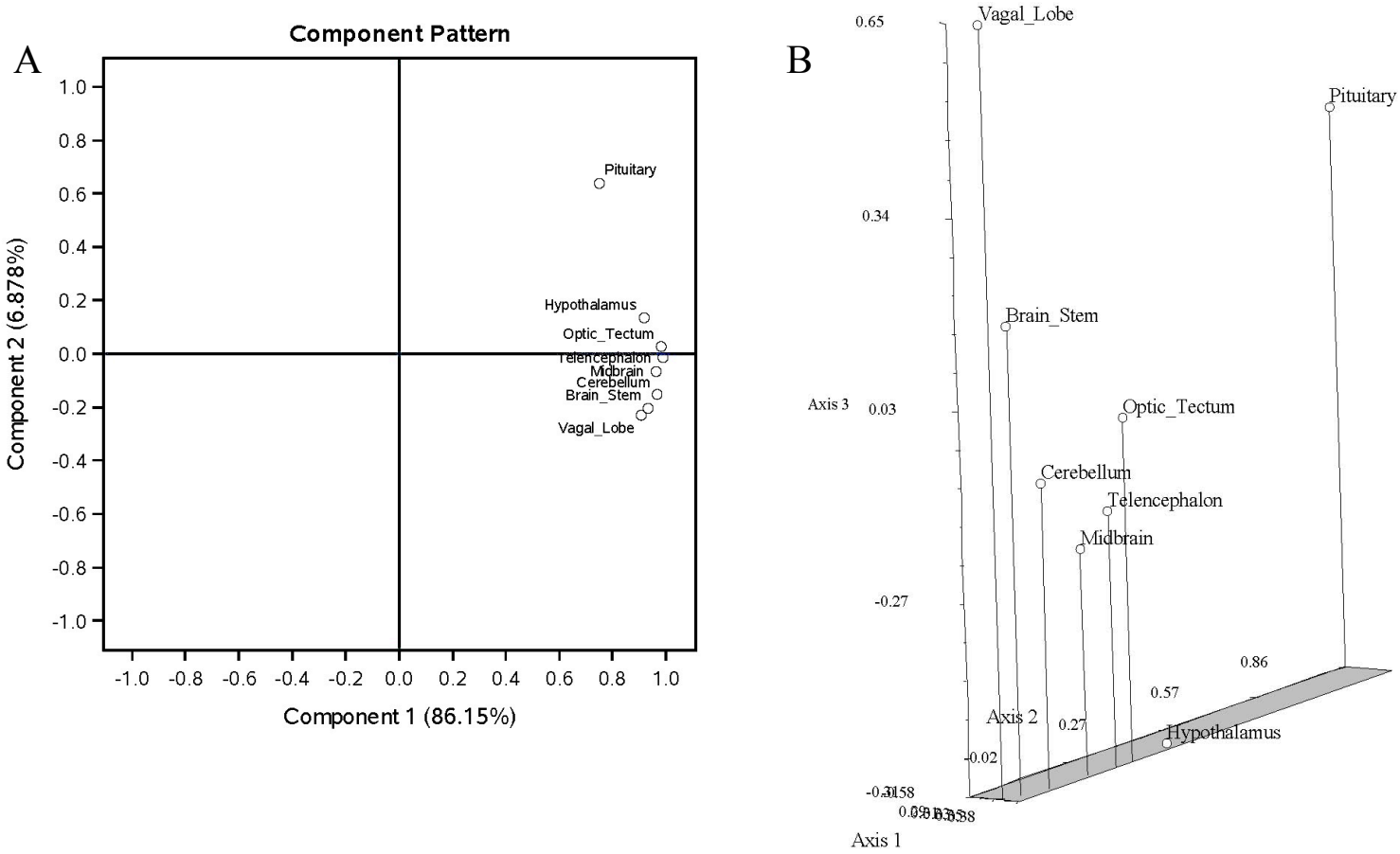

Figure 3.6. A) Canonical analysis of nestin protein expression data obtained from western blots separating the variables pituitary, hypothalamus, telencephalon, optic tectum, midbrain, cerebellum, vagal lobe and brain stem of male goldfish (n=9) on a 2D plot. Variation explained as percent in brackets. B) Three-dimensional score plot of the first three principal components for the nestin protein expression in the male goldfish group (n=9) separating the factors pituitary, hypothalamus, telencephalon, optic tectum, midbrain, cerebellum, vagal lobe and brain stem. Variance of axis 1 explained is 86.15%; axis 2 is 6.88% and axis 3 is 2.71%.

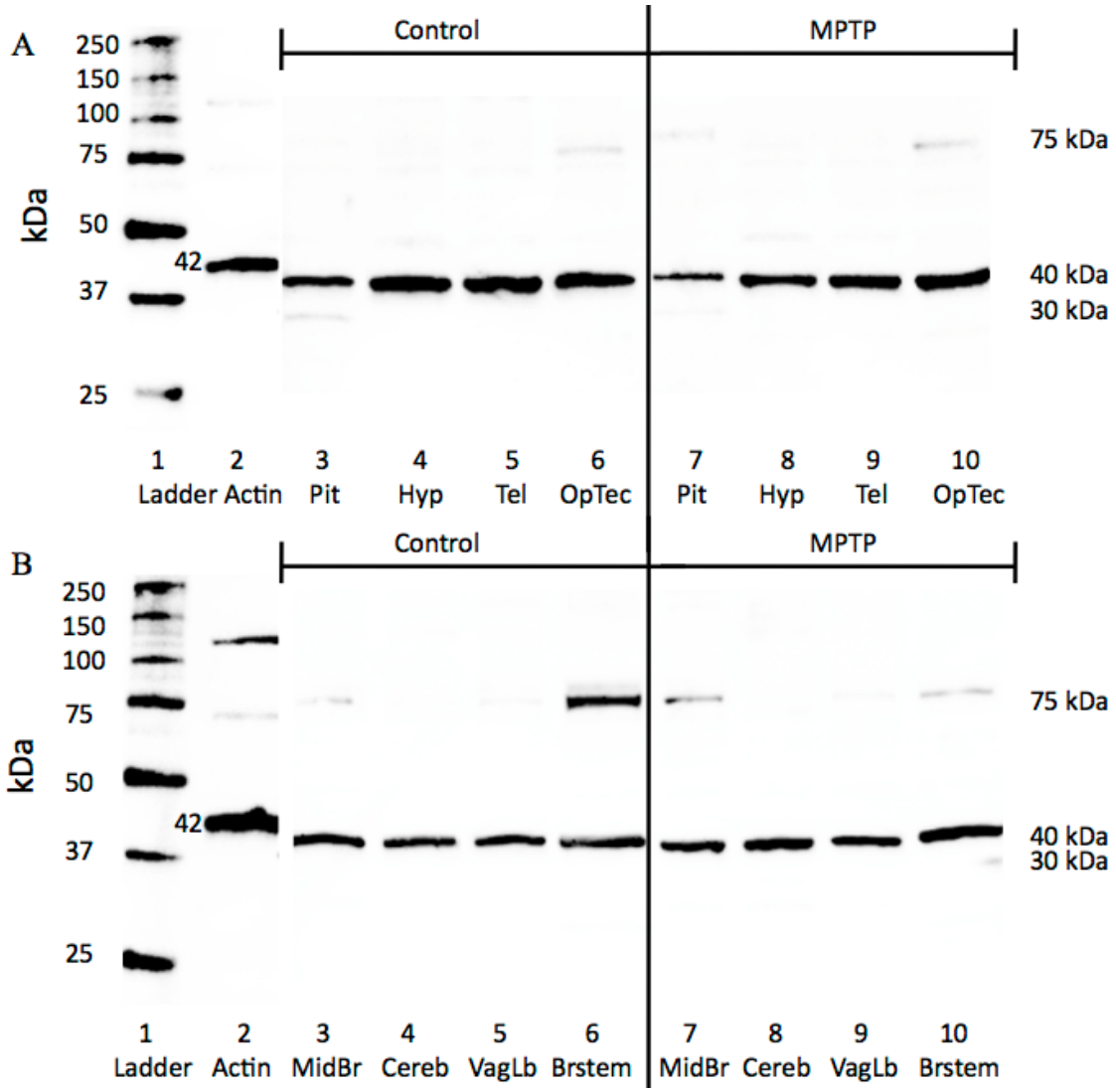

Figure 3.7. Western blot analysis of nestin protein distribution patterns in control and MPTP-treated goldfish in the female brain and whole pituitary at 4 dpi. A) Lane 1 is the standard ladder, lane 2 is the positive control of ß-actin at 42 kDa, lanes 3 to 6 represent female control pituitary (Pit), hypothalamus (Hyp), telencephalon (Tel) and optic tectum (OpTec) in sequential order. Lanes 7 to 10 are MPTP-treated female pituitary, hypothalamus, telencephalon and optic tectum in sequential order. B) Lane 1 is the standard ladder, lane 2 is the positive control of ß-actin at 42 kDa, lanes 3 to 6 represent female control midbrain (MidBr), cerebellum (Cereb), vagal lobes (VagLb) and brainstem (Brstem) in sequential order. Lanes 7 to 10 are MPTP-treated female midbrain, cerebellum, vagal lobes and brainstem in sequential order.

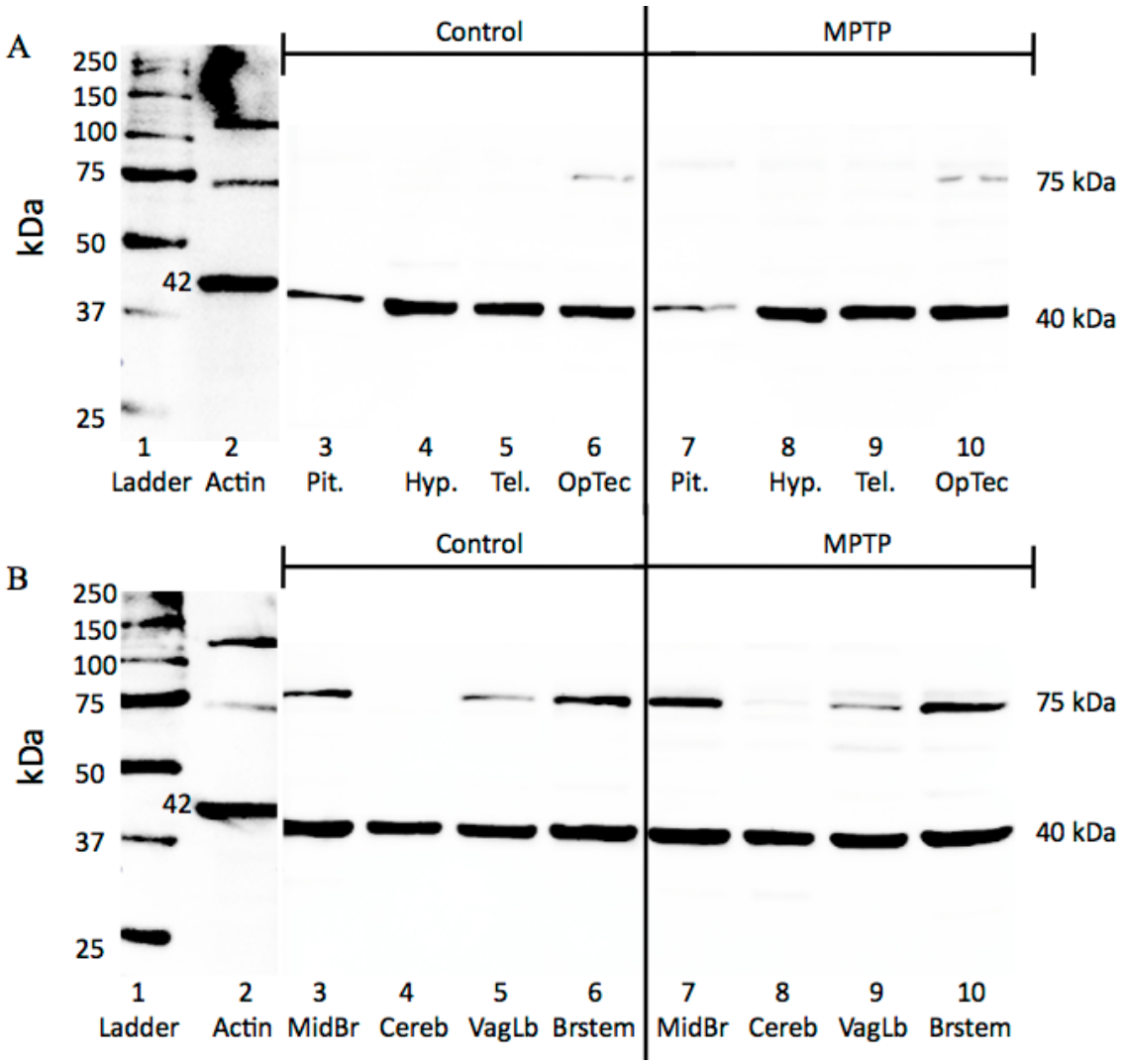

Figure 3.8. Western blot analysis of nestin protein distribution patterns in control and MPTP-treated goldfish in the female brain and whole pituitary at 7 dpi. A) Lane 1 is the standard ladder, lane 2 is the positive control of ß-actin at 42 kDa, lanes 3 to 6 represent female control pituitary (Pit), hypothalamus (Hyp), telencephalon (Tel) and optic tectum (OpTec) in sequential order. Lanes 7 to 10 are MPTP-treated female pituitary, hypothalamus, telencephalon and optic tectum in sequential order. B) Lane 1 is the standard ladder, lane 2 is the positive control of ß-actin at 42 kDa, lanes 3 to 6 represent female control midbrain (MidBr), cerebellum (Cereb), vagal lobes (VagLb) and brainstem (Brstem) in sequential order. Lanes 7 to 10 are MPTP-treated female midbrain, cerebellum, vagal lobes and brainstem in sequential order.

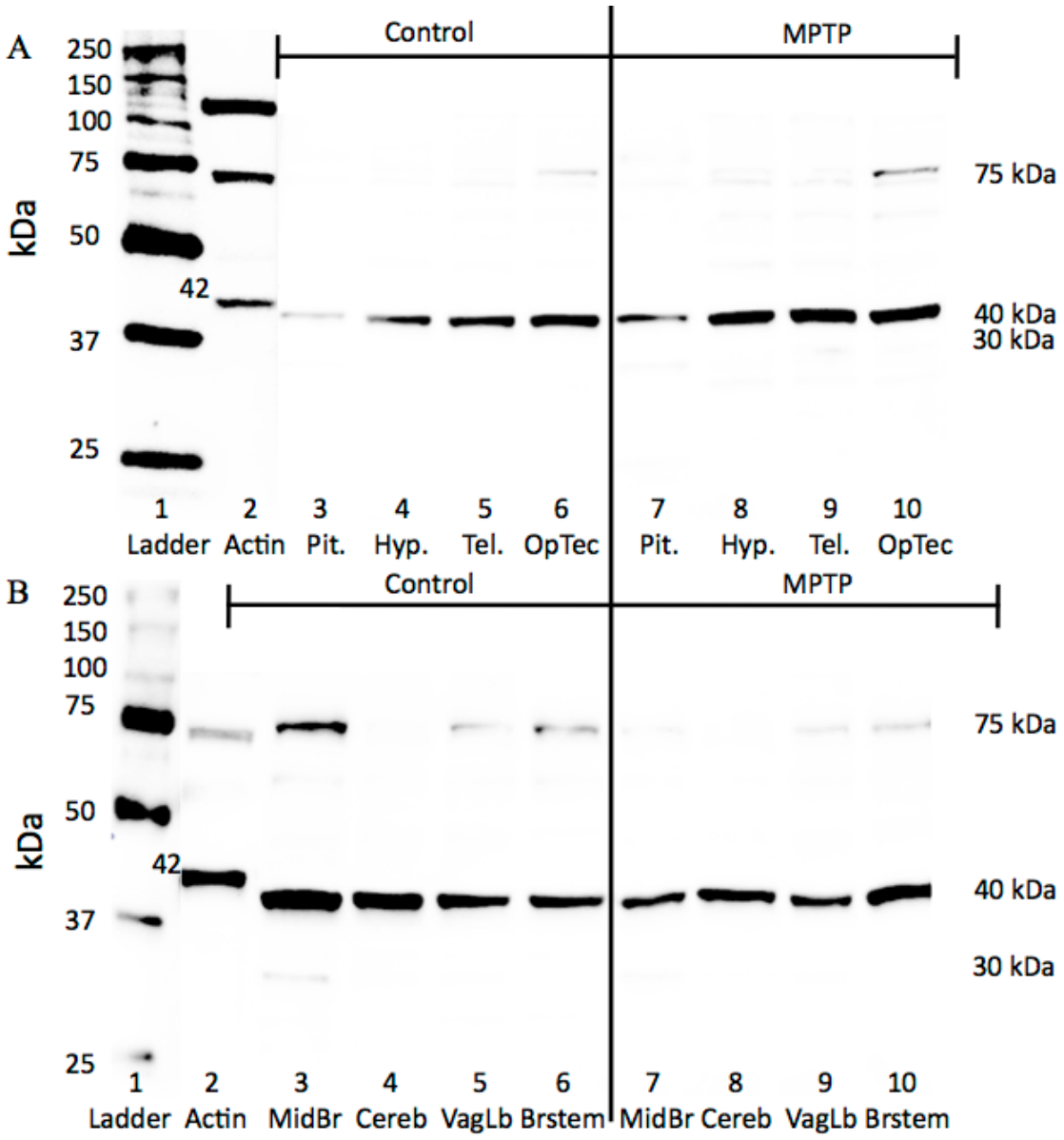

Figure 3.9. Western blot analysis of nestin protein distribution patterns in control and MPTP-treated goldfish in the male brain and whole pituitary at 4 dpi. **A)** Lane 1 is the standard ladder, lane 2 is the positive control of ß-actin at 42 kDa, lanes 3 to 6 represent male control pituitary (Pit), hypothalamus (Hyp), telencephalon (Tel) and optic tectum (OpTec) in sequential order. Lanes 7 to 10 are MPTP-treated male pituitary, hypothalamus, telencephalon and optic tectum in sequential order. **B)** Lane 1 is the standard ladder, lane 2 is the positive control of ß-actin at 42 kDa, lanes 3 to 6 represent male control midbrain (MidBr), cerebellum (Cereb), vagal lobes (VagLb) and brainstem (Brstem) in sequential order. Lanes 7 to 10 are MPTP-treated male midbrain, cerebellum, vagal lobes and brainstem in sequential order.

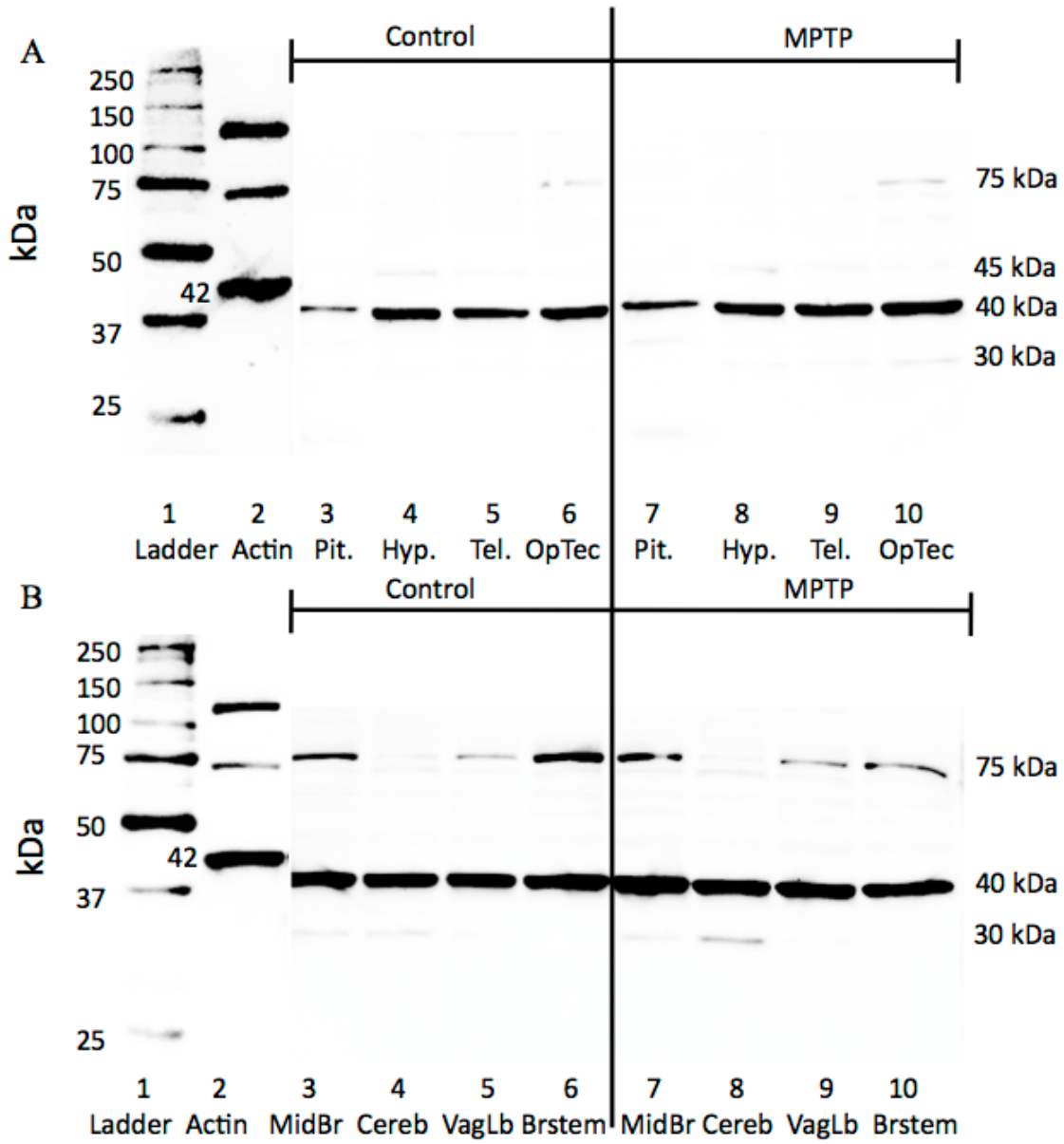

Figure 3.10. Western blot analysis of nestin protein distribution patterns in control and MPTP-treated goldfish in the male brain and whole pituitary at 7 dpi. **A)** Lane 1 is the standard ladder, lane 2 is the positive control of ß-actin at 42 kDa, lanes 3 to 6 represent male control pituitary (Pit), hypothalamus (Hyp), telencephalon (Tel) and optic tectum (OpTec) in sequential order. Lanes 7 to 10 are MPTP-treated male pituitary, hypothalamus, telencephalon and optic tectum in sequential order. **B)** Lane 1 is the standard ladder, lane 2 is the positive control of ß-actin at 42 kDa, lanes 3 to 6 represent male control midbrain (MidBr), cerebellum (Cereb), vagal lobes (VagLb) and brainstem (Brstem) in sequential order. Lanes 7 to 10 are MPTP-treated male midbrain, cerebellum, vagal lobes and brainstem in sequential order.

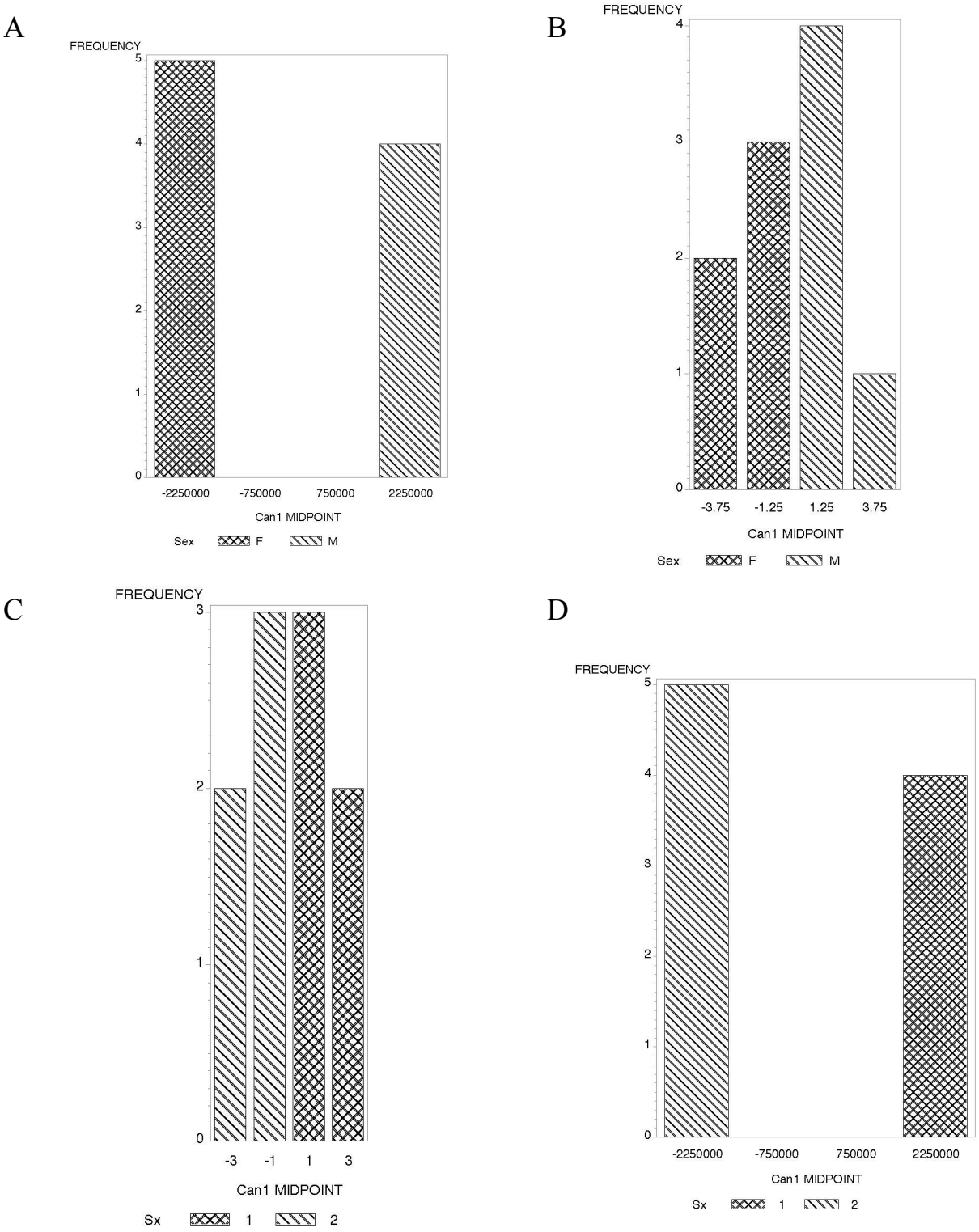

Figure 3.11. Canonical and classificatory discriminant analysis of ß-actin protein expression obtained from western blots of A) control female (n=5; Sex=F) and male (n=4; Sex=M) goldfish at 4 dpi of 0.6% saline; B) control female (n=5; Sex=F) and male (n=5; Sex=M) goldfish at 7 dpi of 0.6% saline; C) control female (n=5; Sx=1) and MPTP-treated female (n=5; Sx=2) goldfish at 4 dpi and D) control male (n=4; Sx=1) and MPTP-treated male (n=5; Sx=2) goldfish at 4 dpi. The bar graph shows the distribution of ß-actin based on sex and treatment.

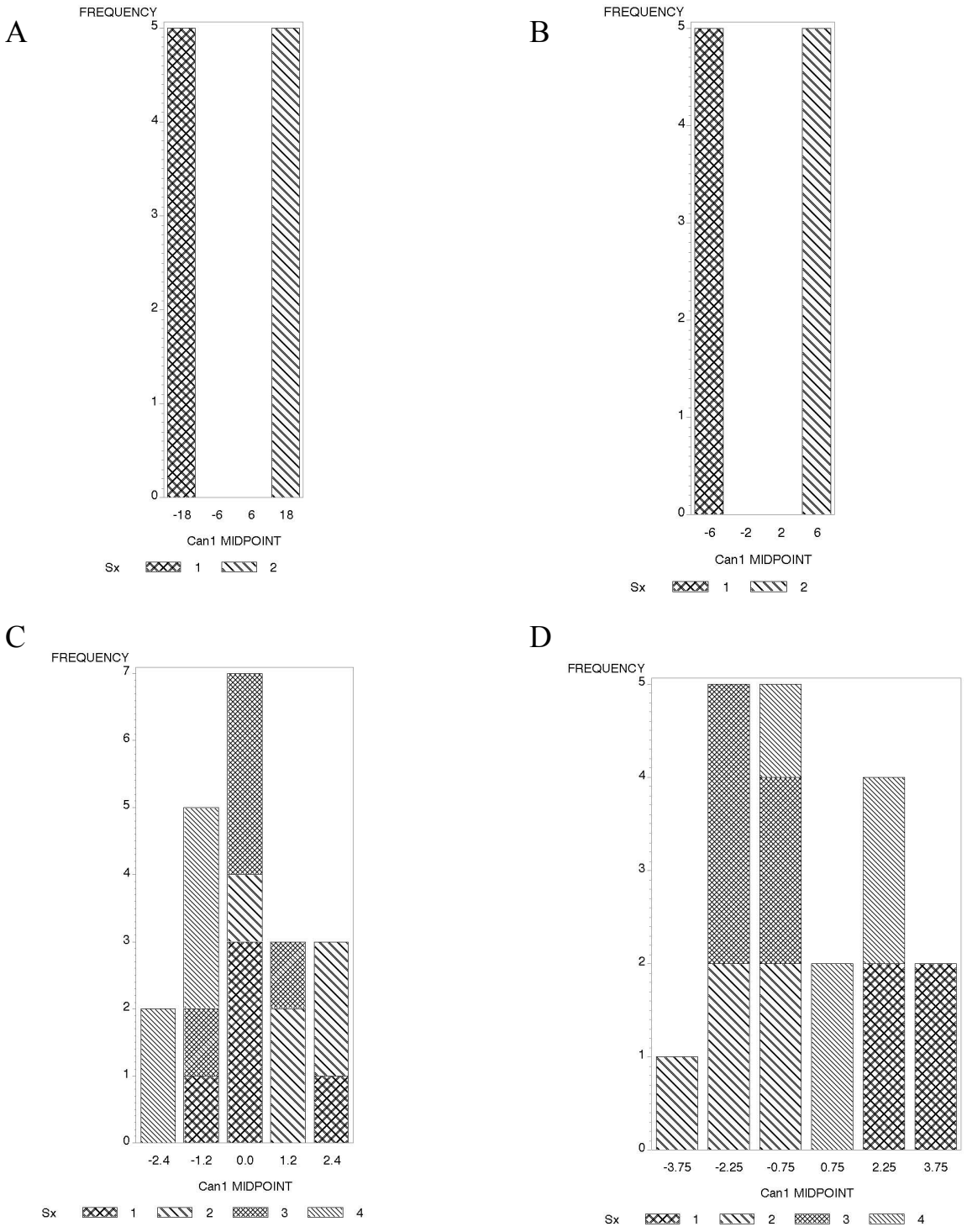

Figure 3.12. Canonical and classificatory discriminant analysis of ß-actin protein expression obtained from western blots of A) control female (n=5; Sx=1) and MPTP-treated female (n=5; Sx=2) goldfish at 7 dpi; B) control male (n=5; Sx=1) and MPTP-treated male (n=5; Sx=2) goldfish at 7 dpi; C) control female goldfish at 4 dpi (n=5; Sx=1); MPTP-treated female at 4 dpi (n=5; Sx=2); control female at 7 dpi (n=5; Sx=3); and MPTP-treated female at 7 dpi (n=5; Sx=4) and D) control male goldfish at 4 dpi (n=4; Sx=1); MPTP-treated male at 4 dpi (n=5; Sx=2); control male at 7 dpi (n=5; Sx=3); and MPTP-treated male at 7 dpi (n=5; Sx=4). The bar graph shows the distribution of ß-actin based on sex and treatment.

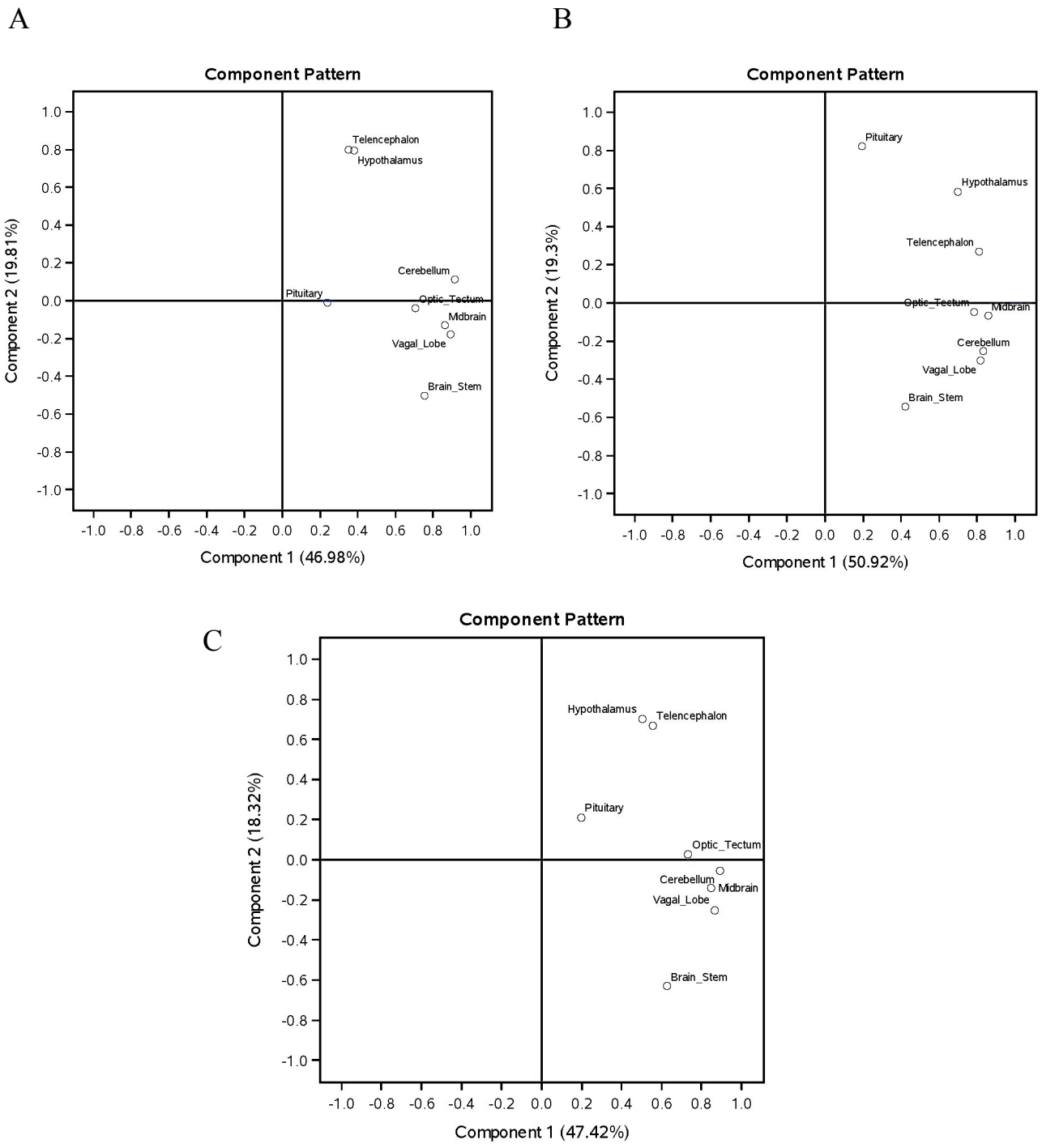

Figure 3.13. Canonical analysis of ß-actin protein expression data obtained from western blots of A) control and MPTP-treated female goldfish at 4 dpi (n=10) and 7 dpi (n=10); B) control and MPTP-treated male goldfish at 4 dpi (n=9) and 7 dpi (n=10) and C) control and MPTP-treated male goldfish at 4 dpi (n=9) and 7 dpi (n=10) separating the variables pituitary, hypothalamus, telencephalon, optic tectum, midbrain, cerebellum, vagal lobe and brainstem on a 2D plot. Variation explained as percent in brackets.

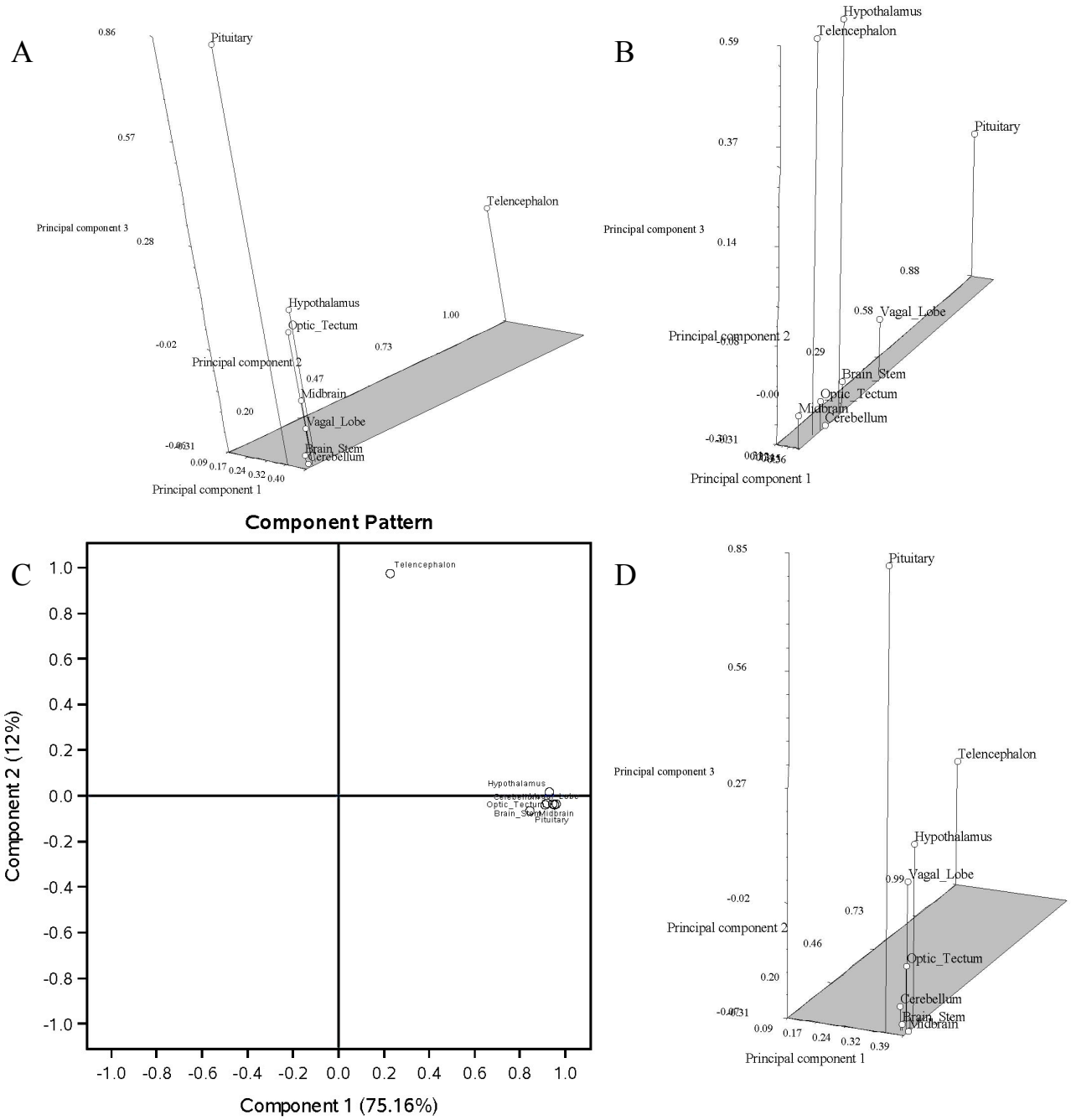

Figure 3.14. Three-dimensional score plot of the first three principal components for the nestin protein expression in the A) control and MPTP-treated 4 dpi female (n=10) and male (n=9) goldfish groups and B) control versus MPTP-treated 7 dpi female (n=10) and male (n=10) goldfish groups separating the factors pituitary, hypothalamus, telencephalon, optic tectum, midbrain, cerebellum, vagal lobe and brainstem. In A) variance of principal component 1 explained is 75.49%; principal component 2 is 12% and principal component 3 is 5.97%. In B), variance of principal component 1 explained is 84.06%; principal component 2 is 5.27% and principal component 3 is 3.52%. C) Canonical analysis of nestin protein expression data obtained from western blots of control and MPTP-treated female goldfish at 4 dpi (n=10) and 7 dpi (n=10) illustrated on a 2D plot. Variation explained as percent in brackets. D) Three-dimensional score plot of nestin protein expression in the control and MPTP-treated female goldfish at 4 dpi (n=10) and 7 dpi (n=10). Variance of component 1 explained is 75.16%; component 2 is 12% and component 3 is 4.56%.

Table 3.1. Primers used for Real-Time RT-PCR (Fw, forward; Rv, reverse).

Primer Name	Primer Sequence (5'->3')
ß-actin Fw	CTGGGATGATATGGAGAAGA
ß-actin Rv	CCAGTAGTACGACCTGAAGC
Nestin Transcript All Fw	TTTGGCTAAGAGAGAAGGTTGG
Nestin Transcript All Rv	TTGAGTTGCTCTGTGGCTGT
Nestin Transcript A Fw	CTCTGGAGATGGAGAAGGACA
Nestin Transcript A Rv	AGTGCGAGAGGAGGTGATTG
Nestin Transcript B Fw	AGAGAAAACCAGCATCAAGTCC
Nestin Transcript B Rv	GGACCCCAACAATTTCCA
Nestin Transcript C Fw	TGCTCTGGAGATGGAGAAGG
Nestin Transcript C Rv	GAGAGGTTGTATTTTGCTGGTG

Total RNA was obtained from goldfish hypothalamus and telencephalon brain tissues at 4 and 7 dpi of control and MPTP-injected fish to perform real-time RT-PCR using the above primer sets.

Table 3.2. Nestin protein band frequency in the different brain tissues and pituitaries based on 10 female goldfish western blots (n=10) (Pit, pituitary; Hyp, hypothalamus; Tel, telencephalon; Mid, midbrain; Cereb, cerebellum; Brainst, brainstem). (Chapter 2 data table)

Nestin protein band	Pit.	Hyp.	Tel.	Optic tectum	Mid.	Cereb.	Vagal lobe	Brainst.
75 kDa	3	0	0	2	3	3	4	4
70 kDa	6	0	1	4	1	3	5	3
40 kDa	10	10	10	10	10	10	10	10
30 kDa	1	3	2	6	6	8	6	2

Table 3.3. Nestin protein band frequency in the different brain tissues and pituitaries based on 9 male goldfish western blots (n=9) (Pit, pituitary; Hyp, hypothalamus; Tel, telencephalon; Mid, midbrain; Cereb, cerebellum; Brainst, brainstem).

Nestin protein band	Pit.	Hyp.	Tel.	Optic tectum	Mid.	Cereb.	Vagal lobe	Brainst.
75 kDa	0	3	1	3	4	0	2	3
70 kDa	1	2	2	1	2	1	2	2
40 kDa	9	9	9	9	9	9	9	9
30 kDa	0	5	2	6	6	6	3	3

Table 3.4. Nestin protein band frequency in the different brain tissues and pituitaries based on 10 female MPTP-treated goldfish western blots (n=10) (Pit, pituitary; Hyp, hypothalamus; Tel, telencephalon; Mid, midbrain; Cereb, cerebellum; Brainst, brainstem).

Nestin protein band	Pit.	Hyp.	Tel.	Optic tectum	Mid.	Cereb.	Vagal lobe	Brainst.
75 kDa	2	0	1	3	7	2	3	4
70 kDa	4	2	2	4	6	5	5	3
40 kDa	10	10	10	10	10	10	10	10
30 kDa	2	5	3	3	4	4	4	2

Table 3.5. Nestin protein band frequency in the different brain tissues and pituitaries based on 10 male MPTP-treated goldfish western blots (n=10) (Pit, pituitary; Hyp, hypothalamus; Tel, telencephalon; Mid, midbrain; Cereb, cerebellum; Brainst, brainstem).

Nestin protein band	Pit.	Hyp.	Tel.	Optic tectum	Mid.	Cereb.	Vagal lobe	Brainst.
75 kDa	2	0	0	1	2	2	3	3
70 kDa	1	1	2	3	3	1	1	1
40 kDa	10	10	10	10	10	10	10	10
30 kDa	0	5	2	6	6	6	3	3

3.4. Discussion

The findings presented reveal sex differences in β–actin and nestin protein distribution in the goldfish brain. Protein distribution was also different from control in response to a neurotoxic insult. Western blotting revealed that nestin-ir protein bands are present in all female and male adult goldfish brain areas and there are sex-specific variations in protein expression patterns. The ~40 kDa band (nestin C) is the most common one and is found in all female and male brain tissues and whole pituitary. The sex differences are only observed in two of the three major nestin isoforms (~30 and 70 kDa) and one minor nestin isoform (~75 kDa). Amongst all the tissues studied, the pituitary was identified as a distinct tissue amongst the 8 observed in the male goldfish group in comparison to the telencephalon and pituitary in the female goldfish group.

We report for the first time male and female sex-specific differences in the expression of the neurogenic marker nestin. We speculate that the variation of nestin-ir observed in the pituitary is associated to nestin B protein levels in the brain. On the other hand, the variation of nestin-ir observed in the telencephalon is likely associated to nestin A protein levels. Further investigation revealed that the ~75 kDa band is also present in all tissues except for the hypothalamus and telencephalon in the female goldfish brain and the pituitary and cerebellum in male goldfish. The cerebellum is known as one of the most mitotically active tissues in teleost where sex-specific differences in neurogenesis exists (Zupanc *et al.* 2005; Ampatzis and Dermon 2007; Delgado and Schmachtenberg 2011). We speculate that the 75 kDa band represents the same protein (nestin A) as the ~70 kDA band but with a post-translational modification. The findings of this study

provide further evidence for tissue-dependent variations in neurogenesis in the male and female goldfish brains.

There were both individual and tissue-dependent variations in the presence and relative abundance of the different goldfish nestins (A, B and C) in both female and male fish in response to MPTP treatment. The findings of the study report on differences between sexes to repair or heal tissues following a neurotoxic insult. Firstly, western blotting revealed MPTP-treatment differences in the two major nestin isoforms (~30 and 70 kDa) and minor nestin isoform (~75 kDa). In the female control group, the ~30 kDa protein band (nestin B) is doubled in frequency in the optic tectum and cerebellum in comparison to the MPTP-treated female group. A decrease in the ~30 kDa band could represent a recruitment of nestin-positive cells to migrate and differentiate into neuronal cells to alleviate MPTP effects. The ~70 kDa band is also differentially expressed where it is absent in the female control hypothalamus in comparison to the MPTP-treated group thus could be inversely related to neurogenic ability in the adult goldfish brain. Furthermore, the ~75 kDa band is present in the telencephalon of MPTP-treated female fish versus the control and this ~75 kDa protein band is more than doubled in frequency in the midbrain in response to MPTP. The presence of the ~70 and 75 kDa bands indicates a differential expression pattern of nestin A protein in the goldfish brain. The telencephalon contains numerous cellular proliferation pools where nestin-positive cells could actively proliferate in preparation for tissue repair following injury (Zupanc and Clint 2003; Mahler and Driever 2007; März *et al.* 2010; Zupanc and Sîrbulescu 2011). Increased or re-expression of nestin following injury suggests a neuroregenerative ability in goldfish similar to the re-expression of nestin observed in the adult mammalian brain

after CNS injury (Lin *et al.* 1995). We can speculate that a change in nestin expression profiles following injury leads to an increase in cellular proliferation and migration to repair damaged cells and tissues. However, the nestin protein expression patterns were complex and necessitated both discriminant and PCA analyses to further investigate the variations observed in the goldfish brain.

At 4 dpi of MPTP, the telencephalon followed by the pituitary and hypothalamus were identified as distinct tissues amongst the 8 studied. Quantitative analysis also revealed a difference in all goldfish nestin mRNAs (*nesa, nesb* and *nesc*) in the MPTP-treated hypothalamus tissue at 4 dpi. Moreover, a significant difference in *nesa* mRNA levels was identified in the telencephalon. The complexity in the expression pattern and levels of nestin protein and mRNA in the telencephalon and hypothalamus suggests functional plasticity of these tissues in response to CNS injury. At 7 dpi of MPTP, the pituitary followed by the telencephalon and hypothalamus were identified as distinct tissues amongst the 8 studied. However, the mRNA levels of all goldfish *nestin* transcripts were not affected by MPTP treatment at this 7 dpi time-point. This suggests a quick turnover of nestin-positive cells in these tissues to alleviate the effects of MPTP-treatment. In mammals, it was suggested that astrocytes could recruit precursor cells for neuronal regeneration after injury (Lin *et al.* 1995). The goldfish brain is abundant in radial glia cells (RGCs) and these are activated following injury providing further evidence for the activation of neuroregeneration in fish (Frisen *et al.* 1995; Lin *et al.* 1995; Michalczyk and Ziman 2005; Pelligrini *et al.* 2007; Carmona *et al.* 2011; Blesa *et al.* 2012; Yokoyama *et al.* 2010).

Goldfish have the ability to regenerate damaged tissues and cells following chemical or physical lesions in the CNS (Contestable *et al.* 1979; Levine 1983; Scherer and Easter 1984; Zupanc and Sîrbulescu 2011). Thus, modifying nestin expression profiles in proliferative cellular pools could be a means to activate or a result of regenerative activity in the adult goldfish brain. Overall, the main determinants indentifying the telencephalon, hypothalamus and pituitary as the most variable tissues of nestin expression are the frequency and intensity of the nestin isoform bands. More specifically, based on the frequency of detection of the nestin-ir bands, nestin isoform A (~70 kDa) and B (~30 kDa) are affected by sex and MPTP-treatment in fish. Unfortunately the mechanisms implicated in the re-expression of nestin in fish after injury still remain unknown.

Western blotting also revealed sex-specific and MPTP-treatment variations in the protein expression pattern of ß-actin in both female and male adult goldfish brain. This suggests sex differences in the control of cytoskeletal dynamics in cells after injury. Extensive brain remodelling could result in variations in cytoskeletal IF organization and partitioning in response to the toxic effects of MPTP and to support cellular demands and activities such as cell migration and protein trafficking. A microarray analysis study supports this idea where DA regulates various biological functions such as cell differentiation, cytoskeleton organization and biogenesis as well as transport (Popesku *et al.* 2012). Discriminant and PCA analyses identified the telencephalon, hypothalamus and pituitary as having the greatest variance in ß-actin protein expression similar to the findings in nestin protein expression. This is important because the hypothalamus and telencephalon are neurogenetic tissues abundant in DA neuronal populations involved in

controlling reproduction and motor activity in fish (Peter and Paulencu 1980; Ball 1981; Kah *et al.* 1987; Hornby et *al.* 1987; Poli et *al.* 1990; Anglade *et al.* 1993; Goping et *al.* 1995; Olanow and Tatton 1999; Dufour *et al.* 2010). These findings are also supported by the quantitative analysis of *ß-actin* mRNA levels in the hypothalamus and telencephalon of female goldfish treated with MPTP. The ability of goldfish to alter cellular components on demand could explain, in part, their remarkable ability for brain plasticity and cellular remodelling.

In conclusion, we have provided evidence to the diversity of goldfish nestin isoform expression as well as ß-actin protein expression based on sex and following neurotoxic treatments. The presence and patterns of distribution of the isoforms were complex, revealing individual and tissue-dependent expression. This could suggest functional specializations of the nestins in the CNS during proliferative and cellular migration events. The most striking finding was the uniqueness of the telencephalon, hypothalamus and pituitary in both nestin and ß-actin expression patterns. Close examination of nestin protein expression patterns in female and male fish revealed that the ~30, 70 and 75 kDa bands were differentially expressed in the animals at the time they were sacrificed for tissue sampling. These data permit speculation of the roles of nestin isoforms in sex-specific neurogenesis and brain remodelling in various brain structures following injury. This brain remodelling could be indicative of the animal preparing or repairing tissues to be able to perform a specific animal behaviour. For example, the ablation of the forebrain or cerebellum in tilapia was linked to impairments in learning abilities (Aronson and Herberman 1960). Similarly, a cerebellar lesion in the goldfish was linked to impairments in emotional fear heart rate conditioning as a

modified emotional learning behaviour (Rodriguez *et al.* 2005). Consequently, it will be important to determine the role of the nestin isoforms in filament formation to support cellular proliferation and migration following CNS injury as well as observe nestin expression variations during various development stages and seasons.

Chapter 4

Neuronal regeneration in the goldfish telencephalon following 1-methyl-4-phenyl-1,2,3,6-tetrahydropyridine (MPTP) insult

4.1. Introduction

Goldfish (*Carassius auratus*) and other teleosts have a remarkable and higher neurogenic rate than mammals and thus a greater ability to regenerate damaged axons and tissues following a central nervous system (CNS) injury (Contestabile *et al.* 1979; Levine 1983; Scherer and Easter 1984; Stuermer 1986; Delgado and Schmachtenberg 2011). The constitutive ability of the goldfish CNS to regenerate after injury makes them an excellent model organism to study neurogenesis (Stevenson and Yoon 1978; Stuermer *et al.* 1992; Sullivan *et al.* 1997). It has been estimated that the rate of neurogenesis in the CNS of teleosts is approximately one order of magnitude higher than that observed mammals (Zupanc and Sîrbulescu 2011). For example, 6000 cells are newly generated in the zebrafish brain within any period of 30 minutes which represents ~0.06% of the total brain cell population (Hinsch and Zupanc 2007; Zupanc and Sîrbulescu 2011). Newly generated neurons are thought to originate from radial glial cells (RGCs) which are known as one of the major progenitor cell populations from which new neurons can arise (Adolf *et al.* 2006; Pellegrini *et al.* 2007; Ganz *et al.* 2010; Chapouton *et al.* 2011; Rothenaigner *et al.* 2011; Xing *et al.* 2014). There are up to 16 proliferative zones in the teleost brain and the telencephalon exhibits numerous cellular pools and is a major source of RGCs (Zupanc and Horschke 1995; Ekström *et al.* 2001; Zupanc *et al.* 2005; Adolf *et al.* 2006; Grandel *et al.* 2006; Zupanc and Zupanc 2006; Kaslin *et al.* 2009; März *et al.* 2010; Schmidt *et al.* 2013; Pelligrini *et al.* 2015).

The neurotoxin, 1-methyl-4-phenyl-1,2,3,6-tetrahydropyridine (MPTP), can destroy DAergic neurons in the brain of teleosts and induce dopamine (DA) depletion and Parkinson-like symptoms (Poli *et al.* 1990; Youdim *et al.* 1992; Pollard *et al.* 1992; Lucchi *et al.* 1998; McKinley *et al.* 2005; Lam *et al.* 2005). The MPTP models of Parkinson's disease (PD) experience many of the symptoms exhibited by humans and primates. This includes neuronal cell body destruction in the CNS motor axis, as well as decreased tyrosine hydroxylase (TH) activity and DA content in the forebrain, midbrain, cerebellum and vagal lobes (Burns *et al.* 1983; Heikkila *et al.* 1984a, 1984b; Chiueh *et al.* 1984; Hallman *et al.* 1985; Adams *et al.* 1989; Poli *et al.* 1990; Pollard *et al.* 1996). The goldfish ventral telencephalon, especially the area telencephali pars dorsalis (Vd) that plays a role in motor control in teleosts, is an area negatively impacted by MPTP toxicity (Goping *et al.* 1995; Wullimann and Mueller 2004; Sallinen *et al.* 2009). The ability of fish to regenerate damaged cells and tissues and reestablish normal behavioural functions following injury has been extensively studied in the spinal cord, cerebellum and retina, but not in the highly regenerative telencephalon tissue (Bernstein 1964; Stuermer *et al.* 1992; Zottoli and Freemer 2003; Matsukawa *et al.* 2004; Becker and Becker 2007, 2008; Sîrbulescu *et al.* 2009; Sîrbulescu and Zupanc 2010a,b; Zupanc and Sîrbulescu 2011). Previous studies have reported reversible changes in DA forebrain levels following MPTP treatment where DA returned to baseline levels ~8 days post-injection (dpi) (Pollard *et al.* 1992; Adeyemo *et al.* 1993).

Bromodeoxyuridine (BrdU) is a synthetic analog of thymidine that incorporates into newly synthesized DNA and is used to study cellular proliferation and neuronal development (Miller and Nowakowski 1988). Previous studies have reported the ability

of fish to incorporate BrdU into mitotically active cells following injury (Zupanc and Horschke 1995; Zupanc 1999; Ekström *et al.* 2001; Zikopoulos *et al.* 2001; Zupanc *et al.* 2005; Ampatzis and Dermon 2007; Delgado and Schmachtenberg 2011; Zupanc and Sîrbulescu 2011). For example, actively dividing cells were visualized 1-10 days following a lesion in the cerebellum of the weakly electric fish *Apteronotus leptorhynchus* (Zupanc and Ott 1999). In this animal model, newly generated cells were able to migrate to specific target areas, differentiate into neurons and integrate into existing neural networks (Zupanc and Zupanc 1992; Stroh and Zupanc 1996; Zupanc *et al.* 1996; Zupanc and Ott 1999). Zupanc and Horschke (1995) showed that BrdU is available for 4 hrs after intraperitoneal injection in *A. leptorhynchus* and another electric fish *Eigenmannia sp,* thus is able to incorporate into new cells and mark the occurrence of neurogenesis following injury.

Teleost species remove damaged or compromised cells almost exclusively via apoptosis following CNS injury in comparison to necrotic cell death observed in mammalian models (Beattie *et al.* 2000; Vajda 2002; Liou *et al.* 2003). The damaged cells resulting from apoptotic events can be detected using a terminal deoxynucleotidyl transferase (TdT)-mediated dUTP nick-end labelling (TUNEL) technique (Gavrieli *et al.* 1992). This technique labels DNA fragments associated to changes in cellular morphology due to cellular apoptosis (Thiry 1992; Migheli *et al.* 1995). Cellular apoptosis occurs as a result of activating apoptotic enzyme cascades that are triggered when cell cycle checkpoints are compromised as observed in neurodegenerative diseases such as PD (Bursch *et al.* 1990; Majno and Joris 1995; Darzynkiewicz *et al*. 1997; Trump *et al.* 1997; Beal 1998; Green and Droemer 2004). The present study investigated the

proliferation of cells and quantified apoptotic activity in the telencephalon of the goldfish brain by using BrdU and TUNEL methods.

In conclusion, we report novel information on the ability of the goldfish to regenerate rapidly (~3-4 dpi) damaged DAergic neurons in telencephalic tissue by observing the rapid incorporation of BrdU into newly generated cells which preceeds recovery of motor function in MPTP-treated animals. The telencephalon was found to be the most distinct tissue in nestin protein expression following MPTP insult in adult female goldfish (Chapter 3). For this reason, this study focuses on the capacity of female goldfish telencephalic tissue to regenerate following MPTP toxicity, specifically in the Vd area associated with fish motor acitivity. The DAergic marker, TH, was used to determine if new DA neurons are generated after the CNS injury in the adult goldfish telencephalon.

4.2. Material and Methods

4.2.1. Animal maintenance

Adult female goldfish (*Carassius auratus*) were purchased from a commercial supplier (Mt. Parnell Fisheries Inc., Mercersburg, PA) and maintained at 18 ˚C under a natural-simulated photoperiod on standard flaked goldfish food. Fish were kept in 70 L tanks (15-18 fish/tank). All procedures were performed according to the guidelines of the Canadian Council on Animal Care and were approved by the University of Ottawa animal care committee. Goldfish were anesthetized using 3-aminobenzoic acid ethylester (MS-222; 0.05% in water, Sigma Chemicals, Oakville, Canada) for all handling and sampling procedures.

4.2.2. Experimental and sampling procedures

The dopaminergic neurotoxin MPTP (Sigma-Aldrich M0896, Oakville, Canada) was dissolved in 0.6% saline to give a dose of 50 µg/g body weight of fish at 2 µL/g. Sexually recrudescent female goldfish (September; ~33g ± 1.6; gonadosomatic index ~2.8 ± 0.5; n=20) either received a single intraperitoneal injection of MPTP or a control 0.6% saline injection at time 0 similar to the treatment schedule used by Pollard's group (Pollard *et al.* 1992; Goping *et al.* 1995). All female goldfish also received a single intraperitoneal injection of BrdU (Life Techonologies B23151, Burlington, Canada) dissolved in 0.6% NaCl at a dose of 150 µg/g body weight at 3 dpi prior to sampling at 4 and 7 dpi. Female goldfish were randomly sampled at time 4 and 7 dpi when they were intracardially perfused with 0.6% saline (~10 ml) and then 4% paraformaldehyde (PFA, Sigma, P6148, Oakville, Canada) freshly depolymerized in phosphate-buffered saline (PBS; pH 7.4). Following perfusion, the brains, whole pituitary and gonads were carefully dissected from the goldfish. The gonadosomatic index was calculated by dividing the gonad weight by body weight of the goldfish x 100.

4.2.3. Immunostaining

Goldfish brains were dissected and collected after intracardial perfusion and postfixed with 4% PFA overnight at 4°C. The following day, the brains were washed in a series of solutions [1xPBS (2x 30 min); 0.85% NaCl (1x 40 min); EtOH 70%/NaCl 0.85% 1:1 (1x 30 min); EtOH 70% 2x 20 min; EtOH 85% (1x 40 min); EtOH 95% (1x 40 min); EtOH 100% (2x 30 min)] at 4 °C in preparation for paraffin embedding [toluene (2x 45 min); melted paraffin (3x 60 min)]. All the brains were embedded in paraffin prior to sectioning. Six micrometer sections were obtained for staining using a motorized

microtome (HM 350, Microm, Heidelberg) and the sections were placed on Superfrost plus microscopic glass slides (Fisher Scientific 12-550-15, Toronto, Canada). To visualize incorporated BrdU, the paraffin sections were deparaffinized by washes in Xilol (2x20 min) and serial dilutions of ethanol (2min/wash) [2x EtOH 100%; EtOH 95%; EtOH 85%; EtOH 70%; EtOH 50%; EtOH 30%]. The sections were then washed with 1x PBS (2x 10 min) prior to incubation with 50% formamide/50% 2xSSC for 3 hrs in a 65 °C water bath. Following the incubation, the sections were washed with 2x saline-sodium citrate (SSC) (20x SSC stock solution: 3M NaCl, 0.3M Sodium citrate, pH 7.0) (2x 5min) prior to DNA denaturation by incubating the sections in 2N HCl for 30 min at 37 °C. This was followed by washing in sodium borate buffer (0.1M, pH 8.5) for 2x 5min at room temperature (RT) and then with 1x PBS with 0.2% TritonX-100 (3x 5min). Nonspecific protein binding sites were blocked with 1% milk with 0.2% Triton X-100 in 1x PBS for 45 min at RT. Sections were then incubated with rat anti-BrdU (dilution 1:300; Abcam ab6326, Cambridge, MA, USA) and rabbit anti-TH antibodies (dilution 1:400; Millipore Ab152, Toronto, Canada) in 1% milk with 0.2% Triton X-100 in 1x PBS at 4 °C overnight in a moist chamber. After 1x PBS with 0.2% TritonX-100 rinses of 3x 10min on a shaker, the sections were incubated in Alexa Fluor 594 goat anti-rat IgG (dilution 1:300; Invitrogen A11007, Burlington, Canada) and Alexa Fluor 488 goat anti-rabbit IgG (dilution 1:300; Life Technologies A11008, Burlington, Canada) secondary antibodies in 1xPBS with 0.2% TritonX-100 for 1.5 hrs at RT. The sections were then washed three times in 1xPBS with 0.2% Triton X-100 for 5 min and mounted with antifading medium Vectashield with 4,6-diamino-2-phenylindole (DAPI) (Vector Laboratories, Burlingame, CA, USA) and kept in the dark until visualization of slides

with a confocal microscope.

In situ TUNEL was used for single-labelling experiments to visualize the distribution of apoptotic cells in the goldfish brain. Adjacent brain sections from the BrdU experiment were used to detect the DNA fragments using the ApopTag Fluorescein in situ plus detection kit (Millipore S7111, Toronto, Canada), which uses antidogoxigenin antibody conjugated to a fluorescein reporter molecule to visualize fluorescent TUNEL nuclei in green. The TUNEL experiment was performed following the manufacturer's protocol. To detect nonspecific labelling, adjacent sections were incubated in the absence of the primary or secondary antibody (data not shown). No labelled cells were observed under these control conditions (data not shown). The sections were mounted with Vectashield and DAPI and kept in the dark until visualization of slides.

4.2.4. Quantification of BrdU, TH and TUNEL labelled cells

The BrdU, TH and TUNEL staining-positive cells were visualized using a fluorescent microscope (Zeiss Axiophot Microscope) at 20 X magnification with the aid of an Olympus DP70 camera. Positive cells were counted in the 4 and 7 dpi goldfish brains to quantify cellular proliferation and apoptosis using ImageJ1.43I software (Rasband 1997-2014). The total number of TH, BrdU and TUNEL-positive cells in goldfish brain sections were counted using unbiased, single-blind, counting of cells in random sections (Guillery 2002). For the TH and BrdU counting, five sections of the ventral telencephalic area at 4 and 7 dpi were analyzed per fish (n=5 per group) where cells were counted the entire length of the ventricular surface along the ventral-dorsal axis of the left brain hemisphere using a specific counting frame of a width of ~ 680 ± 80 μm stretching laterally from the ventricular surface to the apical surface. Cell counting

was confined within neuroanatomical borders of the target area. Quantification of TUNEL staining in sections was performed in the same manner with the analysis of 3 sections per brain (n=5 per group) at 4 dpi. Labelled cells were localized according to the goldfish brain atlas of Peter and Gill (1975). The total number of positive cells between treatment group and control group were first tested for normality and then statistically compared using Student's t-test (two-tailed) in SPSS Statistics (version 21). P-values less than or equal to 0.05 were considered statistically significant. All data are presented as the mean + SEM.

4.2.5. Behavioural Analysis

Female goldfish (December; ~32 g ± 1.4; gonadosomatic index ~1 ± 0.1; n=10) received either a single intraperitoneal injection of MPTP (50 µg/g body weight) or a control 0.6% saline injection at time 0. The mobility measurements were performed once a day at 0, 3 and 7 dpi of MPTP in the late morning where time 0 was measured after the administration of MPTP. The fish movement and swimming motions were recorded using an Olympus Stylus TG-850 camera in individual tanks. The fish were placed in 4 cm of water in a 13 x 30 cm transparent aquarium similar to the experiment performed by Weinreb and Youdim (2007). The fish were allowed to acclimatize for 30 min prior to mobility recordings. The total movement of a single fish, which includes the total distance of swimming and time of rest, was measured over a period of 5 min using a non-commercial Python tracking software specifically programmed for fish mobility measurements (kindly provided by A.D. St-Jacques and M. Vera Chang, unpublished). Statistical analysis was performed using GraphPad Prism v6.0. The total distance traveled data were normally distributed and statistically compared using Student's t-test (two-

tailed) by comparing the control at time 0 group to each of the treatment time-points followed by Bonferroni's correction. The resting time data were not normally distributed and were therefore statistically compared using Mann-Whitney Test (two-tailed) by comparing the control at time 0 group to each of the treatment time-points followed by Bonferroni's correction. P-values less than or equal to 0.02 were considered statistically significant. All data are presented as a mean ± SEM.

4.3. Results

4.3.1. Effects of MPTP on female goldfish swimming behaviour

Female goldfish were treated with MPTP and their swimming movements were measured on different days post MPTP injection. As shown in Fig. 4.1, control goldfish traveled an average of ~2000 cm/ 5 min and rested for ~10 s during the test period. However, there was an observable decrease in total distance traveled and an increase in resting time following the injection of MPTP. At 3 dpi of MPTP goldfish decreased distance traveled by ~50% (P=0.04) (Fig. 4.1). There was a significant increase in resting time (P=0.02) at 3 dpi (Fig. 4.1B). Thereafter, the total distance traveled by MPTP-treated goldfish recovered to control levels at 7 dpi (P=0.98). Reversible changes were also evident for the resting time, which started to return to control levels following 7 days post-MPTP treatment (P=0.17).

4.3.2. Effects of MPTP on TH and BrdU-immunoreactivity in the female goldfish ventral telencephalon

Confocal imaging of MPTP-treated female goldfish at 4 and 7 dpi reveals TH and BrdU-positive cell labelling evidence in the Vd of the telencephalon. Figure 4.2B shows some BrdU-positively labelled cells (red) traveling laterally and dorsally from the

ventricular surface to the Vd area at 4 dpi of MPTP. Control (Fig. 4.2A) and MPTP-treated fish at 4 dpi also contained TH-positive cells (green). At 7 dpi of MPTP, there were no differences in TH or BrdU-positive cells in the MPTP-treated (Fig. 4.2D) or the control fish (Fig. 4.2C).

Confocal imaging also revealed that BrdU-positive cells are colocalized with DAPI (blue nuclear stain) thereby confirming that BrdU was incorporated into newly generated cells in the female goldfish brain (Fig. 4.3A). Several double-labelled BrdU and TH-positive cells were also found in the 4 dpi of MPTP fish group (Fig. 4.3B and 4.3C).

The total number of TH-positive neurons in the ventral telencephalon, which includes the Vd, was counted. At 4 dpi of MPTP, TH-positive cells significantly decreased by 27% compared to control fish (P=0.02) (Fig. 4.4A). No significant differences in TH-immunolabelling were observed at 7 dpi of MPTP (P=0.69) compared to controls (Fig. 4.4C). The BrdU-positive cell counts also revealed a statistically significant difference in the adult goldfish. At 4 dpi of MPTP, BrdU-positive cells significantly increased ~1.9-fold compared to control fish (P=0.02) (Fig. 4.4B). In contrast, no significant differences in BrdU-immunolabelling were observed at 7 dpi of MPTP (P=0.69) (Fig. 4.4D).

4.3.3. Effects of MPTP on cell survival and death in the ventral telencephalon of female goldfish

Fluorescent imaging reveals that cellular apoptosis occurred in the ventral telencephalon following the injection of MPTP at 4 days. TUNEL-positive cells were

elevated in the MPTP-treated brain tissue at 4 dpi (Fig. 4.5B) relative to the control fish (Fig. 4.5A).

TUNEL-positive cell counts revealed a statistically significant difference in the adult goldfish. At 4 dpi of MPTP, the number of positively labelled TUNEL cells (apoptotic cells) in the ventral telencephalon was significantly increased by ~9-fold in comparison to control fish (P=0.0001) (Fig. 4.6).

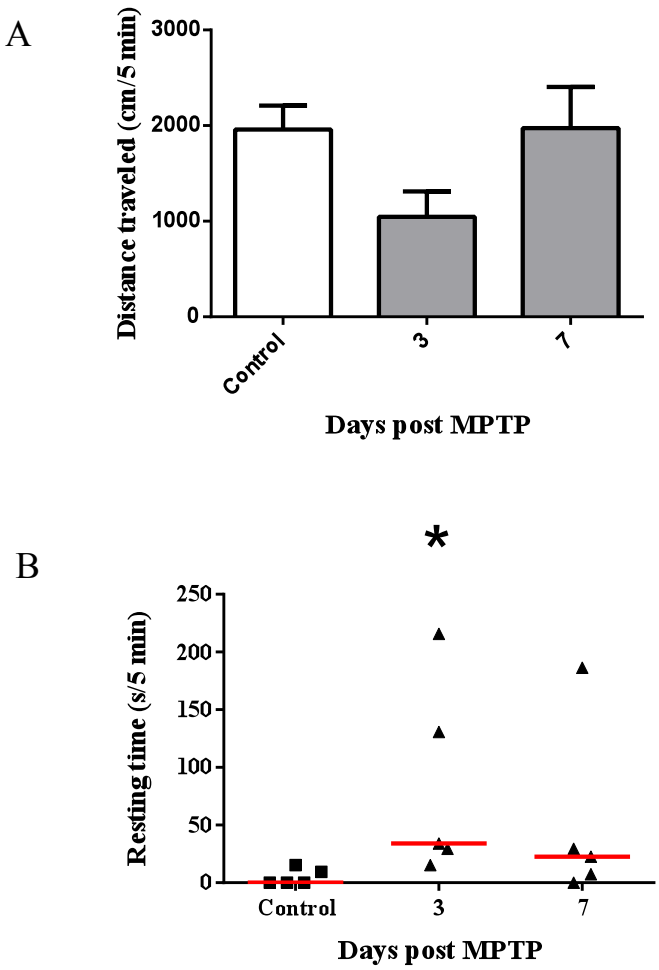

Figure 4.1. Time course for onset and recovery of swimming activity of female goldfish from MPTP toxicity. Goldfish in groups of 5 were treated on day 0 with MPTP (50 µg/g body weight, i.p.) or with 0.6% saline. A) At 3 and 7 days post-MPTP injection fish were tested for the distance travelled in a 5 min period according to a Python tracking software. A Student's t-test was performed to determine the effects of MPTP on distance travelled B) Data were not normally distributed so the distribution and median values (red bars) are presented. Resting time during each 5 min period is presented as determined by the Python tracking program. A Mann-Whitney Test (two-tailed) was performed followed by a Bonferroni correction to determine the effects of MPTP on resting time (P=0.02). Treatment groups marked by an asterisk are significantly different compared to control group (n=5 per treatment group).

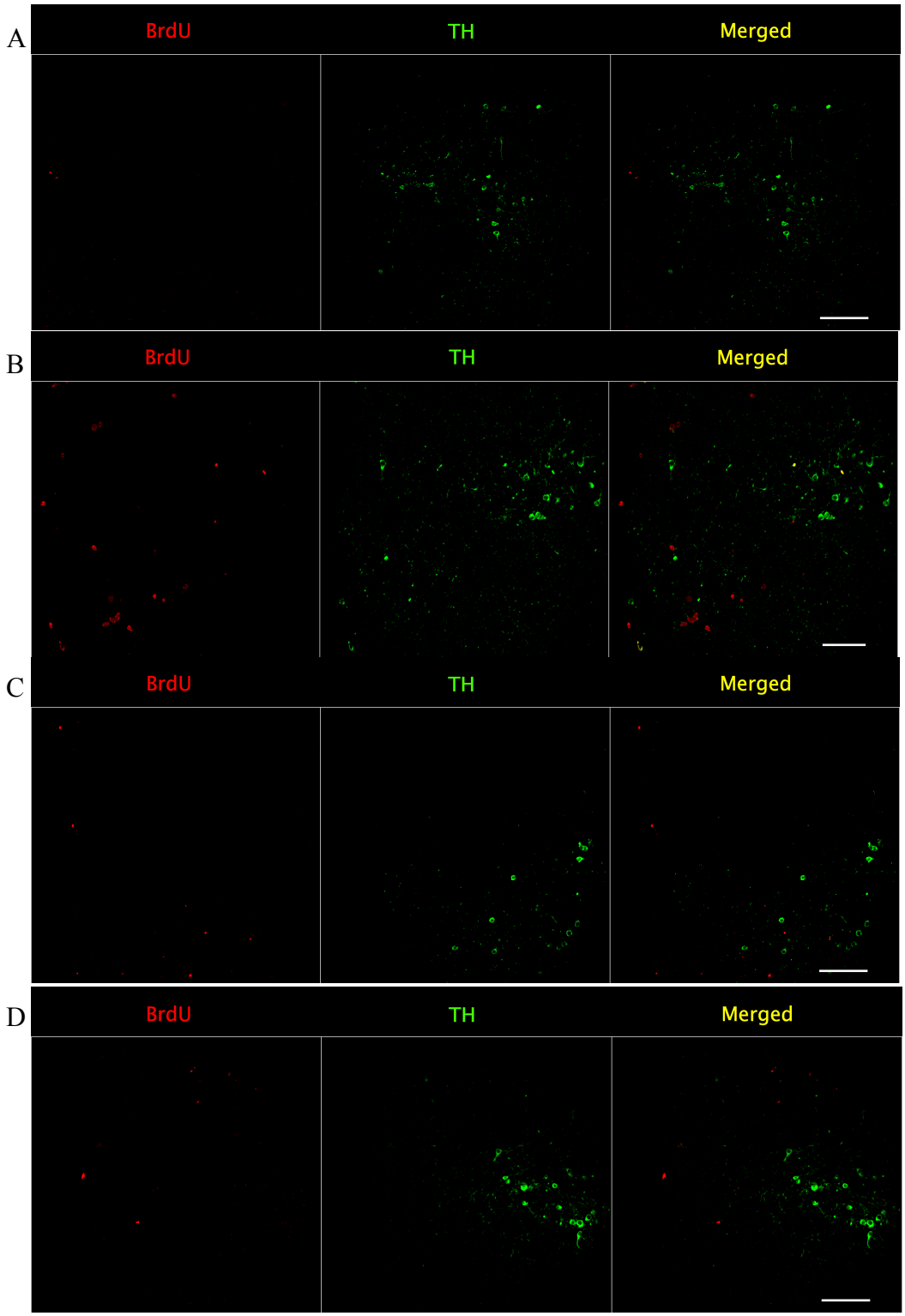

Figure 4.2. Confocal imaging illustrating effects of MPTP on BrdU-positive cells (red) and TH-positive cells (green) in the area telencephali pars dorsalis (Vd) of female goldfish. The images show positively stained BrdU and TH cells in (A) control fish 4 days post injection (dpi); (B) MPTP-treated goldfish at 4 dpi; (C) control goldfish at 7 dpi; and (D) MPTP-treated goldfish at 7 dpi. Scale bars = 100 µm.

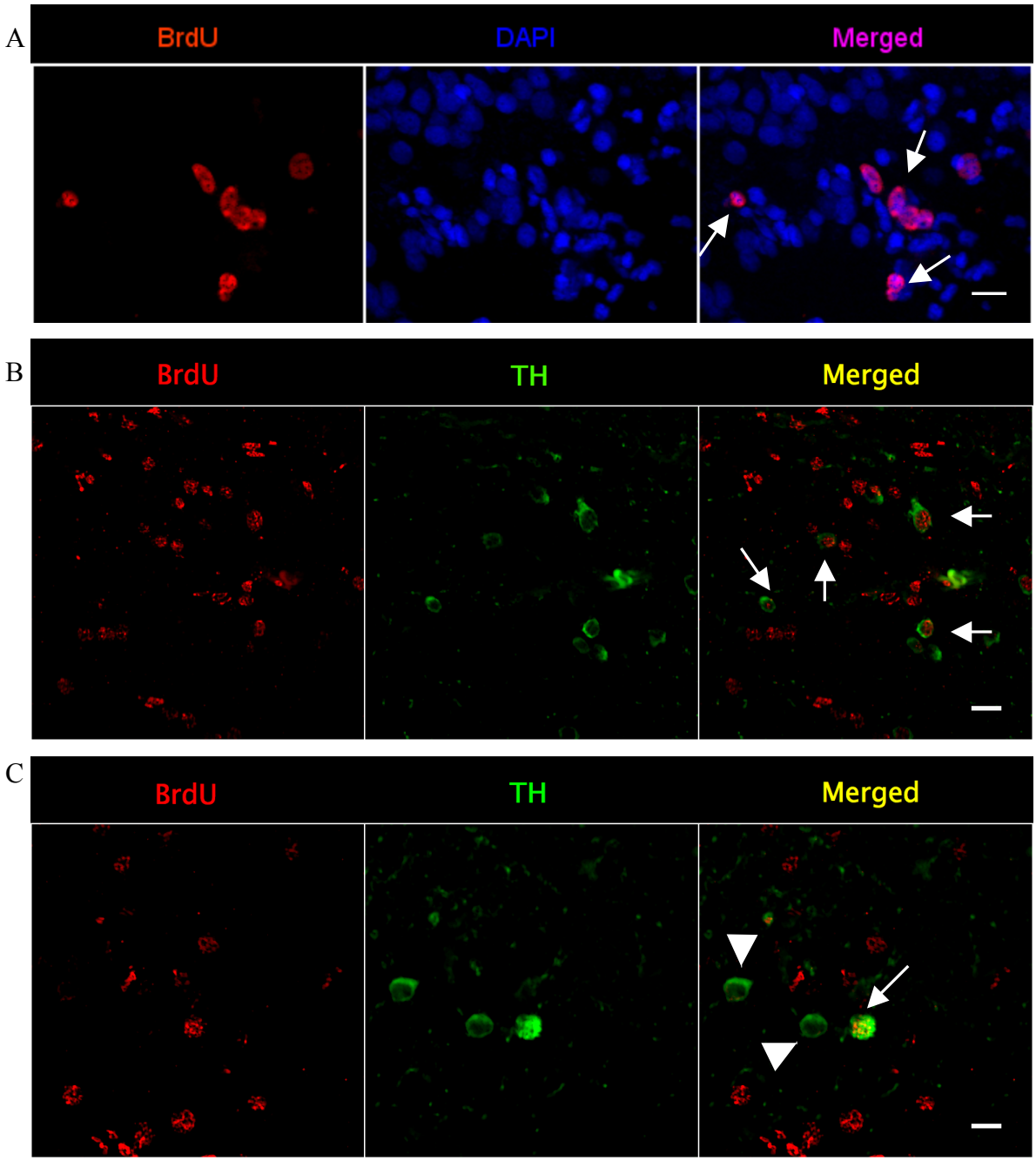

Figure 4.3. Confocal imaging of (A) double-labelled BrdU (red) and DAPI (blue) nuclear staining; B) and C) double-labelled BrdU-positive cells (red) and TH-positive cells (green) in the area telencephali pars dorsalis (Vd) of female goldfish. Arrows show double-labelled cells and arrowheads show TH-positive and BrdU-negative cells. Scale bars = 10 µm.

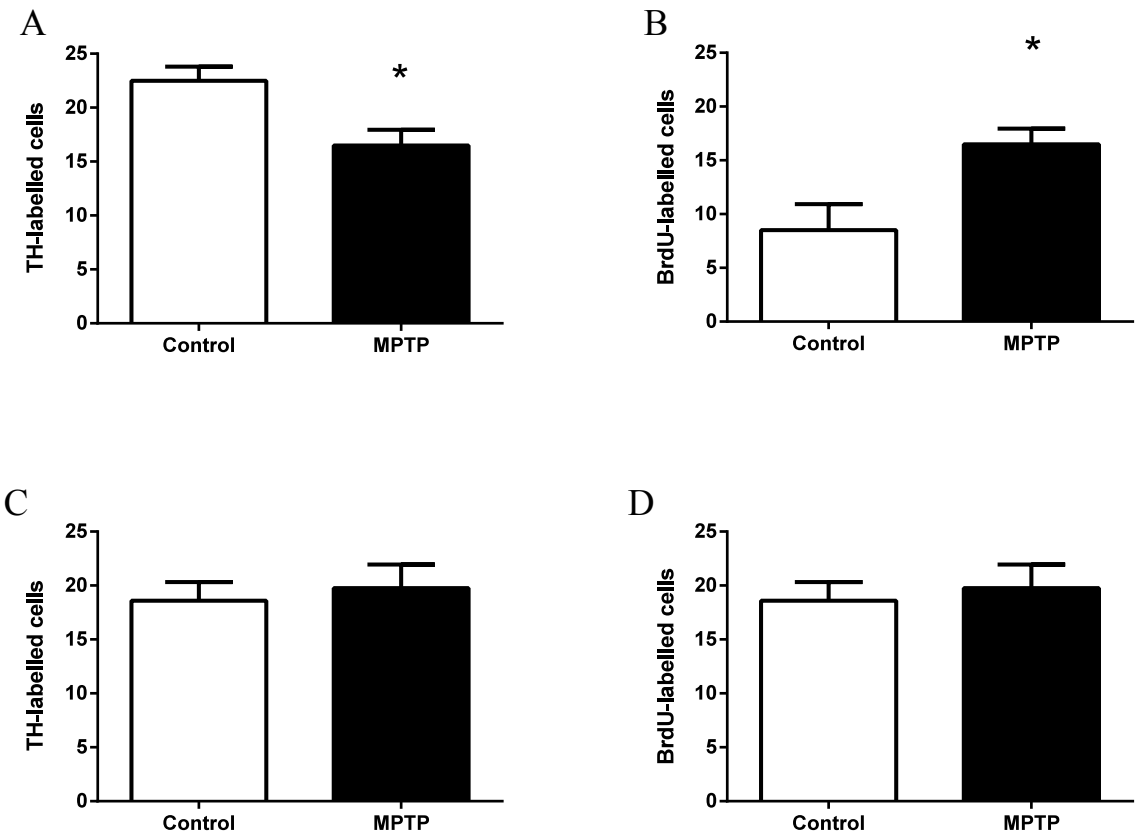

Figure 4.4. The effects of MPTP on the number of TH-positive cells and BrdU-positive cells in female goldfish ventral telencephalon. Female goldfish exposed to MPTP after 4 days had a significant decrease of TH-labelled cells (A) and a significant increase of BrdU-labelled cells (B) compared to control fish. There were no significant changes observed in TH-labelled cells (C) or BrdU-labelled cells (D) in female goldfish exposed to MPTP after 7 days. A Student's t-test was performed to determine the effects of MPTP on TH and BrdU cell numbers. Treatment groups marked by asterisks are significantly different compared to control group (n=5 per treatment group; P=0.02 (A) and P=0.02 (B).

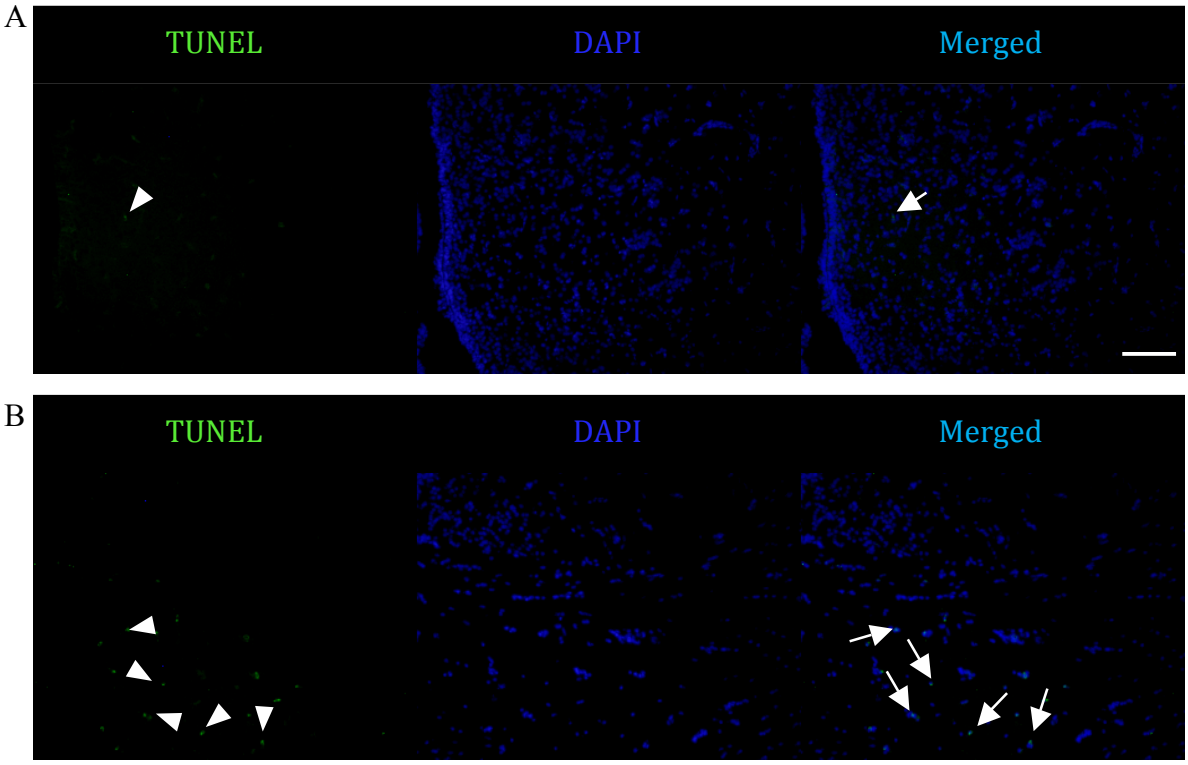

Figure 4.5. Fluorescent images illustrating effects of MPTP on cellular apoptosis by labelling TUNEL-positive cells (green) and DAPI (blue) in the area telencephali pars dorsalis (Vd) of female goldfish. The images show positively stained TUNEL cells in (A) control goldfish at 4 days post injection (dpi) and (B) MPTP-treated goldfish at 4 dpi. Arrows show double-labelled cells for both TUNEL and DAPI staining and arrowheads show TUNEL-positive labelling only. Scale bars = 100 µm.

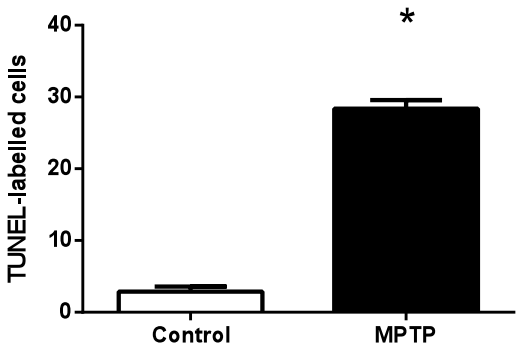

Figure 4.6. The effects of MPTP on the number of TUNEL-labelled cells in female goldfish ventral telencephalon at 4 days post-MPTP treatment. Female goldfish exposed to MPTP after 4 days had a significant increase of TUNEL-labelled cells compared to control fish. A Student's t-test was performed to determine the effects of MPTP on TUNEL-labelled cell numbers. Treatment group marked by an asterisk is significantly different compared to control group (n=5 per treatment group; P=0.0001).

4.4. Discussion

The behavioural MPTP model of PD was validated by first evaluating the motor deficits in goldfish injected with MPTP. In this behavioural study, a significant decrease of ~50% in total distance traveled was observed in goldfish 3 dpi of MPTP coincident with the maximal loss of DA brain content reported in the forebrain by several studies (Poli *et al.* 1992; Pollard *et al.* 1992; Lu *et al.* 2014). Youdim *et al.* 1992 also reported profound bradykinesia in goldfish at 3 dpi of MPTP. We also observed a significant increase in total resting time at 3 dpi of MPTP. Goldfish were able to recover their swimming distance to control levels by 7 dpi and resting time slowly recovered towards control levels at 6 and 7 dpi of MPTP. A similar recovery of total distance traveled and resting time was reported at 7 and 5 dpi respectively (Weinreb and Youdim 2007). The recovery of normal motricity suggests a recovery of neurotransmitter levels i.e., DA, and thus the ability of goldfish to reestablish important biological behaviours which is most likely due to their high neuroregenerative abilities. Although these findings suggest a recovery of mobility due to a recovery of DA levels in the teleost brain, more studies are necessary to directly link the changes in DA neurotransmitter levels to mobility function.

The neuronal cells in the ventral telencephalon were destroyed by the neurotoxin MPTP at 4 dpi as observed by TUNEL assay. This confirms previous studies that apoptotic cell death occurred as a means to remove damaged or compromised cells following injury (Beattie *et al.* 2000; Vajda 2002; Liou *et al.* 2003). The observation of cell death close to the site of injury suggests a role of apoptosis in structural reorganization of cells and tissue networks (Zupanc and Sîrbulescu 2011). The greatest decrease of forebrain DA content following MPTP injection is reached at 3-5 days

(Pollard *et al.* 1992; Adeyemo *et al.* 1993; Sloley and McKenna 1993; Goping *et al.* 1995; Hibbert *et al.* 2004) coincident with the cellular death observed in the goldfish ventral telencephalon. The DAergic marker TH was also quantified in the goldfish ventral telencephalon and was significantly decreased by 27% at 4 dpi of MPTP. Similar findings were reported by Pollard *et al.* (1996) and Goping *et al.* (1995) following immunohistochemistry studies where TH-immmunoreactivity decreased in the goldfish telencephalon at 4 dpi of MPTP. Goldfish have also been reported to recover DA brain content to baseline levels at 7-8 dpi of MPTP (Pollard *et al.* 1992; Adeyemo *et al.* 1993; Popesku 2009) and a full recovery is observed following 6 weeks of MPTP injection (Poli *et al.* 1992). Remarkably, we observed a significant increase of 1.9 fold of BrdU-labelled cells at 4 dpi of MPTP but no significant differences were observed at 7 dpi in comparison to controls. This illustrates that goldfish have a remarkably high and rapid neurogenic rate to recover from MPTP toxicity starting at 4 dpi. This is the first time that neuroregeneration has been observed in the goldfish telencephalon during such a short time-frame (~4 dpi) in response to MPTP toxicity. Furthermore, BrdU-positive cell counts returned to control levels at 7 dpi providing further evidence that neuroregeneration occurs rapidly (between 4-7 dpi) after the neurotoxic insult.

The short-term experiments conducted in this present study, where BrdU was injected 24 hrs prior to the 4 dpi of MPTP, allowed for sufficient time for BrdU to be available for incorporation into newly generated cells. Previous studies have shown that BrdU is readily available for uptake for ~4hrs after intraperitoneal injection (Zupanc and Horschke 1995). Furthermore, the length of the cell cycle in the adult teleost *Haplochromis burtoni* was estimated to be ~25 hrs based on proliferating cell nuclear

antigen (PCNA) and BrdU labelling in the retina (Mack and Fernald 1997). Based on these studies, the positively-labelled BrdU cells in the goldfish telencephalon likely label proliferative cells and their progeny if cellular division occurred. The longer-term experiment, where BrdU was available for a total of 4 days post-injection, proliferative cells that are actively dividing likely went through several cell cycles. Therefore the BrdU observed at this time-point would likely label several cellular generations and also the original cell progeny. In this present study, we observed proliferation and lateral and dorsal migration of BrdU-positive cells towards the Vd area at 4 dpi of MPTP. These newborn cells likely originated from the proliferative cellular pools along the ventricular surface where a large number of RGCs reside that can act as neural stem cells (Zupanc and Clint 2003; Mahler and Driever 2007; Pelligrini *et al.* 2007; März *et al.* 2010; Zupanc and Sîrbulescu 2011). At 7 dpi of MPTP, the majority of proliferative cells remained near the ventricular area in the proliferative cell pools.

Based on the observations of BrdU-positive cells in this study, we postulate that proliferative cells are completing or have completed their migration to the Vd area following MPTP insult shortly after 4 dpi. Previous studies have reported the occurrence of rapid migration of newborn cells following injury based on BrdU cellular labelling. For example, cellular proliferation in the zebrafish cerebellum following injury was observed where cells migrated to their final destination of the granular cell layer after 10 days (Zupanc *et al.* 2005). Ampatzis and Dermon (2007) also found BrdU-labelled cells in the migration state at 24 hrs post-injury in the zebrafish cerebellum. Another study of spinal cord injury in *Apteronotus leptorhynchus* fish reported a several fold increase in the rate of cell proliferation starting at 1 day post-injury and lasting several weeks

(Zupanc and Ott 1999; Takeda *et al.* 2008; Reimer *et al.* 2008; Sîrbulescu *et al.* 2009) providing further evidence to the possibility of rapid goldfish neuroregeneration in the telencephalon.

Remarkably, we observed some colocalization of BrdU and TH-positive cells in the Vd area of the goldfish telencephalon at 4 dpi of MPTP. This provides direct evidence that DAergic neurons are regenerating in the region exhibiting apoptosis following MPTP injections. There were also BrdU-positive cells that were negatively stained for TH illustrating two possible options. Firstly, one possibility is that future DAergic cells could still be migrating to their final target site and do not yet express DAergic differentiation factors such as TH. There could also be the occurrence of cellular differentiation of other cell types in the Vd following a neurotoxic insult. However, this option is unlikely as the majority of catecolaminergic neurons expressing TH in the teleost forebrain consist mainly of DAergic neurons (Kaslin and Panula 2001; Sébert *et al.* 2008). Future studies are needed to characterize the newborn cells in the telencephalon of the goldfish to determine which cell populations are present by using specific cellular markers and immunohistochemistry.

In conclusion, the administration of BrdU revealed development and proliferation of newborn DAergic cells post-MPTP treatment in the ventral telencephalon, specifically in the Vd area. These newborn cells migrate laterally and dorsally from the Vd towards the injured site to replenish DAergic neuronal populations. The findings are novel and provide evidence of neuronal regeneration of DAergic neurons by showing cellular death and double-labelling of BrdU and TH cells at the CNS injury site. Future studies are necessary to test whether the newly generated neurons are integrated into synaptic

circuits to reestablish proper biological functions such as motricity. Another future study should aim at identifying the permissive factors allowing neuregeneration to occur at a rapid rate. The findings of this study provide a platform for future neuronal regeneration studies in the teleost brain as a means to understand normal brain plasticity events as well as healing and repair mechanisms following injury.

Chapter 5

General Discussion

Neuronal regeneration and brain plasticity events in the normal and injured goldfish were investigated. Nestin is an intermediate filament (IF) protein that has been well characterized in mammalian species but has not been well studied in fish. Research presented in this thesis reveals novel findings relating to nestin protein and neuroregeneration in the goldfish brain.

5.1. Nestin isoform expression is sex- and tissue- dependent in the goldfish brain

The generation of the first fish specific nestin antibody provided the tools to localize and identify nestin in the goldfish brain (Chapter 2). Western blotting analysis using the goldfish anti-nestin antibody and RACE-PCR led to the discovery of three different nestin isoforms (nestin A, B and C); the first report of multiple nestin isoforms in teleost species. Phylogenetic analysis determined that goldfish nestin isoform A is closely related to the single nestin isoform identified so far in other teleost species. On the other hand, nestin isoform B and C appear to be distinct. These novel isoforms might work together in a time-dependent manner and thus contribute to the high neurogenesis capacity observed in the CNS of fish. The discovery of multiple nestin proteins in the goldfish brain might provide insight into the reasons why teleosts have unparalleled neuroregenerative abilities relative to the very limited ability in mammals. Adult mammals only have two distinct proliferative brain areas (Alvarez-Buylla and Garcia-Verdugo 2002; Taupin and Gage 2002; Goldman 2003; Garcia *et al.* 2004; Merkle *et al.* 2004; Doetsh and Hen 2005; Lledo and Saghatelyan 2005), but in marked contrast teleosts have up to 16 proliferative pools migrating and differentiating into a range of cell types (Zupanc and Horschke 1995; Ekström *et al.* 2001; Zupanc *et al.* 2005; Adolf *et al.*

2006; Grandel *et al.* 2006; Zupanc and Zupanc 2006; Kaslin *et al.* 2009; März *et al.* 2010; Schmidt *et al.* 2013; Pelligrini *et al.* 2015).

It was found that nestin protein distribution and isoform expression varied significantly across brain regions and the pituitary gland. These included neuroendocrine regions such as the hypothalamus and telencephalon, and also the optic tectum, midbrain, cerebellum, vagal lobes and brainstem. Remarkably, based on PCA analysis, the telencephalon was identified as a distinct tissue with a unique nestin expression pattern in the normal goldfish brain. This is important because the telencephalon is a neuroendocrine region involved in motor control, reproduction and learning and contains numerous proliferative cellular pools capable of recruiting cells to activate neurogenesis (Zupanc and Clint 2003; Mahler and Driever 2007; März *et al.* 2010; Zupanc and Sîrbulescu 2011). The telencephalon is also abundant in RGCs that are also neural stem cells and have multipotency capability to differentiate into numerous cell types (Zupanc and Clint 2003; Mahler and Driever 2007; Pelligrini *et al.* 2007; März *et al.* 2010; Zupanc and Sîrbulescu 2011; Xing *et al.* 2014). However, PCA analysis has some limitations as it only identifies the discriminiating factor providing the most variance in the nestin protein expression pattern in the goldfish brain based on the western blot data. Future studies are necessary to investigate the actual effect of sex and MPTP toxicity on nestin protein expression, i.e., upregulation or downregulation, in the respective neurogenic areas. For example, we could perform western blotting on a greater sample number of female and male fish against nestin to quantifiy and visualize the nestin protein changes in various brain tissues.

Nestin protein expression is also influenced by both seasonality and sex in goldfish (Chapter 3). For example, it was discovered that in individual sexually regressed female goldfish, the nestin protein isoform A and isoform B appear less frequently in the telencephalon compared to sexually mature female fish. Nestin isoform A was expressed at a lower frequency in male versus female goldfish in all brain tissues except for the hypothalamus. Identifying the differences of neurogenetic patterns in different sexes and during the reproductive cycle will help to identify peaks of annual neuronal regeneration that may underly seasonal brain plasticity (Zhang *et al.* 2009).

A differential expression pattern of nestin protein was also observed following the injection of the neurotoxin MPTP at 4 and 7 days. MPTP is a neurotoxin that specifically depletes DA brain content and destroys DAergic neurons in the brain (Singer et *al.* 1987; Poli *et al.* 1990; Pollard *et al.* 1992; Goping *et al.* 1995; Lucchi *et al.* 1998). Previous studies have reported an upregulation of nestin following injury in both fish and mammalian models, suggesting neuronal regeneration as a means to heal and repair damaged cells and tissues in the CNS (Lin *et al.* 1995*;* Zhao *et al.* 2003; Michalczyk and Ziman 2005; Popesku 2009; Carmona *et al.* 2011). In Chapter 3, we explored the neurogenesis potential of various brain structures and whole pituitary of the goldfish by observing the effects of injecting the neurotoxin MPTP on nestin protein expression. Remarkably, MPTP injection affected both the frequency and intensity of nestin protein expression specifically in the pituitary, hypothalamus and telencephalon of female and male goldfish. This is important because some neurons in the telencephalon and hypothalamus control pituitary function and reproductive activity (Peter and Paulencu 1980; Oka and Ueda 1981; Kyle and Peter 1982; Koyama *et al.* 1984; Fryer *et al.* 1985;

Kah *et al.* 1987; Airhart *et al.* 1988; Dufour *et al.* 2010), while others regulate motor activity (Marshall *et al.* 1974; Hornby et *al.* 1987; Sas *et al.* 1990; Poli et *al.* 1992; Goping et *al.* 1995; Olanow and Tatton 1999; Wullimann and Mueller 2004; Sallinen et *al.* 2009). Although the pituitary does not contain neuronal cell bodies, only neuronal terminals, the nestin observed likely marks other cell types. The differential expression of nestin observed following MPTP-induced injury suggests the occurrence of neuronal regeneration in the hypothalamus and telencephalon tissues to alleviate DA loss. One possible neuroregeneration mechanism could be to recruit nestin-positive proliferative cells to differentiate into DA neurons at the site of MPTP-induced injury.

The relative mRNA levels of *nestin a (nesa), b (nesb)* and *c (nesc)* were also measured by qRT-PCR to quantify specific nestin transcripts in the hypothalamus and telencephalon. At 4 dpi of MPTP, *nesa* and *nesc* were significantly decreased in the telencephalon and hypothalamus respectively, but no significant differences were observed at the 7 dpi time-point. Unfortunately, it is not yet possible to link the specific nestin transcript levels to the different nestin protein expression patterns obtained by western blot because the antibody generated for this study labels all three nestin isoforms. A future study is needed to investigate the distribution of individual nestin isoforms, and will require manufacturing specific nestin antibodies for each isoform. In this way it will be possible to understand the direct transcript-protein relationship for each specific nestin subtype.

We propose that the variability in nestin isoform expression patterns is linked to high neurogenic capacity. This higher neurogenic capacity in teleosts could be one possible trigger to activate regenerative mechanisms and increase neuronal populations

from proliferative cells. However, the mechanisms involved in the upregulation of nestin following injury still remain unknown. Several mechanisms could be involved for example, the release of soluble factors from adjacent tissues such as nerve growth factor, changes in cell to cell contact or IF remodeling (Ishikawa *et al.* 1991; Holmin *et al.* 1997; Frisen *et al.* 1995; Johansson *et al.* 2002; Matsuda *et al.* 1996). Furthermore, the nestin antibody was only specific for nestin protein in western blot analyses and did not successfully mark nestin-positive cells when immunohistochemistry (IHC) was performed on goldfish or zebrafish brain sections (data not shown). The epitope recognized by the goldfish nestin antibody is at the N-terminal region of the goldfish nestin protein sequence. We hypothesize that the epitope region recognized by the antibody is unaccessible for binding on fish tissues, perhaps due to protein folding. Further optimization of the IHC protocol could eventually allow the use of the goldfish nestin antibody for IHC purposes on tissue sections. The optimization could include different epitope revealing washes with various buffers as well as attempting to fix the brain tissues in different fixatives. Visualizing nestin upregulation in the areas of motor and reproductive control would provide further evidence for the changes observed in nestin protein expression following injury. In addition, visualizing double-labelling of cells with BrdU and nestin would provide insight into the association between fish regenerative ability and nestin IF remodeling in the cell.

5.2. Dopaminergic neuronal regeneration following MPTP-induced neurotoxic insult

The complex and altered nestin protein expression patterns following MPTP treatments led us to believe that adult neuronal regeneration could be occurring. We

explored the possibility of neuroregeneration of DA neurons, specifically in the area dorsalis of the telencephalon (Vd). In Chapter 4, we first confirmed the occurrence of cellular death by apoptosis in the ventral telencephalon following MPTP injection. These findings provide evidence that apoptosis is a mechanism involved in removing damaged cells and tissue repair at 4 dpi of MPTP. Thereafter, a BrdU experiment revealed that TH-positive neurons regenerate in the ventral telencephalon to alleviate the negative effects of MPTP on DA levels in the brain. Following MPTP treatment, DA neurons were shown to significantly decrease in number in the Vd following 4 dpi of MPTP and recovered to control levels shortly after (~7 dpi). Coincidentally, a string of BrdU-positive cells appear to be migrating from the ventricular surface to the affected Vd area. We specifically visualized the migration of newborn cells laterally and dorsally from the telencephalic ventricular surface towards the Vd where DA neurons are usually found. Remarkably, BrdU colocalized to the nucleus of some TH positive neurons at 4 dpi of MPTP. To our knowledge, this is the first time that neuronal regeneration of DAergic neurons has been observed in the teleost Vd following CNS injury. The data are original and provides direct evidence for neuroregeneration following neuronal death induced by MPTP.

Female goldfish also had observable motor deficits following the injection of MPTP and appeared to recover to control levels following 7 dpi. There is a possible relation between cellular proliferation events observed by nestin and BrdU-positive cells and adult brain plasticity and behaviour. Zupanc (1999) postulated that adding newborn cells could have functional implications for long-term changes in teleost behaviour. We have observed changes in motor behaviour following MPTP similar to that reported in previous studies (Pollard *et al.* 1992; Youdim *et al.* 1992; Adeyemo *et al.* 1993; Weinreb

and Youdim 2007; Lu *et al.* 2014). The high capacity of neurogenesis reported and observed in this thesis in the goldfish telencephalon could help with the discovery of proteins involved in activating neuronal proliferation to heal and repair damaged brain tissues and cells. This is important as the replacement of damaged or dead neurons in the adult mammalian brain as a consequence of neurodegenerative disease is very limited because of a low neurogenic capacity that is highly restricted to a few brain regions (Altman 1962, 1963, 1969a,b; Altman and Das 1965; Mares and Lodin 1974; Kaplan and Hinds 1977; Kaplan 1981; Bayer *et al.* 1982; Kaplan and Bell 1983; Corotto *et al.* 1993; Lois and Alvarez-Buylla 1993, 1994; Gould *et al.* 1998). The research presented in this thesis will therefore advance our knowledge in neuronal brain plasticity and will contribute to our understanding of how the CNS can regenerate in vertebrates.

5.3 Concluding Remarks

This thesis provides evidence that the goldfish neurogenic ability extends to the telencephalon specifically in an area controlling motor activity. The progenitor cell niche of RGCs located near the telencephalic ventricle is the most likely candidate for differentiating into DA neurons following a neurotoxic insult to alleviate the motor difficulties. The increase in expression of neurogenic markers such as nestin followed by an increase in DA neuronal markers such as TH also provides further evidence into DA neuronal regeneration (Popesku 2009).

The goldfish is an amenable model organism to study DA signaling and innervation as pathways are well-conserved relative to other vertebrates (Pollard et *al.* 1992; Popesku et *al.* 2008). However, much remains to be discovered about the

regulation of DA cellular remodeling. Identifying the signals and transcriptional factors and sequence of events controlling stem cell differentiation in the goldfish brain could offer new possibilities in treating diseases and neuroendocrine deficits in fish and even humans. The proposed DA neuronal regeneration pathway activated in the goldfish brain following a neurotoxic insult is presented in Fig. 5.1. Radial glial cells stretch from the apical surface of the ventricle to the dorsal surface of the telencephalon to help newborn DA neurons migrate to the Vd area following MPTP injection. More specifically, we propose the DA neurons arise from progenitor cells located near the telencephalic ventricle that proliferate and migrate along the RGCs. As they are proliferating, the expression of DA differentiation factors such as Notch signaling, Wnt proteins, Otx-2, nurr1, pitx3 factors likely increases coincidentally as progenitor cell factors such as nestin decreases (Riddle and Pollock 2003; Castelo-Branco et *al.* 2005; Michalczyk and Ziman 2005; Dirian et *al.* 2014). The end result is a newborn DA neuron synthesizing and releasing DA thereby alleviating the reproductive and motor deficits observed following MPTP injection.

The study of nestin protein distribution and DAergic neuronal remodeling following a neurotoxic insult increases our understanding of neurogenesis in the CNS. However, further studies are needed to investigate the role of individual nestin isoforms to determine if they cause an increase in fish regenerative capacity or change as a result of regeneration activity. To investigate this possibility, we could use knowdown zebrafish models of each nestin isoform to investigate the role of individual nestin isoforms in neuroregeneration during fish development and adulthood. We could also overexpress

each nestin isoform in a glial cell culture system (Xing et al. 2015) and observe the effects on neurogenic markers and signaling factors such as FGF, GDNF, Shh and Wnt.

The research resulting from this thesis also provides the tools for future studies relating to neurogenesis in the teleost brain. However, more studies are necessary to relate nestin expression and distribution in the CNS to seasonal changes in brain remodeling of neural networks. This is important as fish seasonality cycles vary throughout the year, as do other neurotransmitters and proteins such as dopaminergic activity (Trudeau *et al.* 1993; Senthilkumaran and Joy 1995; Chaube and Joy 2003; Trudeau 1997; Blazquez *et al.* 1998; Zhang *et al.* 2009). Future studies are also necessary to determine if DAergic neurons are regenerating in brain structures involved in the reproductive axis especially in the preoptic telencephalic area (POA), similarly to DAergic neuron regeneration reported in the telencephalic motor axis. The toxin MPTP not only depletes DA neurons in the Vd and Vv areas but also in the POA and hypothalamic region, areas involved in teleost reproduction (Peter and Paulencu 1980; Ball 1981; Kah *et al.* 1987; Poli et *al.* 1990; Anglade *et al.* 1993; Goping et *al.* 1995). Telencephalic projections to the hypothalamus and from hypothalamus to the pituitary regulate spawning behaviour in fish (Oka and Ueda 1981; Kyle and Peter 1982; Koyama *et al.* 1984; Fryer *et al.* 1985). The telencephalon, hypothalamus and pituitary were identified as distinct tissues expressing differential expression of nestin proteins in response to MPTP treatment. These studies could provide a link between nestin and neurogenic mechanisms to regulate DAergic levels during the seasonal reproductive cycle.

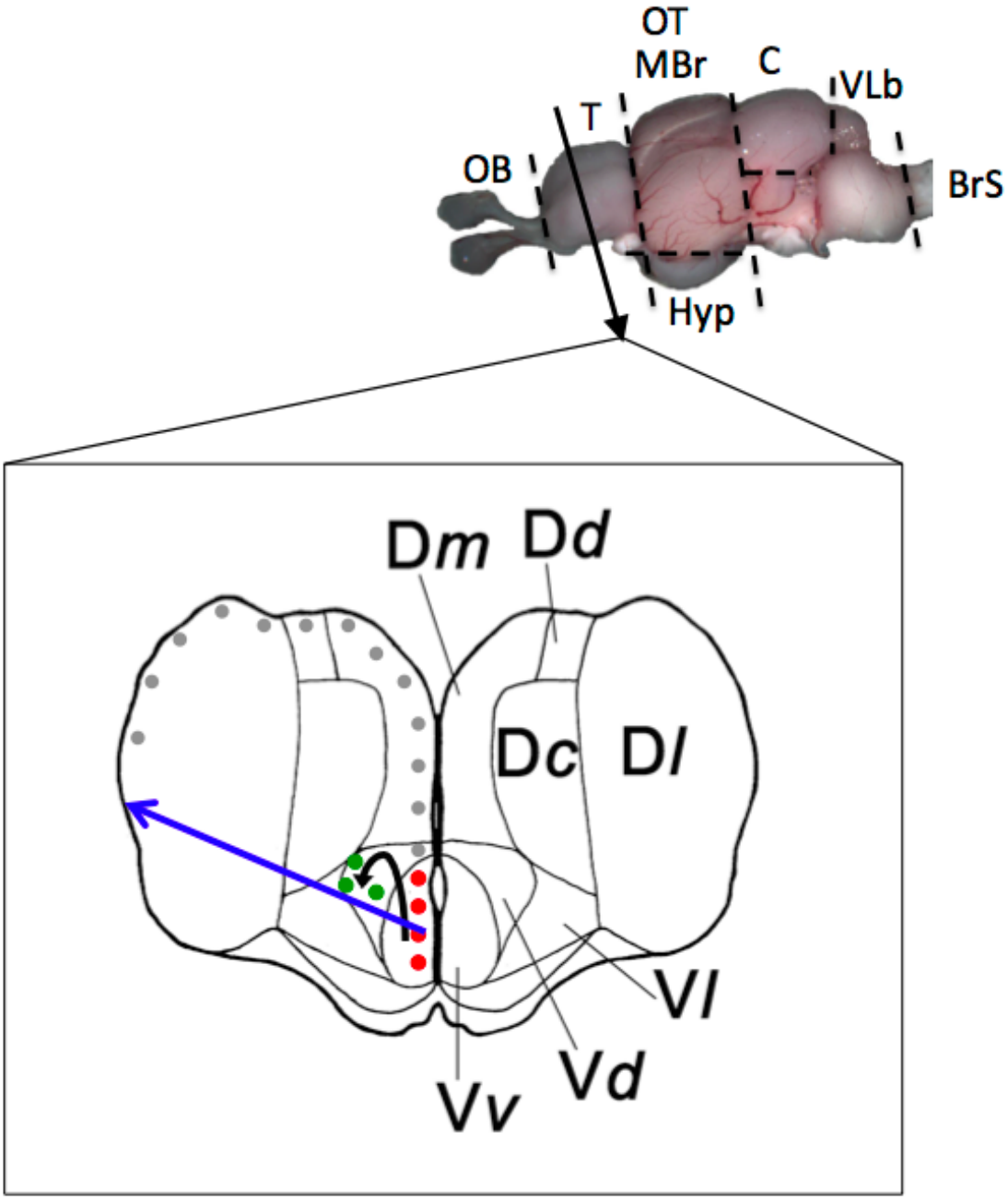

Figure 5.1. Proposed DA neuronal regeneration pathway following neurotoxic insult in the goldfish telencephalon. Radial glial cells stretch from the apical surface of the ventricle to the dorsal telencephalon and directionality is illustrated by the blue arrow. Progenitor cells (red dots) proliferate, migrate along RGCs (black arrow) and differentiate into DA neurons in the telencephalic Vd area. Grey dots represent various progenitor cell niches in the goldfish telencephalon. OB: Olfactory bulb; H: Hypothalamus; T: Telencephalon; MBr: Midbrain; OT: Optic Tectum; C: Cerebellum; VLb: Vagal Lobes; BrS: Brain Stem. Vd: area ventralis telencephali pars dorsalis; Vv: area ventralis telencephali pars ventralis; Vl: area ventralis telecephali pars lateralis; Dc: area dorsalis telencephali pars centralis; Dd: area dorsalis telencephali pars dorsalis; Dl: area dorsalis telencephali pars lateralis; Dm: area dorsalis telencephali pars medialis.

References

Adams J.D., Kalivas P.W. and Miller C.A. (1989). The acute histopathology of MPTP in the mouse CNS. *Brain Res. Bull.* **23**, 1-17.

Adeyemo O.M., Youdim M.B.H., Markey S.P., Markey C.J. and Pollard H.B. (1993). L-Deprenyl confers specific protection against MPTP-induced Parkinson's disease-like movement disorder in the goldfish. *Eur. J. of Pharmacol.* **240**, 185-193.

Airhart M.J., Shirk J.O. and Kriebel R.M. (1988). Telencephalic projections to the goldfish hypothalamus: an anterograde degeneration study. *Brain Res. Bull.* **20**, 503-514.

Adolf B., Chapouton P., Lam C.S., Topp S., Tannhäuser B., Strähle U., Götz M. and Bally-Cuif L. (2006). Conserved and acquired features of adult neurogenesis in the zebrafish telencephalon. *Dev. Biol.* ***295,*** 278–93.

Altman J. (1962). Are new neurons formed in the brains of adult mammals? *Science* **135**, 1127-1128.

Altman J. (1963). Autoradiographic investigation of cell proliferation in the brains of rats and cats. *Anat. Rec.* **145**, 573-591.

Altman J. (1969a). Autoradiographic and histological studies of postnatal neurogenesis: III. Dating the time of production and onset of differentiation of cerebellar microneurons in rats. *J. Comp. Neurol.* **136**, 269-294.

Altman J. (1969b). Autoradiographic and histological studies of postnatal neurogenesis: IV. Cell proliferation and migration in the anterior forebrain, with special reference to persisting neurogenesis in the olfactory bulb. *J. Comp. Neurol.* **137**, 433-458.

Altman J and Das G.D. (1965). Autoradiographic and histological evidence of postnatal hippocampal neurogenesis in rats. *J. Comp. Neurol.* **124**, 319-336.

Alvarez-Buylla, A. (1990) Mechanism of neurogenesis in adult avian brain. *Experientia* **46**, 948–955.

Alvarez-Builla A. and Garcia-Verdugo J.M. (2002). Neurogenesis in adult subventricular zone. *J. Neurosci.* **22**, 629-634.

Alvarez-Buylla A. and Lim D.A. (2004). For the long run: Maintaining germinal niches in the adult brain. *Neuron* **41**, 683-686.

Ampatzis K. and Dermon C.R. (2007). Sex differences in adult cell proliferation within the zebrafish (Danio rerio) cerebellum. *Eur. J. Neurosci.* **25**, 1030-1040.

Anglade I., Zandbergen T. and Kah O. (1993). Origin of the pituitary innervation in the goldfish. *Cell Tissue Res.* **273**, 345-355.

Aronson L.R. and Herberman R. (1960). Persistence of a conditioned response in the cichlid fish, *Tilapia macrocephala*, after forebrain and cerebellar ablations. *Anat. Rec.* **138**, 332.

Ball J.N. (1981). Hypothalamic control of the pars distalis in fishes, amphibians, and reptiles. *Gen. Comp. Endocrinol.* **44** (2), 135-170.

Barry D.S., Pakan J.M.P. and McDermott K.W. (2014). Radial glial cells: Key organisers in CNS development. *Int. J. of Biochem. Cell B.* **46**, 76-70.

Basak A., Boudreault A., Chen A., Chretien M., Seidah N.G. and Lazure C. (1995) Application of the multiple antigenic peptides (MAP) strategy to the production of prohormone convertases antibodies: synthesis, characterization and use of 8-branched immunogenic peptides. *J. Pept. Sci.* **1**, 385–395.

Bayer S.A., Yackel J.W. and Puri P.S. (1982). Neurons in the rat dentate gyrus granular layer substantially increase during juvenile and adult life. *Science* **216**, 890-892.

Beattie M.S., Farooqui A.A. and Bresnahan J.C. (2000). Review of current evidence for apoptosis after spinal cord injury. *J. Neurotrauma* **17**, 915-925.

Becker C.G. and Becker T. (2007). Growth and pathfinding of regenerating axons in the optic projection of adult fish. *J. Neurosci. Res.* **85**, 2793-2799.

Becker C.G. and Becker T. (2008). Adult zebrafish as a model for successful central nervous system regeneration. *Restor. Neurol. Neuros.* **26**, 71-80.

Benowitz L.I., Shashona V.E. and Yoon, M.G. (1981). Specific changes in rapidly transported protein during regeneration of the goldfish optic nerve. *J. Neurosci.* **1**, 300-307.

Benskey M.T., Manfredsson F.P., Lookingland K.J. and Goudreau J.L. (2015). The role of parkin in the differential susceptibility of tuberoinfundibular and nigrostriatal dopamine neurons to acute toxicant exposure. *NeuroToxicology* **46**, 1-11.

Bernstein J.J. (1964). Relation of spinal cord regeneration to age in adult goldfish. *Exp. Neurol.* **9**, 161-174.

Björklund A. and Dunnett S.B. (2007). Dopamine neuron systems in the brain: an update. *TRENDS Neurosci.* **32**, 194-202.

Blazquez M., Bosma P.T., Fraser E.J., Van Look K.J. and Trudeau V.L. (1998). Fish as models for the neuroendocrine regulation of reproduction and growth. *Comp.*

Biochem. Physiol. C. Pharmacol. Toxicol. Endocrinol. **119**, 345-364.

Blesa J., Phani S., Jackson-Lewis V. and Przedborski S. (2012). Classic and new animal models of Parkinson's disease. *J. Biomed. Biotechnol.* **2012**, 1-10.

Blin M., Norton W., Bally-Cuif L. and Vernier P. (2008). NR4A1 controls the differentiation of selective dopaminergic nuclei in the zebrafish brain. *Mol. Cell Neurosci.* **39**, 592-604.

Borodovsky N., Ponomaryov T., Frenkel S. and Levkowitz G. (2009). Neural protein olig2 acts upstream of the transcriptional regulator sim1 to specify diencephalic dopaminergic neurons. *Developmental Dynamics* **238**, 826-834.

Brunne, B., Zhao, S. Derouiche, A., Herz, J., May, P., Frotscher, M. and Bock, H.H., 2010. Origin, maturation, and astroglial transformation of secondary radial glial cells in the developing dentate gyrus. Glia **58**, 1553-1569.

Burns R.S., Chiueh C.C., Markey S.P., Ebert M.H., Jacobowitz D. and Kopin l.J. (1983). A primate model of parkinsonism: selective destruction of dopaminergic neurons in the pars compacta of the substantia nigra by N-methyl-4-phenyl-l,2,3,6-tetrahydropyridine. *Proc. Natl. Acad. Sci.* **80,** 4546-4550.

Carmona I.C., Luesma Bartolomé M.J., Lavoie-Gagnon C. and Junquera Escribano C. (2011). Distribution of nestin protein: Immunohistochemical study in enteric plexus of rat duodenum. *Microsc. Res. Tech.* **74**, 148-152.

Castelo-Branco G., Sousa K.M., Bryja V., Pinto L., Wagner J. and Arenas E., (2005). Ventral midbrain glia express region-specific transcription factors and regulate dopaminergic neurogenesis through Wnt-5a secretion. *Mol. Cell. Neurosci.* **31**, 252-262.

Castillo S.O., Baffi J.S., Palkovits M., Goldstein D.S., Kopin I.J., Witta J., Magnuson M.A. and Nikodem V.M. (1998). Dopamine biosynthesis is selectively abolished in substantia nigra/ventral tegmental area but not in hypothalamic neurons in mice with targeted disruption of the Nurr1 gene. *Mol. Cell. Neurosci.* **11**, 36-46.

Chang J.P. and Peter R.E. (1983). Effects of dopamine on gonadotropin release in female goldfish, Carassius auratus. *Neuroendocrinology* **36**, 351-357.

Chapouton P., Jagasia R. and Bally-Cuif L. (2007). Adult neurogenesis in non-mammalian vertebrates. *Bioessays* **29**, 745-757.

Chapouton P., Webb K.J., Stigloher C., Alunni A., Adolf B., Hesl B., Topp S., Kremmer E. and Bally-Cuif L. (2011). Expression of *haire/enhancer of split* genes in neural profenitors and neurogensis domains of the adult zebrafish brain. *J. Comp. Neurol.* **519**, 1748-1769.

Chaube R. and Joy K.P. (2003). Brain tyrosine hydroxylase in the catfish Heteropneustes fossilis: annual and circadian variations, and sex and regional differences in enzyme activity and some kinetic properties. *Gen. Comp. Endocr.* **130**, 29-40.

Chen H.-L., Yuh C.-H. and Wu K. K. (2010) Nestin is essential for zebrafish brain and eye development through control of progenitor cell apoptosis. *PLoS ONE* 5, e9318.

Chiba K., Trevor A. and Castagnoli N. Jr. (1984). Metabolism of the neurotoxic tertiary amine, MPTP, by brain monoamine oxidase. *Biochem. Biophys. Res. Commun.* **120**, 574-578.

Chen H.L., Yuh C.H. and Wu K.K. (2010). Nestin is essential for zebrafish brain and eye development through control of progenitor cell apoptosis. *PLoS One* **5**, e9318.

Chiueh C.C., Markey S.P., Burns R., Johannensen J.N., Jacobowitz D. Kopin I. (1984). Neurochemical and behavioral effect of MPTP in rat, guinea pig and monkey. *Psychopharmacol. Bull*. **20**, 546-553.

Contestabile A., Friz T. and Caravagio M.V. (1979). Disappearance and recovery of catecholamine innervation in brain regions of adult goldfish following 6-hydroxydopamine treatment. *Neurosci. Lett.* **14**, 333-337.

Corotto F.S., Henegar J.A. and Maruniak J.A. (1993). Neurogenesis persists in the subependymal layer of the adult mouse brain. *Neurosci. Lett.* **149**, 111-114.

Cunningham F., Amode M.R., Barrell D., Beal K., Billis K., Brent S., Carvalho-Silva D., Clapham P., Coates G., Fitzgerald S., Gil L., Garcín Girón C., Gordon L., Hourlier T., Hunt S.E., Janacek S.H., Johnson N., Juettemann T., Kähäri A.K., Keenan S., Martin F.J., Maurel T., McLaren W., Murphy D.N., Nag R., Overduin B., Parker A., Patricio M., Perry E., Pignatelli M., Riat H.S., Sheppard D., Taylor K., Thormann A., Vullo A., Wilder S.P., Zadissa A., Aken B.L., Birney E., Harrow J., Kinsella R., Muffato M., Ruffier M., Searle S.M.J., Spudich G., Trevanion S.J., Yates A., Zerbino D.R. and Flicek P. (2015). Ensembl 2015. *Nucleic Acids Res.* **43** (Database issue), D662-D669.

Dahlstrand J., Zimmerman L.B., McKay R.D. and Lendahl U. (1990). Characterization of the human nestin gene reveals a close evolutionary relationship to neurofilaments. *J Cell Sci* **103**, 589-597.

Date I., Felten D.L. and Felten S.Y. (1990a). Long-term effect of MPTP in the mouse brain in relation to aging: neurochemical and immunocytochemical analysis. *Brain Res.* **519**, 266-276.

Date I., Notter M.F.D., Felten S. and Felten D. (1990b). MPTP-treated young mice but not aging mice show partial recovery of the nigrostriatal dopaminergic system by stereotaxic injection of acidic fibroblast growth factor (aFGF). *Brain Res.* **526**, 156-160.

De Leeuw R., Habibi H.R., Nahorniak C.S. and Peter R.E. (1989). Dopaminergic regulation of pituitary gonadotrophin-releasing hormone receptor activity in the goldfish (*Carassius auratus*). *J. Endocrinol.* **121**, 239 – 247.

Delgado L.M. and Schmachtenberg O. (2011). Neurogenesis in the adult goldfish cerebellum. *Anat. Record* **294**, 11-15.

Diotel N., Le Page Y., Mouriec K., Tong S.K., Pellegrini E., Vaillant C., Anglade I., Brion F., Pakdel F., Chung B.C. and Kah O. (2010). Aromatase in the brain of teleost fish: expression, regulation and putative functions. *Front. Neuroendocrinol.* **31**, 172–192.

Dirian L., Galant S., Coolen M., Chen W., Bedu S., Houart C., Bally-Cuif L. and Foucher I. (2014). Spatial regionalization and heterochrony in the formation of adult pallial neural stem cells. *Developmental Cell* **30**, 123-136.

Doetsh F. and Hen R. (2005). Young and excitable: The function of new neurons in the adult mammalian brain. *Curr. Opin. Neurobiol.* **15**, 121-128.

Dufour S., Weltzien F.A., Sebert M.E., Le Belle N., Vidal B., Vernier P. and Pasqualini C. (2005). Dopaminergic inhibition of reproduction in teleost fishes. Ann.N.Y. Acad. *Science* **1040**, 9-21.

Dufour S., Serbert M.E., Weltzien,F.A., Rousseau K. and Pasqualini C. (2009). Neuroendocrine control by dopamine of teleost reproduction. *J. Fish Biol.* **76**, 129-160.

Dufour S., Sebert M.-E., Weltzien F.-A., Rousseau K., and Pasqualini C. (2010). Neuroendocrine control by dopamine of teleost reproduction. *J. Fish Biol.* **76**, 129-160.

Duggal N., Schmidt-Kastner R. and Hakim A.M. (1997). Nestin expression in reactive astrocytes following focal cerebral ischemia in rats. *Brain Res.* **768**, 1-9.

Echteler S.M. and Saidel W.M. (1981). Forebrain connections in the goldfish support telencephalic homologies with land vertebrate. *Science* **212**, 683-685.

Ekström, P., Johnsson, C.M. & Ohlin, L.M. (2001) Ventricular proliferation zones in the brain of an adult teleost fish and their relation to neuromeres and migration (secondary matrix) zones. *J. Comp. Neurol.* **436**, 92–110.

Esni F., Soffers D.A., Takeuchi T. and Leach S.D. (2004). Origin of exocrine pancreatic cells from nestin-positive precursors in developing mouse pancreas. *Mech. Dev.* **121**, 15-25.

Felsenstein J. (1985). Confidence limits on phylogenies: An approach using the bootstrap. *Evolution* **39**, 783-791.

Filippi A., Durr K., Ryu S., Willaredt M., Holzschuh J. and Driever W. (2007). Expression and function of nr4a2, lmx1b, and pitx3 in zebrafish dopaminergic and noradrenergic neuronal development. *BMC Dev. Biol.* **7**, 135.

Finn R.D., Bateman A., Clements J., Coggill P., Eberhardt R.Y., Eddy S.R., Heger A., Hetherington K., Holm L., Mistry J., Sonnhammer E.K.K., Tate J. and Punta M. (2014). Pfam: the protein families database. *Nucleic Acids Res.* 42 (D1), D222-D230.

Fleige S. and Pfaffl M.W. (2006). RNA integrity and the effect on the real-time qRT-PCR performance. *Mol. Aspects. Med.* **27**, 126-139.

Fraichard A., Chassande O., Bilbaut G., Dehay C., Savatier P. and Samarut J. (1995). In vitro differentiation of embryonic stem cells into glial cells and functional neurons. *J. Cell Sci.* **108**, 3181-3188.

Franzoni M.F., Thibault J., Fasolo A., Marinoli M.G., Scaranari F. and Calas A. (1986). Organization of tyrosine-hydroxylase immunopositive neurons in the brain of the crested newt, *Triturus cristatus carnifex*. *J. Comp. Neurol.* **251**, 121-134.

Frederiksen K. and McKay R.D. (1988). Proliferation and differentiation of rat neuroepithelial precursor cells in vivo. *J. Neurosci.* **8**, 1144-1151.

Frisen J., Johansson C.B., Torok C., Rislin M. and Lendahl U. (1995). Rapid, widespread and longlasting induction of nestin contributes to the generation of glial scar tissue after CNS injury. *J. Cell. Biol.* **131**, 453-464.

Fryer J.N., Boudreault-Chateauvert C. and Kirby R.P. (1985). Pituitary afferents originating in the paraventricular organ (PVO) of the goldfish hypothalamus. *J. Comp. Neurol.* **242**, 475-484.

Fuchs E. and Weber K. (1994). Intermediate filaments: Structure, dynamics, function, and disease. *Annu. Rev. Biochem.* **63**, 345-382.

Gainetdinov R.R., Fumagalli F., Jones S.R. and Caron, M.G. (1997). Dopamine transporter is required for in vivo MPTP neurotoxicity: evidence from mice lacking the transporter. *J. Neurochem.* **69,** 1322-1325.

Ganz J., Kaslin J., Hochmann S., Freudenreich D. and Brand M. (2010). Heterogeneity and Fgf dependence of adult neural profenitors in the zebrafish telencephalon. *Glia* **58**, 1345-1363.

Garcia A.D., Doan N.B., Imura T., Bush T.G. and Sofroniew M.V. (2004). GFAP-expressing progenitors are the principal source of constitutive neurogenesis in adult mouse forebrain. *Nat. Neurosci.* **7**, 1233-1241.

Glasauer S.M.K. and Neuhass S.C.F. (2014). Whole-genome duplication in teleost fishes and its evolutionary consequences. *Mol. Genet. Genomics* **289**, 1045-1060.

Goldman S.A. and Nottebohm F. (1983) Neuronal production, migration, and differentiation in a vocal control nucleus of the adult female canary brain. *Proc. Natl. Acad. Sci. USA* **80**, 2390–2394.

Goldman S. (2003). Glia as neural progenitor cells. *Trends Neurosci.* 26, 590-596.

Goping G., Pollard H.B., Adeyemo O. M. and Kuijpers G.A. (1995). Effect of MPTP on dopaminergic neurons in the goldfish brain: a light and electron microscope study. *Brain Res.* **687**, 35-52.

Götz M. and Barde Y.A. (2005). Radial glial cells: defined and major intermediates between embryonic stem cells and CNS neurons. *Neuron* **46**, 369-372.

Gould E., Tanapat P., McEwen B.S., Flügge G. and Fuchs E. (1998). Proliferation of granule cell precursors in the dentate gyrus of adult monkeys is diminished by stress. *Proc. Natl. Acad. Sci. USA* **95**, 3168-3171.

Goulet M., Morissette M., Grondin R., Falardeau P., Bedard P.J., Rostene W. and Di Paolo T. (1999). Neurotensin receptors and dopamine transporters: effects of MPTP lesioning and chronic dopaminergic treatments in monkeys. *Synapse* **32**, 153-64.

Grandel H., Kaslin J., Ganz J., Wenzel I. and Brand M. (2006). Neural stem cells and neurogenesis in the adult zebrafish brain: origin, proliferation dynamics, migration and cell fate. *Dev. Biol.* **295**, 263–277.

Guarnieri I., Villani L. and Fasolo A. (1989). Tyrosine hydroxylase immunohistochemistry in the normal and 1-methyl-4-phenyl-tetrahydropyridine (MPP+) treated retina of goldfish. *Neurosci. Lett.* **106**, 269-274.

Guilgur L.G., Moncaut N.P., Canario a.v. and Somoza G.M. (2006). Evolution of GnRH ligands and receptors in gnathostomata. *Comp. Biochem. Physiol. A. Mol. Integr. Physiol.* **144**, 272-283.

Guillery R.W. (2002). On counting and counting errors. *J. Comp. Neurol.* **447**, 1-7.

Hallman H., Lange J., Olson L., Stromberg I. and Jonsson G. (1985). Neurochemical and histochemical characterization of neurotoxic effects of 1-methyl-4-phenyl-l,2,3,6-tetrahydropyridine on brain catecholamine neurons in the mouse. *J. Neurochem*. **44,** 117-127.

Hamill C.E., Caudle W.M., Richardson J.R., Yuan H., Pennel K.D., Greene J.G., Miller G.W. and Traynelis S.F. (2007). Exacerbation of dopaminergic terminal damage in a mouse model of Parkinson's disease by the G-protein-couples receptor protease-activated receptor 1. *Mol. Pharmacol.* **72**, 653-664.

Heckmann L.-H., Sorensen P.B., Krogh P.H. and Sorensen J.G. (2011). NORMA-Gene: A simple and robust method for qPCR normalization based on target gene data. *BioMed Central Bioinformatics* **12**, 1471-2105.

Heikkila R.E., Hess A. and Duvoisin R.C. (1984a). Dopaminergic neurotoxicity of 1-methyl-4-phenyl-l,2,5,6-tetrahydropyridine in mice. *Science* **224**, 1451-1453.

Heikkila R.E., Manzino L., Cabbat F.S. and Duvoisin R.C. (1984b). Protection against the dopaminergic neurotxicity of 1-methyl-4-phenyl-1,2,3,6-tetrahydropyridine by monoamine oxidase inhibitors. *Nature* **311**, 467-469.

Herrmann H. and Aebi U. (2000). Intermediate filaments and their associates: multi-talented structural elements specifying cytoarchitecture and cytodynamics. *Curr. Opin. Cell Biol.* **12**, 79-90.

Hibbert B., Fung I., McAuley R., Larivière K., MacNeil B., Bafi-Yeboa N., Livesey J. and Trudeau V. (2004). Increased GAD67 mRNA levels are correlated with in vivo GABA synthesis in the MPTP-treated catecholamine-depleted goldfish brain. *Mol. Brain Res.* **128**, 121-130.

Hidalgo, A., Barami, K., Iversen, K. & Goldman, S.A. (1995) Estrogens and non-estrogenic ovarian influences combine to promote the recruitment and decrease the turnover of new neurons in the adult female canary brain. *J. Neurobiol.* **27**, 470–487.

Hinsch K. and Zupanc G.K.H. (2007). Generation and long-term persistence of new neurons in the adult zebrafish brain: a quantitative analysis. *Neuroscience* **146**, 679-696.

Holmin S., Almqvist P., Lendahl U. and Mathiesen T. (1997). Adult nestin-expressing subependymal cells differentiate to astrocytes in response to brain injury. *Eur. J. Neurosci.* **9**, 65-75.

Holzschuh J., Hauptmann G. and Driever W. (2003). Genetic analysis of the roles of Hh, FGF8, and nodal signaling during catecholaminergic system development in the zebrafish brain. *J. Neurosci.* **23**, 5507– 5519.

Hornby P.J., Piekut D.T. and Demski L.S. (1987). Localization of immunoreactive tyrosine hydroxylase in the goldfish brain. *J. Comp. Neurol.* **261**, 1-14.

Hornby P.J. and Piekut D.T. (1990). Distribution of catecholamine-synthesizing enzymes in goldfish brains: presumptive dopamine and norepinephrine neuronal organization. *Brain Behav. Evol.* **35,** 49-64.

Irwin I., DeLanney L.E., Forno L.S., Finnegan K.T., Di Monte D.A. and Langston J.W. (1990). The evolution of nigrostriatal neurochemical changes in the MPTP-treated squirrel monkey. *Brain Res.* **531**, 242-252.

Ishikawa R., Nishikori K. and Furukawa S. (1991). Appearance of nerve growth factor and acidic fibroblast growth factor with different time courses in the cavity-lesioned cortex of the rat brain. *Neurosci. Lett.* **127**, 70-72.

Itoh T., Satou T., Nishida S., Hashimoto S., Ito H. (2006). Cultured rat astrocytes give rise to neural stem cells. *Neurochem. Res.* **31**, 1381-1387.

Iversen S.D. and Iversen L. (2007). Dopamine: 50 years in perspective. *TRENDS in Neurosciences* **30**, 188-193.

Jacobs F.M., Van Erp S., Van der Linden A.J., Von Oerthel L., Burbach J.P. and Smidt M.P. (2009). Pitx3 potentiates Nurr1 in dopamine neuron terminal differentiation through release of SMRT-mediated repression. *Development* **136**, 531-540.

Javitch J.A. and Snyder S.H. (1984). Uptake of MPP(+) by dopamine neurons explains selectivity of parkinsonism-inducing neurotoxin, MPTP. *Eur. J. Pharmacol.* **106**, 455-456.

Johansson C. B., Lothian C., Molin M., Okano H. and Lendahl U. (2002) Nestin enhancer requirements for expression in normal and injured adult CNS. *J. Neurosci. Res.* **69**, 784-794.

Kabanova A., Pabst M., Lorkowski M., Braganza O., Boehlen A., Nikbakht N., Pothmann L., Vaswani A.R., Musgrove R., Di Monte D.A., Sauvage M., Beck H. and Blaess S. (2015). Function and developmental origin of a mesocortical inhibitory circuit. *Nature Neuroscience* **18**, 872-885.

Kachinsky A.M., Dominov J.A. and Miller J.B. (1995). Intermediate filaments in cardiac myogenesis: nestin in the developing mouse heart. *J. Histochem. Cytochem.* **43**, 843-847.

Kah O., Dulka J.G., Dubourg P., Thibault J. and Peter R.E. (1987). Neuroanatomical substrate for the inhibition of gonadotrophin secretion in goldfish: existence of a dopaminergic preoptico-hypophyseal pathway. *Neuroendocrin.* **45,** 451-458.

Kaplan MS. (1981). Neurogenesis in the 3-month-old rat visual cortex. *J. Comp. Neurol.* **195**, 323–338.

Kaplan M.S. and Hinds J.W. (1977). Neurogenesis in the adult rat: electron microscopic analysis of light radioautographs. *Science* **197**, 1092–1094.

Kaplan M.S. and Bell D.H. (1983). Neuronal proliferation in the 9-month-old rodent-radioautographic study of granule cells in the hippocampus. *Exp. Brain Res.* **52**, 1-5.

Kapsimali M., Bourrat F. and Vernier, P. (2001). Distribution of the orphan nuclear receptor Nurr1 in Medaka (Oryzias latipes): Cues to the definition of homologous cell groups in the vertebrate brain. *J. Comp. Neurol.* **431**, 276-292.

Kaslin J. and Panula P. (2001). Comparative anatomy of the histaminergic and other aminergic systems in zebrafish (*Danio rerio*). *J. Comp. Neurol.* **440**, 342-347.

Kaslin J., Ganz J. and Brand M. (2008). Proliferation, neurogenesis and regeneration in the non-mammalian vertebrate brain. *Philos. Trans. R. Soc. Lond. B. Biol. Sci.* **363**, 101-222.

Kaslin J., Ganz J., Geffarth M., Grandel H., Hans S. and Brand M. (2009). Stem cells in the adult zebrafish cerebellum: initiation and maintenance of a novel stem cell niche. *J. Neurosci*. **29**, 6142–6153.

Kastenhuber E., Kratochwil C.F., Ryu S., Schweitzer J. and Drieve W. (2010). Genetic dissection of dopaminergic and noradrenergic contributions to catecholamineric tracts in early larval zebrafish. *J. Comp. Neurol.* **518**, 439-458.

Kebabian J.W. and Calne D.B. (1979). Multiple receptors for dopamine. *Nature* **277**, 93-96.

Kempermann G., Wiskott L. and Gage F.H. (2004). Functional significance of adult neurogenesis. *Curr. Opin. Neurobiol.* **14**, 186-191.

Klausen C., Chang J.P. and Habibi H.R. (2002). Multiplicity of gonadotropin-releasing hormone signaling: a comparative perspective. *Prog. Brain. Res.* **141**, 111-128.

Koyama Y., Satou M., Oka Y. and Ueda K. (1984). Involvement of the telecephalic hemispheres and the preoptic area in sexual behavior of the male goldfish, Carassius auratus: a brain-lesion study. *Behav. Neurol. Biol.* **40**, 70-86.

Kuhar M.J., Couceyro P.R. and Lambert P.D. (1999). Biosynthesis of catecholamines, in: Siegel G.J., Agranoff B.W. *et al.* (Eds). Basic neurochemistry: Molecular, cellular and medical aspects, 6th edition, Lippincott-Raven, Philadelphia, 243-261.

Kuhn K., Wellen J., Link N., Maskri L., Lubbert H. and Stichel C.C. (2003). The mouse MPTP model: gene expression changes in dopaminergic neurons. *Eur. J. Neurosci.* **17**, 1-12.

Kyle A.L. and Peter R.E. (1982). Effects of forebrain lesions on spawning behavior in the male goldfish. *Physiol. Behav.* **28**, 1103-1109.

Lam C.S., Korzh V. and Strahle U. (2005). Zebrafish embryos are susceptible to the dopaminergic neurotoxin MPTP. *Eur. J. Neurosci.* **21**, 1758-1762.

Langston J.W., Fomo L.S., Rebert C.S. and Irwin I. (1984). Selective nigral toxicity after systemic administration of 1-methyl-4-phenyl-1,2,3,6-tetrahydropyridine (MPTP) in the squirrel monkey. *Brain Res.* **292**, 390-395.

Lardon J. Rooman I. and Bouwens L. (2002). Nestin expression in pancreatic stellate cells and angiogenic endothelial cells. *Histochem. Cell Biol.* **177**, 535-540.

Lees J.F., Shneidman P.S., Skuntz S.F. Carden M.J., Lazzarini R.A. (1988). The structure and organization of the human heavy neurofilament subunit (NF-H) and the gene encoding it. *EMBO J.* **7**, 1947-1955.

Lendahl U., Zimmerman L. and McKay R. (1990). CNS stem cells express a new class of intermediate filament protein. *Cell* **60**, 585-595.

Le Page Y., Diotel N., Vaillant C., Pellegrini E., Anglade I., Mérot Y. and Kah O. (2010). Aromatase, brain sexualization and plasticity: the fish paradigm. *Eur. J. Neurosci.* **32**, 2105-2115.

Lethimonier C., Madigou T., Munoz-Cueto J.A., Lareyre J.J. and Kah O. (2004). Evolutionary aspects of GnRHs, GnRH neuronal systems and GnRH receptors in teleost fish. *Gen. Comp. Endocrinol.* **135**, 1-16.

Levine R.L. (1983). Widespread regeneration of central axons through the central nervous system of the goldfish. *Dev. Brain Res.* **9**, 416.

Lin L.F., Doherty D.H., Lile J.D., Bektesh S. and Collins F. (1993). GDNF: a glial cell line-derived neurotrophic factor for midbrain dopaminergic neurons. *Science* **260,** 1130-2.

Lin R.C.S., Matesic D.F., Marvin M., McKay R.D. and Brüstle O. (1995). Re-expression of the intermediate filament nestin in reactive astrocytes. *Neurobiol. Dis.* **2**, 79-85.

Liou A.K.F., Clark R.S., Henshall D.C., Yin X.-M. and Chen J. (2003). To die or not to die for neurons in ischemia, traumatic brain injury and epilepsy: a review on the

stress-activated signaling pathways and apoptotic pathways. *Prog. Neurobiol.* **69**, 103-142.

Liu X., Bolteus A.J., Balkin D.M., Henschel O. and Bordey A. (2006). GFAP-expressing cells in the postnatal subventricular zone display a unique glial phenotype intermediate between radial glia and astrocytes. *Glia* **54**, 394–410.

Lledo P.M. and Saghatelyan A. (2005). Integrating new neurons into the adult olfactory bulb: Joining the network, life-death decisions, and the effects of sensory experience. *Trends Neurosci.* **28**, 248-254.

Lois C. and Alvarez-Buylla A. (1993). Proliferating subventricular zone cells in the adult mammalian forebrain can differentiate into neurons and glia. *Proc. Natl. Acad. Sci. USA* **90**, 2074–2077.

Lois C. and Alvarez-Buylla A. (1994). Long-distance neuronal migration in the adult mammalian brain. *Science* **264**, 1145–1148.

Lu Z., Wang J., Li M., Liu Q., Wei D., Yang M. and Kong L. (2014). H NMR-based metabolomics study on a goldfish model of Parkinson's disease induced by 1-methyl-4-phenyl-1,2,3,6-tetrahydropyridine (MPTP). *Chemico-Biological Interactions* **223**, 18-26.

Lucchi R., Notari S., Pierantozzi S., Barnabei O., Villani L. and Poli A. (1998). Effect of 1-methyl-4-phenyl-1,2,3,6-tetrahydropyridine in goldfish cerebellum: neurochemical and immunocytochemical analysis. *Brain Res.* **782**, 105-112.

Luo G.R., Chen Y., Li X.P., Liu T.X. and Le W.D. (2008). Nr4a2 is essential for the differentiation of dopaminergic neurons during zebrafish embryogenesis. *Mol. Cell Neurosci.* **39**, 202-210.

Lykissas M.G., Batistatou A.K., Charalabopoulos K.A., Beris A.E. (2007) The role of neurotrophins in axonal growth, guidance, and regeneration. *Curr. Neurovasc. Res.* **4**, 143-151.

Ma P.M. (2003). Catecholaminergic systems in the zebrafish: IV. Organization and projection pattern of dopaminergic neurons in the diencephalon. *J. Comp. Neurol.* **460**, 13– 37.

Mack A.F. and Fernald R.D. (1997). Cell movement and cell cycle dynamics in the retina of the adult teleost *Haplochromis burtoni. J. Comp. Neurol.* **388**, 435-443.

Mahler J. and Driever W. (2007). Expression of the zebrafish intermediate neurofilament nestin in the developing nervous system and in neural proliferation zones at postembryonic stages. *BMC Developmental Biology* **7**, 1-11.

Marchler-Bauer A., Derbyshire M.K., Gonzales N.R., Lu S., Chitsaz F., Geer L.Y., Geer R.C., He J. Gwadz M., Hurwitz D.I., Lanczycki C.J., Lu F., Marchler G.H., Song J.S., Thanki N., Wang Z., Yamashita R.A. Zhang D., Zheng C. and Bryant S.H. (2015). CDD: NCBI's conserved domain database. *Nucleic Acids Res.* **43** (Database issue), D222-226.

Mares, V and Lodin Z. (1974). An autoradiographic study of DNA synthesis in adolescent and adult mouse forebrain. *Brain Res.* **76**, 557–561.

Martinat C., Bacci J.J., Leete T., Kim J., Vanti W.B., Newman A.H., Cha J.H., Gether U., Wang H. and Abeliovich A. (2006). Cooperative transcription activation by Nurr1 and Pitx3 induces embryonic stem cell maturation to the midbrain dopamine neuron phenotype. *Proc. Natl. Acad. Sci. USA* **103**, 2874-2879.

Marshall J.F., Richardson J.S. and Teitelbaum P. (1974). Nigrostriatal bundle damage and the lateral hypothalamic syndrome. *J. Comp. Physiol. Psychol.* **87**, 808-830.

März M., Chapouton P., Diotel N., Vaillant C., Hesl B., Takamiya M., Lam C.S., Kah O., Bally- Cuif, L. and Strähle, U. (2010). Heterogeneity in progenitor cell subtypes in the ventricular zone of the zebrafish adult telencephalon. *Glia* **58**, 870-888.

Matsuda M., Katoh-Semba R., Kitani H. and Tomooka Y. (1996) A possible role of the nestin protein in the developing central nervous system in rat embryos. *Brain Res.* **723**, 177–189.

Matsui H., Taniguchi Y., Inoue H., Uemura K., Takeda S. and Takahashi R. (2009). A chemical neurotoxin, MPTP induces Parkinson's disease like phenotype, movement disorders and persistent loss of dopamine neurons in medaka fish. *Neurosci. Res.* **65**, 263-271.

Matsukawa T., Arai K., Koryama Y., Liu Z. and Kato S. (2004). Axonal regeneration of fish optic nerve after injury. *Biol. Pharm. Bull.* **27**, 445-451.

McKinley E.T., Baranowski T.C., Blavo D.O., Cato C., Doan T.N., Rubinstein A.L. (2005). Neuroprotection of MPTP-induced toxicity in zebrafish dopaminergic neurons. *Brain Res.* **141**, 128-137.

Merkle F.T., Tramontin A.D., Garcia-Verdugo J.M. and Alvarez-Buylla A. (2004). Radial glia give rise to adult neural stem cells in the subventricular zone. *Proc. Natl. Acad. Sci. USA* **101**, 17528-17532.

Michalczyk K. and Ziman M. (2005). Nestin structure and predicted function in cellular cytoskeletal organisation. *Histol. Histopathol.* **20**, 665-671.

Miller R.M., Callahan L.M., Casaceli C., Chen L., Kiser G.L., Chui B., Kaysser-Kranich T.M., Sendera T.J., Palaniappan C. and Federoff, H.J. (2004). Dysregulation of

gene expression in the 1-methyl-4-phenyl-1,2,3,6-tetrahydropyridine-lesioned mouse substantia nigra. *J. Neurosci.* **24**, 7445-7454.

Mogensen G.J., Jones D.L. and Yim C.Y. (1980). From motivation to action: functional interadction between the limbic system and the motor system. *Prog. Neurobiol.* **14** 69-97.

Mokry J. and Nemecek S. (1998). Angiogenesis of extra- and intraembryonic blood vessels is associated with expression of nestin in endothelial cells. *Folia Biol. (Praha)* **44**, 155-161.

Monsma F.J. Jr., McVittie L.D., Gerfen C.R., Mahan L.C. and Sibley D.R. (1989). Multiple D2 dopamine receptors produced by alternative RNA splicing. *Nature* **342**, 926-929.

Murray M. and Grafstein B. (1969). Changes in the morphology and amino acid incorporation of regenerating goldfish optic neuron. *Exp. Neurol.* **23**, 544-560.

Nagatsu T., Levi H. and Udenfriend S. (1964). Tyrosine hydroxylase. The initial step in norepinephrine biosynthesis. *J. Biol. Chem.* **239**, 2910-2917.

Namiki J. and Tator C.H. (1999). Cell proliferation and nestin expression in the ependyma of the adult rat spinal cord after injury. *J. Neuropathol. Exp. Neurol.* **58**, 489-490.

Nilsson M., Perfilieva e., Johansson U., Orwar O. and Eriksson P. (1999). Enriched environment increases neurogenesis in the adult rat dentate gyrus and improves spatial memory. *J. Neurobiol.* **39**, 569-578.

Nordeen, K.W., Nordeen, E.J. & Arnold, A.P. (1987) Estrogen accumulation in zebra finch song control nuclei: implications for sexual differentiation and adult activation of song behavior. *J. Neurobiol.* **18**, 569–582.

Nordeen, E.J. & Nordeen, K.W. (1989) Estrogen stimulates the incorporation of new neurons into avian song nuclei during adolescence. *Brain Res. Dev. Brain Res.* **49**, 27–32.

Ohye T., Ichinose H., Ogawa M., Yoshida M. and Nagatsu, T. (1995). Alterations in multiple tyrosine hydroxylase mRNAs in the substantia nigra, locus coeruleus and adrenal gland of MPTP-treated parkinsonian monkeys. *Neurodegeneration* **4**, 81-85.

Oka Y. and Ueda K. (1981). Telencephlaic projections in the goldfish (*Carassius auratus*): an anterograde degeneration study. *J. Fac. Sci. Univ. Tokyo* **15**, 1-8.

Oki C, Watanabe Y., Yokoyama H., Shimoda T., Kato H. and Araki T. (2008). Delayed

treatment with arundic acid reduces the MPTP-induced neurotoxicity in mice. *Cell Mol. Neurobiol.* **28**, 417-430.

Olanow C.W. and Tatton W.G. (1999). Etiology and pathogenesis of Parkinson's disease. *Annu. Rev. Neuroscience* **22**, 123-144.

Omeljaniuk R.J., Shih S.H. and Peter R.E. (1987). In-vivo evaluation of dopamine receptor-mediated inhibition of gonadotrophin secretion from the pituitary gland of the goldfish, *Carassius auratus*. *J. Endocrinol.* **114**, 449-458.

Omodei D., Acampora D., Mancuso P., Prakash N., Di Giovannantonio L.G., Wurst W. and Simeone A. (2008). Anterior-posterior graded response to Otx2 controls proliferation and differentiation of dopaminergic progenitors in the ventral mesencephalon. *Development* **135**, 3459-3470.

Park D., Xiang A.P., Mao F.F., Zhang L., Di C.G., Liu X.M., Shao Y., Ma B.F., Lee J.H., Ha K.S., Walton N. and Lahn B.T. (2010). Nestin is required for the proper self-renewal of neural stem cells. *Stem Cells* **28**, 2162-2171.

Pellegrini E., Mouriec K., Anglade I., Menuel A., Le Page Y., Gueguen M.M., marmignon M.H., Brion F., Pakdel F. and Kah O. (2007). Identification of aromatase-positive radial glial cells as progenirot cells in teh ventricular layer of the forebrain in zebrafish. *J. Comp. Neurol.* **501**, 150-167.

Pelligirini E., Diotel N., Vaillant C., Pérez Marie R., Gueguen M.M., Nasri A., Cano-Nicolau J. and Kah O. (2015). Steroid modulation of neurogenesis: Focus on radial glial cells in zebrafish. *J. Steroid Biochem. Mol. Biol.*

Peretto P., Giachino C., Panzica G. and Fasolo A. (2001) Sexually dimorphic neurogenesis is topographically matched with the anterior accessory olfactory bulb of the adult rat. *Cell Tissue Res.* **306**, 385–389.

Peter R.E., Crim L.W., Goos H.J.TH., and Crim J.W. (1978) Lesioning studies on the gravid female goldfish: neuroendocrine regulation of ovulation. *General and Comp. Endocrinol.* **35**, 391-401.

Peter R.E. and Gill V.E. (1975). A stereotaxic atlas and technique for forebrain nuclei of the goldfish, *Carassius auratus*. *J. Comp. Neurol.* **159**, 69-101.

Peter R.E. and Palencu C.R. (1980). Involvement of the preoptic region in the gonadotropin release-inhibition in the goldfish. *Neuroendocrinol.* **31**, 133-141.

Poli A., Guarnieri O., Facchinetti F. and Villani L. (1990). Effect of 1-methyl-4-phenyl-1,2,3,6-tetrahydropyridine (MPTP) in goldfish brain. *Brain Res.* **534**, 45-50.

Poli A., Gandolfi O., Lucchi R. and Barnabei O. (1992). Spontaneous recovery of MPTP-

damage catecholamine systems in goldfish brain areas. *Brain Res.* **584**, 128-134.

Pollard H.B., Dhariwal K., Adeyemo O.M., Markey C.J., Caohuy H., Levine M., Markey S. and Youdim M.B.H. (1992). A parkinsonian syndrome induced in the goldfish by the neurotoxin MPTP. *FASEB J.* **6**, 3108-3116.

Pollard H.B., Kuijpers G.A., Adeyemo O.M., Youdim M.B.H. and Goping G. (1996). The MPTP-induced parkinsonian syndrome in the goldfish is associated with major cell destruction in the forebrain and subtle changes in the optic tectum. *Exp.l Neurol.* **142**, 170-178.

Popesku J.T., Martyniuk C.J., Mennigen J., Hiong H., Zhan D., Xia X., Cossins A.R., Trudeau V.L. (2008). The goldfish (Carassius auratus) as a model for neuroendocrine signaling. *Mol. Cell. Endocrinol.* **293**, 43-56.

Popesku J.T. (2009). Dopaminergic regulation of gene expression in the neuroendocrine brain of the goldfish (*Carassius auratus*). PhD Thesis. University of Ottawa, Canada, 1-193.

Popesku J.T., Martyniuk C.J. and Trudeau V.L. (2012). Meta-type analysis of dopaminergic effects on gene expression in the neuroendocrine brain of female goldfish. *Front. Endocrinol.* **3**, 30.

Porter J.C., Kedzierski W., Aguila-Mansilla N., Jorquera B.A. and González H.A. (1990). The tuberoinfundibular dopaminergic neurons of the brain: hormonal regulation. *Adv. Exp. Med. Biol.* **274**, 1-23.

Prakash N. and Wurst W. (2006). Genetic networks controlling the development of midbrain dopaminergic neurons. *J. Physiol.* **575**, 403-410.

Rasband, W.S. (1997-2014). Image J, U.S. National Institutes of Health, Bethesda, Maryland, USA, http://imagej.nih.gov/ij/

Rasika S., Nottebohm F. and Alvarez-Buylla A. (1994). Testosterone increases the recruitment and/or survival of new high vocal center neurons in adult female canaries. *Proc. Natl. Acad. Sci. USA* **91**, 7854–7858.

Raymond P.A. and Easter S.S. Jr (1983). Postembryonic growth of the optic tectum in goldfish. I. Location of germinal cells and numbers of neurons produced. *J. Neurosci.* **3**, 1077–1091.

Reimer M.M., Sörensen I., Kuscha V., Frank R.E., Liu C., Becker C.G. and Becker T. (2008). Motor neuron regeneration in adult zebrafish. *J. Neurosci.* **28**, 8510-8516.

Riddle R. and Pollock J.D. (2003). Making connections: the development of mesencephalic dopaminergic neurons. *Dev. Brain Res.* **147**, 3-21.

Rink E. and Wullimann M.F. (2001). The teleostean (zebrafish) dopaminergic system ascending to the subpallium (striatum) is located in the basal diencephalon (posterior tuberculum). *Brain Res.* **889**, 316-330.

Rink E. and Wullimann M.F. (2002). Connections of the ventral telencephalon and tyrosine hydroxylase distribution in the zebrafish brain (Danio rerio) lead to identification of an ascending dopaminergic system in a teleost. *Brain Res. Bull.* **57**, 385– 387.

Rodriguez F., Duran E., Gomez A., Ocana F.N., Alvarez E., Jimenez-Moya F., Broglio C. and Salas C. (2005). Cognitive and emotional functions of the teleost fish cerebellum. *Brain Res. Bull.* **66**, 365-370.

Rohlf, F. J. 2009. NTSYSpc: numerical taxonomy system. ver. 2.21c. Exeter Software: Setauket: New York.

Rothenaigner I., Krecsmarik M., Hayes J.A., Bahn B., Lepier A., Fortin G., Götz M., Jagasia R. and Bally-Cuif L. (2011). Clonal analysis by distinct viral vector identifies bona fide neural stem cells in the adult zebrafish telencephalon and characterizes their division properties and fate. *Development* **138**, 1459-1469.

Rutherford S., Chen H.-L., Yuh C.-H. and Wu K. K. (2010) Nestin is essential for zebrafish brain and eye development through control of progenitor cell apoptosis. *PLoS ONE* **5,** e9318.

Saijo K., Winner B., Carson C.T., Collier J.G., Boyer L., Rosenfeld M.G., Gage F.H. and Glass C.K. (2009). A Nurr1/CoREST pathway in microglia and astrocytes protects dopaminergic neurons from inflammation-induced death. *Cell* **137**, 47-59.

Saitou N. and Nei M. (1987) The neighbor-joining method: A new method for reconstructing phylogenetic trees. *Mol. Biol. Evol.* **4**, 406-425.

Sakurada K., Ohshima-Sakurada M., Palmer T.D. and Gage F.H. (1999). Nurr1, an orphan nuclear receptor, is a transcriptional activator of endogenous tyrosine hydroxylase in neural progenitor cells derived from the adult brain. *Development* **126**, 4017-4026.

Sallinen V., Torkko V., Sundvik M., Reenilä I., Khrustalyov D., Kaslin J. and Panula P. (2009). MPTP and MPP+ target specific aminergic cell populations in larval zebrafish. *J. Neurochem.* **109**, 719-731.

Santarelli L., Saxe M., Gross C., Surget A., Battaglia F., Dulawa S., Weisstaub N., Lee J., Duman R., Arancio O., Belzung C. and Hen R. (2003). Requirement of hippocampal neurogenesis for the behavioral effects of antidepressants. *Science* **301**, 805-809.

Sas E., Maler L. and TInner B. (1990). Catecholaminergic systems in the brain of a gymnotiform teleost fish: an immunohistochemical study. *J. Comp. Neurol.* **292**, 127-162.

Saucedo-Cardenas O., Quintana-Hau J.D., Le W.D., Smidt M.P., Cox J.J., De Mayo F., Burbach J.P. and Conneely O.M. (1998). Nurr1 is essential for the induction of the dopaminergic phenotype and the survival of ventral mesencephalic late dopaminergic precursor neurons. *Proc. Natl. Acad. Sci. USA* **95**, 4013-4018.

Scatton B., Javoy-Agid F., Rouquier L., Dubois B. and Agid Y. (1983). Reduction of cortical dopamine, noraderenaline, serotonin and their metabolites in Parkinson's disease. *Brain Res.* **275**, 321-328.

Scherer S.S. and Easter S.S. (1984). Degeneration and regeneration changes in the trochlear nerve of the goldfish. *J. Neurocytol.* **13,** 519.

Schmidt R., Strähle U. and Scholpp S. (2013). Neurogenesis in zebrafish – from embryo to adult. *Neural Development* **8**, 1-13.

Schneider J.S. and Markham C.H. (1986). Neurotoxic effects of N-methyl-4-phenyl-l,2,3,6-tetrahydropyridine (MPTP) in the cat. Tyrosine hydroxylase immunohistochemistry. *Brain Res*. **373**, 258-267.

Sébert M-E., Weltzien F.-A., Moisan C., Pasqualini C. and Dufour S. (2008). Dopaminergic systems in the European eel: characterization, brain distribution and potential role in migration and reproduction. *Hydrobiologia* **602**, 27-46.

Sejersen T. and Lendahl U. (1993). Transient expression of the intermediate filament nestin during skeletal muscle development. *J. Cell Sci.* **106**, 1291-1300.

Senthilkumaran B. and Joy K.P. (1995). Changes in hypothalamic catecholamines, dopamine ß hydroxylase, and phenylethanolamine-N-transferase in the catfish, *Heteropneustes fossilis*, in relation to season, raised photoperiod, and temperature, ovariectomy, and estradiol-17ß replacement. *Gen. Comp. Endocrinol.* **97**, 121-134.

Singer T.O., Castagnoli N., Ramsay R.R. and Trevor A.J. (1987). Biochemical events in the development of parkinsonism induced by 1-ethyl-4-phenyl-1,2,3,6-tetrahydropyridine. *J. Neurochem.* **49**, 1-8.

Sîrbulescu R.F., Ilies I. and Zupanc G.K.H. (2009). Structural and functional regeneration after spinal cord injury in the weakly electric teleost fish, *Apteronotus leptorhynchus*. *J. Comp. Physiol.* **195**, 699-714.

Sîrbulescu R.F. and Zupanc G.K.H. (2010a). Inhibition of caspase-3-mediated apoptosis improved spinal cord repair in a regeneration-competent vertebrate system. *Neuroscience* **171**, 599-612.

Sîrbulescu R.F. and Zupanc G.K.H. (2010b). Effect of temperature on spinal cord regeneration in the weakly electric fish, *Apteronotus leptorhynchus*. *J. Comp. Physiol. A*. 196, 359-368.

Sirinathsinghju D.J.S., Heavens R.P. and McBride C.S. (1988). Dopamine-releasing action of 1-methyl-4-phenyl-12,3,6-tetrahydropyridine (MPTP) and 1-methyl-4-phenylpyridine (MPP+) in the neostriatum of the rat as demonstrated in vivo by the push-pull perfusion technique: dependence on sodium but not calcium ions. *Brain Res.* **443**, 101-116.

Sjoberg G., Jiang W.Q., Ringertz N.R., Lendahl U. and Sejersen T (1994). Colocalization of nestin and vimentin/desmin in skeletal muscle cells demonstrated by three-dimensional fluorescence digital imaging microscopy. *Exp. Cell Res.* **214**, 447-458.

Sloley B. and McKenna K.F. (1993). 1-methyl-4-phenyl-1,2,3,6-tetrahydropyridine (MPTP), and γ-vinyl-γ-aminobutyric acit (γ-vinyl GABA) alter neurotransmitter concentrations in the nervous tissue of the goldfish (*Carassius auratus*) but not the cockroach (*Periplaneta Americana*). *Neurochem. Int.* **22**, 197-203.

Smidt M.P. and Burbach J.P. (2007). How to make a mesodiencephalic dopaminergic neuron. *Nat. Rev. Neurosci.* **8**, 21-32.

Smidt M.P., Smits S.M. and Burbach J.P. (2003). Molecular mechanisms underlying midbrain dopamine neuron development and function. *Eur. J. Pharmacol.* **480**, 75-88.

Smits S.M. and Smidt M.P. (2006). The role of Pitx3 in survival of midbrain dopaminergic neurons. *J. Neural. Transm. Suppl.* **70**, 57-60.

Snyder S.H., D'Amato J.R., Nye J.S. and Javitch J.A. (1986). Selective uptake of MPP+ by dopamine neurons is required for MPTP toxicity: studies in brain synaptosomes and PC-12 cells, in *MPTP: A neurotoxin producing a parkinsonian syndrome*, S.P. Markey *et al.*, Editors. Academic Press, Orlando. 191-201.

Springer A.D. and Agranoff B.W. (1977). Effect of temperature on rate of goldfish optic nerve regeneration: a radioautographic and behavioural study. *Brain Res.* **128**, 405-415.

Sriram K., Pai K.S., Boyd M.R. and Ravindranath V. (1997). Evidence for generation of oxidative stress in brain by MPTP: in vitro and in vivo studies in mice. *Brain Res.* **749**, 44-52.

Stacey N.E., Cook A.F. and Peter R.E. (1979). Ovulatory surge of gonadotropin in the goldfish, Carassius auratus. *Gen. Comp. Endocrinol.* **37**, 246-249.

Steinert P.M. and Roop D.R. (1988). Molecular and cellular biology of intermediate filaments. *Ann. Rev. Biochem.* **57**, 593-625.

Stevenson J.A. and Yoon M.G. (1978). Regeneration of optic nerve fibers enhances cell proliferation in the goldfish optic tectum. *Brain Res.* **153**, 345-351.

Strübing C., Ahnert-Hilger G., Shan J., Wiedenmann B., Hescheler J. and Wobus A.M. (1995). Differentiation of pluripotent embryonic stem cells into the neuronal lineage in vitro gives rise to mature inhibitory and excitatory neurons. *Mech. Dev.* **53**, 275-287.

Stuermer C.A.O. (1986). Pathways of regenerated retinotectal axons in goldfish. *J. Embryol. Exp. Morph.* **93**, 1-28.

Stuermer C.A.O., Bastmeyer M., Bähr M., Strobel G. and Paschke K. (1992). Trying to understand axonal regeneration in the CNS of fish. *J. Neurobiol.* **23**, 537-550.

Sullivan S.A., Barthel L.K., Largent B.L. and Raymond P.A. (1997). A goldfish Notch-3 homologue is expressed in neurogenic regions of embryonic, adult, and regenerating brain and retina. *Dev. Genet.* **20**, 209-223.

Stuermer, C.A. (1988) Retinotopic organization of the developing retinotectal projection in the zebrafish embryo. *J. Neurosci.* **8**, 4513–4530.

Tamura K., Peterson D., Peterson N., Stecher G., Nei M. and Kumar S. (2011) MEGA5: Molecular evolutionary genetics analysis using maximum likelihood, evolutionary distance, and maximum parsimony methods. *Mol. Biol. Evol.* **28**, 2731-2739.

Taupin P. and Gage F.H. (2002). Adult neurogenesis and neural stem cells of the central nervous system in mammals. *J. Neurosci. Res.* **69**, 745-749.

Terling C., Rass A., Mitsiadis T.A., Fried K., Lendahl U. and Wroblewski J. (1995). Expression of the intermediate filament nestin during rodent tooth development. *Int. J. Dev. Biol.* **39**, 947-956.

Tipton K.F. and Singer T.P. (1993). Advances in our understanding of the mechanisms of the neurotoxicity of MPTP and related compounds. *J. Neurochem.* **61**, 1191-1206.

Tohyama T., Lee V.M., Rorke L.B., Marvin M., McKay R.D. and Trojanowski J.Q. (1992). Nestin expression in embryonic human neuroepithelium and in human neuroepithelial tumor cells. *Lab. Invest.* **66**, 303-313.

True L.D. (1990). Atlas of diagnostic immunopathology. Gower Medical Publishing, N.Y. p.6.5

Trudeau V.L., Sloley B.D., Wong A.O. and Peter R.E. (1993). Interactions of gonadal steroids with brain dopamine and gonadotropin-releasing hormone in the control of gonadotropin-II secretion in the goldfish. *Gen. Comp. Endocrinol.* **89**, 39-50.

Trudeau V.L. (1997). Neuroendocrine regulation of gonadotrophin II release and gonadal growth in the goldfish, *Carassius auratus*. *Rev. Reprod.* **2**, 55-68.

Trudeau V.K., Spanswick D., Fraser E.J., Lariviere K., Crump D., Chiu S., MacMillan M. and Schulz R.W. (2000). The role of amino acid neurotransmitter in the regulation of pituitary gonatropin release in fish. *Biochem. Cell Biol.* **78**, 241-259.

Tsujimura T., Makiishi-Shimobayashi C., Lundkvist J., Lendahl U., Nakasho K., Sugihara A., Iwasaki T., Mano M., Yamada N., Yamashita K., Toyosaka A. and Terada N. (2001). Expression of the intermediate filament nestin in gastrointestinal stromal tumors and interstitial cells of Cajal. *Am. J. Pathol.* **158**, 817-823.

Vaittinen S., Lukka R., Sahlgren C., Hurme T., Rantanen J., Lendahl U., Eriksson J.E. and Kalimo H. (2001). The expression of intermediate filament protein nestin as related to vimentin and desmin in regenerating skeletal muscles. *J. Neuropathol. Exp. Neurol.* **60**, 588-597.

Vajda F.J. (2002). Neuroprotection and neurodegenerative disease. *J. Clin. Neurosci.* **9**, 4-8.

Vankelecom H. (2007). Stem cells in the postnatal pituitary? *Neuroendocrinology* **85**, 110-130.

Vankelecom H. and Gremeaux L. (2009). Stem cells in the pituitary gland: A burgeoning field. *Gen. Comp. Endocrinol.* **166**, 478-488.

Ven den Heuvel D.M.A. and Pasterkamp R.J. (2008). Getting connected in the dopamine system. *Prog. Neurobiol.* **85**, 75-93.

Vernay B., Koch M., Vaccarino F., Briscoe J., Simeone A., Kageyama R. and Ang S.L. (2005). Otx2 regulates subtype specification and neurogenesis in the midbrain. *J. Neurosci.* **25**, 4856-4867.

Vyas I., Heikkila R.E. and Nicklas W.J. (1986). Studies on the neurotoxicity of 1-methyl-4-phenyl-1,2,3,6-tetrahydropyridine: inhibition of NADH-linked substrate oxidation by its metabolite 1-methyk-4-phenylpyridinium. *J. Neurochem.* **46**, 1501-1507.

Walcott J.C. and Provis J.M. (2003). Müller cells express the neuronal progenitor cell

marker nestin in both differentiated and undifferentiated human foetal retina. *Clin. Experiment. Ophthalmol.* **31**, 246-249.

Waters C.M., Hunt S.P., Jenner P. and Marsden C.D. (1987). An immunohistochemical study of the acute and long-term effects of 1-methyl-4-phenyl-l,2,3,6-tetrahydropyridine in the marmoset. *Neuroscience* **23,** 1025-1039.

Weinreb O. and Youdim M.B.H. (2007). A model of MPTP-induced Parkinson's disease in the goldfish. *Nature Protocols* **2**, 3016-3021.

Westlund K.N., Denney R.M., Kochenperger L.M., Rose R.M. and Abell C.W. (1985). Distinct monoamine oxidase A and B populations in primate brain. *Science* **230**, 181-183.

Wiese D.C., Rolletschek A., Kania G., Blyszczuk P., Tarasov K.V., Tarasova Y., Werstor R.P., Boheler K.R., and Wobus A.M. (2004). Nestin expression – a property of multi-lineage progenitor cells. *Cell. Mol. Life Sci.* **61**, 2510-2522.

Wullimann M.F. and Rink E. (2001). Detailed immunohistology of Pax6 protein and tyrosine hydroxylase in the early zebrafish brain suggests role of Pax6 gene in development of dopaminergic diencephalic neurons. *Dev. Brain Res.* **131**, 173–191.

Wullimann M.F. and Rink E. (2002). The teleostean forebrain: a comparative and developmental view based on early proliferation, Pax6 activity and catecholaminergic organization. *Brain Res. Bull.* **57**, 363– 370.

Wullimann M.F. and Mueller T. (2004). Teleostean and mammalian forebrains contrasted: Evidence from genes to behavior. *J. Comp. Neurol.* **475**, 143-162.

Xing L., Goswami M. and Trudeau V. L. (2014). Radial glial cell: critical functions and new perspective as a steroid synthetic cell. *Gen. Comp. Endocrinol*. **203**, 181–185.

Xing L., McDonald H., DaFonte D.F., Gutierrez-Villagomex J.M. and Trudeau V.L. (2015). Dopamine D1 receptor activation regulates the expression of the estrogen synthesis gene aromatase B in radial glial cells. *Front. Neurosci.* **9**, 1-12.

Yamaguchi M., Saito H., Suzuki M. and Mori K. (2000). Visualization of neurogenesis in the central nervous system using nestin promoter-GFP transgenic mice. *Neuroreport* **11**, 1991-1996.

Yamamoto K., Ruuskanen J.O., Wullimann M.F. and Vernier P. (2011). Differential expression of dopaminergic cell markers in the adult zebrafish forebrain. *J. Comp. Neurol.* **519**, 576-598.

Yang J., Cheng L., Yan Y., Bian W., Tomooka Y., Shiurba R. and Jing N. (2001). Mouse nestin cDNA cloning and protein expression in the cytoskeleton of transfected cells. *Biochem. Biophys. Acta.* **1520**, 251-254.

Yasuhara T., Shingo T. and Date I. (2007) Glial cell line-derived neurotrophic factor (GDNF) therapy for Parkinson's disease. *Acta. Med. Okayama* **61**, 51.

Yokoyama, H., Uchida, H., Kuroiwa, H., Kasahara, J., Araki, T., 2010. Role of glial cells in neurotoxin-induced animal models of Parkinson's disease. *Neurol. Sci.* **32,** 1-7.

Yoon, M.G. (1975) Effects of post-operative visual environments on reorganization of retinotectal projection in goldfish. *J. Physiol. (Lond.)* **246**, 673–694.

Youdim M.B.H., Dhariwal K., Levine M., Markey C.J., Markey S., Caohuy H., Adeyemo O.M. and Pollard H.B. (1992). MPTP induced "parkinsonism" in the goldfish. *Neurochem. Int.* **20**, 275-278.

Yu K.L. and Peter R.E. (1990). Dopaminergic regulation of brain gonadotropin-releasing hormone in male goldfish during spawning behaviour. *Neuroendocrinology* **52**, 276-283.

Zhang D., Xiong H., Mennigen J.A., Popesku J.T., Marlatt V.L., Martyniuk C.J., Crump K., Cossins A.R., Xia X. and Trudeau V.L. (2009). Defining global neuroendocrine gene expression patterns associated with reproductive seasonality in fish. *PLoS One* **4**, 1-11.

Zhao M., Momma S., Delfani K., Carlen M., Cassidy R.M., Johansson C.B., Brismar H., Shupliakov O., Frisen J. and Janson A.M. (2003). Evidence for neurogenesis in the adult mammalian substantia nigra. *Proc. Natl. Acad. Sci. USA* **100**, 7925-7930.

Zikopoulos, B., Kentouri, M. & Dermon, C.R. (2000) Proliferation zones in the adult brain of sequential hermaphrodite teleost species (Sparus aurata). *Brain Behav. Evol.* **56**, 310–322.

Zikopoulos B. Kentouri M. and Dermon C.R. (2001). Cell genesis in the hypothalamus is associated to the sexual phase of a hermaphrodite teleost. *Neuroreport* **12**, 2477-2481.

Zimmerman L., Parr B., Lendahl U., Cunningham M., McKay R., Gavin B., Mann J., Vassileva G. and McMahon A. (1994). Independent regulatory elements in the nestin gene direct transgene expression to neural stem cells or muscle precursors. *Neurons* **12**, 11-24.

Zottoli S.J. and Freemer M.M. (2003). Recovery of C-starts, equilibrium and targeted feeding after whole spinal cord crush in the adult goldfish *Carassius auratus*. *J. Exp. Biol.* **206**, 3015-3029.

Zuckerkandl E. and Pauling L. (1965) Evolutionary divergence and convergence in proteins. Edited in *Evolving Genes and Proteins* by V. Bryson and H.J. Vogel, pp. 97-166. Academic Press, New York.

Zupanc G.K.H. and Heiligenberg W. (1989). Sexual maturity-dependent changes in neuronal morphology in the prepacemaker nucleus of adult weakly electri knifefish, *Eigenmannia. J. Neurosci.* **9** 3816-3827.

Zupanc G.K.H. (1991). The synaptic organization of the prepacemaker nucleus in weakly electric knifefish, *Eigenmannia*: a quantitative ultrastructural study. *J. Neurocytol.* **20**, 818-833.

Zupanc G.K.H. and Horschke I. (1995). Proliferation zones in the brain of adult gymnotiform fish: A quantitative mapping study. *J. Comp. Neurol.* **353**, 213-233.

Zupanc G.K.H. (1997). Towards a cellular understanding of motivation. *Adv. Ethol.* **32**, 19.

Zupanc G.K.H. (1999). Neurogenesis, cell death and regeneration in the adult gymnotiform brain. *J. Exp. Biol.* **202**, 1435-1446.

Zupanc G.K.H. and Ott R. (1999). Cell proliferation after lesions in the cerebellum of adult teleost fish: time course, origin, and type of new cells produced. *Exp. Neurol.* **160**, 78-87.

Zupanc G.K.H. (2001) Adult neurogenesis and neuronal regeneration in the central nervous system of teleost fish. *Brain Behav. Evol.* **58**, 250–275.

Zupanc G.K. and Clint S.C. (2003). Potential role of radial glia in adult neurogenesis of teleost fish. *Glia* **43**, 77-86.

Zupanc G.K.H., Hinsch K. and Gage F.H. (2005). Proliferation, migration, neuronal differentiation, and long-term survival of new cells in the adult zebrafish brain. *J. Comp. Neurol.* **488**, 290-319.

Zupanc G.K.H. and Zupanc M.M. (2006). New neurons for the injured brain: mechanisms of neuronal regeneration in adult teleost fish. *Regen. Med.* **1**, 207–216.

Zupanc G.K.H. (2008). Adult neurogenesis and neuronal regeneration in the brain of teleost fish. *J. Physiol. Paris* **102**, 357-373.

Zupanc G.K. and Sîrbulescu R.F. (2011). Adult neurogenesis and neuronal regeneration in the central nervous system of teleost fish. *Eur. J. Neurosci.* **34**, 917-929.

Appendix A

MPTP toxicity in the goldfish brain: A light microscopy study

A.1. Introduction

Goldfish (*Carassius* auratus*)* are an excellent model organism for neuroendocrine studies including the study of the catecholamine dopamine (DA) (Popesku *et al.* 2008). Dopamine plays an important role in movement and reward mechanisms in vertebrates including lower vertebrates such as the goldfish. Abnormalities in the functioning and signaling pathways of DAergic neurons can lead to neurodegenerative diseases such as Parkinson's disease (PD). A parkinsonian syndrome can be induced in goldfish by injecting the neurotoxin 1-methyl-4-phenyl-1,2,3,6-tetrahydropyridine (MPTP) (Poli *et al.* 1990, 1992; Goping *et al.* 1995; Popesku 2009). Previous studies of MPTP-induced goldfish animal models of PD have illustrates that the basic neural circuits of DA signaling are conserved between goldfish and primates making the goldfish an attractive model organism (Poli *et al.* 1992; Pollard *et al.* 1992; Adeyemo *et al.* 1993; Goping *et al.* 1995; Popesku 2009). The present study investigates neuroanatomical effects of MPTP on tyrosine hydroxylase immunoreactive neurons in the goldfish brain.

MPTP is a neurotoxin that is selectively taken up by DAergic neurons via a dopamine transporter and leads to DAergic cellular death (Chiba *et al.* 1984; Javitch and Snyder 1984; Westlund *et al.* 1985; Snyder *et al.* 1986; Vyas *et al.* 1986; Singer *et al.* 1987; Pollard *et al.* 1992, 1996; Tipton and Singer 1993; Gainetdinov *et al.* 1997; Sriram *et al.* 1997). Goping et *al.* (1995) demonstrated, using microscopy studies, that injection of MPTP in the goldfish leads to neuronal cell irregularities such as disrupted nuclei.

Pollard *et al.* (1992) and Popesku (2009) observed a maximal decrease in DA brain and hypothalamus content, respectively, following 4-5 days post injection (dpi) of MPTP. Coincidentally, Poli et *al.* (1992) showed full recovery of DA levels in the brain of the goldfish after 6 weeks of MPTP injection. Popesku (2009) reported that hypothalamic DA levels recovered to baseline levels at about 7 dpi. Similarly, Pollard *et al.* 1992 reported that DA content in the brain recovered to baseline levels by 8 dpi. Visualization of DA neurons in the brain of the goldfish can be accomplished by performing immunohistochemistry (IHC) against tyrosine hydroxylase (TH). Tyrosine hydroxylase plays an important role in the biosynthesis of DA in adrenergic neurons and is therefore used as a marker of DA neurons (Nagatsu *et al.* 1964; Kuhar *et al.* 1999). Hornby et *al.* (1987) also showed the presence of TH-immunoreactivity (-ir) in the cell bodies of DAergic neurons making TH a good DAergic neuronal marker.

The highest TH-ir has been reported in the goldfish forebrain, which includes the telencephalon and the optic tectum (Hornby *et al.* 1987; Youdim *et al.* 1992; Goping *et al.* 1995), both areas are the focus of this study. The TH-ir was observed in the telencephalon, in the area telencephali pars dorsalis (Vd), the nucleus telencephali pars medialis (NPM), and the preoptic area (POA) as well as in the optic tectum in control and MPTP-treated goldfish brains using a monoclonal and polyclonal anti-TH antibody. The NPM and Vd brain areas are thought to be involved in motor control and are likely homologous to the substantia nigra pars compacta (SNc) and the dorsal striatum respectively, two mammalian brain structures involved in movement control (Franzoni *et al.* 1986; Sas *et al.* 1990; Pollard *et al.* 1992; Goping *et al.* 1995). The present study investigated qualitatively the effects of MPTP in the goldfish brain following 4,7, 21, 28

and 52 dpi and served to confirm previous reports (Hornby *et al.* 1987; Poli *et al.* 1990; Pollard *et al.* 1996; Goping *et al.* 1995), and set the stage for the main experiments described in the thesis.

A.2. Materials and Method

A.2.1. Animal maintenance

Adult female goldfish (*Carassius auratus*) were purchased from a commercial supplier (Mt. Parnell Fisheries Inc., Mercersburg, PA, USA) and maintained at 18˚C under a natural-simulated photoperiod on standard flaked goldfish food. Fish were kept in 70L tanks (15-18 fish/tank). All procedures were performed according to the guidelines of the Canadian Council on Animal Care and were approved by the University of Ottawa animal care committee. Goldfish were anesthetized using 3-aminobenzoic acid ethylester (MS-222; 0.05% in water, Sigma Chemicals) for all handling and sampling procedures.

A.2.2. Experimental and sampling procedures

The dopaminergic neurotoxin, 1-methyl-4-phenyl-1,2,3,6-tetrahydropyridine (MPTP), was purchased from Sigma-Aldrich (M0896, Oakville, Canada) and dissolved in 0.6% saline to give a dose of 50 μg/g body mass of fish at 2 μL/g. Female goldfish (February-April; ~21 g ± 0.7 body weight; ~0.8 ± 0.1 gonadosomatic index; n=40) either received a single intraperitoneal injection of MPTP at time t_0 or a control saline 0.6% injection (2 μL/g). The gonadosomatic index was calculated by dividing the gonad weight by body weight of the goldfish x 100.

A.2.3. Tissue preparation

Female goldfish were sacrificed randomly at 4, 7, 21, 28 and 52 days post-injection (dpi). All brain dissections were performed in mid-afternoon. Female goldfish were intracardially perfused with 0.6% saline following by perfusion with Bouin's fixative. Afterwards, the brains were dissected and postfixed by immersion in Bouin's solution for 12 hours at room temperature (RT). The intact brains were then immersed in 70% ethanol for 4 days prior to paraffin embedding. Fixed brains were washed in a series of ethanol solutions increasing in concentration from 96% to 100% and then placed in a solution containing both xilol and 100% ethanol (1:1) before being immersed in xilol then in melted paraffin. Each brain was placed in an embedding mold, covered with paraffin and placed on ice. The embedded paraffin brains were placed at -20˚C until sectioning. Brains were then cut coronally into 6 µm sections using a microtome, mounted on superfrost glass slides and placed at 4˚C until immunohistochemical studies.

A.2.4. Immunohistochemistry

Brain tissue sections mounted on glass slides were immunolabeled for tyrosine hydroxylase (TH) using polyclonal and monoclonal antibodies. Firstly, the tissues were deparaffinized by immersion in 2 different xylol solutions for 20 minutes and then immersed in a series of ethanol solutions decreasing in concentration from 100% to 70% for 10 minutes each. Afterwards, washing was done in 1x PBS (1x10min) prior to blocking nonspecific protein binding sites using 3% hydrogen peroxide (H_2O_2) for 45 minutes at RT. Sections were then washed with 1x PBS (2x10min) before immersion in a blocking solution of 0.5% skim milk, 0.3% triton X-100 and 1x PBS for 30 min at RT.

Serial sections were then incubated overnight in either monoclonal anti-TH mouse antibody (Chemicon, Temecula, CA, MAB318) or polyclonal anti-TH rabbit antibody (Chemicon, Temecula, CA, AB152) in 1:200 dilutions. The monoclonal antibody MAB318 (Matsui *et al.* 2009) and the polyclonal antibody Ab152 (Yamamoto *et al.* 2011) were both previously used by other groups to visualize TH in the fish brain. In the control samples, the primary antiserum was omitted and the sections were processed in identical solutions without the primary antibody. The next day, the sections were washed in 1x PBS (2x10min) and incubated in biotinylated secondary antibody for 45 minutes at RT and then washed with 1x PBS (2x10min) prior to incubation with streptavidin-horseradish peroxidase (HRP) solution for 1 hour at RT. Afterwards, the sections were washed with 1x PBS (2x10min) and the antigen-antibody complex was revealed with 3,3'-diaminobenzidine, 30% H_2O_2 and 1x PBS. The sections were then washed with tap water, stained with hemocytoxylin and then washed with alcohol acid for light microscopy. All sections were dehydrated in a series of ethanol solutions in increasing concentrations (70% to 100%), cleared in xylol and coverslipped in Permount for microscopy visualization.

A.3. Results

A.3.1. Tyrosine hydroxylase-immunoreactivity in the goldfish brain

Tyrosine hydroxylase-immunoreactivity (TH-ir) was observed in the telencephalon and the optic tectum using a monoclonal and a polyclonal antibody against TH in the goldfish brain. The polyclonal anti-TH rabbit antibody provided a more pronounced TH staining pattern (Fig. A.1A) than the monoclonal anti-TH mouse

antibody (Fig. A.2). Tyrosine hydroxylase-ir was not observed in control sections where the primary antibody was omitted from the incubation period. MPTP-induced depletion of DAergic neurons was only observed at 4 dpi by TH immunolabeling. There were no observable differences in TH-ir at the later time-points of 7, 21, 28 and 52 dpi (data not shown) and thus the 4 dpi treatment group was the focus of this study.

A.3.1.1. Telencephalon

A large group of TH-ir cells and fibers are present in the Vd and the preoptic area of the telencephalon. These TH-ir cells were observed in the control goldfish brain following immunostaining against TH (Fig. A.1A and A.1B). In addition, many TH fibers observed in the Vd extend dorsally and ventrally innervating other areas in the goldfish brain (Fig. A.1B). However, the Vd and preoptic area were almost devoid of TH-ir fibers and showed minimal TH-positive cell bodies when immunostaining was performed with the monoclonal anti-TH mouse antibody in control fish (Fig. 2). Also, the TH-ir fibers and cell bodies in the ventral telencephalon were drastically reduced in number in MPTP-treated goldfish at 4 dpi and these cell bodies showed minimal cytoplasmic processes (Fig. A.1C). Furthermore, TH-positive neurons were present in the nucleus telencephali pars medialis (NPM) of control fish (Fig. A.4).

A.3.1.2. Optic Tectum

TH-ir fibers are located throughout the optic tectum of control fish (Fig. A.1E), however, TH-ir cell bodies were only present in very small numbers (Fig. A.1E and A.1F). At the level of the optic tectum, the control and MPTP-treated goldfish brains at 4 dpi showed a pattern of stained TH-positive cell bodies and fibers traveling through the

optic tectum (Fig. A.1D and A.1E), however, the TH-ir was more pronounced in the control brain. In MPTP-treated goldfish, TH-positive cell bodies and fibers were drastically reduced in number in the optic tectum (Fig. 1D).

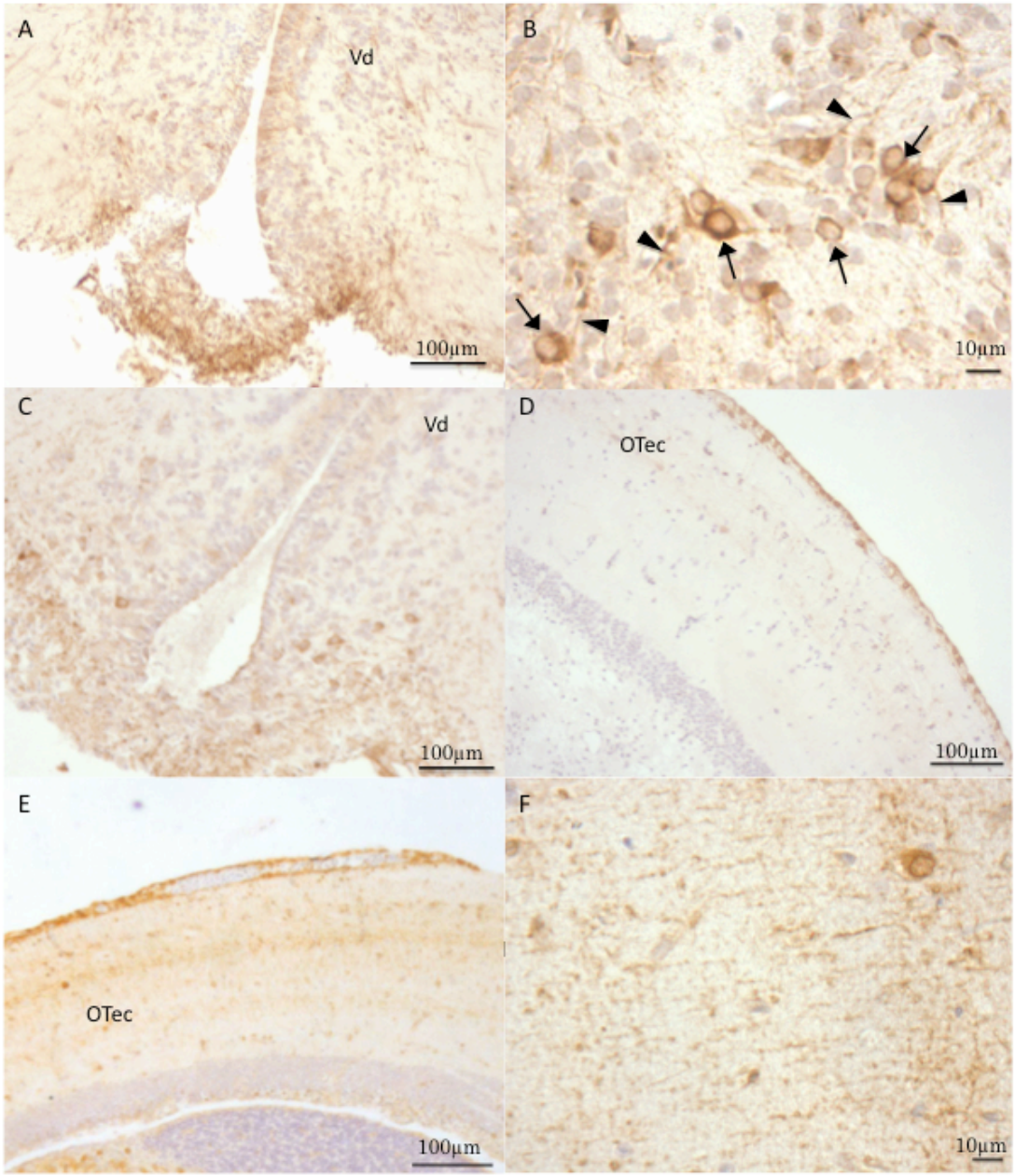

Figure A.1. Light micrographs of TH-immunoreactive cell bodies and fibers in the rostral telencephalon of the goldfish brain at 10x and 40x. Micrographs were immunostained with a polyclonal anti-TH rabbit antibody (1:200) on 6 µm goldfish brain sections. (A) A micrograph illustrating normal distribution of TH-immunoreactivity in the ventral telencephalon. (B) A micrograph focusing on the TH-immunoreactive cellbodies (arrows) and fibers (arrowheads) of the preoptic area of the goldfish telencephalon. (C) A micrograph of the ventral area of the telencephalon of goldfish treated with 50µg/g MPTP. The micrograph illustrates the reduction of TH-immunoreactive cell bodies and fibers in the preoptic area and the area dorsalis (Vd) of a MPTP-treated goldfish. (D) A micrograph of a MPTP-treated goldfish brain showing the reduction of TH-immunoreactive cell fibers in the optic tectum. (E) A micrograph of a non-treated goldfish brain showing TH-immunoreactive cell bodies and fibers in the optic tectum. (F) A micrograph of a non-treated goldfish brain showing neuronal processes traveling though the optic tectum.

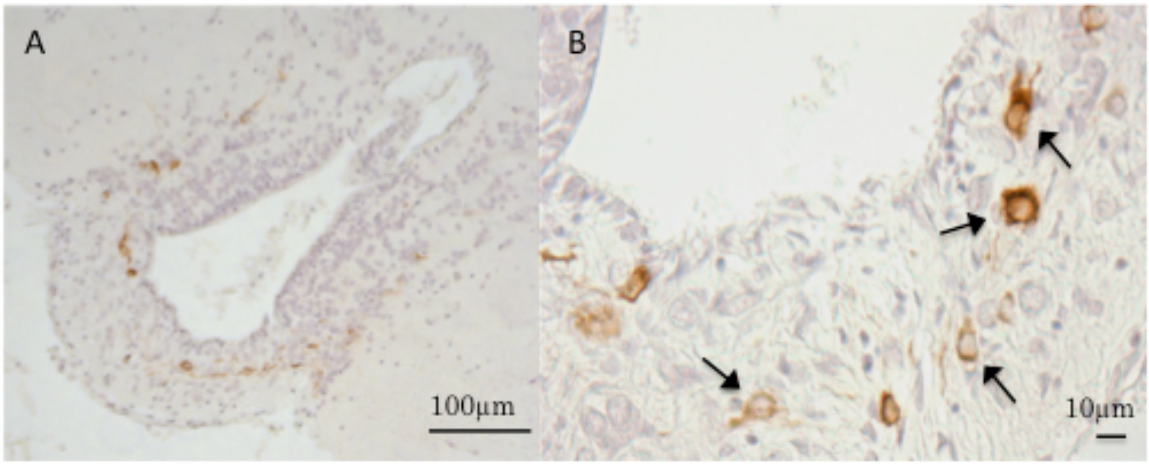

Figure A.2. Light micrographs of 6 µm-thick coronal brain sections of the goldfish telencephalon at 10x and 40x respectively. Both micrographs were immunostained with the monoclonal anti-TH mouse antibody at 1:200 dilution. (A) A micrograph showing incomplete TH-immunoreactivity of cell bodies and fibers in normal goldfish brain. B) A micrograph illustrating partial TH-immunoreactivity in a normal goldfish brain. Several TH-immunoreactive cell bodies are labelled with arrows.

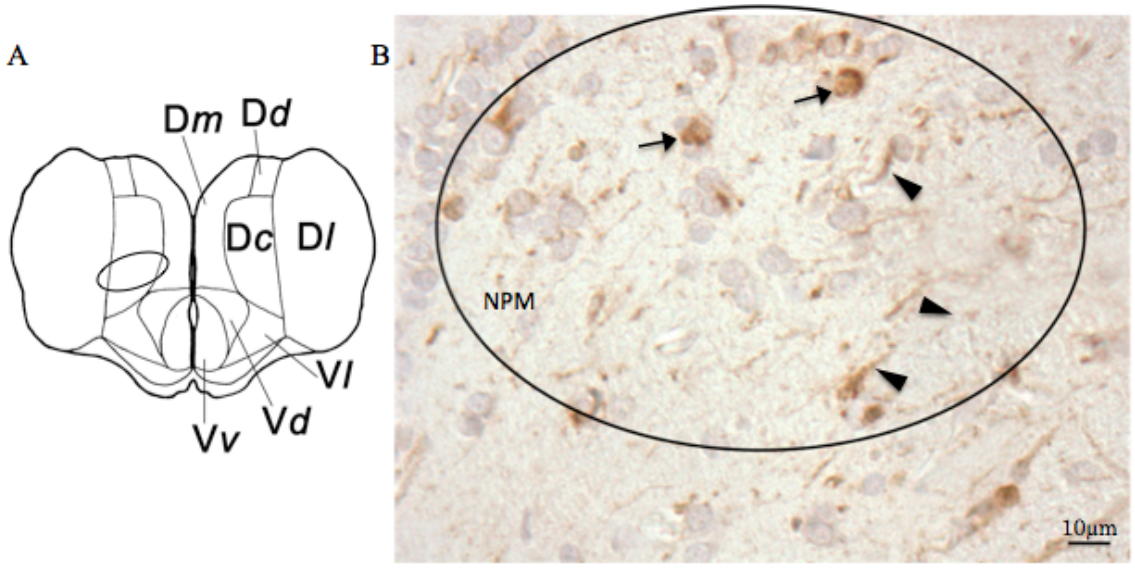

Figure A.3. A) A telencephalic brain diagram illustrating the nucleus telencephali pars medialis (NPM) area denoted by an oval circle. B) A light microscopy micrograph of a 6 µm-thick coronal section of a normal goldfish brain at 40x. The micrograph focuses on TH-immunoreactive nerve fibers (arrowheads) and cell bodies (arrows) in the NPM indicated in the circle.

A.4. Discussion

In the present study, DA depletion following MPTP injection was observed by performing immunohistochemistry (IHC) against TH. The polyclonal anti-TH rabbit antibody provided a consistent pattern of TH-ir in accordance to other IHC studies (Hornby *et al.* 1987; Goping *et al.* 1995; Pollard *et al.* 1996). However, the TH-ir staining pattern obtained with the monoclonal anti-TH mouse antibody was not convincing and was only partially in agreement with other studies (Hornby *et al.* 1987; Goping *et al.* 1995; Pollard *et al.* 1996). It appears that the polyclonal antibody is more specific in binding the desired TH epitope in the goldfish brain. The monoclonal anti-TH mouse antibody recognized an epitope outside of the regulatory N-terminus region of TH (Antibody data sheet, Millipore, Temecula, CA, USA). As a result, there is a possibility that the epitope was only partially present in the goldfish TH sequence explaining its low level of expression when performing IHC. Unfortunately, we were unable to compare the sequences as the manufacturer of the monoclonal antibody did not disclose the TH epitope sequence.

The TH-ir pattern observed in control and MPTP-treated goldfish at 4 dpi are in accordance with the TH expression pattern observed in the Vd and NPM areas reported by Hornby *et al.* (1987) and Goping *et al.* (1995). The TH-positive neurons appear in clusters throughout the telencephalon similarly to those findings presented by Goping *et al.* (1995) and Poli *et al.* (1990). In addition, the presence of many TH-ir fibers in the goldfish Vd is consistent to those observed in zebrafish IHC studies (Rink and Wullimann 2001). Tyrosine hydroxylase-ir fibers are also located in the optic tectum with

a small number of cell bodies, these findings are in accordance with the data reported by Hornby *et al.* (1987), Goping *et al.* (1995) and Pollard *et al.* (1996).

Cytochemical damage induced by MPTP injection was only qualitatively observed at 4 dpi in DAergic neurons of the goldfish brain especially in the telencephalon and the optic tectum. There were no visual differences in the staining pattern or intensity of TH-ir between control and MPTP-treated goldfish following 7, 21, 28 and 52 dpi. This is in agreement with multiple studies that reported DA content recovery starting at 7-8 dpi of MPTP in the goldfish brain (Pollard *et al.* 1992, 1996; Goping *et al.* 1995; Popesku 2009). However, it is important to note that neurons with abnormal and normal appearances were always observed in the MPTP-treated goldfish at 4 dpi similar to that reported by Goping *et al.* (1995). In addition, Poli *et al.* (1990) observed a decrease in TH-ir in the telencephalon following 7 dpi of MPTP. However, no TH-ir differences were observed at the 7 dpi time-point in this study.

To elaborate, the TH-ir fibers and cell bodies in the Vd area of MPTP-treated goldfish brain were drastically reduced in comparison to control goldfish. Goping *et al.* (1995) reported drastic reduction of TH-ir and cell processing throughout the ventral mid-telencephalon following MPTP injection. Poli *et al.* (1990) also reported a decrease in TH-ir at the mid-telencephalic level of the goldfish brain following MPTP injection. Tyrosine hydroxylase positive neurons were present in the NPM in control goldfish. Following MPTP injection, Pollard *et al.* (1996) reported a reduction in the number of TH-positive neurons in the NPM. The damage observed in the NPM following MPTP injection is similar to that observed in substantia nigra neurons in higher vertebrates (Pollard *et al.* 1992; Goping *et al*. 1995; Lucchi *et al.* 1998). The optic tectum also

exhibited a decrease in TH-ir fibers travelling across the tissue following 4 dpi of MPTP. Pollard *et al.* (1996) observed the effects of MPTP on the optic tectum and they report that a higher dose of MPTP (200 μg/g body weight) disrupts TH-ir fibers in the optic tectum at 4 dpi.

The present study explored the goldfish brain regions depleted of TH-ir induced by MPTP by localizing and comparing TH-ir cell bodies and fibers in control and MPTP-treated goldfish brain. The expression patterns of TH-ir in the telencephalon and the optic tectum appear to reflect the location of DAergic neurons in the goldfish brain. A decrease in TH-ir was only observed following 4 dpi of MPTP followed by a recovery of TH-ir starting at 7 dpi of MPTP.

Appendix B

Supplemental Material

B.1. Chapter 2 Supplementary Figures

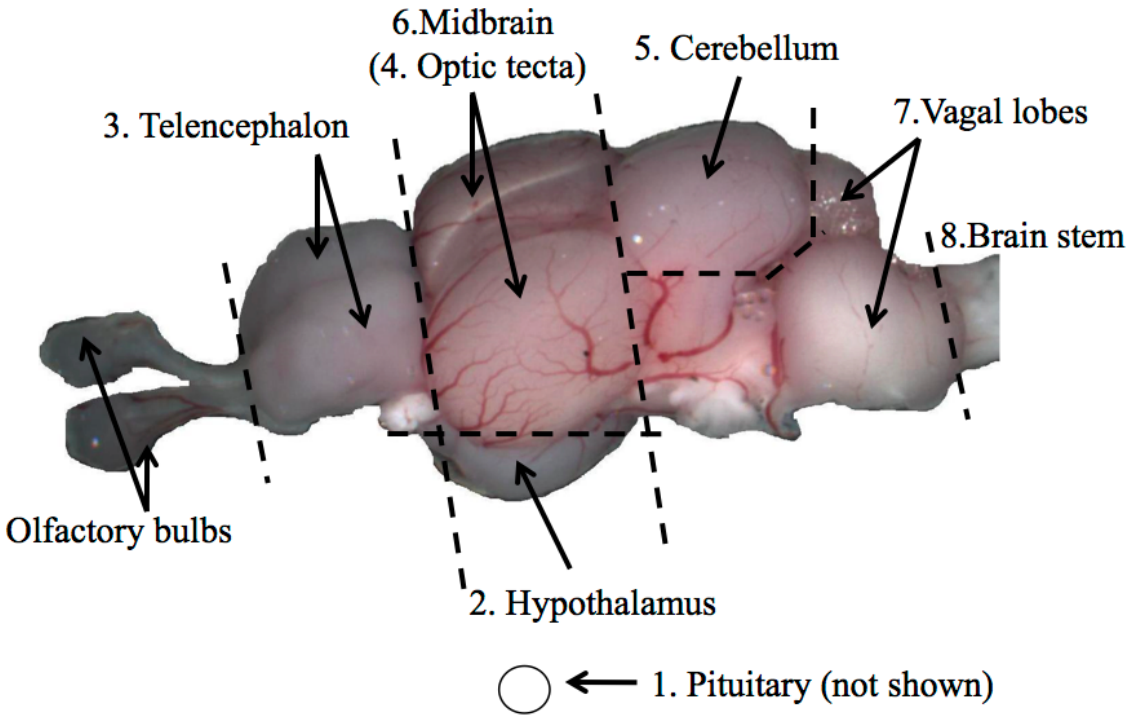

Supplementary Figure 1. Goldfish brain dissection. The numbers indicate the sequence of dissected tissues. Note that the pituitary (#1) is not shown in the figure but was collected. The optic tecta were peeled off from the midbrain region. The olfactory bulbs were not analyzed in this study.

```
Nestin_Transcript_B      GAAAATTCAGCCACTGGGCACTGGGACTGTGGTCCAGACCTCACCCTCAAGCCTGTCATT 60
Nestin_Transcript_C      GAAAATTCAGCCACTGGGCACTGGGACTGTGGTCCAGACCTCACCCTCAAGCCTGTCATT 60
                         ************************************************************

Nestin_Transcript_B      ATAATAACTCAGCAGCCACAAAGACCTCCAGCCATTCACAGCCTCTGTGCACAGTTCTAG 120
Nestin_Transcript_C      ATAATAACTCAGCAGCCACAAAGACCTCCAGCCATTCACAGCCTCTGTGCACAGTTCTAG 120
                         ************************************************************

Nestin_Transcript_B      TGAGACTTAACACTTTCCACCACTCTAAGATGGAGCTTTTGGGTGCCCGACTGCCCTTCA 180
Nestin_Transcript_C      TGAGACTTAACACTTTCCACCACTCTAAGATGGAGCTTTTGGGTGCCCGACTGCCCTTCA 180
                         ************************************************************

Nestin_Transcript_B      CCCAGTTTCAGGAGGAAAAGTACCAGATGCTGGAGCTGAACCAGCGTCTTGAATCATACT 240
Nestin_Transcript_C      CCCAGTTTCAGGAGGAAAAGTACCAGATGCTGGAGCTGAACCAGCGTCTTGAATCATACT 240
                         ************************************************************

Nestin_Transcript_B      TAGGCCGCGTGAAGCTTCTGGAGGAGGAAAACAAGCTACTGCATGAGGAGATCCACACTC 300
Nestin_Transcript_C      TAGGCCGCGTGAAGCTTCTGGAGGAGGAAAACAAGCTACTGCATGAGGAGATCCACACTC 300
                         ************************************************************

Nestin_Transcript_B      TCAAGAGCAGCAGGGAACCAGCAGGCCAGCGCAAAGCTCAAGAGGAGGCTCTCAGCCAGG 360
Nestin_Transcript_C      TCAAGAGCAGCAGGGAACCAGCAGGCCAGCGCAAAGCTCAAGAGGAGGCTCTCAGCCAGG 360
                         ************************************************************

Nestin_Transcript_B      CCAGGAGGATGCTGGAGGAGGCCTGGAGGAAGAAAGACCATGTGGAACTGGAAGTCGAGA 420
Nestin_Transcript_C      CCAGGAGGATGCTGGAGGAGGCCTGGAGGAAGAAAGACCATGTGGAACTGGAAGTCGAGA 420
                         ************************************************************

Nestin_Transcript_B      ACTTGATGGAGGATATAGAGGTGGTGAGTATTCAAAGACAGAAGGCAAAGAACGCTCAGG 480
Nestin_Transcript_C      ACTTGATGGAGGATATAGAGGTGGTGAGTATTCAAAGACAGAAGGCAAAGAACGCTCAGG 480
                         ************************************************************

Nestin_Transcript_B      CTGAGGCACAGAGAAAACTCATGGAGAGCAGGAAGGAGCTTGAAGAGGAGCGTAGAGCTC 540
Nestin_Transcript_C      CTGAGGCACAGAGAAAACTCATGGAGAGCAGGAAGGAGCTTGAAGAGGAGCGTAGAGCTC 540
                         ************************************************************

Nestin_Transcript_B      AGATTTGGCTAAGAGAGAAGGTTGGCCAACTTGAGAAAGACCTCCTGCTACAGATGCAAG 600
Nestin_Transcript_C      AGATTTGGCTAAGAGAGAAGGTTGGCCAACTTGAGAAAGACCTCCTGCTACAGATGCAAG 600
                         ************************************************************

Nestin_Transcript_B      TCCACCAGGAGAACATGGAAACCATGCAGGCCTCTCTGAAACAGACAAAACAAGTCTTGA 660
Nestin_Transcript_C      TCCACCAGGAGAACATGGAAACCATGCAGGCCTCTCTGAAACAGACAAAACAAGTCTTGA 660
                         ************************************************************

Nestin_Transcript_B      TGGCCCCACAGCACACTCAGACTGCCAGCATCCCAGACCTGGGACAAGAGTACAGCCACA 720
Nestin_Transcript_C      TGGCCCCACAGCACACTCAGACTGCCAGCATCCCAGACCTGGGACAAGAGTACAGCCACA 720
                         ************************************************************

Nestin_Transcript_B      GAGCAACTCAAGCATGGCAGGAGGCAACCAACAACTATCAGAGACTGGTTGGACGTCTTG 780
Nestin_Transcript_C      GAGCAACTCAAGCATGGCAGGAGGCAACCAACAACTATCAGAGACTGGTTGGACGTCTTG 780
                         ************************************************************

Nestin_Transcript_B      AGGAAAGTCTGAACCAGGCCAAAGCTAACATGACAAAGATTCATCAAGAAAAGAGAGAAA 840
Nestin_Transcript_C      AGGAAAGTCTGAACCAGGCCAAAGCTAACATGACAAAGATTCATCAAGAAAAGAGAGAAA 840
                         ************************************************************

Nestin_Transcript_B      ACCAGCATCAAGTCCAGCATCTGGCAAAGGAGCTCGAGAGCACTAAGACTAAGAGGCAGA 900
Nestin_Transcript_C      ACCAGCATCAAGTCCAGCATCTGGCAAAGGAGCTCGAGAGCACTAAGACTAAGAGGCAGA 900
                         ************************************************************

Nestin_Transcript_B      TGTTGGAGAAAAACTTAGTGCAGCAGAAAGAAGAGCATAAACAGGAGCTTCAACATTTTC 960
Nestin_Transcript_C      TGTTGGAGAAAAACTTAGTGCAGCAGAAAGAAGAGCATAAACAGGAGCTTCAACATTTTC 960
                         ************************************************************

Nestin_Transcript_B      AGGTAATAGTTTAAACTTATGGACTTCTGTCTTCATTTACTCGCTCTAACCTTTATGATA 1020
Nestin_Transcript_C      AGG------------------------------------------------------------ 963
                         ***

Nestin_Transcript_B      TTTTGAGAAATGTTTCATCTGGTTTAGTCCATACGATGGAAATTGTTGGGGTCCAAAACA 1080
Nestin_Transcript_C      ------------------------------------------------------------


Nestin_Transcript_B      ACACTGGACCCCGCTTTTGTTTCAGGGATAAAAAGTACTGAGACATTTTTCTACAGAAGA 1140
Nestin_Transcript_C      ------------------------------------------------------------
```

```
Nestin_Transcript_B      CAGAAGTCCATAAAGGTTTGGAACAGGACACATGTATTTAACTGGGTTCTTTTCATTTTG 1200
Nestin_Transcript_C      ------------------------------------------------------------

Nestin_Transcript_B      TGAAATTTCTATTGCAATTTTCCACATATTCTTCACTTTAATATATATTTCTGAAGAAAA 1260
Nestin_Transcript_C      ------------------------------------------------------------

Nestin_Transcript_B      AATGTCTCATATCTTTGCACAGGCTCAAGTAGATGCTCTGGAGATGGAGAAGGACAGCCT 1320
Nestin_Transcript_C      ----------------------CTCAAGTAGATGCTCTGGAGATGGAGAAGGACAGCCT 1000
                                              ************************************

Nestin_Transcript_B      GGGGCAGCAGATAGACAGCCTAATGGTGGACAGACAAAACTTGCTGCAGGTCAAGATGTC 1380
Nestin_Transcript_C      GGGGCAGCAGATAGACAGCCTAATGGTGGACAGACAAAACTTGCTGCAGGTCAAGATGTC 1060
                         ************************************************************

Nestin_Transcript_B      TCTTGGGCTGGAGGTGGCCACATACAGGTACCTGTCTTCAAAATCATCATCAACACCAGC 1440
Nestin_Transcript_C      TCTTGGGCTGGAGGTGGCCACATACAGGTACCTGTCTTCAAAATCATCATCAACACCAGC 1120
                         ************************************************************

Nestin_Transcript_B      AAAATACAACCTCTCTTTATTAAGAACTTCAGAACCATCTTTACATGATGTAAAATATGC 1500
Nestin_Transcript_C      AAAATACAACCTCTCTTTATTAAGAACTTCAGAACCATCTTTACATGATGTAAAATATGC 1180
                         ************************************************************

Nestin_Transcript_B      ATAGCTATTTCCCTTTCCTCTCTAAATGGGATTCCCCACATTGTGGGATTTGCAGTTTAT 1560
Nestin_Transcript_C      ATAGCTATTTCCCTTTCCTCTCTAAATGGGATTCCCCACATTGTGGGATTTGCAGTTTAT 1240
                         ************************************************************

Nestin_Transcript_B      GGAGGACAAACTAATATGATCATGCATCAGTGGCTCTAAAAAGCATCTCAGACACCCTGA 1620
Nestin_Transcript_C      GGAGGACAAACTAATATGATCATGCATCAGTGGCTCTAAAAAGCATCTCAGACACCCTGA 1300
                         ************************************************************

Nestin_Transcript_B      GAGGGGCAACTTTAGATCAGTCAAGCAGAATGGACCCTCTCCAATTTCCCACCCGGCACT 1680
Nestin_Transcript_C      GAGGGGCAACTTTAGATCAGTCAAGCAGAATGGACCCTCTCCAATTTCCCACCCGGCACT 1360
                         ************************************************************

Nestin_Transcript_B      GACCCCGATCCATCTGCTTGGAGGAGGGGCAGTGAAACAGGGGGGTGGGCAATTCATTCA 1740
Nestin_Transcript_C      GACCCCGATCCATCTGCTTGGAGGAGGGGCAGTGAAACAGGGGGGTGGGCAATTCATTCA 1420
                         ************************************************************

Nestin_Transcript_B      ATAACTTCCTTCAGATCTGACCGATTTATGTCTGTCGAGAGCACACTGAAATTAATTTTG 1800
Nestin_Transcript_C      ATAACTTCCTTCAGATCTGACCGATTTATGTCTGTCGAGAGCACACTGAAATTAATTTTG 1480
                         ************************************************************

Nestin_Transcript_B      ACCAAGCGTTTTAGCTGTCACTTTTTTCATGGTCCTTCATATCATGAAGTTGCATTGCAT 1860
Nestin_Transcript_C      ACCAAGCGTTTTAGCTGTCACTTTTTTCATGGTCCTTCATATCATGAAGTTGCATTGCAT 1540
                         ************************************************************

Nestin_Transcript_B      TCGATGCACAGGTACTGGATGGGGATGGGACAGGGGTTTTAAATATGTGAGGTTATTAAC 1920
Nestin_Transcript_C      TCGATGCACAGGTACTGGATGGGGATGGGACAGGGGTTTTAAATATGTGAGGTTATTAAC 1600
                         ************************************************************

Nestin_Transcript_B      CATTTTTTATTTCATATGGTTACAATATGATAAGCCTATCTCTTTAAAGTCTTTTCAAGT 1980
Nestin_Transcript_C      CATTTTTTATTTCATATGGTTACAATATGATAAGCCTATCTCTTTAAAGTCTTTTCAAGT 1660
                         ************************************************************

Nestin_Transcript_B      TTTTGAATACATTTTTTTGTAATAAAAAAATAAAAATCCACTTTGTTTTTAAAAATATGA 2040
Nestin_Transcript_C      TTTTGAATACATTTTTTTGTAATAAAAAAATAAAAATCCACTTTGTTTTTAAAAATATGA 1720
                         ************************************************************

Nestin_Transcript_B      TTGTGTGATGATTTTTGTAAATGAAATTACATGCATTTGGCAGGCTAACTGTTACATTGT 2100
Nestin_Transcript_C      TTGTGTGATGATTTTTGTAAATGAAATTACATGCATTTGGCAGGCTAACTGTTACATTGT 1780
                         ************************************************************

Nestin_Transcript_B      GTATGTATGTAAATTAGTTTGTAAATTCCAACCCTTGCGATTGCTCAGTGCTGCATGCAG 2160
Nestin_Transcript_C      GTATGTATGTAAATTAGTTTGTAAATTCCAACCCTTGCGATTGCTCAGTGCTGCATGCAG 1840
                         ************************************************************


Nestin_Transcript_B      GAGGTAGATGAACTGATGTCAAACCAAATCCTGCAATGACAAATCTGACATACTATTTGC 2220
Nestin_Transcript_C      GAGGTAGATGAACTGATGTCAAACCAAATCCTGCAATGACAAATCTGACATACTATTTGC 1900
                         ************************************************************

Nestin_Transcript_B      ATAACAACAGAACTAATAAGCACAAGAATGCAGCTCAAGAACCCGACTCCATCTCATTAA 2280
Nestin_Transcript_C      ATAACAACAGAACTAATAAGCACAAGAATGCAGCTCAAGAACCCGACTCCATCTCATTAA 1960
                         ************************************************************
```

```
Nestin_Transcript_B      ACCCACCCCTCACATTAAAGAAATTGCTGTGATGCTGACAAATGCTCTGTTGCTTCTTTC 2340
Nestin_Transcript_C      ACCCACCCCTCACATTAAAGAAATTGCTGTGATGCTGACAAATGCTCTGTTGCTTCTTTC 2020
                         ************************************************************

Nestin_Transcript_B      CAGAGCTTTGCTGGACAGCGAGGGGCTGAGAACTGACAGACCAACAACAAAAAAGACCAG 2400
Nestin_Transcript_C      CAGAGCTTTGCTGGACAGCGAGGGGCTGAGAACTGACAGACCAACAACAAAAAAGACCAG 2080
                         ************************************************************

Nestin_Transcript_B      CTCTGCTTTCTTTTTAGGTAACATAAAAAAAAAAAAAAAAAAAAAA 2446
Nestin_Transcript_C      CTCTGCTTTCTTTTTAGGTAACATAAAAAAAAAAAAAAAAAAAAAA 2126
                         **********************************************
```

Supplementary Figure 2.2. Sequence alignment (CLUSTAL 2.1, European Bioinformatics Institute, http://www.ebi.ac.uk/Tools/msa/clustalw2/) of goldfish *nestin* transcript B and C outlining the deletion of 320 nucleotides in goldfish *nestin* transcript C.

```
> Nestin_A    MELLGARLPFTQFQEEKYQMLELNQRLESYLGRVKLLEEENKLLH
> Nestin_B    MELLGARLPFTQFQEEKYQMLELNQRLESYLGRVKLLEEENKLLH
> Nestin_C    MELLGARLPFTQFQEEKYQMLELNQRLESYLGRVKLLEEENKLLH

> Nestin_A    EEIHTLKSSREPAGQRKAQEEALSQARRMLEEAWRKKDHVELEVE
> Nestin_B    EEIHTLKSSREPAGQRKAQEEALSQARRMLEEAWRKKDHVELEVE
> Nestin_C    EEIHTLKSSREPAGQRKAQEEALSQARRMLEEAWRKKDHVELEVE

> Nestin_A    NLMEDIEVVSIQRQKAKNAQAEAQRKLMESRKELEEERRAQIWLR
> Nestin_B    NLMEDIEVVSIQRQKAKNAQAEAQRKLMESRKELEEERRAQIWLR
> Nestin_C    NLMEDIEVVSIQRQKAKNAQAEAQRKLMESRKELEEERRAQIWLR

> Nestin_A    EKVGQLEKDLLLQMQVHQENMETMQASLKQTKQVLMAPQHTQT
> Nestin_B    EKVGQLEKDLLLQMQVHQENMETMQASLKQTKQVLMAPQHTQT
> Nestin_C    EKVGQLEKDLLLQMQVHQENMETMQASLKQTKQVLMAPQHTQT

> Nestin_A    ASIPDLGQEYSHRATQAWQEATNNYQRLVGRLEESLNQAKANMT
> Nestin_B    ASIPDLGQEYSHRATQAWQEATNNYQRLVGRLEESLNQAKANMT
> Nestin_C    ASIPDLGQEYSHRATQAWQEATNNYQRLVGRLEESLNQAKANMT

> Nestin_A    KIHQEKRENQHQVQHLAKELESTKTKRQMLEKNLVQQKEEHKQE
> Nestin_B    KIHQEKRENQHQVQHLAKELESTKTKRQMLEKNLVQQKEEHKQE
> Nestin_C    KIHQEKRENQHQVQHLAKELESTKTKRQMLEKNLVQQKEEHKQE

> Nestin_A    LQHFQAQVDALEMEKDSLGQQIDSLMVDRQNLLQVKMSLGLEVA
> Nestin_B    LQHFQVIV----------------------------------------------------------------------
> Nestin_C    LQHFQAQVDALEMEKDSLGQQIDSLMVDRQNLLQVKMSLGLEVA

> Nestin_A    TYRALLDSEGLRTDRPTTKKTSSAFFLDVLSKPTGTHPASQTTAAS
> Nestin_B    ----------------------------------------------------------------------------
> Nestin_C    TYRYLSSKSSSTPAKYNLSLLRTSEPSLHDVKYA----------------------

> Nestin_A    CHVSNAVPTSHRSITSSRTLLTSVTPSWTPTRRGTPQKTPTRASVTV
> Nestin_B    ----------------------------------------------------------------------------
> Nestin_C    ----------------------------------------------------------------------------

> Nestin_A    KAEVHIPEETENAAEKSVDQLQQERAHVKLALATTLTKTAAEPKP
> Nestin_B    ----------------------------------------------------------------------------
> Nestin_C    ----------------------------------------------------------------------------
```

```
> Nestin_A    ELKPEDIEIQEEDESKQFQEDQVVESETVASASVSVSADQLINLTQT
> Nestin_B    ------------------------------------------------------------------------------------------
> Nestin_C    ------------------------------------------------------------------------------------------

> Nestin_A    PEIESWAGPFADPAGVSEEGKDEDTEVSVEMARISHAPKVAWEEN
> Nestin_B    ------------------------------------------------------------------------------------------
> Nestin_C    ------------------------------------------------------------------------------------------

> Nestin_A    KTVAEDEKDDASEMDVRSENISESHTDAYGDDENDNDTLKSSHIS
> Nestin_B    ------------------------------------------------------------------------------------------
> Nestin_C    ------------------------------------------------------------------------------------------

> Nestin_A    ADTSKLGSSFLEQGTLDLVRDFGYHDDLMRVDEQDNVSNISEEVT
> Nestin_B    ------------------------------------------------------------------------------------------
> Nestin_C    ------------------------------------------------------------------------------------------

> Nestin_A    EQMDSETEAAIDSINKGDKQENKGDGQEETEEENETKVMSPDSKV
> Nestin_B    ------------------------------------------------------------------------------------------
> Nestin_C    ------------------------------------------------------------------------------------------

> Nestin_A    EAEDEMNINTNMKDKTDENVTEIEEEEIEVIKSDISVQGEGVDHQE
> Nestin_B    ------------------------------------------------------------------------------------------
> Nestin_C    ------------------------------------------------------------------------------------------

> Nestin_A    TLEKTVTPTEPHPYPTVNEEDPLPEESVEEEENQGEDDDSPNISASC
> Nestin_B    ------------------------------------------------------------------------------------------
> Nestin_C    ------------------------------------------------------------------------------------------

> Nestin_A    RTDPGECDSYSQENTLADTRPLIHYKSDEETDGKVQASHLMGETS
> Nestin_B    ------------------------------------------------------------------------------------------
> Nestin_C    ------------------------------------------------------------------------------------------

> Nestin_A    DSEEEKERMEGSLWNQSASKRFNTMDWRSHRRTRHGGHWRDGR
> Nestin_B    ------------------------------------------------------------------------------------------
> Nestin_C    ------------------------------------------------------------------------------------------

> Nestin_A    RCCF
> Nestin_B    --------
> Nestin_C    --------
```

Supplementary Figure 2.3. Amino acid sequence alignment of nestin isoform A, B and C illustrating sequence identity. The black highlighted sequence illustrates high sequence identity between the goldfish nestin isoforms.

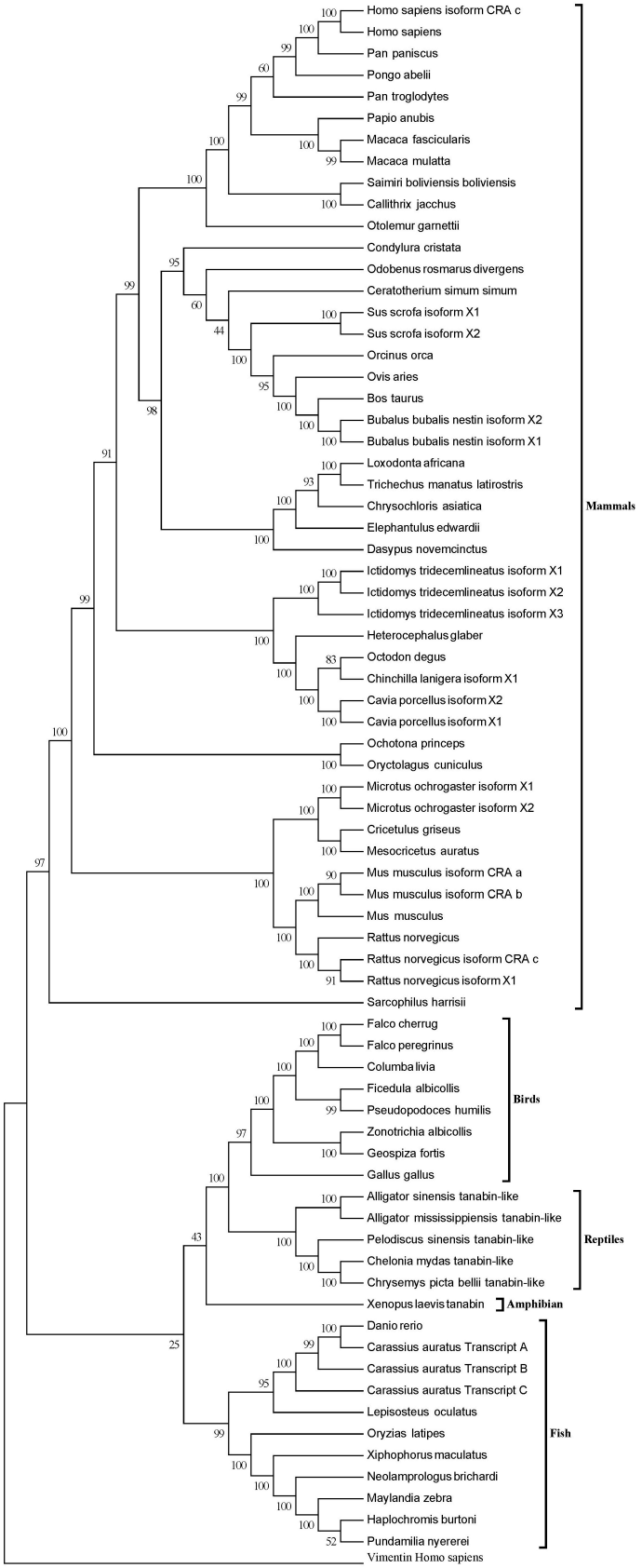
Homo sapiens isoform CRA c
Homo sapiens
Pan paniscus
Pongo abelii
Pan troglodytes
Papio anubis
Macaca fascicularis
Macaca mulatta
Saimiri boliviensis boliviensis
Callithrix jacchus
Otolemur garnettii
Condylura cristata
Odobenus rosmarus divergens
Ceratotherium simum simum
Sus scrofa isoform X1
Sus scrofa isoform X2
Orcinus orca
Ovis aries
Bos taurus
Bubalus bubalis nestin isoform X2
Bubalus bubalis nestin isoform X1
Loxodonta africana
Trichechus manatus latirostris
Chrysochloris asiatica
Elephantulus edwardii
Dasypus novemcinctus
Ictidomys tridecemlineatus isoform X1
Ictidomys tridecemlineatus isoform X2
Ictidomys tridecemlineatus isoform X3
Heterocephalus glaber
Octodon degus
Chinchilla lanigera isoform X1
Cavia porcellus isoform X2
Cavia porcellus isoform X1
Ochotona princeps
Oryctolagus cuniculus
Microtus ochrogaster isoform X1
Microtus ochrogaster isoform X2
Cricetulus griseus
Mesocricetus auratus
Mus musculus isoform CRA a
Mus musculus isoform CRA b
Mus musculus
Rattus norvegicus
Rattus norvegicus isoform CRA c
Rattus norvegicus isoform X1
Sarcophilus harrisii
Mammals
Falco cherrug
Falco peregrinus
Columba livia
Ficedula albicollis
Pseudopodoces humilis
Zonotrichia albicollis
Geospiza fortis
Gallus gallus
Birds
Alligator sinensis tanabin-like
Alligator mississippiensis tanabin-like
Pelodiscus sinensis tanabin-like
Chelonia mydas tanabin-like
Chrysemys picta bellii tanabin-like
Reptiles
Xenopus laevis tanabin
Amphibian
Danio rerio
Carassius auratus Transcript A
Carassius auratus Transcript B
Carassius auratus Transcript C
Lepisosteus oculatus
Oryzias latipes
Xiphophorus maculatus
Neolamprologus brichardi
Maylandia zebra
Haplochromis burtoni
Pundamilia nyererei
Fish
Vimentin Homo sapiens

Supplementary Figure 2.4. Phylogenetic tree of nestin showing evolutionary relationship between nestin protein sequences. The evolutionary history was inferred using the Neighbor-Joining method (Saitou and Nei 1987). The bootstrap consensus tree inferred from 1000 replicates is taken to represent the evolutionary history of the taxa analyzed (Felsenstein 1985). Branches corresponding to partitions reproduced in less than 80% bootstrap replicates are collapsed. The percentage of replicate trees in which the associated taxa clustered together in the bootstrap test (1000 replicates) are shown next to the branches. The evolutionary distances were computed using the Poisson correction method (Zuckerkandl and Pauling 1965) and are in the units of the number of amino acid substitutions per site. The analysis involved 73 amino acid sequences. All ambiguous positions were removed for each sequence pair. There were a total of 2886 positions in the final dataset. Evolutionary analyses were conducted in MEGA5 (Tamura *et al.* 2011).

B.2. Chapter 3 Supplementary Figures

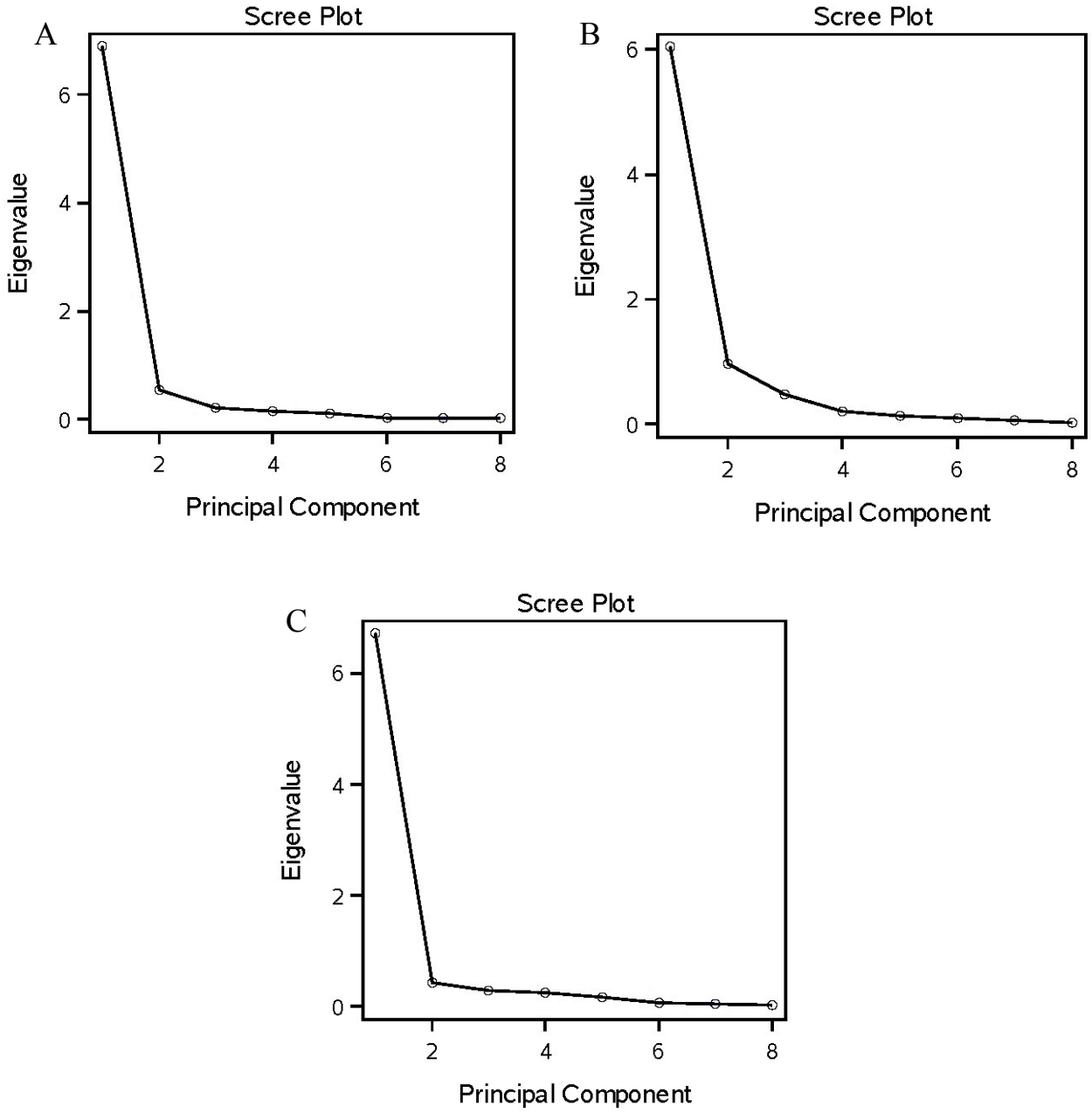

Supplementary Figure 3.1. A principal component analysis of nestin protein expression obtained from western blots and displayed as a scree plot of A) male goldfish (n=9); B) control and MPTP-treated 4 dpi female (n=10) and male (n=9) goldfish groups and C) control versus MPTP-treated 7 dpi female (n=10) and male (n=10) goldfish groups. The scree plots shows the number of principal components that best describes the variation within the data set. The remaining components explain a very small proportion of the variance of nestin protein expression.

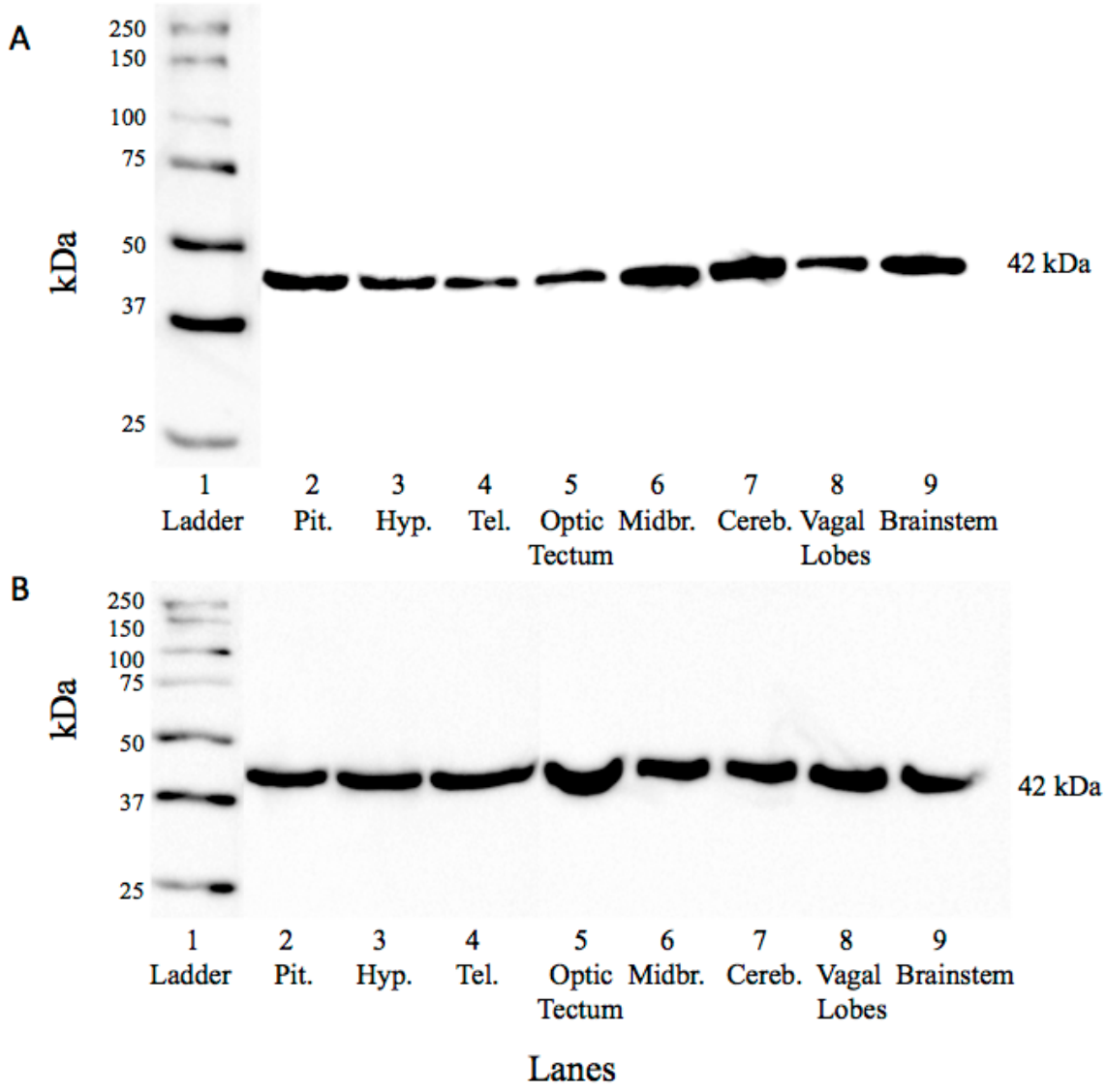

Supplementary Figure 3.2. Western blot analysis of ß-actin protein distribution patterns (42 kDa) in the female MPTP-treated goldfish brain and whole pituitary at A) 4 dpi of MPTP and B) 7 dpi of MPTP. Lane 1 is the standard ladder, lane 2 is goldfish pituitary (Pit), lane 3 is hypothalamus (Hyp), lane 4 is telencephalon (Tel), lane 5 is optic tectum, lane 6 is midbrain (Midbr), lane 7 cerebellum (Cereb), lane 8 is vagal lobes and lane 9 is brainstem.

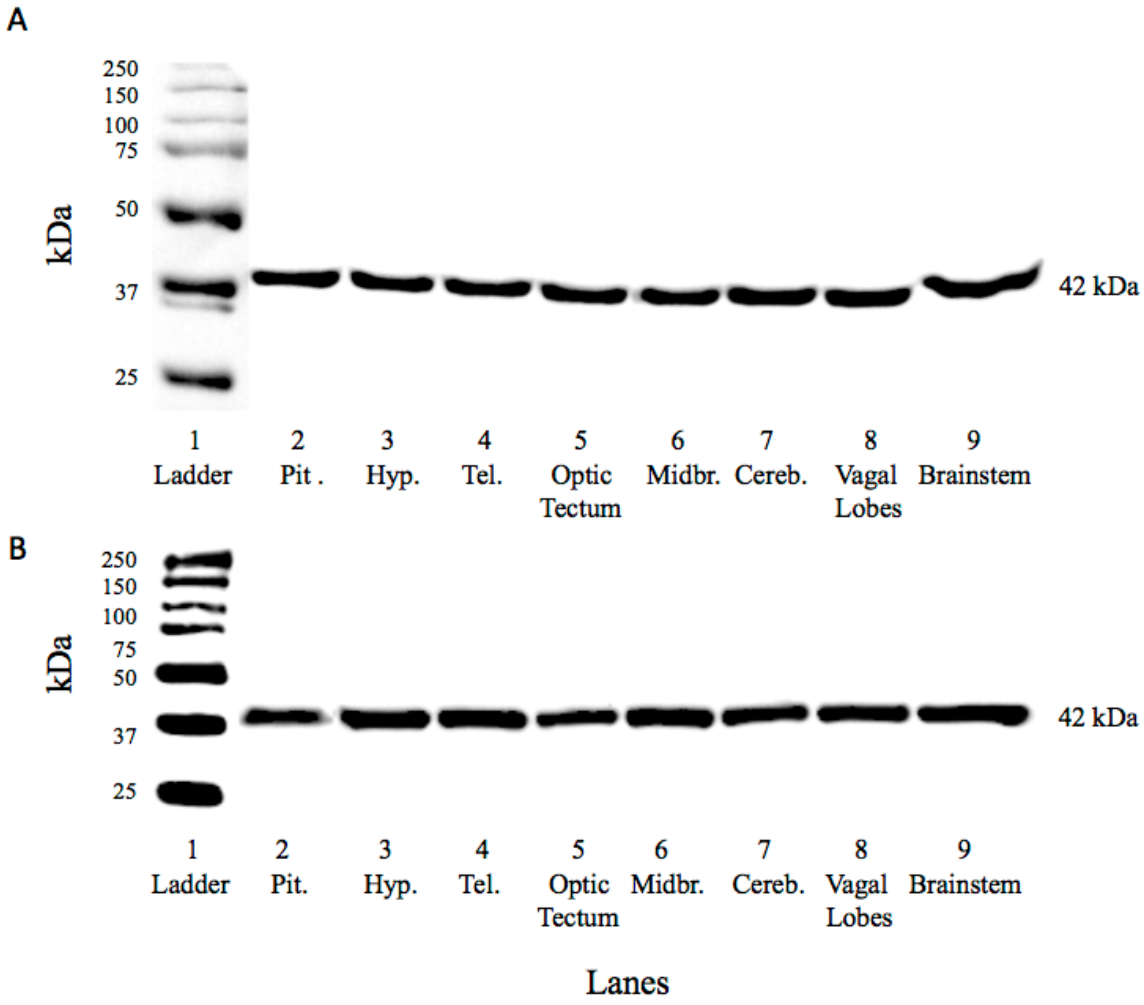

Supplementary Figure 3.3. Western blot analysis of ß-actin protein distribution patterns (42 kDa) in the male MPTP-treated goldfish brain and whole pituitary at A) 4 dpi of MPTP and B) 7 dpi of MPTP. Lane 1 is the standard ladder, lane 2 is goldfish pituitary (Pit), lane 3 is hypothalamus (Hyp), lane 4 is telencephalon (Tel), lane 5 is optic tectum, lane 6 is midbrain (Midbr), lane 7 cerebellum (Cereb), lane 8 is vagal lobes and lane 9 is brainstem.

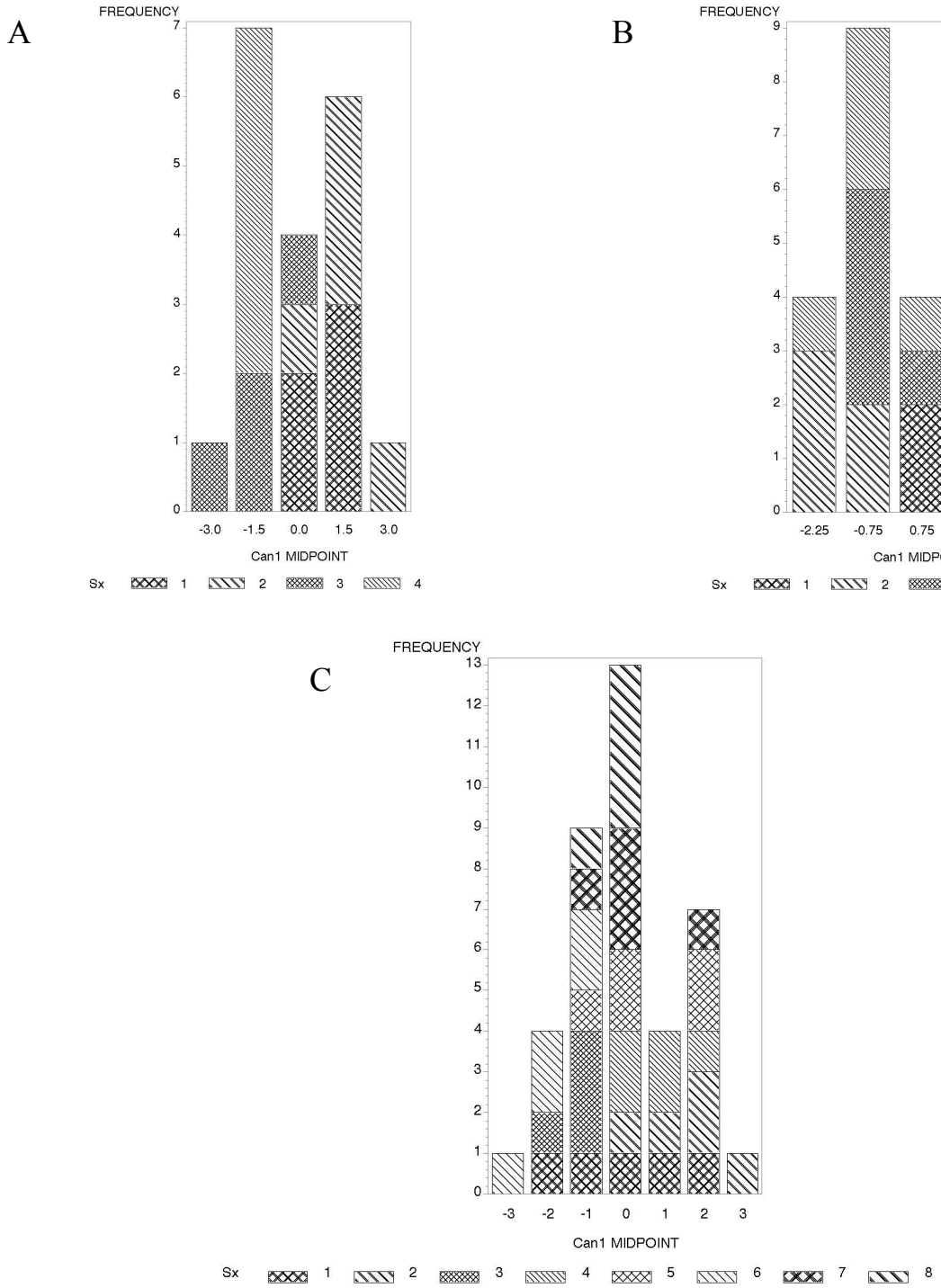

Supplementary Figure 3.4. Canonical and classificatory discriminant analysis of ß-actin protein expression obtained from western blots of A) control female (n=5; Sx=1); MPTP-treated female (n=5; Sx=2); control male (n=4; Sx=3); and MPTP-treated male (n=5; Sx=4) goldfish at 4 dpi; B) control female (n=5; Sx=1); MPTP-treated female (n=5; Sx=2); control male (n=5; Sx=3); and MPTP-treated male (n=5; Sx=4) goldfish at 7 dpi and C) control female at 4 dpi (n=5; Sx=1); MPTP-treated female at 4 dpi (n=5; Sx=2); control male at 4 dpi (n=4; Sx=3); MPTP-treated male at 4 dpi (n=5; Sx=4); control female at 7 dpi (n=5; Sx=5); MPTP-treated female at 7 dpi (n=5; Sx=6); control male at 7 dpi (n=5; Sx=7); and MPTP-treated male at 7 dpi (n=5; Sx=8). The bar graph shows the distribution of ß-actin based on sex and treatment.

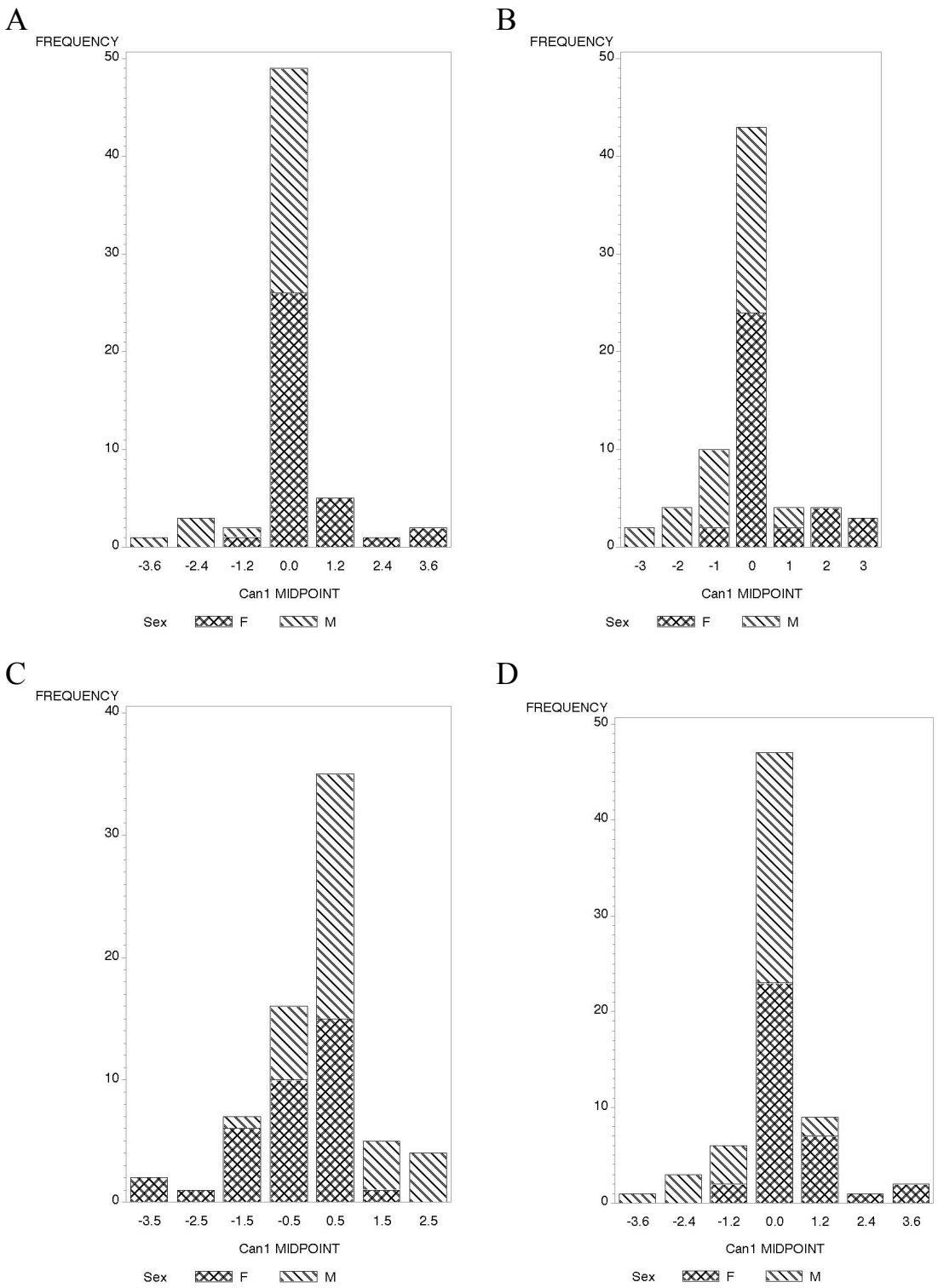

Supplementary Figure 3.5. Canonical and classificatory discriminant analysis of nestin protein expression obtained from western blots of A) control female (n=5; Sex=F) and male (n=4; Sex=M) goldfish at 4 dpi; B) control female (n=5; Sex=F) and male (n=5; Sex=M) goldfish at 7 dpi, C) MPTP-treated female (n=5; Sex=F) and MPTP-treated male (n=5; Sex=M) goldfish at 4 dpi and D) MPTP-treated female (n=5; Sex=F) and MPTP-treated male (n=5; Sex=M) goldfish at 7 dpi. The bar graph shows the distribution of nestin based on sex.

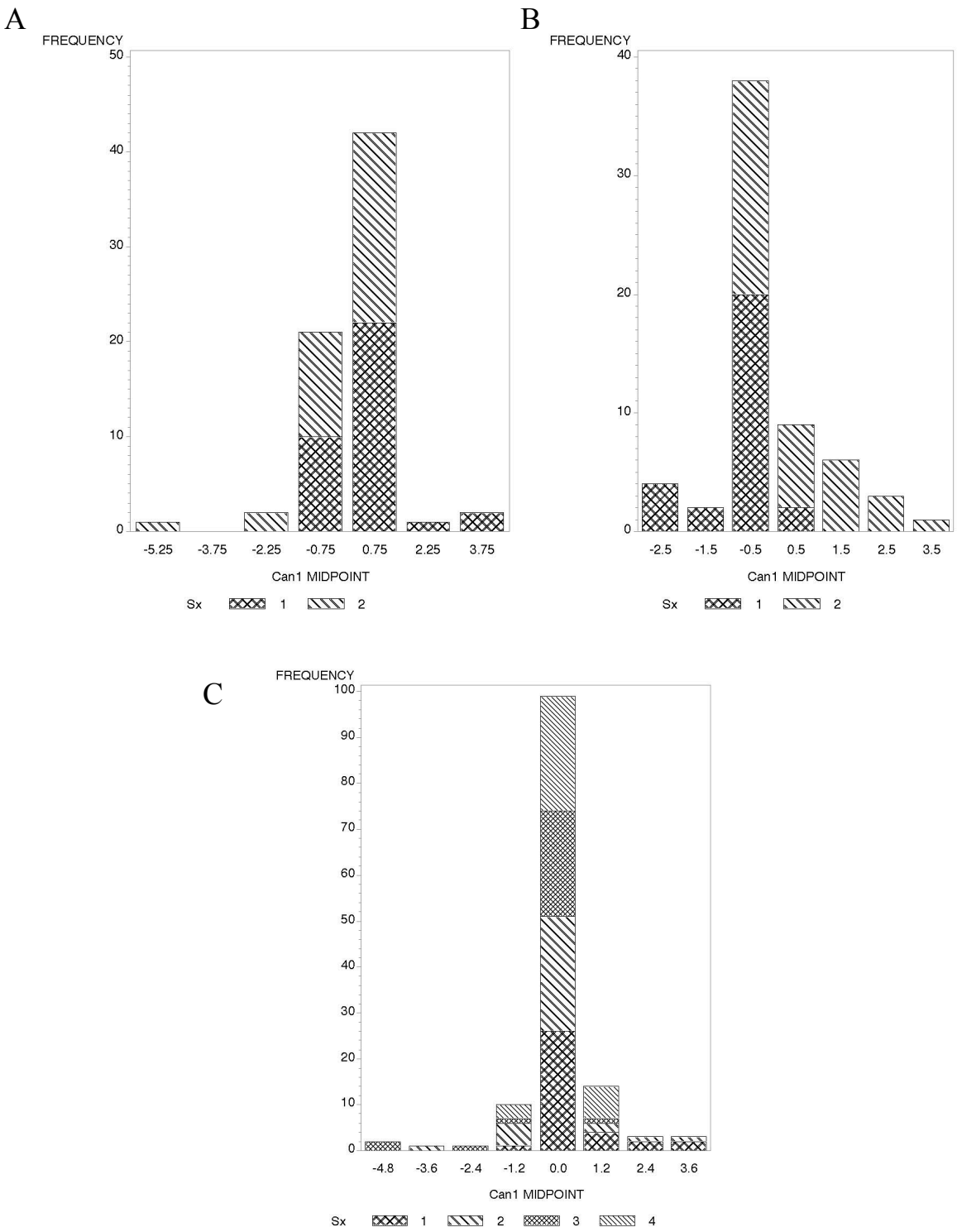

Supplementary Figure 3.6. Canonical and classificatory discriminant analysis of nestin protein expression obtained from western blots of A) control female (n=5; Sx=1) and MPTP-treated female (n=5; Sx=2) goldfish at 4 dpi and B) control male (n=4; Sx=1) and MPTP-treated male (n=5; Sx=2) goldfish at 4 dpi. The bar graph shows the distribution of nestin based on treatment. C) Analysis of control female (n=5; Sx=1); MPTP-treated female (n=5; Sx=2); control male (n=4; Sx=3); and MPTP-treated male (n=5; Sx=4) goldfish at 4 dpi. The bar graph shows the distribution of nestin based on sex and treatment.

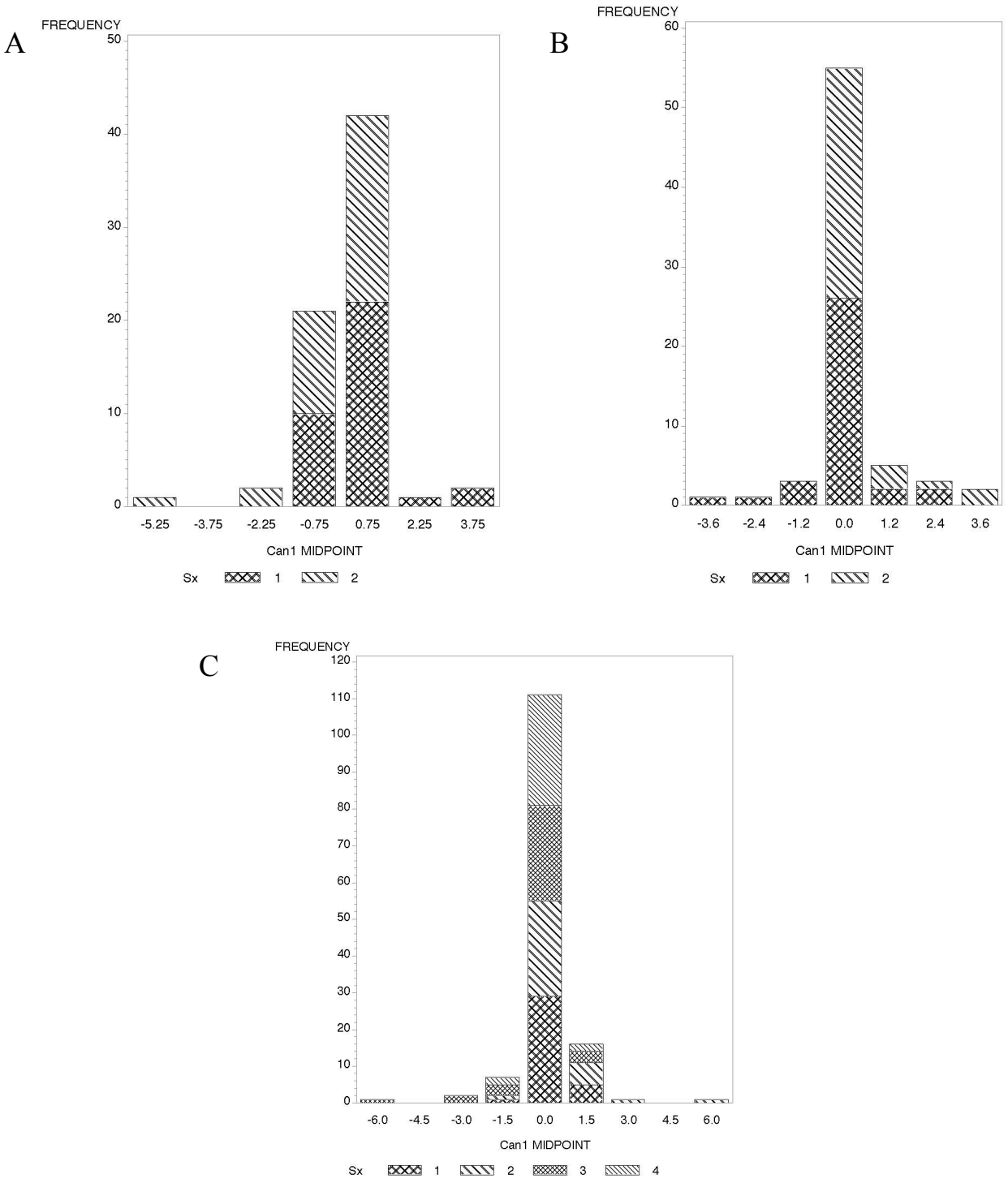

Supplementary Figure 3.7. Canonical and classificatory discriminant analysis of nestin protein expression obtained from western blots of A) control female (n=5; Sx=1) and MPTP-treated female (n=5; Sx=2) goldfish at 7 dpi and B) control male (n=4; Sx=1) and MPTP-treated male (n=5; Sx=2) goldfish at 7 dpi. The bar graph shows the distribution of nestin based on treatment. C) Analysis of control female (n=5; Sx=1); MPTP-treated female (n=5; Sx=2); control male (n=5; Sx=3); and MPTP-treated male (n=5; Sx=4) goldfish at 7 dpi. The bar graph shows the distribution of nestin based on sex and treatment.

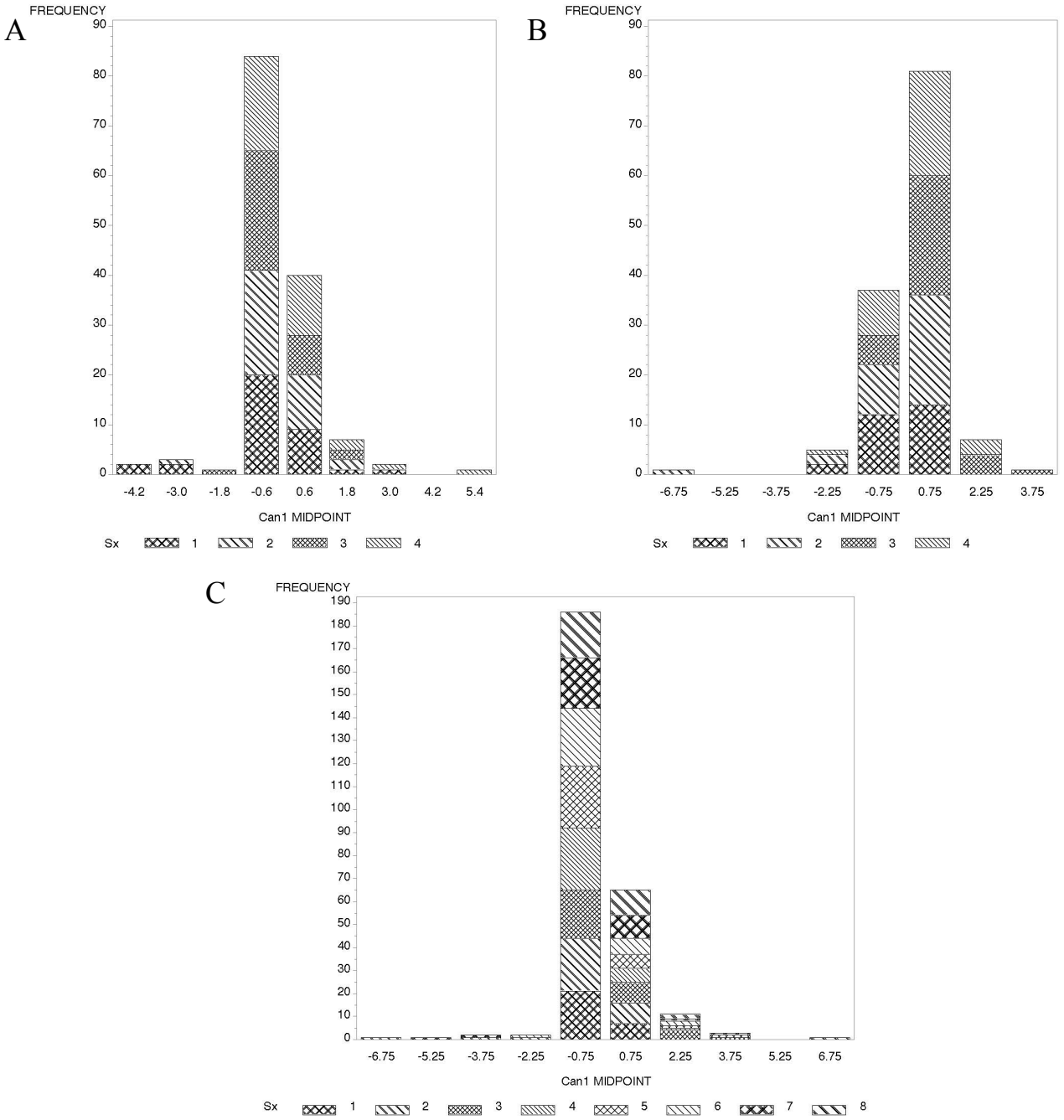

Supplementary Figure 3.8. Canonical and classificatory discriminant analysis of nestin protein expression obtained from western blots of A) control female goldfish at 4 dpi (n=5; Sx=1); control female at 7 dpi (n=5; Sx=2); MPTP-treated female at 4 dpi (n=5; Sx=3); and MPTP-treated female at 7 dpi (n=5; Sx=4) and B) control male goldfish at 4 dpi (n=4; Sx=1); control male at 7 dpi (n=5; Sx=2); MPTP-treated male at 4 dpi (n=5; Sx=3); and MPTP-treated male at 7 dpi (n=5; Sx=4). The bar graph shows the distribution of nestin based on treatment. C) Analysis of control male goldfish at 4 dpi (n=4; Sx=1); control male at 7 dpi (n=5; Sx=2); MPTP-treated male at 4 dpi (n=5; Sx=3); MPTP-treated male at 7 dpi (n=5; Sx=4); control female at 4 dpi (n=5; Sx=5); control female at 7 dpi (n=5; Sx=6); MPTP-treated male at 4 dpi (n=5; Sx=7); and MPTP-treated male at 7 dpi (n=5; Sx=8). The bar graph shows the distribution of nestin based on sex and treatment.

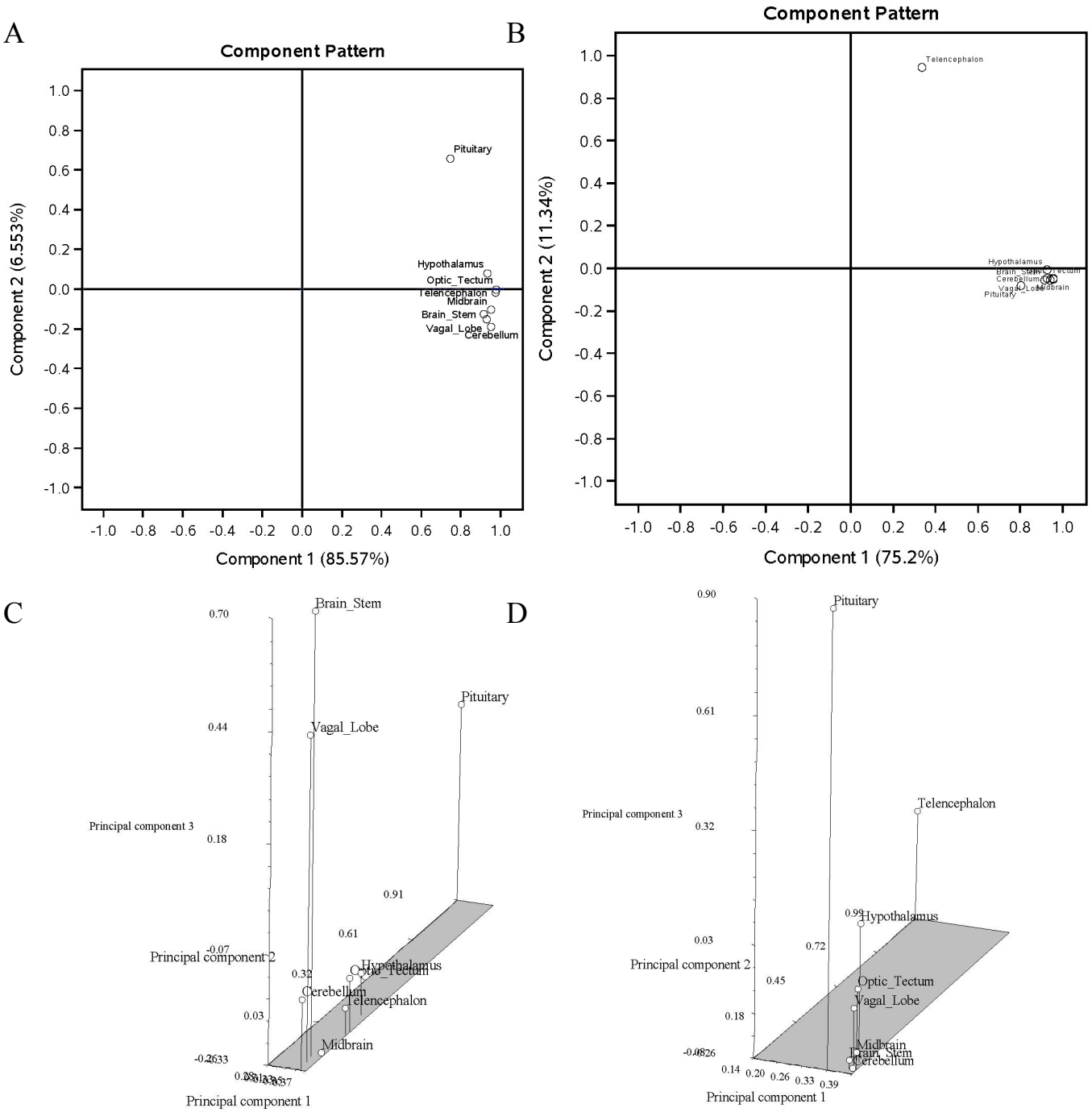

Supplementary Figure 3.9. Canonical analysis of nestin protein expression data obtained from western blots of A) control and MPTP-treated male goldfish at 4 dpi (n=9) and 7 dpi (n=10) and B) control and MPTP-treated female and male goldfish at 4 and 7 dpi separating the variables pituitary, hypothalamus, telencephalon, optic tectum, midbrain, cerebellum, vagal lobe and brainstem on a 2D plot. Variation explained as percent in brackets. Three-dimensional score plot of the first three principal components for the nestin protein expression in the C) control and MPTP-treated male goldfish at 4 dpi (n=9) and 7 dpi (n=10) and D) control and MPTP-treated female and male goldfish at 4 and 7 dpi separating the factors pituitary, hypothalamus, telencephalon, optic tectum, midbrain, cerebellum, vagal lobe and brainstem. In C), variance of component 1 explained is 85.57%; component 2 is 6.55% and component 3 is 2.54% and in D) variance of component 1 explained is 75.2%; component 2 is 11.34% and component 3 is 5.26%.